Doctorado en Biomedicina y Farmacia
FACULTAD DE FARMACIA
UNIVERSIDAD DE VALENCIA

Innovative *In Vitro* Method and Permeability Estimation Procedure to Predict Drug Transport across the Blood-Brain Barrier

Víctor Mangas Sanjuán

Supervisors:

Vicente G. Casabó Alós

Mª del Val Bermejo Sanz

Isabel González Álvarez

Doctorado en Biomedicina y Farmacia
FACULTAD DE FARMACIA
UNIVERSIDAD DE VALENCIA

Tesis Doctoral

Innovative *In Vitro* Method and Permeability Estimation Procedure to Predict Drug Transport across the Blood-Brain Barrier

Trabajo presentado por Víctor Mangas Sanjuán para obtener el grado de Doctor en Farmacia

Fdo.: Víctor Mangas Sanjuán

D. VICENTE GERMÁN CASABÓ ALÓS, Doctor en Farmacia y Catedrático de la Universidad de Valencia, Dña. MARIA DEL VAL BERMEJO SANZ, Doctora en Farmacia y Catedrática de la Universidad Miguel Hernández de Elche y Dña. ISABEL GONZÁLEZ ÁLVAREZ, Doctora en Farmacia y Contratada Doctor en la Universidad Miguel Hernández de Elche certifican que:

> El presente trabajo: ***"Innovative In Vitro Method and Permeability Estimation Procedure to Predict Drug Transport across the Blood-Brain Barrier"***, presentado por D. Víctor Mangas Sanjuán para optar al grado de Doctor ha sido realizado bajo su dirección y una vez revisado, no encuentran objeciones para que sea presentado a su lectura y su defensa.

Y para que así conste, firman el presente certificado en Valencia, a 6 de mayo de dos mil catorce.

Fdo.: Vicente G. Casabó Alós Fdo.: Mª del Val Bermejo Sanz

Fdo.: Isabel González Álvarez

Doctorado en Biomedicina y Farmacia
FACULTAD DE FARMACIA
UNIVERSIDAD DE VALENCIA

Innovative *In Vitro* Method and Permeability Estimation Procedure to Predict Drug Transport across the Blood-Brain Barrier

Víctor Mangas Sanjuán

Valencia, 2014

A mi familia

A Berta

A mi jefe, Vicente

Acknowledgements

Son muchos los sentimientos, momentos y conocimientos que han dejado su huella en mi persona y en esta Tesis. Por ello, quisiera agradecer:

A mi directora, Marival. Por haberme enseñado y guiado durante este tiempo. Porque lo que era un sueño hace un tiempo cuando entré en tu despacho, tú lo has hecho realidad.

A mi directora, Isa. Por todas las horas y consejos que aquí están guardados. Por convertir un trabajo en una pasión, por contagiarme la ilusión por lo que hago día a día.

A mi director, Vicente. Porque lo más importante que he aprendido de ti no está escrito en esta tesis. Por maravillarme con cada momento sentado a tu lado en tu despacho, encontrando la manera de que lo descubriera sólo. Por ser un Genio, al que todos recordamos con una sonrisa.

A Marta, Carmen, Ana y Carlos por su paciencia y dedicación desde el primer día. Por los grandes momentos juntos y por los que aún quedan por vivir.

Al Departamento de Farmacia y Tecnología Farmacéutica de la Universidad de Valencia. Especialmente, a la Prof. Matilde y Prof. Virginia por su cariño y ayuda. Agradecer también a Juana, Jose, Pilar, Carmina y Carolina su sonrisa y disponibilidad siempre.

A mis compañeros y grupo de investigación Nacho, Vero, Sarín, Isa, Mayte, Alejandro, Adrián, Tere, Nasim, Ana y Andrés por su paciencia y ayuda siempre que lo he necesitado. Gracias a vosotros, somos un grupo de compañeros.

Al Grupo de Modeling & Experimental Biopharmaceutics la Universidad de Central "Marta Abreu" de las Villas, Cuba y muy especialmente, a Hai, Alcides y Reinaldo. Al Prof. Miguel Ángel por su consejo, confianza y amistad en este tiempo.

Prof. Liebeth de Lange for her guidance during my stay at LACDR. I will take care of all your advices and knowledge learned from you. I would like also to thank Robin, Jan, Nick, Shinji and Sinziana for their patience and support.

Al Departamento de la Universidad de Navarra, especialmente a los Prof. Iñaki y Prof. Maria Jesús por sus conocimientos y dedicación durante mi estancia en Pamplona. Así mismo, a Maria, Núria, Martín, Ana, Yolanda, Hilda, Simon, Ana Margarita, Sara, Maria, Koldo, Laura, Hugo y demás compañeros del departamento por los increíbles y buenos momentos vividos.

Al Área de Farmacia y Tecnología Farmacéutica de la Universidad Miguel Hernández de Elche.

Contents

Abbrevations

Abbreviation	Definition
AD	Alzheimer Disease
BBB	Blood-Brain Barrier
BCE	Barrera Cerebroespinal
BCEC	Brain Capillary Endothelial Cells
BCS	Biopharmaceutical Classification System
BCSFB	Blood cerebrospinal Fluid Barrier
BHE	Barrera Hematoencefálica
BUI	Brain Uptake Index
CNS	Central Nervous System
CSF	Cerebrospinal Fluid
ECF	Brain Extracellular Fluid
EMA	European Medicines Agency
ENT	Equilibrative Nucleoside Transporter
FDA	Food and Drug Administration
$f_{u,brain}$	Unbound fraction in brain
$f_{u,plasma}$	Unbound fraction in plasma
GLUT	Glucose Transporter
hPSC	Human Pluripotent Stem Cells
IAM	Immobilized Artificial Chromatography
ICF	Brain Intracellular Fluid
$K_{p,uu}$	Partition coefficient of unbound fraction in plasma and unbound fraction in brain
LAT	Large neutral Amino acid Transporter
MCT	Monocarboxylate Transporter

MDCK	Madin-Darby Canine Kidney
MDR	Multidrug Resistance gene
MNS	Modified Non-Sink
NS	Non-Sink
OATP	Organic Anion-Transporting Polypeptide
PAMPA	Parallel Artificial Membran Permeability Assay
P_{eff}	Permeability
PET	Positron Emission Tomography
P-gp	P-Glycoprotein
PKPD	Pharmacokinetic and Pharmacodynamic
PS	Permeability Surface product
PSA	Polar Surface Area
S	Sink
SC	Sink Corrected
SNC	Sistema Nervioso Central
TEER	Transepithelial Electrical Resistance
$V_{u,brain}$	Unbound volumen in brain

Summary. Resumen

La Barrera Hematoencefálica (BHE) es una entidad caracterizada por su naturaleza restrictiva al paso de sustancias. Las propiedades de la barrera están determinadas por la confluencia de tres componentes principales: 1) uniones celulares endoteliales con presencia de proteínas especificas intramembrana y citoplasmáticas unidas estrechamente al citoesqueleto. Esta circunstancia restringe la difusión paracelular de compuestos. Adicionalmente a las células endoteliales, la barrera presenta una membrana basal, en la cual se localizan pericitos y astrocitos, que conforman una capa que refuerza las propiedades de la barrera; 2) la presencia de transportadores de absorción y la sobreexpresión de transportadores de secreción combinada con el escaso transporte vesicular y la falta de fenestraciones y 3) metabolismo debido a la presencia de enzimas específicas, cuya función es proteger al cerebro. Todos estos componentes de la BHE son esenciales para mantener su integridad estructural, funcionalidad y estabilidad. En el Capítulo 1 de la Tesis se revisa con detalle la anatomía y fisiología de la BHE así como los mecanismos de transporte a través de esta barrera.

La BHE permite el paso de sustancias esenciales al cerebro, tales como glucosa, oxigeno, iones, aminoácidos esenciales y algunas sustancias lipídicas. En situaciones fisiopatológicas, también permite el paso de macrófagos y otras células del sistema inmune. Sin embargo, debido a su naturaleza protectora de la homeostasis del cerebro, limita el transporte de sustancias potencialmente tóxicas, como son los fármacos. Estas restricciones son necesarias para mantener un óptimo ambiente que permita el desarrollo de las funciones neuronales, aunque

pueda limitar el acceso de tratamientos farmacológicos cuando son requeridos. La BHE, la Barrera Cerebroespinal (BCE) y otras estructuras son un obstáculo enorme para la administración de fármacos con finalidad diagnóstica o terapéutica en el interior del cerebro. Actualmente, existe un número creciente de patologías que afectan al Sistema Nervioso Central (SNC) y según las investigaciones más recientes en muchas de ellas existe una desregulación o disfunción de la BHE. Numerosos investigadores trabajan hoy en día para entender los principales determinantes de la velocidad y magnitud de acceso al cerebro a fin de mejorar el desarrollo de sistemas de liberación dirigidos a optimizar el paso a través de la BHE. En este sentido hay numerosas propuestas novedosas que facilitarán el desarrollo de candidatos capaces de acceder al SNC que se describen en el Capítulo 2 de la memoria.

Con el fin de garantizar que los fármacos alcanzan su diana terapéutica es necesario evaluar la habilidad de los candidatos para cruzar la BHE, preferiblemente en las primeras fases de desarrollo de medicamentos. La determinación de los parámetros farmacocinéticos de los compuestos en desarrollo se ha facilitado gracias al uso de métodos experimentales *in silico, in vitro* e *in vivo.* Particularmente, los métodos *in vitro* basados en cultivos y co-cultivos de líneas celulares se han utilizados como métodos de cribado rápido para seleccionar los mejores candidatos en las etapas siguientes. Los modelos *in vitro* deben cumplir una serie de requisitos como un valor alto de resistencia transepitelial (TEER), baja capacidad permeable y la expresión de diferentes transportadores en su membrana. Mediante los coeficientes de permeabilidad obtenidos, se puede predecir la velocidad de acceso al cerebro y el momento del inicio de la acción, pero no es posible determinar la cantidad de fármaco que se alcanzaría en estado

estacionario. Sólo la fracción de fármaco libre en plasma es capaz de atravesar las barreras biológicas, tales como la BHE, y alcanzar la diana terapéutica. Por ello son necesarios nuevos modelos *in vitro* experimentales capaces de considerar todos los factores mencionados y predecir velocidad y cantidad de fármaco que alcanza la diana terapéutica, en este caso en el cerebro.

Otro objetivo de los modelos *in vitro* consiste en reproducir las condiciones fisiopatológicas de la BHE. La morfología, la fisiología y consecuentemente la permeabilidad de la BHE se ven alteradas en numerosas enfermedades y todavía no se conoce claramente como esos cambios afectan al acceso de fármacos al SNC. Modelos *in vitro* de condiciones patológicas podrían ser muy útiles para encontrar soluciones aplicables a estas situaciones. En este sentido, el aislamiento de capilares se ha utilizado para estudiar ciertas condiciones patológicas y, recientemente, se están investigando con este propósito modelos de redes de fibras en 3D, modelos de chip de microfluidos y otros modelos de cultivos celulares. Los diversos métodos *in silico*, *in vitro* e *in vivo* se discuten en cuanto a ventajas y limitaciones en el Capítulo 3 y se justifica la necesidad del desarrollo de un nuevo sistema de predicción como objetivo central de esta Memoria.

Durante las fases preclínicas del desarrollo de medicamentos, los experimentos para la determinación de la permeabilidad son esenciales a la hora de seleccionar moléculas candidatas para su posterior desarrollo clínico. La estimación del valor de permeabilidad de estas moléculas es un punto crítico que permitirá incorporar o descartar a los candidatos para las fases posteriores, por lo que el valor de permeabilidad obtenido debe ser lo más exacto y preciso posible. Para ello es necesario controlar los factores pre-experimentales,

experimentales y post-experimentales que pueden influir en la obtención de dicho valor.

En el Capítulo 4 se revisan estas metodologías de cálculo y se propone un nuevo método de estimación. Tavelin y col. habían propuesto en 2002 una nueva ecuación para calcular la permeabilidad cuando el experimento de transporte no cumplía las condiciones sink o sumidero. También describieron la presencia de perfiles atípicos en los que la velocidad inicial está alterada debido a factores propios del investigador, o factores asociados a las características fisicoquímicas del compuesto, así como condicionantes propios del diseño experimental. El modelo non-sink clásico presenta una infra- o sobreestimación del valor de permeabilidad en situaciones de perfiles atípicos, es por ello que surgió la necesidad de diseñar una nuevo modelo para calcular la permeabilidad que se ha llamado MNS (modificación de la ecuación non-sink.). Mediante la simulación de experimentos de transporte, se ha explorado la capacidad predictiva del nuevo modelo MNS, para diferentes perfiles de cantidad-concentración frente al tiempo, incluyendo aquellos en los cuales la permeabilidad se ve alterada en las primeras fases del ensayo experimental y se ha comparado frente a los métodos clásicos sink y no-sink. El modelo se ha probado considerando diferentes niveles de variabilidad experimental y, finalmente se ha explorado su utilidad para la clasificación de fármacos según el sistema BCS (Biopharmaceutical Classification System).

Los resultados han demostrado que el método MNS es preciso y exacto para el cálculo de la permeabilidad en cualquier tipo de perfil y en diferentes escenarios de variabilidad, bajo condiciones sink y no-sink, mientras que el modelo estándar No-Sink presenta una peor capacidad predictiva en aquellas situaciones dónde se ve alterado el paso de

fármaco a través de la monocapa en las fases iniciales del ensayo experimental. Los modelos de regresión lineal, Sink y Sink corregida, no son válidos en condiciones no-sink, debido a que no se cumplen las asunciones necesarias para su utilización, pero tampoco en condiciones sink donde hay una alta variabilidad experimental.

Otros factores que pueden afectar el valor de permeabilidad calculado son los relativos a los protocolos o procedimientos normalizados de trabajo de la técnica experimental. Este aspecto se aborda en el Capítulo 5. En esta tesis doctoral se ha realizado un estudio para comparar los resultados obtenidos utilizando distintos protocolos que se diferenciaban fundamentalmente en la edad de las monocapas utilizadas (pases) y en la distinta maduración de las células antes de realizar el experimento (días post-sembrado), así como en el uso de insertos recubiertos o no con colágeno. Los resultados obtenidos demostraron diferencias estadísticamente significativas en el valor de permeabilidad según las distintas condiciones ensayadas. Es por ello que, la estandarización y la demostración de la idoneidad de los métodos experimentales son pasos necesarios para la utilización de los valores de permeabilidad con fines regulatorios o de predicción del comportamiento *in vivo* durante el desarrollo clínico. Generalmente, se ha prestado más atención a la validación de los procesos experimentales y menos al análisis matemático de los resultados, aunque los modelos matemáticos estándar presenten una serie de asunciones que no siempre se mantienen experimentalmente.

Una vez controlada la fiabilidad en la obtención de la permeabilidad para fármacos candidatos a atravesar la BHE se procede al cálculo de los parámetros que rigen dichos procesos. Los parámetros más relevantes para la predicción de la velocidad y cantidad que

atraviesa la BHE son: $f_{u, plasma}$ (fracción de fármaco libre en plasma), $Kp_{uu, brain}$ (relación entre la concentración de fármaco libre en plasma y cerebro) y $V_{u, brain}$ (volumen de distribución en el cerebro). Su estimación requiere todavía de modelos *in vivo* y de experimentos *in vitro* de cribado rápido conjuntamente, lo cual dificulta el cribado rápido de moléculas candidatas a actuar en el SNC en las fases iniciales de desarrollo clínico.

El objetivo principal de este trabajo es el desarrollo de un nuevo método *in vitro* de cribado rápido para la predicción de la velocidad y cantidad de fármaco que atraviesa la BHE y se discute en el Capítulo 6. El sistema permite estimar los parámetros anteriormente descritos en un único método experimental, utilizando monocapas celulares *in vitro* bajo diferentes condiciones. A partir de relaciones entre los valores de permeabilidad obtenidos bajo cada condición y con el adecuado análisis matemático, se estiman todos los parámetros relevantes.

Se seleccionaron diez compuestos y se estimaron sus valores de permeabilidad utilizando líneas celulares MDCKII y MDCKII-MDR1 en ausencia o presencia de albúmina y homogeneizado de cerebro. Los ratios entre las permeabilidades obtenidas en presencia y ausencia de albúmina permiten estimar la fracción libre en plasma *in vitro*. Por otro lado, los ratios entre las permeabilidades en presencia y ausencia de homogeneizado de cerebro permiten la estimación de la fracción libre en cerebro *in vitro*. $Kp_{uu, brain}$ y $V_{u, brain}$ se estiman a partir de la relación entre las permeabilidades apical y basal en condiciones estándar. Los parámetros *in vitro* se correlacionaron con los parámetros de los mismos compuestos obtenidos en experimentos *in vivo*. Con ello, se ha demostrado una alta capacidad predictiva del comportamiento *in vivo* de los compuestos utilizando el sistema experimental propuesto. La línea celular MDCKII presentó un mayor nivel de correlación frente a los

valores *in vivo* de $f_{u,\ plasma,}$ $Kp_{uu,\ brain}$ y $V_{u,\ brain}$ (R=0.93, R=0.85 y R=0.99, respectivamente). Debido a su sencillez, destaca notablemente el nivel de correlación obtenido, a pesar del número reducido de compuestos con características fisicoquímicas y mecanismos de transporte asociados tan diversos. Modificaciones experimentales posteriores serán necesarias, con el fin de optimizar el método, pero los resultados obtenidos hasta el momento demuestran su viabilidad. Del mismo modo que otros modelos de cultivos celulares *in vitro*, el sistema es adecuado para la miniaturización y robotización con el objetivo de establecer mecanismos de cribado rápido de candidatos en el desarrollo de medicamentos.

Introduction

BLOOD-BRAIN BARRIER

Brain is the most protected organ in the body. Due to a very controlled brain homeostasis, there are three physiological barriers that restrict the access of endogenous substances and xenobiotics (drugs or toxins) to the central nervous system (CNS): the blood-brain barrier (BBB), the blood cerebrospinal fluid barrier (BCSFB) and the ependyma (the epithelial layer of cells covering the brain) (Figure 1) [1].

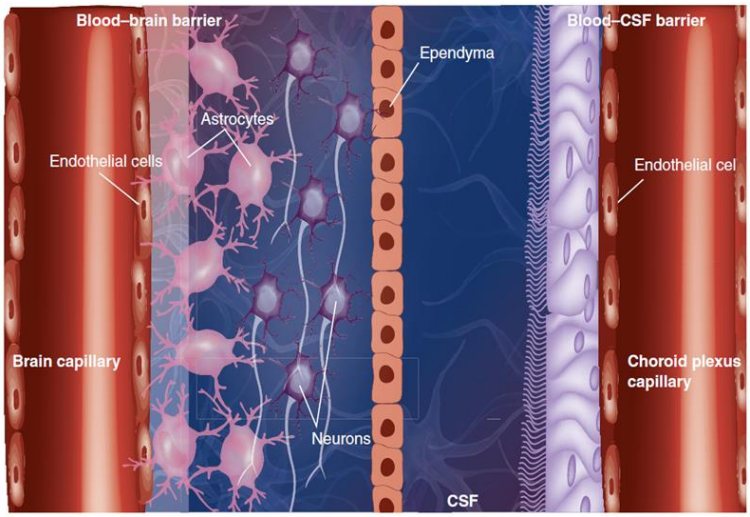

Figure 1. Localization and structure of BBB and BCSF barriers. Adapted from Pavan et al, 2008 [1].

Even today, the majority of new drugs discovered do not cross the BBB [2]. In the last decade, a growing number of spin-off biotechnological companies from academia have started to develop new methods and strategies to help pharmaceutical companies target the brain. The CNS discovery and development paradigm in those companies is slowly changing to acknowledge the need for earlier BBB access in order to avoid clinical failures. The development programs

should include the use of *in silico*, *in vitro* and *in situ* models from the beginning to reduce the attrition rate later on. Nevertheless, there is still room for research and many unanswered questions.

In upcoming years it will be desirable to improve the quality of *in silico* models to screen better new families of compounds, taking into account passive diffusion in combination with influx and efflux mechanisms.

More research is required to improve *in vitro* cell methods to obtain barriers keeping the BBB phenotype, while also being easy to handle and offering similar dynamic properties of the human BBB vessels.

Research in the area of transporters at BBB level, tight junction formation and changes under pathological conditions will help to design strategies for targeting the brain. There is a need for BBB genomic research to identify specific targets on the brain vasculature. Carrier-mediated transport or receptor-mediated transport are successful strategies that offer a wide scenario for the development of new brain targeted molecules.

Chapter 1 and 2 review the anatomy and physiology of Blood Brain Barrier and the latest developments in Drug Delivery Methodologies to access the Central Nervous System (CNS).

IN VITRO MODELS OF BBB AND PHARMACOKINETICS PARAMETERS OF BRAIN DELIVERY AND DISTRIBUTION.

Blood-brain barrier (BBB) controls the access of endogenous substances and xenobiotics to the extracellular fluid (ECF) and intracellular cerebral fluid (ICF). BBB is an active barrier with important functions for brain homeostasis and protection, formed by endothelial cells with high expression of tight junctions and transporters. Only the unbound fraction of drug in plasma can permeate through the BBB and interact with the target in the brain [3-6]. The most important parameters that govern the pharmacokinetics of drug in the CNS are $f_{u,\ plasma}$, $Kp_{uu,\ brain}$ and $V_{u,\ brain}$. $f_{u,\ plasma}$ is the unbound fraction of drug in plasma, $Kp_{uu,\ brain}$ represents the ratio between unbound drug concentrations in brain and in blood and $V_{u,\ brain}$ is the apparent distribution volume in brain. ECF concentrations could only be obtained using microdialysis. For ethical reasons, human cerebrospinal fluid concentrations (CSF) have been used as a surrogate measure of the ECF concentrations. De Lange et al. has recently published the utility of human $Kp_{uu,\ CSF}$ as reference of the ECF concentrations in brain [3].

In silico, *in vitro*, *in situ* or *in vivo* methodologies have been employed to evaluate the pharmacokinetic of new drug candidates in the CNS [7]. Chapter 3 review the *in silico*, *in vitro* and *in vivo* methods used in drug development for CNS candidate screening. *In vitro* cell culture experiments are used as a high throughput method to select best candidates for further stages of the drug development process, however permeability coefficients (P_{app}) are relevant only for the rate of access

and the onset of action but do not determine the extent as in a steady state drug administration there is not a limited time for the permeation process. Consequently the range of adequate permeability values for BBB barrier is wider than that used for intestinal permeability screening [5, 8]. Different *in vitro* cell models have been used to mimic the blood-brain barrier (BBB) [9-13]. Madin-Darby canine kidney II (MDCKII) cells and MDCKII transfected with the human multidrug resistance gene 1 (encoding P- glycoprotein, P-gp) (MDCKII-MDR1) are commonly used to evaluate the blood–brain barrier permeability of drugs [10, 14, 15] MDCK I cells show much higher transepithelial electric resistance (TEER) than MDCK II cells, although they bear similar numbers of tight junction (TJ) strands [16]. These cells display morphological, enzymatic, and antigenic cell markers, also found in cerebral endothelial cells and have been reported as a suitable model for this barrier. The MDCKII-MDR1 cell line was identified as the most promising cell line among several cell lines, for qualitative predictions of brain distribution, and to distinguish between compounds that pass the blood–brain barrier by passive diffusion and those that are substrates for active efflux by P-glycoprotein, P-gp [14, 15]. The P-gp transporter and other membrane transporters belonging to the ATP-binding cassette family of transporters have been extensively described to regulate intracellular concentrations of different compounds [17-19].

The *in vivo* microdialysis is the gold standard technique, allowing continuous monitoring with high-resolution concentration profiles of drugs and metabolites from (freely moving) individual subjects. Measurements are obtained from brain extracellular fluid, inserting one probe into the brain tissue and from peripheral blood stream. Then, unbound brain and plasma concentrations are estimated as the best

reference to explore drug permeation and distribution across the BBB [4, 5, 20-22]. However, the main disadvantage of this technique is the high time-consuming, which reduces its application as a high screening method for new drug candidates.

PERMEABILITY ESTIMATION METHODS.

The permeability is calculated from the drug concentrations and accumulated amounts in acceptor chamber using either linear or nonlinear regression models, depending of the assumption about sink conditions on the receptor side [23, 24]. Tavelin et al.[24] described the different profiles that are usually observed between accumulated amounts of drug in the acceptor side versus time. Three examples of these profiles are represented in Figure 2.

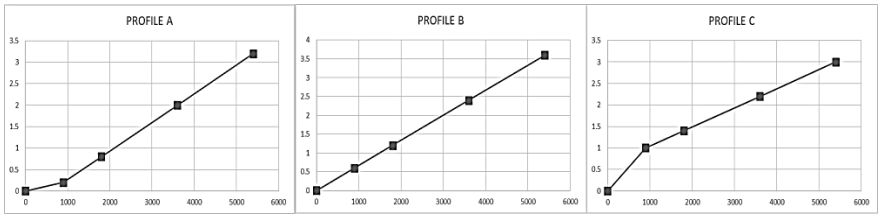

Figure 2. Profiles of accumulated amounts of drug in acceptor chamber versus time in permeability experiments in cell monolayers. Profile A: Drug is transported during the first sampling interval at a lower rate than expected; Profile B: Drug is transported linearly with a constant rate; Profile C: Drug is transported at a higher rate during the first sampling interval.

Tavelin et al. [24] highlighted the existence of atypical profiles (Profiles A and C on Figure 2) and explained the possible reasons to these profiles. Profile A may be caused by poor temperature control at the beginning of the experiment, or by the fact that partitioning of the drug into the cell monolayer is the rate-limiting step. Profile C is sometimes observed when the transport of radiolabeled drugs is

studied. The reason may be that radiolabeled low molecular weight impurities (such as 3H-water) are present in the drug solution and are transported at a higher rate than the drug. Another reason may be that the cell monolayer is affected by a too harsh application of the drug solution. In such cases, the estimation of the permeability by the standard linear regression methods or even non-linear regression methods may not be correct. Therefore, a good estimation of permeability is needed to correctly classify drugs under BCS criteria. Chapter 4 focuses on the development of a new estimation method able to be used under sink and non-sink conditions and to capture the alteration of the initial permeation rate without biasing the permeability estimation.

Simulation is an important tool for the evaluation of pharmacokinetic models that allows analyzing different scenarios and a more efficient decision making during drug development [25-33]. Regulatory agencies, FDA and EMA, encourage model simulation as a tool to increase predictability and efficiency in preclinical and clinical phases [34, 35].

A second aim of this study was to use a simulation strategy to explore the performance of a Modified Non-Sink equation, MNS; (in terms of precision and accuracy) for permeability estimation in different types of profiles and scenarios of variability, to compare the new proposed model with the classical sink and non-sink approaches and to explore its usefulness for BCS classification. Data from cell culture experiments representing the different experimental profiles have been analyzed with all the equations to validate the new approach. The limitations ad advantages of the MNS equation are discussed.

PROTOCOL OPTIMIZATION.

Chapter 5 deals with the factors affecting permeability estimation and its variability intra- and inter-laboratory. Permeability values and their associated variability from cell culture transport experiments are influenced by several factors that can be classified in three groups, pre-experimental, experimental and post-experimental factors. The adequate standardization of these factors can help to reduce the inter- and intra-laboratory variability in permeability values. For instance, the variability in permeability estimations complicates the comparison and combination of data from different laboratories and it makes necessary the careful validation of the model and the continuous suitability demonstration.

Among the pre-experimental factors the most relevant are the cell type and source and passage number which could affect the monolayer differentiation, membrane composition, transporter expression and tight junction resistance [36, 37]. In fact, some research works describe differences in cell shape and size, multilayer formation and actin staining between the same cell sources [38]. Several cellular lines have been traditionally used in order to determine the *in vitro* permeability values. Caco-2, MDCK or MDCK-MDR1 cell lines are the most commonly used for this purpose. Caco-2 cells are the most widely used model for estimation of drug intestinal permeability despite its colonic origin [39, 40]. On the other hand MDCK epithelial cells, despite of its non-human and non-intestinal origin, have demonstrated a good correlation with Caco-2 cells results and good predictive performance of human oral fraction absorbed [41, 42]. MDCK-MDR1 cells correspond to the P-gp transfected clone from MDCK and are

used for the study of P-gp substrates [43, 44]. MDCK and MDCK-MDR1 lines with low values of trans-epithelial resistance (TEER) are used also as blood brain barrier model [10, 14, 15]. These three cell lines have been included in this study as the most representative barrier models to compare its intrinsic variability when used with the same protocol. The culture conditions, such as the components of the culture medium or the cell density, the pH or the temperature also affect the final characteristics of the monolayer [45, 46]. Subculture details such as the frequency of culture media renewal affect the expression of several enzymes and the kinetic parameters of the transport substrates [47, 48].

Regarding the passage number, many researchers have demonstrated that changes in TEER, cell growth, mannitol flux and active transport are observed with passage number [49-51]. However, there is no consensus regarding the optimal interval of passages for conducting assays in order to obtain adequate and reproducible permeability values.

The experimental factors can also affect the monolayer absorption and metabolic properties. The literature describe parameters involved in monolayer permeability such as media composition and pH of both chambers, seeding density, system shaking, plastic support material type, solute concentration, temperature, etc. which also affect the barrier properties (integrity, permeability and transporter expression) and the thickness of the unstirred water layer [10, 14, 15, 37-39, 41, 43-54]. Differentiation period after confluence is a crucial parameter in order to obtain reproducible results as the cells suffer important changes in morphology, barrier properties and expression of transporters with time [49-51, 55, 56]. With increasing age, changes in cell height and shape, cell junction formation, TEER values, metabolic

activity, P-gp, MRP2, OATB OCTN2 and PePT1 transporters expression and brush border microvilli were observed [57]. The challenge is to determine the optimum culture period for performing transport assays. Moreover, features such as the sampling schedule (only acceptor chamber or both, number of samples, media replacement), the maintenance or not of sink conditions are determinant of the calculation method and thus influence the permeability estimate obtained.

Among the post experimental factors, the variability associated with the analytical method is an important aspect to take into account as well as the estimation method (and its underlying mathematical assumptions) that it is an aspect often neglected [58].

The objective of this part of the work was the evaluation of the effect of passage number, experimental protocol, maturation time after seeding and calculation method on the permeability values and their associated variability in cell culture transport experiments conducted in our laboratory using three cell lines, Caco-2, MDCK and MDCK-MDR1. The final goal is to select the best experimental conditions for further method validation and to determine the sample size for detecting a given difference in permeability values. Three compound markers of transcellular permeability (Metoprolol), paracellular permeability (Lucifer Yellow) and P-gp functionality (Rhodamine-123) were used to check the performance of the cell lines and their ability to reach pre-established specifications.

NEW *IN VITRO* MODEL DEVELOPMENT.

The main aim of the present work was to develop a new whole *in vitro* high throughput method to predict drug rate and extent of access across the BBB. This new method is presented in Chapter 6. The system permits using apparent permeability values (P_{app}) from *in vitro* cell monolayers experiments in different conditions to estimate $f_{u,\ plasma}$, $V_{u,\ brain}$, and $Kp_{uu,\ brain}$.

In order to explore the feasibility of the *in vitro* system as a screening method for CNS compounds the predicted *in vitro* values have been correlated to *in vivo* $f_{u,\ plasma}$, $Kp_{uu,\ brain,\ human}$, $Kp_{uu,\ CSF}$ and $V_{u,\ brain}$ values obtained by microdialysis by Friden et al. [59] (Table 1). Cell cultures of MDCKII and MDCKII-MDR1 have been used to compare its prediction performance and to determine the transport mechanism for each compound tested.

The BBB parameters obtained with our new method were predictive of the *in vivo* behavior of candidates. *in vitro* $f_{u,\ plasma}$, $Kp_{uu,\ brain}$ and $V_{u,\ brain}$ calculated with P_{app} from MDCKII cell line presented a good correlation with *in vivo* $f_{u,\ plasma}$, $Kp_{uu,\ brain}$ and $V_{u,\ brain}$ published values ($r=0.93$; $r=0.85$ and $r=0.99$ respectively). Despite its simplicity the predictive performance is fairly good considering the reduced number of tested compounds with different physicochemical and transport properties. Further experimental modifications could be checked to optimize the method but the present data support its feasibility. As other *in vitro* cell culture models the system is suitable for miniaturization and robotization to allow high throughput performance.

Aim and Objectives

The overall aim of this work was to develop a new ***Innovative In Vitro Method and Permeability Estimation Procedure to Predict Drug Transport across the Blood-Brain Barrier.*** In order to attain this general goal, specific objectives were considered as detailed below:

- To review the state of the art of the *in vitro* models for Blood Brain Barrier and to identify the relevant parameters that a model should be able to predict to identify CNS drug candidates.

- To review the mathematical estimation methods of permeability values from cell culture experimental data and their underlying assumptions and limitations.

- To propose a new estimation method with a broader applicability in any experimental situation i.e. sink and non-sink and in the presence of initial rate alterations.

- To optimize the experimental conditions for cell culture permeability experiments in order to minimize system variability

and to ensure the consistency of the experimental results in our laboratory.

- To develop a new whole *in vitro* BBB model able to predict all the relevant parameters for CNS access $Kp_{u,u}$, $V_{u,\,brain}$ and $f_{u,\,plasma}$.

- To validate the prediction ability of the new *in vitro* models of $Kp_{uu,\,brain}$, $V_{u,\,brain}$ and $f_{u,\,plasma}$ by comparison with *in vivo* data from model drugs and to compare the prediction performance of the *in vitro* model based on MDCK cells versus the system based on MDCK-MDR1.

Chapter 1

Drug Penetration Across the BBB: An Overview

Mangas-Sanjuan, V.[1,2]; Gonzalez-Alvarez, M.[2]; Gonzalez-Alvarez, I.[2]; Bermejo, M[2].

[1]Pharmaceutics and Pharmaceutical Technology Department. University of Valencia.
[2]Department of Engineering, Pharmaceutics and Pharmaceutical Technology Area. University Miguel Hernández, Elche.

Therapeutic Delivery, 2010
Volume I, Issue 4, Pages 535-62

The brain is one of the most protected organs in the body. There are three barriers that control the access of endogenous substances and xenobiotics (drugs or toxins) to the CNS. These physiological structures are the blood–brain barrier (BBB), the blood–cerebrospinal fluid barrier (BCSFB) and the ependyma (the epithelial layer of cells covering the brain). Figure 1 shows a scheme of the localization and organization of these barriers [1]. The BBB represents the main determinant of the effective delivery of drugs to the CNS [2-4]. The development of new drugs targeted to the CNS require a better knowledge of the factors affecting BBB permeation, as well as predictive tools *in vitro* and *in silico* to optimize the screening at early stages of drug development, and to reduce the attrition rate at later stages. On the other hand, it is important to characterize the alteration of the BBB in pathological conditions.

A good permeability through the BBB is essential if the target site is located in the CNS or, in contrast, can be disadvantageous if the action site is outside the CNS, when the drug could cause adverse reactions at central level. For instance, drug penetration of the BBB is the most challenging issue in brain tumor therapy. In addition, there is a growing demand of new drugs for neurodegenerative conditions such as Alzheimer's, Huntington's and Parkinson's diseases or multiple sclerosis [5].

The physicochemical factors affecting BBB permeability include lipophilicity, polar surface area (PSA), charge state, molecular size, flexibility and hydrogen-bonding potential. Nevertheless, these characteristics mainly affect permeability through the barrier, while the overall access in extent and rate (and, thus, the concentration at the receptor site) is also determined by other factors, such as plasma protein

binding, active uptake into the CNS, efflux out of the CNS and the degree of binding to components of brain tissue [6–9]. In this review, the characteristics of the BBB are described and the *in vitro*, *in situ* and *in vivo* methods to measure BBB transport, as well as the possibilities to enhance the BBB permeability for drugs targeted to treat brain diseases or injuries. The overall aim is to identify the key factors to be considered, when developing new, active and safe CNS drugs in an efficient manner.

GENERAL CHARACTERISTICS OF THE BBB

The structure of the BBB is formed by endothelial cells lining the cerebral microvessels [10] and is characterized by its tight-junctions and lack of fenestrae. The barrier function is determined not only for the inter-endothelial tight junctions but also for the presence of enzymes (such as glutamyl transpeptidase, alkaline phosphatase, esterases and monoamine oxidase, which are either absent or expressed at low levels in peripheral vessels) and the expression of uptake and efflux transport systems. Around the endothelial cells there is a large number of pericytes, perivascular antigen-presenting cells. Covering the vessels there is a sheath of astrocytes and the associated parenchymal basement membrane [11]. All these structures ensure CNS homeostasis and the correct neuronal function, preventing the entrance of many endogenous and pharmacological compounds. A basic scheme of the BBB architecture is provided in Figure 2 [10].

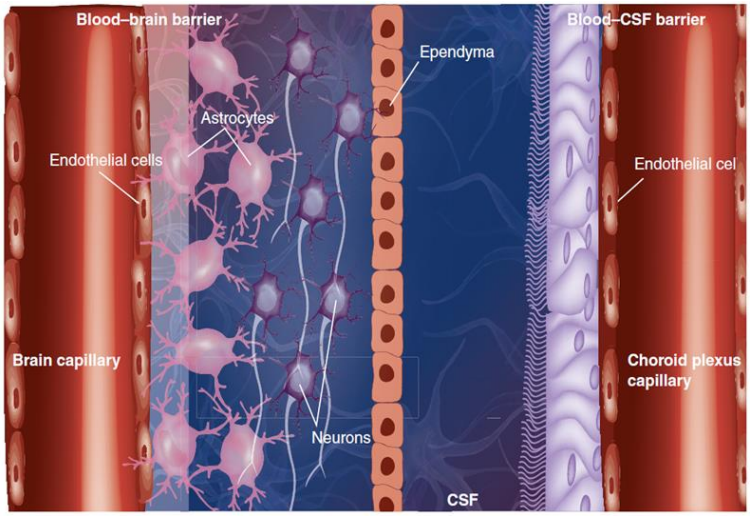

Figure 1. Localization and structure of blood-brain barrier and brain-cerebrospinal fluid barrier. Adapted with permission from [1].

Endothelial cell–cell junctions in the CNS

The effectiveness of the BBB as a restrictive barrier is due to the tight junctions, which provide a high trans-endothelial electrical resistance of 2000Ω·cm^2, compared with 3–30Ω·cm^2 in peripheral vessels. In addition, the BBB endothelial cells have a low vesicular transport capacity and also lack fenestrations. The inter-endothelial tight junctions in CNS microvessels are an intricate complex of transmembrane (claudins, occludin and junctional adhesion molecule [JAM-A] and cytoplasmic zonula occludens [ZO]-1 and [ZO]-2, cingulin, AF-6 and 7H6) proteins linked to the actin cytoskeleton [11-13].

Astrocytes & pericytes

The astrocytic glia endfeet and leptomeningeal cells constitute a covering layer that is connected to the CNS microvessels. It has been

suggested that the ability of CNS endothelial cells to form a barrier is not intrinsic to these cells but induced by the CNS environment [14]. The inducing factors are likely to be low-molecular-weight molecules. Not fully considered is whether the basement membrane itself also contributes to the tightness of the brain endothelial cell monolayer and influences expression and or function of BBB-specific structural (tight junctions) and molecular (transporters and enzymes) characteristics (see upcoming discussion). In addition to astrocytes, epithelial cells from the meninges can be associated with CNS blood vessels. The role of astrocytes in the formation of the BBB is of great interest to scientists and is one of the main aspects considered during the development of *in vitro* BBB models [11]. Pericytes are cells of microvessels including capillaries, venules and arterioles that wrap around the endothelial cells. They are thought to provide structural support and vasodynamic capacity to the microvasculature. Although astrocytes cover 99% of the abluminal surface of the capillary basement membrane in brain, their precise role in the BBB is not well investigated. The *in vitro* models incorporating pericytes and astrocytes show significantly increased transendothelial electrical resistance compared with the models combining only endothelial cells and astrocytes [15,16]. Nakagawa et al. demonstrated that the presence of astrocytes elevated the trans-endothelial electrical resistance (TEER) values by approximately 250% in 5 days compared with the TEER values of endothelial cells alone [17]. The TEER values of the triple co-cultured models were higher than the values of the double co-cultures. The level of TEER increased up to 700% in triple co-cultures compared with endothelial cells. Their exact role in BBB function is still an open question due to the difficulty

in obtaining these cells and the fact that their physiological function seems to be influenced by the tissue environment [11].

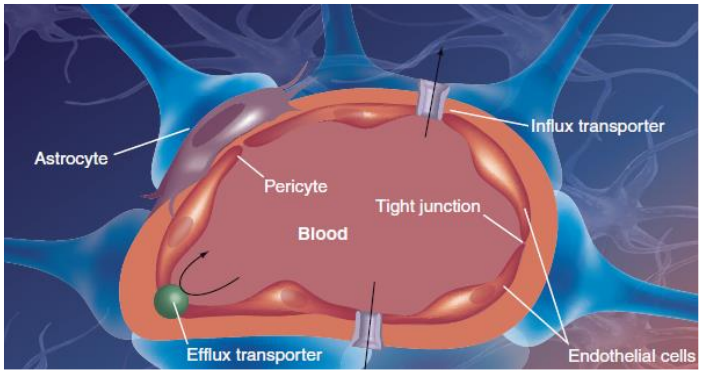

Figure 2. Structure of blood–brain barrier: the endothelial cells of brain micro-vessels lack fenestrations and present tight-junctions that restrict paracellular permeation of solutes. The presence of transporters (at both sides of the endothelial cells) and metabolizing enzymes contribute to the barrier properties. Astrocytes form a sheath covering the vessels and play a role in inducing barrier properties. Pericytes provide structural support and their role in the blood–brain barrier is an open question. Adapted with permission from [10].

Acellular layers: basement membranes

The potential role of the acellular extracellular matrix in the BBB is not well known. CNS inflammation studies highlighted the contribution of vascular basement membranes to leukocyte extravasation processes and, hence, barrier functions at the level of postcapillary venules. Although data on the basement membrane composition of CNS vessels exist, the data is fragmentary and lacks specificity both with regards to vessel type and specific extracellular matrix isoforms [18–22]. Nevertheless, existing data suggest that biochemical variations are present between endothelial and parenchymal basement membranes and that basement membrane components contribute to microvessel integrity and function [11].

Extracellular matrix receptors

It is known that endothelial cells and astrocytes express several integrins and dystroglycan (a major non-integrin receptor) [20,23]. Microglia express some integrins also. There is evidence for the role of these receptors in the maintenance of BBB integrity [24-26].

BBB PERMEATION

Transport processes in the CNS

There are two controlled pathways for molecules to cross the BBB, namely paracellular (junctional) and trans-endothelial routes. In Figure 3 the most important and currently known permeation routes to access the brain are depicted.

Due to the restrictive paracellular pathway (regulated by inter-endothelial tight junctions) the transport of hydrophilic and low-molecular-weight compounds for this route is limited. The trans-endothelial pathway is also restricted to hydrophilic substances due to the lipophilic nature of the membrane and a lower rate of pinocytosis than in the peripheral endothelium. Passive diffusion depends mainly on the lipophilicity and molecular weight. The alternative route for molecules that cannot cross the barrier via passive diffusion is to enter the CNS by interaction with endogenous transport systems located within the brain capillary endothelium or the neuroepithelial cells of the choroid plexus. The transport mechanisms are classified into three groups [27]:

- Carrier-mediated transport (CMT), is responsible for the transport of low-molecular-weight (less than 600Da) compounds into the CNS. There are active and facilitated

diffusion carriers [28]. Many nutrients such as glucose, amino acids and purine bases use some CMT systems to enter into the brain. At least eight different nutrient transport systems have been identified. These systems are substrate selective but could be used by drugs that closely mimic the endogenous carrier substrates;

- Receptor-mediated transport (RMT), allows the entrance to relatively large compounds (peptide and proteins) via an endocytotic process. Classical examples of receptors involved in receptor-mediated transcytosis are the insulin receptor, transferrin receptor and transporters for low density lipoprotein, leptin and insulin-like growth factors. These systems are studied for targeted delivery of drugs with high molecular weight to the brain [28];
- Active efflux transport (AET), is responsible for the active secretion of multiple drugs from the CNS into the bloodstream. As a consequence, AET substrates cannot effectively penetrate the brain. The best known AET system is P-glycoprotein (P-gp), which limits the transport of a wide range of cationic and lipophilic compounds such as cytotoxic anticancer drugs, antibiotics, hormones and HIV protease inhibitors, into the brain [29,30]. Other active efflux transporters identified at the BBB are the MRP proteins [31–34]. The development of co-drugs in order to inhibit the AET systems can be a strategy for increasing brain penetration of drugs [5]. The term 'co-drug' refers to two or more therapeutic compounds active against the same disease and bonded via a covalent chemical linkage. In

Table 1 a summary of some of the transporters identified in the brain endothelial cells is shown [35,36].

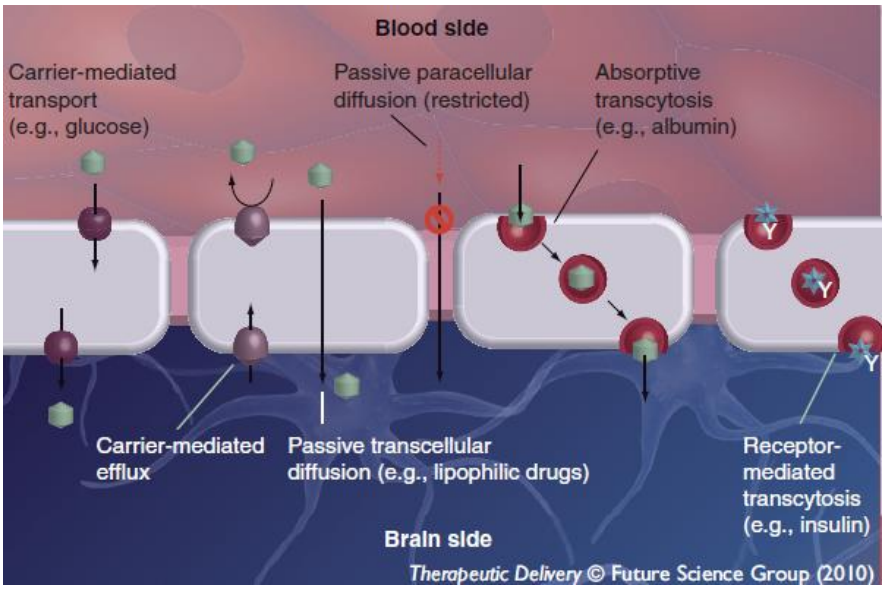

Figure 3. Permeation mechanisms through the endothelial cells. Paracellular diffusion is restricted. Transcellular route includes passive diffusion, carrier-mediated transport or endocytosis. The presence of efflux transporters contributes to limiting the access of xenobiotics to the CNS.

Factors involved in drug permeation through BBB & distribution into the brain

If the CNS is considered as a separate pharmacokinetic compartment, the concentration of compounds in the brain and its evolution with time (i.e., the rate and extent of drug access to the brain) will depend on several factors, as follows:

- The plasma concentration, defined by the drug absorption, distribution, metabolism and excretion characteristics;
- The degree of plasma–protein binding as only the unbound fraction diffuses across the barrier;

- The effective permeability across the BBB, which depends on the combination of the passive permeability and the contribution of efflux and influx CMT;
- The metabolic modification by barrier enzymes and the 'sink effect' of the continual drainage of cerebrospinal fluid (CSF);
- The nonspecific binding to brain tissue [37,38]. On the other hand the relevant pharmacological information is the unbound drug concentration in the interstitial fluid (ISF) if the drug receptor is outside the cells or the intracellular concentrations (ICF) if the target is inside the cells.

As can be deduced from the BBB structure, the permeability of the molecules is based on a number of physicochemical factors, which the most relevant are lipophilicity and PSA [6,39]. Lipophilicity is the main factor for the transcellular passage of drugs through biological membranes. Nevertheless, the correlations between lipophilicity and BBB permeability are far from perfect, and lipophilicity alone is not always predictive of permeability [38]. It is neither easy nor straightforward to identify what parameters should be used to define 'good brain penetration'.

Two parameters, the ratio of brain and plasma concentrations at steady state denoted as Kp, and its logarithm (log BB), and BBB permeability, quantified as the permeability surface area product (PS), have been used to describe brain penetration. The first one is indicative of extent, while the second represents the rate of access. Kp is the most commonly used parameter in literature to evaluate brain penetration. However, this parameter represents the drug partitioning into the brain and not necessarily indicative of the drug unbound concentrations in

the ISF or the drug concentrations in the intracellular fluid in the brain (ICF). The relevant parameter to be measured is the ratio of the unbound concentration in brain over the unbound concentration in plasma $Kp_{,uu}$ [8]. In order to obtain $Kp_{,uu}$ values from Kp and fraction unbound in plasma, it is necessary another parameter $V_{u,\ brain}$ according to Equation 1 [7,8].

Table 1. Active (ATP-binding cassette family) and facilitated diffusion (solute-carrier family) transporters that have been identified at the blood–brain barrier level[†].

Family gene name	Old name	Substrates
Nutrients		
SLC2A(x)	GLUT(x)1	d-glucose
SLC16	MCT1	l-lactate
SLC6A20	SIT	Na^+-imino acid
SLC6A8	CRT	Creatine
SLC7A5	LAT1	Large neutral amino acids
SLC15A2	PEPT2	Oligopeptides
SLC15A3	PHT2	Oligopeptides
SLC27A5	FATP5	Long-chain fatty acids
SLC19A1	FOLT	Folates
SLC19A2	THTR1	Thiamines
SLC23A1	SVCT1	l-ascorbic acid
SLC23A2	SVCT2	l-ascorbic acid
SLC7A1	CAT1	Cationic amino acids
SLC38A2	ATA2	Small neutral amino acids
SLC6A6	TAUT	Taurine
SLC1A5	ASCT2	l-Ala and others
SLC16A2	SYSTEM T	Thyroid hormones
Neurotransmitters		
SLC6A13	GAT2/BGT1	GABA
SLC6A4	5HTT	Serotonin
SLC29	ENT	Norepinephrine
Endogenous substrates and xenobiotics		
SLC14A1	HST1341	Urea
SLCO1A4	OATP1A4	Cation or anion
SLCO1A6	OATP1A6	Cation or anion
SLC22A3	OCT3	Monoamine
SLC22A7	OAT2	Organic anion
SLC22A8	OAT3	Organic anion
SLC30A1	ZRC1	Zinc
SLCO1A2	OATP1A2	Ostreone-3-sulfate, methotrexate, digoxin, statins and levofloxacin
SLCO1C1	OATP1C1	Thyroid hormones
SLC22A8	OAT3	Polycyclic aromatic hydrocarbons, HVA, indoxyl sulfate, nonsteroidal anti-inflammatory drugs, ostreone-3-sulphate, cefaclor,

			ceftizoxime, bumetanide and furosemide
SLCO1B1	OATP2		Digoxin and organic anions
SLC22A5	OCTN2		Carnitine
SLC28	CNT2		Nucleosides
ABCB1	MDR1		Vincristine, cyclosporin A, digoxin, loperamide, doxorubicin, vinblastine, docetaxel, paclitaxel, irinotecan and morphine
ABCC1	MRP1		Leukotriene C_4 and others
ABCC4	MRP4		Topotecan, methotrexate, furosemide, cyclic AMP and cyclic GMP
ABCC5		MRP5	
ABCG2	BCRP		Mitoxantrone, topotecan, irinotecan, methotrexate, anthracyclines, flavopiridol, quinazolines and imatinib

Data from [35,36]. ABC: ATP-binding cassette family; HVA: Homovanillic acid; SLC: Solute carrier family.

$$Kp_{,uu} = \frac{Cu_{brain\ ISF}}{Cu_{plasma}} = \frac{A_{brain}/Vu_{brain}}{Cp \cdot fu} = \frac{Kp}{fu \cdot Vu_{brain}} \qquad \text{Eq. 1}$$

Where $V_{u,\,brain}$ represents an apparent volume of distribution or, in other words, the relationship between the amount of drug in the brain and the unbound drug concentration (its interpretation is analogous to V_{ss} in pharmacokinetics not being a real aqueous volume, but the ratio between drug amount in the body and steady state drug concentration in plasma). If this value is much higher than the combination of ISF and ICF volumes (~ 0.8 ml/g brain) it indicates that the drug nonspecifically binds to the brain tissue.

Considering the rate of access, the time to reach brain equilibrium, defined as the half-life, allows one to evaluate how quickly a compound can enter the brain. In general, however, rate of access is assessed through the measurement f PS product [40]. The best index of BBB permeability is the BBB PS product, which has units of microliter per min per gram and is a measure of unidirectional clearance from

blood to brain across the BBB. The BBB PS product drug is determined by the total drug concentration in plasma and the unbound fraction in plasma that is available for transport into the brain. Nevertheless, the PS product per se cannot predict the unbound concentrations in brain [41,42]. On the other hand, unidirectional permeability per se is less relevant than the efflux ratio (defined as the ratio between permeability from basal to apical chamber (P_{ba}) to permeability from apical to basolateral chamber (P_{ab}) permeability in an *in vitro* cell model or as the ratio of the brain uptake clearance in the P-gp-deficient mice over the rain uptake clearance in P-gp-competent mice [43]), as this ratio reflects the potential limitation of brain penetration due to efflux processes. Another factor to take into account is that the efflux ratio depends on the drug concentration, and in bidirectional studies in cell culture experiments P_{ba} to P_{ab} ratio becomes one once the efflux transporter is saturated and its contribution is negligible [44]. Delineating the components of transport, that is, the passive diffusional permeability and the V_{MAX} and K_M parameters, is essential as a high passive permeability could overcome the P-gp efflux at physiological concentrations [45].

METHODS TO MEASURE DRUG TRANSPORT INTO THE BRAIN

There is a wide range of technologies to characterize the mechanisms of brain penetration and to evaluate the rate and extent of CNS access. As the complexity of the model is increased, the cost is higher and the throughput decreases. Therefore, methods should be selected with care by having in mind the main objective of the analysis, such as screening or lead optimization [7,8,34,46–48]. The recent

developments of combinatorial chemistry call for systems that can be used for high-throughput screening. Costly and labor-intensive *in vivo* measurements and traditional low-throughput *in vivo* assays of CNS pharmacokinetic properties are not adequate for this purpose. For this reason, there has been an increasing interest in *in silico* and high-throughput *in vitro* methods for predicting *in vivo* properties early in the drug discovery process. A single *in vitro* method cannot describe or predict the *in vivo* properties of a new drug as it is necessary to integrate information about rate, extent and distribution in the brain. The consequence of this new concept, is that it is necessary to understand the meaning of the read-out of each *in silico*, *in vitro* or *in vivo* method, and integrate these data with the adequate interpretation of the results [6,7,46,47].

In silico methods

In silico models of drug brain penetration attempt to predict BBB permeability and brain distribution on the basis of physicochemical parameters such as hydrogen bonding, lipid solubility and molecular weight. Most *in silico* models have been based on *in vivo* log BB values [15,49,50]. In the past, *in silico* models were only qualitative and classify the compounds as CNS(+) (penetrates into the brain) or CNS(-) (does not penetrate into the brain). This classification was based on whether a compound showed *in vivo* CNS efficacy or had a Kp value above certain level [51].

In general, Lipinski's rule of five as well as Abraham's equation can be used to predict the passive transport of a drug molecule across the BBB [52]. Other sets of rules that have been proposed to predict

BBB permeation are the rules of Norinder and Haeberlein [53] and Clark [49] (box 1).

As mentioned previously, BB is the brain to blood ratio at some defined time: it is a measure of the extent of drug overall brain access or its partitioning into the brain but not necessarily indicative of the pharmacological active concentrations. The significant pharmacological value is Kp free (defined as the steady-state unbound brain to plasma ratio) [7,8] and the most recent structure–brain exposure relationships are focused on predicting this value (Table 2) [6].

Regarding *in silico* models for BBB permeability, the availability of logPS data has limited the development and validation of models also complicated by the lack of detailed knowledge on the structure activity relationship of transporter proteins and enzymes, but this situation has changed with the appearance of hybrid (*in vitro*/*in silico*) models capable of predicting both passive and transport-mediated function and software tools for screening drugs of chemical features likely to make them P-gp substrates [54–56]. The log PS models may be used in conjunction with *in vivo* log PS data to explore the presence of efflux or uptake transporter mechanisms. For example, the PS values of uptake transporter substrates phenylalanine and levodopa were underpredicted, and the PS values of P-gp substrates, digoxin, CP-141938 and quinidine were overpredicted [57]. It would be desirable to extend the current *in silico* models to include predictions about other transporters at the BBB [10].

Box 1. Rules proposed to predict blood–brain barrier permeation.

Norinder & Haeberlein†.
Rule 1: if the sum of Ns and Os atoms is five or less in a molecule, it has a high chance of entering the brain
Rule 2: if log P - (Ns + Os) is greater than 0, then logBB is positive
Clark‡, rules for good brain access:
The sum of Ns and Os atoms should be 5 or less
C log P – (Ns + Os) should be greater than 0
Polar surface area should be less than 60–90 Å2
Molecular weight should be less than 450 Da
log D in the range of 1–3 is recommended

†*Data from* [53]. ‡*Data from* [49].

Table 2. Summary of *in silico* models and physicochemical parameters used to predict brain penetration.

Parameter predicted	**Predictor variables**	**Refs.**
Log BB	D Log P = log $P_{octanol}$-log $P_{cyclohexane}$	[58]
Log BB	V_m; PSA	[59]
Log BB	MW; Log $P_{cyclohexane}$	[60]
Log BB	PSA; C log P	[61]
Log BB	(N + O); Log $P_{octanol}$	[53]
Log BB	Log BB= log (C_{brain}/C_{blood})	[62]
Log BB	Molar excess refraction; dipolarity/polarizability; hydrogen bond acidity, hydrogen bond basicity and characteristic volumen of McGowan	[63]
Log BB	Hydrogen bonds accepting oxygen; nitrogen atoms and the number of hydrogen atoms bonded to these	[64]
Log BB	Net charge at pH 7.4; lipophilicity; PSA and size (reflected by the total number of aromatic and aliphatic ring systems (Nb[rings])	[65]
Log BB	Number of hydrogen-bond donors, acceptors, rotatable bonds, hydrophobes, log P, molecular weight, PSA Topological índices (randic, electrotopological, atomistic, and functional group). Based on eigenvalues of modified adjacency matrices (CIMI) and atomic charges binned into fingerprints	[66]
Log BB	Quantum chemical descriptors; topological índices; chemical descriptors	[67]

Log BB	Molecular polarizability; the maximum positive charge; the sum of all positive partial atomic charges for all atoms in the molecule; the sum of H-bond factor values for all acceptor substructures in the molecule; the sum of H-bond factor values for all donor atoms in a molecule; the maximum H-bond acceptor descriptor in a molecule	[68]
Kp,uu	PSA Hydrogen-bonding acceptor groups	[6]
Log PS	Molar excess refraction; dipolarity/polarizability; hydrogen bond acidity, hydrogen bond basicity and characteristic volumen of McGowan	[52]
Log PS	VSA_{base}; Log D; TPSA	[57]

CIMI: Chemically intuitive molecular index; PSA: Polar surface area; TPSA: Topological polar surface area; VSA: van der Waals surface area.

In Table 2 a summary of some *in silico* models to predict brain penetration are shown [58–68]. As evident, the predicted variables used to be log BB or log PS, while the most used predictor variables were lipophilicity, MW and polar surface area. On the other hand, if the most relevant pharmacological parameter $Kp_{,uu}$ is considered, the most significant molecular descriptors are those related with hydrogen bonding as PSA and hydrogen bonding acceptor groups [6].

In general, development of software for predicting BBB permeation is particularly useful for compound prioritization and may be applied in different phases of the drug discovery process, from compounds to be synthesized to those to be assayed. Nevertheless, the effort to develop *in silico* methods should be based on a holistic concept of CNS access including rate (permeability or PS) and extent (Kp free) as well as intrabrain distribution ($V_{u,\ brain}$) in order to construct meaningful predictions of the pharmacologically active concentrations [46].

In vitro methods

Research on drug transport across the BBB changed considerably with the availability of *in vitro* BBB systems. The advantages associated with any *in vitro* BBB model include lower compound requirement, the use of physiological buffers; greater throughput relative to *in vivo* models; ability to assess transport mechanisms; identification of early signs of cell toxicity and, generally, lower cost [69]. Moreover, these systems allow a detailed investigation without interferences from the rest of the body. However, in order to appropriately mimic the BBB *in vivo* there are some basic characteristics that an *in vitro* model must possess, as summarized in Figure 4 [10,70]. The *in vitro* model that is chosen should possess as many of these characteristics as possible, while at the same time remaining practical and feasible for moderate- to high-throughput screening [10].

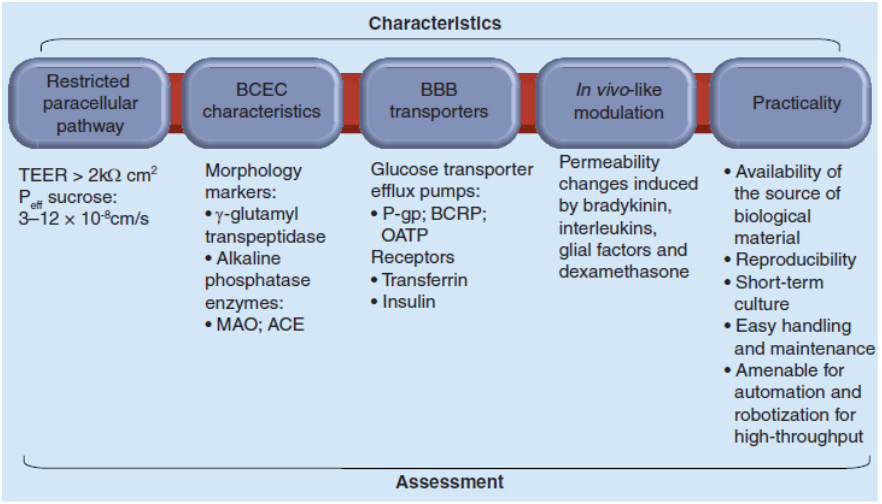

Figure 4. Characteristics of an ideal in vitro blood–brain barrier model. ACE: Angiotensin-converting enzyme; BBB: Blood–brain barrier; BCEC: Brain capillary endothelial cells; BCRP: Breast cancer resistance protein; MAO: Monoamine oxidase; OATP: Organic anion transporter protein; P-gp: P-glycoprotein; Peff: Effective permeability TEER: Trans-endothelial electrical resistance. Adapted with permission from [10].

Physicochemical methods for BBB

Immobilized artificial membrane chromatography

The immobilized artificial membrane (IAM) stationary phase consists of a monolayer of phosphatidylcoline covalently bound to an inert silica support. The resulting IAM surface is a chemically stable chromatographic material that simulates the lipid phase of a biological cell membrane and thereby affects the retention of compounds on the basis of solute-IAM partitioning [71]. This model has been designed as an alternative for estimate drug permeability through cell membranes [10,72]. The greater the retention time, the greater the membrane permeability for the drug candidate. In one study, the uptake of 26 drugs into the brain (basic, neutral and acidic) appeared to correlate weakly to the immobilized artificial membrane retention factors, although an improvement in regression was observed when the effects of ionization and solute size were taken into account [10]. The method has poor predictive power when brain uptake is affected by plasma protein-binding active transport, efflux or metabolism. The main application of this method is the screening of multiple compounds in drug-discovery projects.

Parallel artificial permeability assay

This technology was successfully introduced to the pharmaceutical industry to allow useful predictions of passive oral absorption. Over the last 5 years researchers have modified the lipid composition of the artificial membrane to evaluate passive BBB permeability [73,74]. Parallel artificial permeability assay (PAMPA) model identified compounds that pass the BBB (CNS+) and those that poorly penetrate the BBB (CNS-). PAMPA method only shows a

relationship with passive diffusion permeability, that is, it does not offer information about active transport processes. PAMPA may, therefore be used as an early screen for passive BBB permeation [75–77]. Other methods that provide information on relevant active transporters can be used as an additional screen to improve the PAMPA results [78,79].

Lipophilicity measurements

Lipophilicity is a parameter that affects BBB permeation and brain distribution. Lipophilic molecules have better access to the brain than hydrophilic molecules, thanks to higher membrane permeability and nonspecific binding to proteins and lipids in brain tissue. Any lipophilicity measure as n-Octanol partition coefficient could be used for initial screening of passive permeability (as it is reflected in the rules of Norinder, Haeberlein and Clark [80,81]). From the current experimental data available it could be possible to establish the lipophilicity cut off to ensure a passive permeability above 150 nm/s [45], without forgetting that a poor passive permeability could be compensated by other properties of the compound and that it does not imply necessarily poor brain penetration due to the fact that it occurs in the gastrointestinal system, there is no limit in the transit time [6,46].

Cell-based *in vitro* methods

Primary or low passage brain capillary endothelial cell cultures

Preparation of the *in vitro* BBB from primary isolated cells involves the isolation of capillaries and culture of endothelial cells alone or in combination with astrocytes or astrocyte-conditioned medium. Although human cells would be most ideal from a scientific point of view, there are ethical and tissue access constraints. The most common animal endothelial cells are bovine or porcine due to their availability. The isolation procedures that have been used most frequently can be

classified into nonenzymatic mechanical, combined mechanical-enzymatic or enzymatic procedures [28,82]. The principal advantage is that these cells represent the closest phenotypic resemblance to the *in vivo* BBB phenotype [69]. Unfortunately, passing primary cultured cells will eventually lead to a loss of BBB properties as some features, such as BBB transporters and enzymes, can be downregulated when the endothelial cells are removed from the brain and grown in culture [10,83]. Nevertheless, the advantages of cultured endothelium include the potential for using pure cell populations as well as their relative viability compared with isolated arterioles ex situ [84].

Although primary cultures of brain endothelium alone may form tight intercellular junctions, co-culture with astrocytes [85–87] resulted in the increased formation and complexity of endothelial tight junctions and induced the expression of specific BBB markers including GGTP, the glucose transporter isotype (GLUT-1), mouse antibody against human and rat transferrin receptor (OX-26) and P-gp [84]. Astrocytes can also be grown on the bottom of the culture well plate (no contact). Figure 5 illustrates both situations.

Astrocytes isolated from newborn rats together with bovine or porcine endothelial cells are used as xenogenic co-culture systems, which are very useful in studying drug transport and BBB functionality.

Other cells that can be included in the co-cultures are pericytes and fibroblasts, neurons, microglia and monocytes in order to obtain an optimal model. Pericytes are of special relevance because they are normally present at the BBB surrounded by the basement membrane and are responsible for inducing specific enzymes. So, it has been argued that pericytes are necessary to establish a cell culture model [88].

The major disadvantages associated with these *in vitro* systems are the time and resources required to isolate, seed and incubate the primary cells and the astrocytes. Furthermore, the intra- and inter-batch reproducibility of the primary or low passage brain capillary endothelial cells (BCECs) regarding phenotypic and permeability properties is another important disadvantage [60].

Accepted criteria for monitoring the quality of monolayers in transport studies include TEER and permeability to hydrophilic markers such as 14C-sucrose, which reflect the degree of tight junction formation. Using these criteria, none of the primary endothelial cell culture models yet matched the *in vivo* conditions (TEER in the range >2 $k{\cdot}\Omega{\cdot}cm^2$ ≤ 8 $k{\cdot}\Omega{\cdot}cm^2$ [89] and sucrose permeability of approximately $0.3{\cdot}10^{-7} cm{\cdot}s^{-1}$) [90].

Immortalized brain endothelial cells

To overcome the disadvantages of primary culture systems, various immortalized brain capillary endothelial cell lines have been derived but none of them generate complete tight junctions, resulting in 'leaky' barriers [70]. Therefore, these cell lines are not recommended for BBB permeability screening [91] but are more suited to assessing endothelial cell uptake of compounds and have proved to be useful in mechanistic and biochemical studies [60,92,93]. For this reason, developing immortalized cell lines that preserve a stable BBB phenotype is of great interest and still an area of active research. The advantage of immortalized cell lines is their ease of culture, their purity and the fact that there is no need for a periodic isolation of capillaries from brains. This has resulted in the generation of a number of immortalized, transformed, transfected and transduced cell lines. Some of the cell lines that have been generated by transfection of primary rat endothelial cells

include the RBE4 cell line [29], RBEC1 cell line [94] and TR-BBB13 cell line [95]. A recent review listed 18 brain-derived endothelial cell lines [70]. Some strategies can be used to enhance their barriers properties as the inclusion of phosphodiesterase inhibitors, glucocorticoids and interferon-a, b, which increase the tightness of these monolayers [96–99]. In addition, a human brain immortalized endothelial cell line was established by transfection of the human telomerase or SV40 T antigen. This cell line (hCMEC/D3) represents a stable, well characterized and cell differentiated human brain endothelial cell line [100].

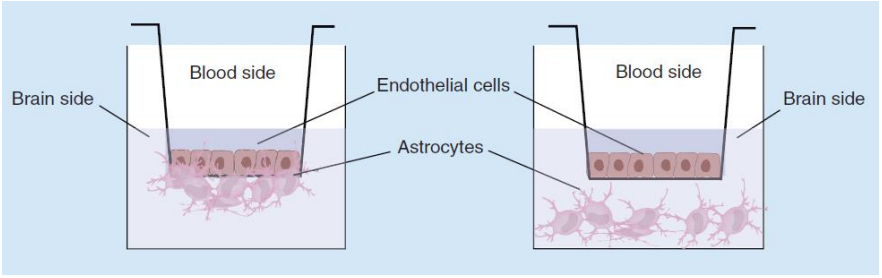

Figure 5. Structure of co-cultures of endothelial cells and astrocytes.

Tridimensional hollow-fiber BBB model

Since monolayer methods ignore the presence of intraluminal blood cells, and blood flow lack the presence of shear stress, few research groups have reported on the use of flow-based hollow-fiber models [101]. In the hollow-fiber apparatus, the endothelial cells are seeded intraluminally and are exposed to flow conditions, whereas glia cells are cultured on the extraluminal surface of the hollow-fiber tube. The hollow-fiber *in vitro* models represent an innovative development in *in vitro* BBB models with increased BBB properties [102–104].

Cells of non-cerebral origin

Due to the difficulties associated with studying BBB transport using brain endothelial cell lines, several methods based on the use of noncerebral peripheral epithelial cell lines have been proposed to study the permeability of pharmacological compounds. Interestingly, even non-brain endothelial cells (EC) such as bovine aortic EC can be induced by glia to form complex tight junctions and express a barrier phenotype [84]. A well-characterized cell line is the Madin-Darby Canine Kidney (MDCK) cell line, which is easy to grow, achieves a reproducible TEER value and can be transfected with the MDR1 gene, resulting in the polarized expression of P-gp [10]. This transfected cell line has been used as a model of BBB barrier to assess the effect of P-gp on the permeability of various compounds [105,106] and a recent collaborative study found that MDR1-transfected MDCK cells were the most representative of *in vivo* BBB permeability compared with other *in vitro* models, including brain capillary endothelial cells/astrocytes, human brain endothelial cells/astrocytes and Caco-2 cell lines (human colon adenoma derived cell line) [15,107]. MDR1- transfected MDCK cells have also shown high absorptive transport for CNS(+) drugs and low absorptive transport for CNS(-) drugs [107] and, consequently, may be a suitable model for BBB permeation. One important characteristic is that this cell line has sufficient restrictive paracellular transport, although the MDCK epithelial cells differ from brain endothelial cells in factors including growth, metabolism and transport properties, and also morphologically. The BCEC is squamous with a large surface area and so there is a lower cell density per unit surface area of endothelium (<1000 cells mm^{-2}), whereas the kidney cell is cuboidal in shape, resulting in a smaller surface area, and a consequent greater cell density per unit area of membrane (>10,000 cells mm^{-2}) [108]. Therefore,

MDCK cells produce a relatively higher transverse area of intercellular junctions (compared with brain endothelial cells) and paracellular transport could be overestimated with this cell line. In addition, while P-gp is one of the most important efflux transporters at the BBB and transfection of MDCK cells with the MDR1 gene compensates for this, there are also other efflux proteins, such as breast cancer resistance protein [109] and organic anion transporting polypeptide [110], present in brain capillary endothelial cells, that may also play a role in overall CNS penetration. If using the MDR1- transfected MDCK cell line, it is important not to rule out the potential effects of these other efflux transporters present in the *in vivo* BBB [111]. Another kind of endothelial cell, LLC-PK1 (Lewis Lung porcine kidney cells), is characterized by the expression of endogenous drug transporters. This cell line has also been used to examine the possible role of P-gp as a determinant of brain penetration in co-cultures with astrocytes [112].

Other noncerebral epithelial cell lines, such as Caco-2 cells, have also been employed to determine the drug permeability in the BBB. Caco-2 was developed as a permeation model for gastrointestinal absorption and some companies have extended its use to screening BBB permeability. Caco-2 incorporates lipid bilayer membranes, P-gp efflux and some other transporters. However, they present some disadvantages, as with MDCK cells, such as different morphological characteristics, lower tight-junction resistance and different lipid composition resulting in significant differences with co-cultures of endothelial cells and astrocytes [69]. In addition, ECV304 cell line, which is a bladder carcinoma cell with epithelial and endothelial properties, has been proposed as a model for the BBB [108]. This cell line has been co-cultured with C6 glioma cells or in C6-conditioned

media; however, although it demonstrated many of the key features of the BBB, it was found to have low TEER values (indicative of poor paracellular restrictive properties) and a lack of P-gp expression [113,114]. The basal TEER of this cell line monolayer could be enhanced by human 1321N1 astrocytes and primary rat astrocytes [98]. On the other hand, stem cells are potential barrier precursors. Human umbilical vein endothelial cells (HUVECs) were transplanted in athymic mouse brain and neovascularization of grafted endothelial cells was studied. Results indicate that endothelial cells from an ectopic origin have the potential to form a BBB after grafting in the CNS [115]. An associated problem of the use of *in vitro* cell cultures is the variability. BBB culture systems has been the subject of a concerted action funded by the European Commission entitled 'Drug transport across the BBB: new experimental strategies' involving 21 research groups from nine European countries [82]. The focus of this action was on the optimization, harmonization and validation of cell cultures and to develop and study new strategies for drug transport to the brain. In the same line of research, several academic researchers working on BBB formed the International Brain Barriers Society in the summer of 2006 [302]. Their aim is to encourage scientific and clinical research on the biological barriers in the CNS. This demonstrates the scientific community's awareness about the need for more efforts to develop effective CNS therapies. Another EU-funded project (oriented towards the validation of intestinal cell models) 'Memtrans' used an approach that could be extrapolated to other barriers than the BBB. The objective of the Memtrans project was to characterize the cell systems in different laboratories using markers of the critical model variables as the paracellular permeability, transcellular one and transporters expression

levels. The next step would be using these markers as weighting factors to translate (or to convert) permeability values of one laboratory to another allowing to the combination of data from different sources or even different cell models [116,117]. This last point would be of particular impact in the QSAR model development where one of the main limitations is the size of the databases.

New *in vitro* methods

Equilibrium dialysis with brain homogenates

A standard equilibrium dialysis assay, described by Maurer et al., is used to measure the transport of the test compound through two chambers separated by a dialysis membrane. The compound is dialyzed between plasma and buffer, then between brain homogenate and buffer. From this, the free drug in brain ($f_{u,\ brain}$) and free drug in plasma ($f_{u,\ plasma}$) are calculated. This is an inexpensive method that is easy to perform [118,119].

Binding studies in brain slices

Becker and Liu [120] and Friden [6] have proposed a new method to estimate free fraction in brain ($f_{u\ ,brain}$) in which they used brain slices instead of brain homogenate. This modification of the technique retains the cellular structure of the brain and, in consequence, any differences between ISF and ICF can be captured in the obtained $f_{u,\ brain}$ values. Table 3 summarized all the above *in vitro* methods: PAMPA-BBB [73,75–77,121,122], immobilized artificial membrane [121,122], lipophilicity measurement-partition methods [80,81], equilibrium dialysis [118,119], isolated brain capillaries [97,23–128], primary isolated cells [90,97,124–126, 129–138], immortalized endothelial cell lines [91,102–104,139,140], tridimensional hollow-fiber

BBB model [101–104], non-brain endothelial cell lines [74,106–107,112–115,141–145] and brain slices [6,120].

Table 3. Main *in vitro* methods for permeability predictions.

Method	Use advantages	Ref.
PAMPA-BBB	Prediction of passive permeability High-throughput	[73,75–77,121,122]
Immobilized artificial membrane	Prediction of passive permeability Chromatographic method	[121,122]
Lipophilicity measurement–partition methods	Correlation with passive permeability	[80,81]
Equilibrium dialysis	Provides insights on brain distribution, Kp,uu	[118,119]
Isolated brain capillaries	Morphologic and biochemical studies	[97,123–128]
Primary isolated cells		
BCEC		
Bovine	Morphologic and transport studies	[129–136]
Porcine	Transport studies	[137,138]
Co-culture BCEC-astrocytes		
Transport studies		[90,97,124–126]
Immortalized endothelial cell lines		
RBE4	Mechanistic and biochemical studies	[91,102–104, 139,140]
Tridimensional hollow-fiber BBB model	Paracellular transport	[101–104]
Nonbrain endothelial cell lines		
Caco-2	P-gp efflux assay	[141]
MDCK	Passive BBB permeability predictions	[74,106,107,142]
MDCK-MDR1	Passive and efflux transport	[74,107]
ECV304/C6	Permeability across the BBB (limited)	[113,114,143–145]
LLC-PK1	Passive and efflux transport	[112]
Stem cells	Passive BBB permeability predictions Transplant to mice brain	[115]
Brain slices	Determination of the free fraction (fu, plasma, fu, brain)	[6,120]

BBB: Blood–brain barrier; BCEC: Brain capillary endothelial cells; P-gp: P-glycoprotein; PAMPA: Parallel artificial permeability assay.

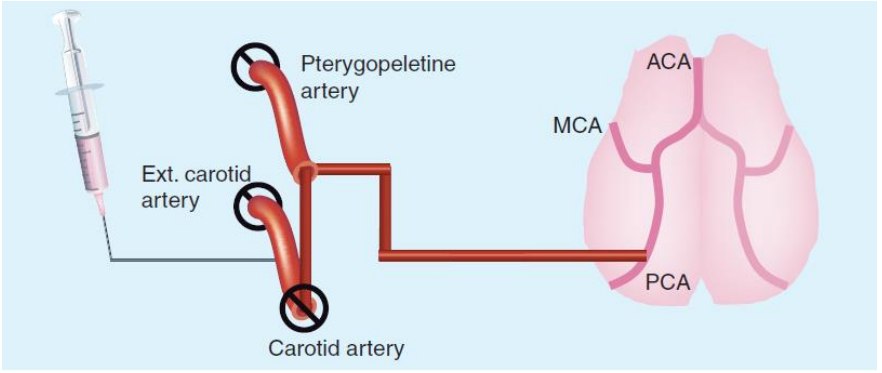

Figure 6. The procedure of brain perfusion. ACA: Anterior cerebral artery; MCA: Middle cerebral artery; PCA: Posterior cerebral artery. Adapted with permission from [10].

In situ methods

In situ perfusion technique

The *in situ* perfusion method provides high quality BBB permeability data [146]. The procedure is shown in Figure 6 [10]. A catheter is placed in the common carotid artery of an anesthetized animal while closing the external carotid. In this way the blood flow is stopped and the pump is switched in line. The perfusate, which contains the reference (radiolabeled substance) and test compounds provide the fluid flow to the brain. Following the perfusion (conducted over a short time), the animal is decapitated and the compound concentration is determined in order to calculate a BBB PS product [5]. The particular advantage of the *in situ* perfusion technique is that there is no systemic exposure of the compound, and thus metabolism is avoided, except for that which occurs within the brain microcirculation [147]. The other major advantage is that there is total control over the perfusate solute concentration, and other constituents of the perfusion fluid can be varied, allowing ready characterization of saturable transport systems, plasma protein binding and the effects of regulatory modifiers,

hormones and neurotransmitters that can be presented to the brain at defined concentrations [148]. In addition, the effects of pH, ionic content and flow rate can be monitored [149]. Moreover, the short time periods allow minimization of nonspecific binding. Co-administration of transporter inhibitor or application of techniques to transgenic animals that lack a transporter allows the study of the extent of transporter contribution to the penetration of a particular compound [146,150]. The major disadvantages are the number of animals, the significant analytical time and the level of experimental difficulty [148]. This makes the technique unsuitable for high-throughput screening, however it can be used to provide mechanistic data and information on factors that may be limiting brain uptake. Another disadvantage of this technique is that prolonged perfusion times (>20 min) are impossible owing to cerebral hypoxemia [90].

In vivo methods

As mentioned previously, although the *in vitro* systems have evolved into sophisticated and functional models of the BBB, they may result in quantitative and qualitative differences in BBB transport due to up or downregulation of transporters and species differences. Therefore, *in vitro* data alone cannot be used to select drug candidates. For example, it has been observed that the permeability can differ by more than 100-fold among compounds that can penetrate the brain [57]. No clear association was observed between the permeability and efflux transport in a recent study [9]. Rather, it is necessary to correlate observations made using an *in vitro* BBB model to *in vivo* studies [27]. *In vivo* brain experiments provide the most reliable reference information for testing and validating other models. There are various *in vivo*

methods that have been used to assess drug uptake into the brain, including the single carotid injection technique, *in situ* perfusion technique, intravenous injection technique, brain efflux index and intracerebral microdialysis [42]. Although not suitable for high-throughput compound screening, various imaging techniques (i.e., quantitative autoradiography [QAR], MRI, positron emission tomography [PET] and single photon emission computed tomography) may be used to assess the transport properties of the BBB and are also more useful in the diagnosis of various CNS diseases. Moreover, in recent years, knockout and gene-deficient animals have been obtained owing to their value in assessing the role of uptake carriers and efflux transporters and identifying their substrates [150–152].

In vivo brain/plasma ratio, Kp (logBB)

In this experiment several animals are dosed (time zero) and at designated time points the animals are sacrificed. A sample of blood is retained and the brain is removed. The compound concentrations in the plasma and brain homogenate are measured. The concentrations are plotted versus time. Kp (and its logarithm logBB) is calculated as brain area under the curve (AUC) over plasma AUC. This parameter depends upon the passive diffusion characteristics, the transporters (uptake and efflux) at the BBB, metabolism and the relative drug binding affinity differences between the plasma proteins and brain tissue [34,43]. An advantage is that this experiment provides other pharmacokinetics insights, such as Cmax and the AUC. Nevertheless, Kp has limitations. First, the experiment requires considerable resources and it does not provide data for the free drug concentration in the extracellular fluid of the brain. Only free drug interacts with the receptor or enzyme to

produce the pharmacological action [83,153]. Recent studies demonstrated the need for an integrated approach in which permeability, efflux/influx data, plasma protein and tissue binding were used for improved CNS penetration [6–8,41,43,46,118,119,154–156].

Brain uptake index

This is one of the oldest techniques (1970) to estimate the uptake of drugs into the brain. A quantity of radiolabeled drug is injected into the common carotid artery of the animal along with tritiated water. The purpose of including the internal standard is to define the amount of injected material that actually distributes to the brain [149]. The bolus passes through the brain within 2 s after the single injection; the animal is decapitated 5–15 s after injection. Following decapitation, the brain concentrations of test and reference compounds are measured and related to the plasma concentrations to calculate the brain uptake index (BUI) [147]. The assumptions of the BUI are that the reference compound is freely diffusible across the BBB, the drug does not back-diffuse from brain to blood and no metabolism occurs before decapitation [149]. The advantages of the BUI technique include the fact that it is fast, technically easy and relatively cheap and many compounds can be evaluated in a short period of time, which is ideal in the high-throughput setting. This procedure is very suitable for compounds that are labile or fast metabolized. The major disadvantage is that BUI offers an indirect calculation of the PS product [147] and, from an experimental point, of view brain extraction must be carried out over a very short limited time, making it difficult to estimate PS products less than 10 ml min-1g-1 [147]. As the external arteries are not ligated, the compound may also diffuse throughout the whole body with only 10% of the compound reaching the brain [149].

Results are dependent on blood flow, brain region and time between injection and decapitation time, making this procedure unsuitable for poorly penetrating compounds [82].

Intravenous injection technique

In a review on BBB transport techniques, the intravenous injection technique was referred to as the 'gold standard' for assessing BBB permeability [148]. With this technique, a femoral vein of rats or mice is cannulated and the test compound is injected or, alternatively, a tail-vein injection may be used. At various time points during the experiment, arterial blood is collected either by cannulation of a femoral artery in rats, or by humanely killing the mice. In addition to the compound of interest, a plasma volume marker must also be administered, to correct for the amount of compound present in the brain microvasculature. Brain levels can be determined at the predetermined time points (if animals are killed over time) or at the end of the experiment (if arterial samples are being taken) [147,157]. One of the main advantages of this technique is that plasma and brain pharmacokinetics can be obtained, allowing for direct pharmacokinetic parameters to be calculated. In addition, there is increased sensitivity (due to greater exposure to cerebral microvessels) and it is quite easy to measure BBB PS products less than 0.5 $ml \cdot min^{-1} \cdot g^{-1}$ [147]. Other advantages of this technique include the BBB remaining intact and cerebral metabolic pathways not being compromised [14]. In addition, the degree of experimental difficulty is lower than that of the brain uptake index or *in situ* perfusion technique [90]. However, the major disadvantage with the intravenous technique is that there may be extensive metabolism by, and distribution into, peripheral organs, resulting in an inaccurate calculation of the BBB PS product, given the

concentration within the brain microvasculature is unknown [157]. In addition, at later time points, there is the possibility of back-diffusion from brain to plasma, which may confound BBB PS product calculations [90]. Nevertheless, this technique provides a realistic evaluation of the brain levels that might be expected in humans, given that it most closely resembles the human situation. The intravenous technique described above is similar to the mouse brain uptake assay used by Raub, where a single intravenous dose of solute is administered, followed by blood and brain sampling at 5 min post-dose [158]. The five-min brain and plasma concentrations are used to calculate a permeability coefficient, with the presumption that metabolism, back-flux and tissue accumulation are negligible at that time point [15]. It is a useful screen for BBB penetration, and may be utilized in a high-throughput setting, to distinguish between poor and promising CNS candidates [10].

Brain efflux index

The brain efflux index technique was developed to estimate the efflux of drugs from brain, following microinjection of the compound of interest and a reference compound (^{14}C-carboxyinulin) that has a limited BBB permeability. Following decapitation at variable times, the brain and plasma concentration of compound and reference can be calculated. The brain efflux index is expressed as the ratio of drug effluxed from the brain and the drug injected into the brain. Although this technique does provide useful information on the involvement of various efflux transporters in the brain, it is not commonly used for permeability screening purposes [148,159,160].

Intracerebral microdialysis

This is an invasive method that measures local concentrations of compounds in the extracellular fluid of the brain or the CSF. Intracerebral microdialysis involves direct sampling of brain interstitial fluid by implanting a dialysis fiber into the brain [161–165]. The concentration of compound that has permeated the brain following oral, intravenous or subcutaneous administration can be monitored over time within the same animal. The microdialysis probe consists of a semipermeable membrane, which is perfused with a physiological solution, whereby compounds that are small enough to traverse the semipermeable membrane diffuse from higher to lower concentration [166]. Therefore, any drug that enters the brain interstitial fluid will permeate the physiological solution and may be subsequently assayed by an appropriate technique. The major advantage of this technique is that it provides pharmacokinetic profiles of compounds in the brain without the need to kill many animals at different time points [105]. In addition, since both plasma and brain levels of compound can be determined over time, it is possible to determine the kinetics of influx and efflux from the brain [105]. Moreover, it can distinguish between parent compound and metabolite. More interestingly, the probe can be placed in any region of the brain, which may be useful when targeting a compound to a specific area of the brain (such as in brain tumors or the substantia nigra in Parkinson's disease). However, if one is not interested in localized concentrations, this raises the issue of where to place the probe and whether multiple probes should be used in order to get an appropriate representation of drug levels throughout the brain [149]. Another limitation of this technique is that it greatly depends on, and is limited by, the sensitivity of the assay method [166], since only low concentrations may be present in the dialysate. Therefore the spatial

resolution of this technique depends on the analytical technique. HPLC combined with MS methods result in high selectivity and sensitivity. The other major disadvantage associated with intracerebral microdialysis is that insertion of the probe can result in chronic BBB disruption, as has been demonstrated by the passage of the normally impermeable inulin from blood to dialysate and extensive extravasation of serum albumin [10].

Imaging techniques

More recently, there has been some focus on the use of various imaging techniques to assess the permeability of compounds across the BBB, including QAR, MRI, PET and single photon emission computed tomography. Although these techniques are not used in high-throughput drug discovery, they are less invasive techniques that may be useful for assessing BBB permeability in pathological conditions. The major disadvantages associated with these techniques are their inherent costs, labor intensity and inability to differentiate between parent compound and metabolites (in the case of labeled compounds).

Quantitative autoradiography is used to visualize the distribution of radioactive tracers across the BBB. It involves intravenous administration of a radiolabeled compound into an animal, followed by blood sampling and brain removal after various times. The brain is frozen immediately and is subsequently sectioned into slices, placed in X-ray cassettes with a sheet of x-ray film and, following sufficient exposure, autoradiographs are developed and analyzed for the distribution-quantification of radioactivity by a computer-driven densitometer [167,168]. QAR has been a valuable tool in visualizing the brain uptake and distribution of various compounds [169–171], in addition to demonstrating the role of P-gp on the uptake of other

compounds [172]. The limitations of this technique compared with other imaging-based techniques is that this one is an invasive technique and brain concentration/distribution of a substance can only be measured at a single exposure time in a single animal whereas multiple data points can be derived from a single drug exposure using MRI or PET techniques described below.

MRI involves administration of the contrasting agent (gadolinium-based compounds) whose appearance in the brain is related to the degree of BBB damage. It allows evaluation of parameters in the brain related to anatomy, physiology and metabolism such as macrophage infiltration, cytotoxic edema, cerebral blood flow, BBB permeability and leakage involved in brain diseases [173–175].

Positron emission tomography has been shown to be a noninvasive, quantitative approach to measure the BBB PS product and drug transport in humans under normal and disease-state conditions [90]. This technique involves the intravenous administration of a positron-emitting radionuclide or a compound labeled with an isotope that emits positrons. Subsequently, one analyzes the data by pharmacokinetic models that describe the transport of tracers (uptake, distribution and elimination) [149,176–179]. The advantage of this technique is that the transport of tracers can be visualized and studied in whole brain over time. It is useful for diagnosis purposes such as the localization of tumors in the brain and also for studying BBB permeability and BBB transport [179–181]. This technique may provide a benefit in screening the brain uptake of P-gp substrates using inhibition experiments [90]. PET is a good method for measuring the rate of drug uptake into the brain and possible drug interactions at the BBB. Regarding the extent of uptake, PET provides information on

total brain to blood ratios but not unbound drug ratio [7]. The RatCAP is a novel miniature PET scanner designed to acquire fully 3D images of the rat's brain while directly attached to its head. This allows the animal to be completely mobile, eliminating the confounding effects of anesthesia on image quantitation [301]. Single photon emission computed tomography has also been useful as a noninvasive measure of BBB permeability. Following administration of a g-emitting compound, g scintigraphic images can be acquired using a g camera and distribution of the compound throughout the body can be examined. With this method it has been shown that technetium-labeled compounds may be used to assess P-gp transport activity *in vivo*. Although this technique may be useful in characterizing efflux transporters and BBB permeability in disease states, it will have a limited role in screening of compounds for potential brain uptake [10].

Regarding the use and selection of the different methods described above, it is advisable to start with higher throughput methods, such as *in silico*, physicochemical properties, even though this approach requires the development and validation of the *in silico* models, which is a feedback mechanism from good experimental data. These techniques would provide initial insights on whether project compounds are expected to have any problems with penetrating to the therapeutic target. As a second step, and in parallel with the *in vitro* assays of drug absorption, distribution, metabolism and excretion optimization, three *in vitro* assays to characterize CNS properties are recommended: bidirectional cell permeability experiments to estimate permeability and efflux ratio (in a P-gp expressing system), equilibrium dialysis of blood plasma to calculate fu, plasma and dialysis with brain homogenate or brain slices to obtain fu brain [6,7,46]. After this step, screening-selected

compounds can be transferred to the *in vivo* experiments. The *in vivo* experiments will provide more in-depth assessment of penetration into the brain as well as feedback (validation) of the *in vitro* methodologies. If the *in vivo* and *in vitro* brain penetration data differ significantly, the contribution of other mechanisms, such as P-gp efflux, hepatic clearance, plasma protein binding and nonspecific brain tissue finding can be assessed using other *in vitro* assays. The limiting mechanisms can be discerned and structure modifications can be undertaken to improve the brain penetration properties of the compounds series [51].

STRATEGIES FOR ENHANCED DRUG DELIVERY INTO THE BRAIN

A brief description of the strategies to enhance drug delivery into the brain is included in this section. Our aim was not to give an exhaustive description and the reader is advised to refer to specific reviews on this topic, including those by Gabathuler [182] and Alam et al. [183].

Local brain delivery

Direct injection of macromolecular drugs

Intracerebral ventricular or intrathecal drug infusion comprises direct injection/infusion of drug into CSF. However, in order to again access the brain, drugs administered in this way still have to cross ependymal BCSFB. Only small molecules can penetrate brain parenchyma. Large compounds very poorly penetrated the brain even when administered intraventricularly [184].

Direct administration into the brain parenchyma has also been applied [185,186]. Amgen carried out an experiment for the treatment of Parkinson's disease that involved the direct infusion of glial cell-derived neurotrophic factor into the putamen. First, they observed a general improvement, but in the second phase the assay was stopped because the results indicated that this treatment could potentially cause permanent damage in patients [187–189].

Another strategy, known as 'convection enhanced drug delivery,' performs a positive pressure infusion in brain parenchyma to increase drug uptake. There are no positive results as yet [190,191].

Furthermore, polymeric brain implants have been successfully used for the local delivery of drugs to the brain, but it has not been possible to obtain a global delivery into the brain [192].

Direct injection/infusion of viral vectors

Viruses are applicable as a biological vector system to deliver genetic material to brain cells. The most commonly used are adeno-associated virus vectors and lentivirus. Important issues in viral gene delivery are stable transgene expression, limited immunogenicity, induction of an inflammatory response, cell-specific targeting efficiency, safety, toxicity and the need for packaging cell lines. Some viral vectors must be injected into the brain and they must have affinity for specific brain cells where genetic material is targeted. Gene transcription and the desired protein synthesis takes place inside the cells. Many applications have been demonstrated for brain gene therapy, especially using lentivirus as a vector [193–204]. However, some studies indicated that application of such elements could induce tumorgenecity. So, further investigation in this promising direction is needed. For instance, neurotropic viruses cross the BBB and are also able to infect brain cells.

This means that the strategy used by the viruses to cross the BBB could also be used to deliver molecules to the brain. Kumar et al. have shown that peptides derived from rabies virus enable the transvascular delivery of siRNA to the brain [205].

Global brain delivery

Enhancing of passive drug delivery

The objective of this approach is to get an enhanced passive transport across the BBB in order to allow large molecules to reach their targets. Enhanced drug delivery to the brain has been achieved in various ways.

- Osmotic disruption/shrinking of the BBB by intracarotid administration of a hypertonic mannitol solution. After injection the BBB is temporarily opened and drug can access the brain. However, unwanted blood components can access neurons too and cause damage [206].
- Intracarotid administration of alkylglycerol that enhances drug transport by the paracellular route [207].
- Application of bradykinin-analog that opens tight junctions via a receptor-mediated mechanism [208].
- Application of 'protein-transduction domains'. These are amino acid sequences that are capable of enhancing delivery of large molecules into cells mainly by increased adsorptive-mediated endocytosis [209].

These approaches are able to enhance uptake into various tissues but the problem is that they do not provide the selectivity needed to target drugs to the brain.

Design of prodrugs

Prodrugs are defined as therapeutically inactive agents that can be predictably transformed into active metabolites. In another words, prodrugs are inactive precursors of parent drugs [1]. The most common strategy for designing effective prodrugs relies on the increase of parent drug lipophilicity. Moreover, it is necessary to take into account the availability of the BBB for the enzymatic/chemical/spontaneous process to release the active drug in order to obtain a selective and effective prodrugs bioconversion in the brain.

Prodrug bioconversion strategies

- Esterase activation: this strategy consists of the lipidization of the active drug by forming an ester derivative [210,211]. The esterification reaction must be reversible and, once in the brain, the molecule is enzymatically converted back to the parent compound. This approach has been successfully used to deliver morphine into brain using heroin prodrugs [1]. They cross BBB easier and later and are converted to morphine in the brain, which interacts with opioid receptors [211]. Other examples are (R)-a-methylhistamine [212], ketoprofen [213], nipecotic acid [214], niflumic acid [215] and some peptides [216]. Although ester formation is the most commonly employed approach for increasing lipophilicity of polar molecules exhibiting limited CNS penetration, there are some limitations. Ester prodrugs should be stable to plasma enzymes, but sensitive to those present in brain tissues. This result is difficult to achieve. An interesting approach might be the involvement of specific esterases, thus drugs could be converted into ester prodrugs stable to plasma esterase but suitable for degradation induced

by specific esterases introduced in the brain by gene therapy strategies [217].

- Adenosine deaminase activation: several studies have confirmed that adenosine deaminase activated prodrugs significantly enhance CNS delivery since the activity of adenosine deaminase is higher in brain than in plasma [218].
- Oxidase activation: another approach may involve BBB enzymes in the delivery of drugs to CNS. In addition to esterase and adenosine deaminase, a variety of oxidative enzymes, including xanthine oxidase, monoamine oxidase and cytochrome-P450 enzymes, are of particular interest for their role in the enzymatic activity of BBB. These enzymes could be utilized as a biotransformation system in the conversion of drugs unable to cross the BBB.

Redox chemical delivery system

In addition to enzyme activation, other techniques to obtain higher drug delivery to the brain have been developed. One of most interesting is the chemical delivery system approach. The method is similar to that of prodrug formation but with the attachment of three different functional groups, a lipophilic group (L), a spacer (S) and a targetor (T). The enhanced lipophilic molecule crosses the BBB and then the targetor undergoes enzymatic oxidation and turns the molecule into a membrane impermeable moiety. The membrane impermeable conjugates 'locked' into the brain undergo sequential metabolism and yield the drug in the brain. The spacer function is to control the enzymatic rate of drug release inside the brain [1,183]. This approach has been used to achieve successful brain delivery of dopamine,

diclofenac, ibuprofen, ketoprofen, tiaprofenic acid, tolmetin, enkephalin TRH and kyotorphin analogues [219]. Until now, there have not been good results in the delivery of peptides because they can be rapidly inactivated by ubiquitous peptidases.

Prodrugs & carrier mediated transport

As discussed previously, CMT systems carry nutrients, vitamins or hormones into the CNS. This type of transport was firstly investigated *in vivo* with physiologic techniques [27,220]. The progress of molecular cloning of transporter genes and their expression in cultured cells, has increased our knowledge of how the transporters can be employed for the brain targeting of drugs [221]. The transporters of neutral amino acids (LAT 1), hexose (GLUT 1), monocarboxylic acids (MCT 1), cationic amino acids (CAT 1) and nucleosides (CNT2) are widely expressed at the BBB level, whereas the ascorbic acid transporter (SVCT2) is mainly expressed in the choroid plexus.

In general, CMT systems are highly stereospecific for their substrates and one consequence of this is that neuroactive drugs are not transported by CMT. However, prodrugs approaches could resolve this problem by two different strategies: the modification of drug structure, enabling transport by a CMT system; or conjugating the drug with a nutrient able to be CMT transported. In both cases, the drugs are released after enzymatic cleavage from their prodrugs following targeting into the CNS. Both strategies may be useful or not, depending on the drug structure and on the transporter chosen. These approaches have been developed for the carriers LAT 1, GLUT 1 and SVCT 2 [1].

The LAT 1 carrier system has been used to transport dopamine and 7-chlorokynurenic acid to the brain using a modified structure of their molecule [5]. Prodrugs transported by LAT 1 were also obtained

by means of the conjugation of neuroactive drugs with neutral amino acids [222]. A prodrug of nipecotic acid was obtained by conjugation with tyrosine [223].

GLUT 1 transports mainly d-glucose. Conjugation of drugs with d-glucose has been proposed as a strategy to improve their uptake into the brain. This strategy has been successfully used with opioid agonist peptides [224], 7-chlorokynurenic acid [225,226] and dopamine [227].

Prodrugs & receptor mediated transcytosis:

Trojan horses

The RMT system is used to transport endogenous large-molecules peptides across the BBB and can be used to ferry large therapeutic molecules such as protein, nucleotides or nonviral plasmid DNA to the human brain [228]. A molecular Trojan horse is an endogenous peptide, or peptidomimetic monoclonal antibody, which enters the brain from blood via receptor-mediated transport on endogenous BBB transporters. (Further information is available elsewhere in the most recent and extensive reviews [229–232]).

Strategies to inhibit efflux

The development of molecules that inhibit the AET system can be a strategy of increasing brain bioaccesibility of the active drugs [5].

Recently, codrugs l-Dopa and sulfur-containing antioxidants have been developed as new pharmacological tools against Parkinson's disease [233] and ibuprofen and lipoic acid diamines are being used as potential codrugs with neuroprotective activity [234]. Rigor et al. [235] have demonstrated that activation of PKC isoform bI at the BBB rapidly decreases P-gp activity and enhances drug delivery to the brain.

Nasal delivery

Intranasal administration is a strategy that has obtained increasing consideration in enabling brain uptake of drugs because the olfactory region is located at the top of the nasal cavity and it is the only place in the body where the CNS is in contact with the external environment [236,237]. In this way, drugs can be transported across the nasal membrane of the respiratory region via a transcellular (lipophilic molecules) or paracellular mechanism (hydrophilic drugs) into the CNS [238,239]. Intranasal delivery does not necessarily require any modification to therapeutic agents and is a noninvasive method of bypassing the BBB to deliver drugs to the CNS, as for instance morphine, butorphanol, capsaicin, lidocaine, dihydroergotamine, olanzapine, ondansetron, metaclopramide and others [240]. This strategy has been used in the administration of dopamine solutions. It has obtained promising results by combining prodrug approach and nasal administration with dopamine, estradiol or nipecotic acid. In a mouse model of Alzheimer's disease, intranasally administered nerve growth factor both reduces neurodegeneration and improves performance in memory tasks [236,241,242]. Intranasal insulin improves memory, attention and functioning in patients with Alzheimer's disease or mild cognitive impairment and even improves memory and mood in normal adult humans. This new method of delivery could revolutionize the treatment of Alzheimer's disease [243–246], stroke [247] and other brain disorders [248–250].

Nanoparticles

Nanoparticle drug carriers consist of solid biodegradable particles ranging in size from 10 to 1000 nm (50–300 nm generally)

[251,252]. An interesting application of nanoparticles is the drug brain delivery of the new large molecule therapeutics now available to treat CNS disorders: peptides, proteins, genes and antisense drugs [253–260]. Nanoparticles cannot freely diffuse through the BBB and require receptor mediated transport through brain capillary endothelium to deliver their content into the brain parenchyma. They may be advantageously formulated in brain-targeted protective nanocontainers due to their poor stability in biological fluids. Nanoparticles have good safety profiles and provide sustained drug release. It is possible to prepare target-specific nanoparticles by conjugation with cell surface ligands. Using peptidomimetic antibodies, BBB transcytosis receptor brain-targeted immunoparticles can be synthesized that should make the delivery of entrapped actives into the brain parenchyma without inducing BBB permeability alteration possible. Nanoparticles made of polybutylcyanoacrylate have been intensively investigated, showing that when coated with polybutylcyanoacrylate they can deliver drugs to the brain by a still debated mechanism. Nanoparticles of polylactide homopolymers or poly(lactide-coglycolide) heteropolymers may be a promising alternative. However, the nanoparticle approach has limitations for its clinical application: potential toxicity, BBB permeabilization and short or lasting delivery. But this methodology, nevertheless, opens great opportunities for drug delivery into the brain [261–265].

FUTURE PERSPECTIVE

Even today, the majority of new drugs discovered do not cross the BBB [266]. In the last decade, a growing number of spin-off biotechnological companies from academia have started to develop new

methods and strategies to help pharmaceutical companies target the brain. The CNS discovery and development paradigm in those companies is slowly changing to acknowledge the need for earlier BBB access in order to avoid clinical failures. The development programs should include the use of *in silico*, *in vitro* and *in situ* models from the beginning to reduce the attrition rate later on. Nevertheless, there is still room for research and many unanswered questions.

In upcoming years it will be desirable to improve the quality of *in silico* models to screen better new families of compounds, taking into account passive diffusion in combination with influx and efflux mechanisms.

More research is required to improve *in vitro* cell methods to obtain barriers keeping the BBB phenotype, while also being easy to handle and offering similar dynamic properties of the human BBB vessels.

Research in the area of transporters at BBB level, tight junction formation and changes under pathological conditions will help to design strategies for targeting the brain. There is a need for BBB genomic research to identify specific targets on the brain vasculature. Carrier-mediated transport or receptor-mediated transport that are successful strategies that offer a wide scenario for the development of new brain targeted molecules.

Acknowledgements

The authors would like to thank the reviewers for all the insightful comments that greatly improved this manuscript.

Financial & competing interests disclosure

The authors acknowledge the funds from the following public funded projects: Bancaja-UMH grant IPYD01, Spanish Ministry of Science and Education SAF2009–12768 and AGL2005–06191-C02–01, Spanish Ministry of Science and Education and Spanish Ministry of Science and Technology: Consolider-Ingenio CSD2007–00063. The authors have no other relevant affiliations or financial involvement with any organization or entity with a financial interest in or financial conflict with the subject matter or materials discussed in the manuscript apart from those disclosed. No writing assistance was utilized in the production of this manuscript.

REFERENCES

1. Pavan B, Dalpiaz A, Ciliberti N, Biondi C, Manfredini S ,Vertuani S. Progress in drug delivery to the central nervous system by the prodrug approach. Molecules. 13, 1035-1065 (2008)

2. Abbott NJ. Inflammatory mediators and modulation of blood-brain barrier permeability. Cell Mol Neurobiol. 20, 131-147 (2000)

3. Gaillard PJ, de Boer AB ,Breimer DD. Pharmacological investigations on lipopolysaccharide-induced permeability changes in the blood-brain barrier *in vitro*. Microvasc Res. 65, 24-31 (2003)

4. Lo EH, Singhal AB, Torchilin VP ,Abbott NJ. Drug delivery to damaged brain. Brain Res Brain Res Rev. 38, 140-148 (2001)

5. Pardridge WM. The blood-brain barrier: bottleneck in brain drug development. NeuroRx. 2, 3-14 (2005)

6. Nicolazzo JA, Charman SA ,Charman WN. Methods to assess drug permeability across the blood-brain barrier. J Pharm Pharmacol. 58, 281-293 (2006)

7. Engelhardt B ,Sorokin L. The blood-brain and the blood-cerebrospinal fluid barriers: function and dysfunction. Semin Immunopathol. 31, 497-511 (2009)

8. Hawkins BT ,Davis TP. The blood-brain barrier/neurovascular unit in health and disease. Pharmacol Rev. 57, 173-185 (2005)

9. Wolburg H ,Lippoldt A. Tight junctions of the blood-brain barrier: development, composition and regulation. Vascul Pharmacol. 38, 323-337 (2002)

10. Bauer HC ,Bauer H. Neural induction of the blood-brain barrier: still an enigma. Cell Mol Neurobiol. 20, 13-28 (2000)

11. Garberg P, Ball M, Borg Net al. *In vitro* models for the blood-brain barrier. Toxicol *In Vitro*. 19, 299-334 (2005)

12. Betsholtz C, Lindblom P, Bjarnegard M, Enge M, Gerhardt H ,Lindahl P. Role of platelet-derived growth factor in mesangium development and vasculopathies: lessons from platelet-derived growth factor and platelet-derived growth factor receptor mutations in mice. Curr Opin Nephrol Hypertens. 13, 45-52 (2004)

13. Sixt M, Engelhardt B, Pausch F, Hallmann R, Wendler O ,Sorokin LM. Endothelial cell laminin isoforms, laminins 8 and 10, play decisive roles in T cell recruitment across the blood-brain barrier in experimental autoimmune encephalomyelitis. J Cell Biol. 153, 933-946 (2001)

14. del Zoppo GJ ,Milner R. Integrin-matrix interactions in the cerebral microvasculature. Arterioscler Thromb Vasc Biol. 26, 1966-1975 (2006)

15. Del Zoppo GJ, Milner R, Mabuchi T, Hung S, Wang X ,Koziol JA. Vascular matrix adhesion and the blood-brain barrier. Biochem Soc Trans. 34, 1261-1266 (2006)

16. Agrawal S, Anderson P, Durbeej Met al. Dystroglycan is selectively cleaved at the parenchymal basement membrane at sites of leukocyte extravasation in experimental autoimmune encephalomyelitis. J Exp Med. 203, 1007-1019 (2006)

17. Wu C, Ivars F, Anderson Pet al. Endothelial basement membrane laminin alpha5 selectively inhibits T lymphocyte extravasation into the brain. Nat Med. 15, 519-527 (2009)

18. Durbeej M, Henry MD, Ferletta M, Campbell KP ,Ekblom P. Distribution of dystroglycan in normal adult mouse tissues. J Histochem Cytochem. 46, 449-457 (1998)

19. Milner R. Microglial expression of alphavbeta3 and alphavbeta5 integrins is regulated by cytokines and the extracellular matrix: beta5 integrin null microglia show no defects in adhesion or MMP-9 expression on vitronectin. Glia. 57, 714-723 (2009)

20. Proctor JM, Zang K, Wang D, Wang R ,Reichardt LF. Vascular development of the brain requires beta8 integrin expression in the neuroepithelium. J Neurosci. 25, 9940-9948 (2005)

21. Zhu J, Motejlek K, Wang D, Zang K, Schmidt A ,Reichardt LF. beta8 integrins are required for vascular morphogenesis in mouse embryos. Development. 129, 2891-2903 (2002)

22. Abraham MH. The factors that influence permeation across the blood-brain barrier. Eur J Med Chem. 39, 235-240 (2004)

23. Norinder U ,Haeberlein M. Computational approaches to the prediction of the blood-brain distribution. Adv Drug Deliv Rev. 54, 291-313 (2002)

24. Clark D. Computational prediction of blood-brain barrier permeation. Annual Report in Medicinal Chemistry. 40, 403-415 (2005)

25. Pardridge WM. Blood-brain barrier delivery. Drug Discov Today. 12, 54-61 (2007)

26. de Boer AG, van der Sandt IC ,Gaillard PJ. The role of drug transporters at the blood-brain barrier. Annu Rev Pharmacol Toxicol. 43, 629-656 (2003)

27. Begley DJ. Efflux mechanisms in central nervous system: a powerful influence on drug distribution within the brain. Elsevier, (2004)

28. Loscher W ,Potschka H. Drug resistance in brain diseases and the role of drug efflux transporters. Nat Rev Neurosci. 6, 591-602 (2005)

29. Katsura T ,Inui K. Intestinal absorption of drugs mediated by drug transporters: mechanisms and regulation. Drug Metab Pharmacokinet. 18, 1-15 (2003)

30. Dahlin A, Royall J, Hohmann JG ,Wang J. Expression profiling of the solute carrier gene family in the mouse brain. J Pharmacol Exp Ther. 329, 558-570 (2009)

31. Mannhold R. The impact of lipophilicity in drug research: a case report on beta-blockers. Mini Rev Med Chem. 5, 197-205 (2005)

32. Bergstrom CA. *In silico* predictions of drug solubility and permeability: two rate-limiting barriers to oral drug absorption. Basic Clin Pharmacol Toxicol. 96, 156-161 (2005)

33. Alavijeh MS, Chishty M, Qaiser MZ ,Palmer AM. Drug metabolism and pharmacokinetics, the blood-brain barrier, and central nervous system drug discovery. NeuroRx. 2, 554-571 (2005)

34. Feng MR. Assessment of blood-brain barrier penetration: *in silico*, *in vitro* and *in vivo*. Curr Drug Metab. 3, 647-657 (2002)

35. Hammarlund-Udenaes M, Friden M, Syvanen S ,Gupta A. On the rate and extent of drug delivery to the brain. Pharm Res. 25, 1737-1750 (2008)

36. Liu X, Yeo, H., Yau, A., Van Natta, K., Vilenski, O., Weller, P. Brain unbound drug concentration calculated from *in vitro* brain unbound fraction is consistent with brain extracellular fluid drug concentration measured by brain microdialysis for four model compounds. AAPS J. 9, 2439 (2007)

37. Young RC, Mitchell RC, Brown THet al. Development of a new physicochemical model for brain penetration and its application to the design of centrally acting H2 receptor histamine antagonists. J Med Chem. 31, 656-671 (1988)

38. Calder JA ,Ganellin CR. Predicting the brain-penetrating capability of histaminergic compounds. Drug Des Discov. 11, 259-268 (1994)

39. Mensch J, Oyarzabal J, Mackie C ,Augustijns P. *In vivo*, *in vitro* and *in silico* methods for small molecule transfer across the BBB. J Pharm Sci. 98, 4429-4468 (2009)

40. Clark DE. Rapid calculation of polar molecular surface area and its application to the prediction of transport phenomena. 2. Prediction of blood-brain barrier penetration. J Pharm Sci. 88, 815-821 (1999)

41. Mehdipour AR ,Hamidi M. Brain drug targeting: a computational approach for overcoming blood-brain barrier. Drug Discov Today. 14, 1030-1036 (2009)

42. Abraham MH, Chadha HS ,Mitchell RC. Hydrogen bonding. 33. Factors that influence the distribution of solutes between blood and brain. J Pharm Sci. 83, 1257-1268 (1994)

43. Norinder U. Refinement of Catalyst hypotheses using simplex optimisation. J Comput Aided Mol Des. 14, 545-557 (2000)

44. Bendels S, Kansy M, Wagner B ,Huwyler J. *In silico* prediction of brain and CSF permeation of small molecules using PLS regression models. Eur J Med Chem. 43, 1581-1592 (2008)

45. Winkler DA ,Burden FR. Modelling blood-brain barrier partitioning using Bayesian neural nets. J Mol Graph Model. 22, 499-505 (2004)

46. Hemmateenejad B, Miri R, Akhond M ,Shamsipur M. Quantitative structure-activity relationship study of recently synthesized 1,4-dihydropyridine calcium channel antagonists. Application of the Hansch analysis method. Arch Pharm (Weinheim). 335, 472-480 (2002)

47. Zhang H. A new nonlinear equation for the tissue/blood partition coefficients of neutral compounds. J Pharm Sci. 93, 1595-1604 (2004)

48. Liu X, Tu M, Kelly RS, Chen C ,Smith BJ. Development of a computational approach to predict blood-brain barrier permeability. Drug Metab Dispos. 32, 132-139 (2004)

49. Mensch J, Melis A., Mackie C., Mortishire-Smith, R., Vanhoutte K., De Maesschalk R., Augustijns P., Brewster ME. (2007) Evaluation of a combined

high throughput *in vitro* permeability assay with *in silico* P-gp estimations for the prediction of *in vivo* log BB data in, AAPS, San Diego.

50. Engkvist O, Wrede P ,Rester U. Prediction of CNS activity of compound libraries using substructure analysis. J Chem Inf Comput Sci. 43, 155-160 (2003)

51. Pardridge WM. Log(BB), PS products and *in silico* models of drug brain penetration. Drug Discov Today. 9, 392-393 (2004)

52. Ecker GF ,Noe CR. *In silico* prediction models for blood-brain barrier permeation. Curr Med Chem. 11, 1617-1628 (2004)

53. Kerns EH ,Di L. Drug-like properties : concepts, structure design, and methods : from ADME to toxicity optimization, Academic Press, Burlington (USA).•(2008)

54. Abbott NJ. Prediction of blood-brain barrier permeation in drug discovery from *in vivo*, *in vitro* and *in silico* models. Drug Discov Today. 1, (2004)

55. Didziapetris R, Japertas P, Avdeef A ,Petrauskas A. Classification analysis of P-glycoprotein substrate specificity. J Drug Target. 11, 391-406 (2003)

56. Usansky HH ,Sinko PJ. Computation of log BB values for compounds transported through carrier-mediated mechanisms using *in vitro* permeability data from brain microvessel endothelial cell (BMEC) monolayers. Pharm Res. 20, 390-396 (2003)

57. Lundquist S ,Renftel M. The use of *in vitro* cell culture models for mechanistic studies and as permeability screens for the blood-brain barrier in the pharmaceutical industry--background and current status in the drug discovery process. Vascul Pharmacol. 38, 355-364 (2002)

58. Reichel A, Begley DJ ,Abbott NJ. An overview of *in vitro* techniques for blood-brain barrier studies. Methods Mol Med. 89, 307-324 (2003)

59. Pidgeon C, Ong S, Liu Het al. IAM chromatography: an *in vitro* screen for predicting drug membrane permeability. J Med Chem. 38, 590-594 (1995)

60. Stein W. Transport and diffusion across cell membranes, Academic Press, Orlando.•(1986)

61. Di L, Kerns EH, Fan K, McConnell OJ ,Carter GT. High throughput artificial membrane permeability assay for blood-brain barrier. Eur J Med Chem. 38, 223-232 (2003)

62. Carrara S, Reali V, Misiano P, Dondio G ,Bigogno C. Evaluation of *in vitro* brain penetration: optimized PAMPA and MDCKII-MDR1 assay comparison. Int J Pharm. 345, 125-133 (2007)

63. Wexler DS, Gao L, Anderson Fet al. Linking solubility and permeability assays for maximum throughput and reproducibility. J Biomol Screen. 10, 383-390 (2005)

64. Rodriguez-Franco MI, Fernandez-Bachiller MI, Perez C, Hernandez-Ledesma B ,Bartolome B. Novel tacrine-melatonin hybrids as dual-acting drugs for Alzheimer disease, with improved acetylcholinesterase inhibitory and antioxidant properties. J Med Chem. 49, 459-462 (2006)

65. Pavon FJ, Bilbao A, Hernandez-Folgado Let al. Antiobesity effects of the novel *in vivo* neutral cannabinoid receptor antagonist 5-(4-chlorophenyl)-1-(2,4-dichlorophenyl)-3-hexyl-1H-1,2,4-triazole--LH 21. Neuropharmacology. 51, 358-366 (2006)

66. Mensch J, Melis A, Mackie C, Verreck G, Brewster ME ,Augustijns P. Evaluation of various PAMPA models to identify the most discriminating method for the prediction of BBB permeability. Eur J Pharm Biopharm.

67. Kerns EH, Di L, Petusky S, Farris M, Ley R ,Jupp P. Combined application of parallel artificial membrane permeability assay and Caco-2 permeability assays in drug discovery. J Pharm Sci. 93, 1440-1453 (2004)

68. Hartmann T, Schmitt J. Lipophilicity beyond octanol/water: a short comparison of modern technologies. Drug Discov Today. 1, 431-439 (2004)

69. Comer JEA. High-throughput measurement of log D and pKa. Wiley-VCH, Weinheim, Germany, (2004)

70. Maurer TS, Debartolo DB, Tess DA ,Scott DO. Relationship between exposure and nonspecific binding of thirty-three central nervous system drugs in mice. Drug Metab Dispos. 33, 175-181 (2005)

71. Summerfield SG, Stevens AJ, Cutler Let al. Improving the *in vitro* prediction of *in vivo* central nervous system penetration: integrating permeability, P-glycoprotein efflux, and free fractions in blood and brain. J Pharmacol Exp Ther. 316, 1282-1290 (2006)

72. de Boer AB, de Vries, H.E., Gaillard, P.J., Breimer D.D. Drug Transport Across the Blood-Brain Barrier: New Esperimental Strategies, Harwood Scientific, Amsterdam.•(1997)

73. Pardridge WM. Holy grails and *in vitro* blood-brain barrier models. Drug Discov Today. 9, 258 (2004)

74. Grant GA, Abbott NJ ,Janigro D. Understanding the Physiology of the Blood-Brain Barrier: *In Vitro* Models. News Physiol Sci. 13, 287-293 (1998)

75. Gaillard PJ, van der Sandt IC, Voorwinden LHet al. Astrocytes increase the functional expression of P-glycoprotein in an *in vitro* model of the blood-brain barrier. Pharm Res. 17, 1198-1205 (2000)

76. Janzer RC ,Raff MC. Astrocytes induce blood-brain barrier properties in endothelial cells. Nature. 325, 253-257 (1987)

77. Meresse S, Dehouck MP, Delorme Pet al. Bovine brain endothelial cells express tight junctions and monoamine oxidase activity in long-term culture. J Neurochem. 53, 1363-1371 (1989)

78. Kim JA, Tran ND, Li Z, Yang F, Zhou W ,Fisher MJ. Brain endothelial hemostasis regulation by pericytes. J Cereb Blood Flow Metab. 26, 209-217 (2006)

79. Butt AM, Jones HC ,Abbott NJ. Electrical resistance across the blood-brain barrier in anaesthetized rats: a developmental study. J Physiol. 429, 47-62 (1990)

80. Bickel U. How to measure drug transport across the blood-brain barrier. NeuroRx. 2, 15-26 (2005)

81. Rist RJ, Romero IA, Chan MW, Couraud PO, Roux F ,Abbott NJ. F-actin cytoskeleton and sucrose permeability of immortalised rat brain microvascular

endothelial cell monolayers: effects of cyclic AMP and astrocytic factors. Brain Res. 768, 10-18 (1997)

82. Toimela T, Maenpaa H, Mannerstrom M ,Tahti H. Development of an *in vitro* blood-brain barrier model-cytotoxicity of mercury and aluminum. Toxicol Appl Pharmacol. 195, 73-82 (2004)

83. Lauer R, Bauer R, Linz Bet al. Development of an *in vitro* blood-brain barrier model based on immortalized porcine brain microvascular endothelial cells. Farmaco. 59, 133-137 (2004)

84. Nagasawa K, Ito S, Kakuda Tet al. Transport mechanism for aluminum citrate at the blood-brain barrier: kinetic evidence implies involvement of system Xc- in immortalized rat brain endothelial cells. Toxicol Lett. 155, 289-296 (2005)

85. Tetsuka K, Takanaga H, Ohtsuki S, Hosoya K ,Terasaki T. The l-isomer-selective transport of aspartic acid is mediated by ASCT2 at the blood-brain barrier. J Neurochem. 87, 891-901 (2003)

86. Rubin LL, Hall DE, Porter Set al. A cell culture model of the blood-brain barrier. J Cell Biol. 115, 1725-1735 (1991)

87. Gaillard PJ, Voorwinden LH, Nielsen JLet al. Establishment and functional characterization of an *in vitro* model of the blood-brain barrier, comprising a co-culture of brain capillary endothelial cells and astrocytes. Eur J Pharm Sci. 12, 215-222 (2001)

88. Tan KH, Dobbie MS, Felix RA, Barrand MA ,Hurst RD. A comparison of the induction of immortalized endothelial cell impermeability by astrocytes. Neuroreport. 12, 1329-1334 (2001)

89. Franke H, Galla HJ ,Beuckmann CT. An improved low-permeability *in vitro*-model of the blood-brain barrier: transport studies on retinoids, sucrose, haloperidol, caffeine and mannitol. Brain Res. 818, 65-71 (1999)

90. Weksler BB, Subileau EA, Perriere Net al. Blood-brain barrier-specific properties of a human adult brain endothelial cell line. Faseb J. 19, 1872-1874 (2005)

91. Neuhaus W, Lauer R, Oelzant S, Fringeli UP, Ecker GF ,Noe CR. A novel flow based hollow-fiber blood-brain barrier *in vitro* model with immortalised cell line PBMEC/C1-2. J Biotechnol. 125, 127-141 (2006)

92. Stanness KA, Guatteo E ,Janigro D. A dynamic model of the blood-brain barrier "*in vitro*". Neurotoxicology. 17, 481-496 (1996)

93. Stanness KA, Westrum LE, Fornaciari Eet al. Morphological and functional characterization of an *in vitro* blood-brain barrier model. Brain Res. 771, 329-342 (1997)

94. Janigro D, Leaman SM ,Stanness KA. Dynamic modeling of the blood-brain barrier: a novel tool for studies of drug delivery to the brain. Pharm Sci Technolo Today. 2, 7-12 (1999)

95. Dai H ,Elmquist WF. Drug transport studies using quantitative microdialysis. Methods Mol Med. 89, 249-264 (2003)

96. Polli JW, Baughman TM, Humphreys JEet al. P-glycoprotein influences the brain concentrations of cetirizine (Zyrtec), a second-generation non-sedating antihistamine. J Pharm Sci. 92, 2082-2089 (2003)

97. Wang Q, Rager JD, Weinstein Ket al. Evaluation of the MDR-MDCK cell line as a permeability screen for the blood-brain barrier. Int J Pharm. 288, 349-359 (2005)

98. Gumbleton M ,Audus KL. Progress and limitations in the use of *in vitro* cell cultures to serve as a permeability screen for the blood-brain barrier. J Pharm Sci. 90, 1681-1698 (2001)

99. Eisenblatter T ,Galla HJ. A new multidrug resistance protein at the blood-brain barrier. Biochem Biophys Res Commun. 293, 1273-1278 (2002)

100. Gao B, Stieger B, Noe B, Fritschy JM ,Meier PJ. Localization of the organic anion transporting polypeptide 2 (Oatp2) in capillary endothelium and choroid plexus epithelium of rat brain. J Histochem Cytochem. 47, 1255-1264 (1999)

101. Doran A, Obach RS, Smith BJet al. The impact of P-glycoprotein on the disposition of drugs targeted for indications of the central nervous system:

evaluation using the MDR1A/1B knockout mouse model. Drug Metab Dispos. 33, 165-174 (2005)

102. Hurst RD ,Fritz IB. Properties of an immortalised vascular endothelial/glioma cell co-culture model of the blood-brain barrier. J Cell Physiol. 167, 81-88 (1996)

103. Ramsohoye PV ,Fritz IB. Preliminary characterization of glial-secreted factors responsible for the induction of high electrical resistances across endothelial monolayers in a blood-brain barrier model. Neurochem Res. 23, 1545-1551 (1998)

104. Memtrans Project EC. (2009) Alternative Testing Strategies- Progress Report 2009. Replacing, reducing and Refining use of animals in research in (Luxembourg, G. B. f. H., ed), Official Publications of the european Comission,

105. Centelles-Sanguesa A, Gunday N, Zengerly Iet al. (2009) Prevalidation of *in vitro* models for prediction of secretion processes at intestinal level in PharmSci Fair Exhibition Nice.

106. Lazaro E, Rafols C, Abraham MH ,Roses M. Chromatographic estimation of drug disposition properties by means of immobilized artificial membranes (IAM) and C18 columns. J Med Chem. 49, 4861-4870 (2006)

107. Salminen T, Pulli A ,Taskinen J. Relationship between immobilised artificial membrane chromatographic retention and the brain penetration of structurally diverse drugs. J Pharm Biomed Anal. 15, 469-477 (1997)

108. Pardridge WM. Isolated brain capillaries: an *in vitro* model of blood-brain barrier research., Cambridge University Press, Cambridge, 49-61 (1998)

109. de Boer AG ,Gaillard PJ. *In vitro* models of the blood brain barrier: When to use which? Curr Med Chem Central Nerv Syst Agents. 2, 203-209 (2002)

110. Cecchelli R, Dehouck B, Descamps Let al. *In vitro* model for evaluating drug transport across the blood-brain barrier. Adv Drug Deliv Rev. 36, 165-178 (1999)

111. Dehouck MP, Meresse S, Delorme P, Fruchart JC ,Cecchelli R. An easier, reproducible, and mass-production method to study the blood-brain barrier *in vitro*. J Neurochem. 54, 1798-1801 (1990)

112. Audus KL ,Borchardt RT. Characterization of an *in vitro* blood brain barrier model system for studying drug transport and metabolism. Pharm Res. 3, 81-87 (1986)

113. Audus KL, Rose JM, Wang W ,Borchardt RT. Brain microvessel endothelial cell culture system., Cambridge University Press, New York, 86-93 (1998)

114. Lundquist S, Renftel M, Brillault J, Fenart L, Cecchelli R ,Dehouck MP. Prediction of drug transport through the blood-brain barrier *in vivo*: a comparison between two *in vitro* cell models. Pharm Res. 19, 976-981 (2002)

115. Raub TJ, Kuentzel SL ,Sawada GA. Permeability of bovine brain microvessel endothelial cells *in vitro*: barrier tightening by a factor released from astroglioma cells. Exp Cell Res. 199, 330-340 (1992)

116. Glynn SL ,Yazdanian M. *In vitro* blood-brain barrier permeability of nevirapine compared to other HIV antiretroviral agents. J Pharm Sci. 87, 306-310 (1998)

117. Rochat B, Baumann P ,Audus KL. Transport mechanisms for the antidepressant citalopram in brain microvessel endothelium. Brain Res. 831, 229-236 (1999)

118. Bachmeier CJ, Spitzenberger TJ, Elmquist WF ,Miller DW. Quantitative assessment of HIV-1 protease inhibitor interactions with drug efflux transporters in the blood-brain barrier. Pharm Res. 22, 1259-1268 (2005)

119. Dingemanse J, Sollie FA, Breimer DD ,Danhof M. Pharmacokinetic modeling of the anticonvulsant response of oxazepam in rats using the pentylenetetrazol threshold concentration as pharmacodynamic measure. J Pharmacokinet Biopharm. 16, 203-228 (1988)

120. Hilbert JM ,Battista D. Quazepam and flurazepam: differential pharmacokinetic and pharmacodynamic characteristics. J Clin Psychiatry. 52 Suppl, 21-26 (1991)

121. Pardridge WM, Boado RJ ,Farrell CR. Brain-type glucose transporter (GLUT-1) is selectively localized to the blood-brain barrier. Studies with quantitative western blotting and *in situ* hybridization. J Biol Chem. 265, 18035-18040 (1990)

122. Hoheisel D, Nitz T, Franke Het al. Hydrocortisone reinforces the blood-brain properties in a serum free cell culture system. Biochem Biophys Res Commun. 247, 312-315 (1998)

123. Kido Y, Tamai I, Nakanishi Tet al. Evaluation of blood-brain barrier transporters by co-culture of brain capillary endothelial cells with astrocytes. Drug Metab Pharmacokinet. 17, 34-41 (2002)

124. Reichel A, Begley DJ ,Abbott NJ. Carrier-mediated delivery of metabotrophic glutamate receptor ligands to the central nervous system: structural tolerance and potential of the L-system amino acid transporter at the blood-brain barrier. J Cereb Blood Flow Metab. 20, 168-174 (2000)

125. Begley DJ, Lechardeur D, Chen ZDet al. Functional expression of P-glycoprotein in an immortalised cell line of rat brain endothelial cells, RBE4. J Neurochem. 67, 988-995 (1996)

126. Lohmann C, Huwel S ,Galla HJ. Predicting blood-brain barrier permeability of drugs: evaluation of different *in vitro* assays. J Drug Target. 10, 263-276 (2002)

127. Polli JW, Humphreys JE, Wring SAet al. A comparison of Madin-Darby Canine kidney cells and bovine brain endothelial cells as a blood-brain barrier screen in early drug discovery., Elsevier Sciences, Amsterdam, 271-289 (2000)

128. Hurst RD, Heales SJ, Dobbie MS, Barker JE ,Clark JB. Decreased endothelial cell glutathione and increased sensitivity to oxidative stress in an *in vitro* blood-brain barrier model system. Brain Res. 802, 232-240 (1998)

129. Kuchler-Bopp S, Delaunoy JP, Artault JC, Zaepfel M ,Dietrich JB. Astrocytes induce several blood-brain barrier properties in non-neural endothelial cells. Neuroreport. 10, 1347-1353 (1999)

130. Scism JL, Laska DA, Horn JWet al. Evaluation of an *in vitro* coculture model for the blood-brain barrier: comparison of human umbilical vein endothelial cells (ECV304) and rat glioma cells (C6) from two commercial sources. *In Vitro* Cell Dev Biol Anim. 35, 580-592 (1999)

131. Dagenais C, Rousselle C, Pollack GM ,Scherrmann JM. Development of an *in situ* mouse brain perfusion model and its application to mdr1a P-glycoprotein-deficient mice. J Cereb Blood Flow Metab. 20, 381-386 (2000)

132. Pardridge WM. Transport of small molecules through the blood-brain barrier: Biology and methodology. Adv Drug Deliv. 15, 5-36 (1995)

133. Smith QR. A review of blood-brain barrier transport techniques. Human Press, 193-208 (2003)

134. Bonate PL. Animal models for studying transport across the blood-brain barrier. J Neurosci Methods. 56, 1-15 (1995)

135. Cisternino S, Mercier C, Bourasset F, Roux F ,Scherrmann JM. Expression, up-regulation, and transport activity of the multidrug-resistance protein Abcg2 at the mouse blood-brain barrier. Cancer Res. 64, 3296-3301 (2004)

136. Summerfield SG, Read K, Begley DJet al. Central nervous system drug disposition: the relationship between *in situ* brain permeability and brain free fraction. J Pharmacol Exp Ther. 322, 205-213 (2007)

137. Schinkel AH. P-Glycoprotein, a gatekeeper in the blood-brain barrier. Adv Drug Deliv Rev. 36, 179-194 (1999)

138. Sisodiya SM, Martinian L, Scheffer GLet al. Major vault protein, a marker of drug resistance, is upregulated in refractory epilepsy. Epilepsia. 44, 1388-1396 (2003)

139. Liu X, Chen C ,Smith BJ. Progress in brain penetration evaluation in drug discovery and development. J Pharmacol Exp Ther. 325, 349-356 (2008)

140. Kalvass JC, Maurer TS ,Pollack GM. Use of plasma and brain unbound fractions to assess the extent of brain distribution of 34 drugs: comparison of unbound concentration ratios to *in vivo* p-glycoprotein efflux ratios. Drug Metab Dispos. 35, 660-666 (2007)

141. Reichel A. The role of blood-brain barrier studies in the pharmaceutical industry. Curr Drug Metab. 7, 183-203 (2006)

142. Martin I. Prediction of blood-brain barrier penetration: are we missing the point? Drug Discov Today. 9, 161-162 (2004)

143. Jeffrey P ,Summerfield SG. Challenges for blood-brain barrier (BBB) screening. Xenobiotica. 37, 1135-1151 (2007)

144. Bostrom E, Simonsson US ,Hammarlund-Udenaes M. *In vivo* blood-brain barrier transport of oxycodone in the rat: indications for active influx and implications for pharmacokinetics/pharmacodynamics. Drug Metab Dispos. 34, 1624-1631 (2006)

145. Gupta A, Chatelain P, Massingham R, Jonsson EN ,Hammarlund-Udenaes M. Brain distribution of cetirizine enantiomers: comparison of three different tissue-to-plasma partition coefficients: K(p), K(p,u), and K(p,uu). Drug Metab Dispos. 34, 318-323 (2006)

146. Liu X, Smith BJ, Chen Cet al. Use of a physiologically based pharmacokinetic model to study the time to reach brain equilibrium: an experimental analysis of the role of blood-brain barrier permeability, plasma protein binding, and brain tissue binding. J Pharmacol Exp Ther. 313, 1254-1262 (2005)

147. Banks WA, Kastin AJ ,Ehrensing CA. Endogenous peptide Tyr-Pro-Trp-Gly-NH2 (Tyr-W-MIF-1) is transported from the brain to the blood by peptide transport system-1. J Neurosci Res. 35, 690-695 (1993)

148. Raub TJ. (2004) Strategies for optimizing blood-brain barrier penetration in Workshop on optimization of drug-like properties during lead optimization Parsippany, NJ. USA.

149. Kusuhara H, Sekine T, Utsunomiya-Tate Net al. Molecular cloning and characterization of a new multispecific organic anion transporter from rat brain. J Biol Chem. 274, 13675-13680 (1999)

150. Kitazawa T, Terasaki T, Suzuki H, Kakee A ,Sugiyama Y. Efflux of taurocholic acid across the blood-brain barrier: interaction with cyclic peptides. J Pharmacol Exp Ther. 286, 890-895 (1998)

151. Chen YF, Chang CH, Wang SC ,Tsai TH. Measurement of unbound cocaine in blood, brain and bile of anesthetized rats using microdialysis coupled with liquid chromatography and verified by tandem mass spectrometry. Biomed Chromatogr. 19, 402-408 (2005)

152. Qiao JP, Abliz Z, Chu FMet al. Microdialysis combined with liquid chromatography-tandem mass spectrometry for the determination of 6-aminobutylphthalide and its main metabolite in the brains of awake freely-moving rats. J Chromatogr B Analyt Technol Biomed Life Sci. 805, 93-99 (2004)

153. de Lange EC, Ravenstijn PG, Groenendaal D ,van Steeg TJ. Toward the prediction of CNS drug-effect profiles in physiological and pathological conditions using microdialysis and mechanism-based pharmacokinetic-pharmacodynamic modeling. AAPS J. 7, E532-543 (2005)

154. Langenbucher F. Numerical convolution/deconvulution as a tool for correlating *in vitro* with *in vivo* drug availability. Pharm Ind. 44, 1166-1172 (1982)

155. Vaughan DP ,Dennis M. Mathematical basis of point-area deconvolution method for determining *in vivo* input functions. J Pharm Sci. 67, 663-665 (1978)

156. Fenstermacher DA ,Joseph DR. Analysis of promoter and androgen regulatory sequences required for optimal transcription of the rat androgen-binding protein gene. J Androl. 19, 81-91 (1998)

157. Wei L, Craven K, Erinjeri Jet al. Local cerebral blood flow during the first hour following acute ligation of multiple arterioles in rat whisker barrel cortex. Neurobiol Dis. 5, 142-150 (1998)

158. Hazai I, Patfalusi M, Klebovich I ,Urmos I. Whole-body autoradiography and quantitative organ-level distribution study of deramciclane in rats. J Pharm Pharmacol. 51, 165-174 (1999)

159. Coloma MJ, Lee HJ, Kurihara Aet al. Transport across the primate blood-brain barrier of a genetically engineered chimeric monoclonal antibody to the human insulin receptor. Pharm Res. 17, 266-274 (2000)

160. Plenevaux A, Weissmann D, Aerts Jet al. Tissue distribution, autoradiography, and metabolism of 4-(2'-methoxyphenyl)-1-[2' -[N-2"-pyridinyl)-p-[(18)F]fluorobenzamido]ethyl]piperazine (p-[(18)F]MPPF), a new serotonin 5-HT(1A) antagonist for positron emission tomography: An *In vivo* study in rats. J Neurochem. 75, 803-811 (2000)

161. Polli JW, Jarrett JL, Studenberg SDet al. Role of P-glycoprotein on the CNS disposition of amprenavir (141W94), an HIV protease inhibitor. Pharm Res. 16, 1206-1212 (1999)

162. Jiang Q, Ewing JR, Ding GLet al. Quantitative evaluation of BBB permeability after embolic stroke in rat using MRI. J Cereb Blood Flow Metab. 25, 583-592 (2005)

163. Wuerfel J, Bellmann-Strobl J, Brunecker Pet al. Changes in cerebral perfusion precede plaque formation in multiple sclerosis: a longitudinal perfusion MRI study. Brain. 127, 111-119 (2004)

164. Floris S, Blezer EL, Schreibelt Get al. Blood-brain barrier permeability and monocyte infiltration in experimental allergic encephalomyelitis: a quantitative MRI study. Brain. 127, 616-627 (2004)

165. Bart J, Dijkers EC, Wegman TDet al. New positron emission tomography tracer [(11)C]carvedilol reveals P-glycoprotein modulation kinetics. Br J Pharmacol. 145, 1045-1051 (2005)

166. Sasongko L, Link JM, Muzi Met al. Imaging P-glycoprotein transport activity at the human blood-brain barrier with positron emission tomography. Clin Pharmacol Ther. 77, 503-514 (2005)

167. Luurtsema G, Molthoff CF, Schuit RC, Windhorst AD, Lammertsma AA ,Franssen EJ. Evaluation of (R)-[11C]verapamil as PET tracer of P-glycoprotein function in the blood-brain barrier: kinetics and metabolism in the rat. Nucl Med Biol. 32, 87-93 (2005)

168. Nagaraja TN, Patel P, Gorski M, Gorevic PD, Patlak CS ,Fenstermacher JD. In normal rat, intraventricularly administered insulin-like growth factor-1 is rapidly cleared from CSF with limited distribution into brain. Cerebrospinal Fluid Res. 2, 5 (2005)

169. Patel NK, Bunnage M, Plaha P, Svendsen CN, Heywood P ,Gill SS. Intraputamenal infusion of glial cell line-derived neurotrophic factor in PD: a two-year outcome study. Ann Neurol. 57, 298-302 (2005)

170. Slevin JT, Gerhardt GA, Smith CD, Gash DM, Kryscio R ,Young B. Improvement of bilateral motor functions in patients with Parkinson disease through the unilateral intraputaminal infusion of glial cell line-derived neurotrophic factor. J Neurosurg. 102, 216-222 (2005)

171. Amgen PR. (2005) in

172. Mardor Y, Rahav O, Zauberman Yet al. Convection-enhanced drug delivery: increased efficacy and magnetic resonance image monitoring. Cancer Res. 65, 6858-6863 (2005)

173. Ohata K ,Marmarou A. Clearance of brain edema and macromolecules through the cortical extracellular space. J Neurosurg. 77, 387-396 (1992)

174. Wells DJ. Opening the floodgates: clinically applicable hydrodynamic delivery of plasmid DNA to skeletal muscle. Mol Ther. 10, 207-208 (2004)

175. Wolff JA ,Budker V. The mechanism of naked DNA uptake and expression. Adv Genet. 54, 3-20 (2005)

176. Krewson CE, Klarman ML ,Saltzman WM. Distribution of nerve growth factor following direct delivery to brain interstitium. Brain Res. 680, 196-206 (1995)

177. Daly TM. Overview of adeno-associated viral vectors. Methods Mol Biol. 246, 157-165 (2004)

178. Burger C, Nash K ,Mandel RJ. Recombinant adeno-associated viral vectors in the nervous system. Hum Gene Ther. 16, 781-791 (2005)

179. Gao G, Alvira MR, Somanathan Set al. Adeno-associated viruses undergo substantial evolution in primates during natural infections. Proc Natl Acad Sci U S A. 100, 6081-6086 (2003)

180. Grimm D ,Kay MA. From virus evolution to vector revolution: use of naturally occurring serotypes of adeno-associated virus (AAV) as novel vectors for human gene therapy. Curr Gene Ther. 3, 281-304 (2003)

181. Tsuji D, Kuroki A, Ishibashi Y, Itakura T ,Itoh K. Metabolic correction in microglia derived from Sandhoff disease model mice. J Neurochem. 94, 1631-1638 (2005)

182. Kobayashi H, Carbonaro D, Pepper Ket al. Neonatal gene therapy of MPS I mice by intravenous injection of a lentiviral vector. Mol Ther. 11, 776-789 (2005)

183. Fjord-Larsen L, Johansen JL, Kusk Pet al. Efficient *in vivo* protection of nigral dopaminergic neurons by lentiviral gene transfer of a modified Neurturin construct. Exp Neurol. 195, 49-60 (2005)

184. Georgievska B, Jakobsson J, Persson E, Ericson C, Kirik D ,Lundberg C. Regulated delivery of glial cell line-derived neurotrophic factor into rat striatum, using a tetracycline-dependent lentiviral vector. Hum Gene Ther. 15, 934-944 (2004)

185. Vezzani A. Gene therapy in epilepsy. Epilepsy Curr. 4, 87-90 (2004)

186. Crozet C, Lin YL, Mettling Cet al. Inhibition of PrPSc formation by lentiviral gene transfer of PrP containing dominant negative mutations. J Cell Sci. 117, 5591-5597 (2004)

187. Steffens S, Tebbets J, Kramm CM, Lindemann D, Flake A ,Sena-Esteves M. Transduction of human glial and neuronal tumor cells with different lentivirus vector pseudotypes. J Neurooncol. 70, 281-288 (2004)

188. Wong LF, Ralph GS, Walmsley LEet al. Lentiviral-mediated delivery of Bcl-2 or GDNF protects against excitotoxicity in the rat hippocampus. Mol Ther. 11, 89-95 (2005)

189. Miller G. Drug targeting. Breaking down barriers. Science. 297, 1116-1118 (2002)

190. Erdlenbruch B, Alipour M, Fricker Get al. Alkylglycerol opening of the blood-brain barrier to small and large fluorescence markers in normal and C6 glioma-bearing rats and isolated rat brain capillaries. Br J Pharmacol. 140, 1201-1210 (2003)

191. Prados MD, Schold SJS, Fine HAet al. A randomized, double-blind, placebo-controlled, phase 2 study of RMP-7 in combination with carboplatin administered intravenously for the treatment of recurrent malignant glioma. Neuro Oncol. 5, 96-103 (2003)

192. Dietz GP ,Bahr M. Delivery of bioactive molecules into the cell: the Trojan horse approach. Mol Cell Neurosci. 27, 85-131 (2004)

193. Oldendorf WH ,Szabo J. Amino acid assignment to one of three blood-brain barrier amino acid carriers. Am J Physiol. 230, 94-98 (1976)

194. Oldendorf WH. Brain uptake of radiolabeled amino acids, amines, and hexoses after arterial injection. Am J Physiol. 221, 1629-1639 (1971)

195. Krause M, Stark H ,Schunack W. Azomethine prodrugs of (R)-alpha-methylhistamine, a highly potent and selective histamine H3-receptor agonist. Curr Med Chem. 8, 1329-1340 (2001)

196. Deguchi Y, Hayashi H, Fujii Set al. Improved brain delivery of a nonsteroidal anti-inflammatory drug with a synthetic glyceride ester: a preliminary attempt at a CNS drug delivery system for the therapy of Alzheimer's disease. J Drug Target. 8, 371-381 (2000)

197. Frey HH, Popp C ,Loscher W. Influence of inhibitors of the high affinity GABA uptake on seizure thresholds in mice. Neuropharmacology. 18, 581-590 (1979)

198. el Kihel L, Bourass J, Richomme P, Petit JY ,Letourneux Y. Synthesis and evaluation of the anti-inflammatory effects of niflumic acid lipophilic prodrugs in brain edema. Arzneimittelforschung. 46, 1040-1044 (1996)

199. Hersh LB, Aboukhair N ,Watson S. Immunohistochemical localization of aminopeptidase M in rat brain and periphery: relationship of enzyme localization and enkephalin metabolism. Peptides. 8, 523-532 (1987)

200. Danks MK, Yoon KJ, Bush RAet al. Tumor-targeted enzyme/prodrug therapy mediates long-term disease-free survival of mice bearing disseminated neuroblastoma. Cancer Res. 67, 22-25 (2007)

201. Singhal D, Morgan ME ,Anderson BD. Role of brain tissue localized purine metabolizing enzymes in the central nervous system delivery of anti-HIV agents 2'-beta-fluoro-2',3'-dideoxyinosine and 2'-beta-fluoro-2',3'-dideoxyadenosine in rats. Pharm Res. 14, 786-792 (1997)

202. Perioli L, Ambrogi V, Bernardini Cet al. Potential prodrugs of non-steroidal anti-inflammatory agents for targeted drug delivery to the CNS. Eur J Med Chem. 39, 715-727 (2004)

203. Pardridge WM. Drug targeting to the brain. Pharm Res. 24, 1733-1744 (2007)

204. Tamai I ,Tsuji A. Transporter-mediated permeation of drugs across the blood-brain barrier. J Pharm Sci. 89, 1371-1388 (2000)

205. Killian DM, Hermeling S ,Chikhale PJ. Targeting the cerebrovascular large neutral amino acid transporter (LAT1) isoform using a novel disulfide-based brain drug delivery system. Drug Deliv. 14, 25-31 (2007)

206. Bonina FP, Arenare L, Palagiano Fet al. Synthesis, stability, and pharmacological evaluation of nipecotic acid prodrugs. J Pharm Sci. 88, 561-567 (1999)

207. Bilsky EJ, Egleton RD, Mitchell SAet al. Enkephalin glycopeptide analogues produce analgesia with reduced dependence liability. J Med Chem. 43, 2586-2590 (2000)

208. Battaglia G, La Russa M, Bruno Vet al. Systemically administered D-glucose conjugates of 7-chlorokynurenic acid are centrally available and exert anticonvulsant activity in rodents. Brain Res. 860, 149-156 (2000)

209. Bonina FP, Arenare L, Ippolito Ret al. Synthesis, pharmacokinetics and anticonvulsant activity of 7-chlorokynurenic acid prodrugs. Int J Pharm. 202, 79-88 (2000)

210. Bonina F, Puglia C, Rimoli MGet al. Glycosyl derivatives of dopamine and L-dopa as anti-Parkinson prodrugs: synthesis, pharmacological activity and *in vitro* stability studies. J Drug Target. 11, 25-36 (2003)

211. Yang C, Tirucherai GS ,Mitra AK. Prodrug based optimal drug delivery via membrane transporter/receptor. Expert Opin Biol Ther. 1, 159-175 (2001)

212. Hanson LR ,Frey WH, 2nd. Intranasal delivery bypasses the blood-brain barrier to target therapeutic agents to the central nervous system and treat neurodegenerative disease. BMC Neurosci. 9 Suppl 3, S5 (2008)

213. Vyas TK, Shahiwala A, Marathe S ,Misra A. Intranasal drug delivery for brain targeting. Curr Drug Deliv. 2, 165-175 (2005)

214. Frey WH, 2nd. Bypassing the blood-brain barrier to delivery therapeutics agents to the brain and spinal cord. Drug Delivery Technology. 5, 46-49 (2002)

215. Illum L. Is nose-to-brain transport of drugs in man a reality? J Pharm Pharmacol. 56, 3-17 (2004)

216. Matsuoka Y, Gray AJ, Hirata-Fukae Cet al. Intranasal NAP administration reduces accumulation of amyloid peptide and tau hyperphosphorylation in a transgenic mouse model of Alzheimer's disease at early pathological stage. J Mol Neurosci. 31, 165-170 (2007)

217. Matsuoka Y, Jouroukhin Y, Gray AJet al. A neuronal microtubule-interacting agent, NAPVSIPQ, reduces tau pathology and enhances cognitive function in a mouse model of Alzheimer's disease. J Pharmacol Exp Ther. 325, 146-153 (2008)

218. Visochek L, Steingart RA, Vulih-Shultzman Iet al. PolyADP-ribosylation is involved in neurotrophic activity. J Neurosci. 25, 7420-7428 (2005)

219. Steen E, Terry BM, Rivera EJet al. Impaired insulin and insulin-like growth factor expression and signaling mechanisms in Alzheimer's disease--is this type 3 diabetes? J Alzheimers Dis. 7, 63-80 (2005)

220. Liu XF, Fawcett JR, Hanson LR ,Frey WH, 2nd. The window of opportunity for treatment of focal cerebral ischemic damage with noninvasive intranasal insulin-like growth factor-I in rats. J Stroke Cerebrovasc Dis. 13, 16-23 (2004)

221. Reger MA, Watson GS, Green PSet al. Intranasal insulin administration dose-dependently modulates verbal memory and plasma amyloid-beta in memory-impaired older adults. J Alzheimers Dis. 13, 323-331 (2008)

222. Reger MA, Watson GS, Green PSet al. Intranasal insulin improves cognition and modulates beta-amyloid in early AD. Neurology. 70, 440-448 (2008)

223. Jin K, Xie L, Childs Jet al. Cerebral neurogenesis is induced by intranasal administration of growth factors. Ann Neurol. 53, 405-409 (2003)

224. Wissing SA, Kayser O ,Muller RH. Solid lipid nanoparticles for parenteral drug delivery. Adv Drug Deliv Rev. 56, 1257-1272 (2004)

225. Soppimath KS, Aminabhavi TM, Kulkarni AR ,Rudzinski WE. Biodegradable polymeric nanoparticles as drug delivery devices. J Control Release. 70, 1-20 (2001)

226. Ross TM, Martinez PM, Renner JC, Thorne RG, Hanson LR ,Frey WH, 2nd. Intranasal administration of interferon beta bypasses the blood-brain barrier to target the central nervous system and cervical lymph nodes: a non-invasive treatment strategy for multiple sclerosis. J Neuroimmunol. 151, 66-77 (2004)

227. Alyautdin RN, Gothier, D., Petrov, V., Kharkevich, D., kreuter, J. Analgesic activity of the hexapeptide dalargin absorbed on the surface of polysrbate 80-coated poly(butyl cyanoacrylate) nanoparticles. Eur J Pharm Biopharm. 41, 44-48 (1995)

228. Kreuter J, Alyautdin RN, Kharkevich DA ,Ivanov AA. Passage of peptides through the blood-brain barrier with colloidal polymer particles (nanoparticles). Brain Res. 674, 171-174 (1995)

229. Steiniger SC, Kreuter J, Khalansky ASet al. Chemotherapy of glioblastoma in rats using doxorubicin-loaded nanoparticles. Int J Cancer. 109, 759-767 (2004)

230. Thorne RG, Pronk GJ, Padmanabhan V ,Frey WH, 2nd. Delivery of insulin-like growth factor-I to the rat brain and spinal cord along olfactory and trigeminal pathways following intranasal administration. Neuroscience. 127, 481-496 (2004)

231. Yu YP, Xu QQ, Zhang Q, Zhang WP, Zhang LH ,Wei EQ. Intranasal recombinant human erythropoietin protects rats against focal cerebral ischemia. Neurosci Lett. 387, 5-10 (2005)

232. Wang D, Gao Y ,Yun L. Study on brain targeting of raltitrexed following intranasal administration in rats. Cancer Chemother Pharmacol. 57, 97-104 (2006)

233. Barakat NS, Omar SA ,Ahmed AA. Carbamazepine uptake into rat brain following intra-olfactory transport. J Pharm Pharmacol. 58, 63-72 (2006)

234. Olivier JC. Drug transport to brain with targeted nanoparticles. NeuroRx. 2, 108-119 (2005)

235. Onishi H, Machida Y ,Machida Y. Antitumor properties of irinotecan-containing nanoparticles prepared using poly(DL-lactic acid) and poly(ethylene glycol)-block-poly(propylene glycol)-block-poly(ethylene glycol). Biol Pharm Bull. 26, 116-119 (2003)

236. Feng SS, Mu L, Win KY ,Huang G. Nanoparticles of biodegradable polymers for clinical administration of paclitaxel. Curr Med Chem. 11, 413-424 (2004)

237. Fishbein I, Chorny M, Rabinovich L, Banai S, Gati I ,Golomb G. Nanoparticulate delivery system of a tyrphostin for the treatment of restenosis. J Control Release. 65, 221-229 (2000)

238. Elamanchili P, Diwan M, Cao M ,Samuel J. Characterization of poly(D,L-lactic-co-glycolic acid) based nanoparticulate system for enhanced delivery of antigens to dendritic cells. Vaccine. 22, 2406-2412 (2004)
239. http://www.ibbsoc.org
240. http://www.chemistry.bnl.gov/ratcap/index.html

Chapter 2

Blood-Brain Barrier and Drug Delivery

Mangas-Sanjuan, V.[1,2]; Gonzalez-Alvarez, M.[2]; Gonzalez-Alvarez, I.[2]; Bermejo, M.[2]

[1]Pharmaceutics and Pharmaceutical Technology Department. University of Valencia.
[2]Department of Engineering, Pharmaceutics and Pharmaceutical Technology Area. University Miguel Hernández, Elche.

Advances in Non-Invasive Drug Delivery to the Brain
Future Science
Accepted

INTRODUCTION

The development of neuropharmaceutic drugs is the most promising sector in the pharmaceutical industry around the world. Diseases affecting the Central Nervous System (CNS) such as stroke, Alzheimer Parkinson or HIV have global population prevalence around 25% and are among the leading causes of mortality and morbidity. One of the reasons of the high prevalence is the aging population. Treatment associated with CNS diseases has increased in recent decades and, consequently, the cost has also increased [1]. In fact, the cost associated with the treatment of these diseases is one of the highest in the healthcare systems worldwide. However, the high cost is not proportional to therapeutic efficiency because in most of cases treatments are directed to alleviate the symptoms of diseases, rather than to act on the etiology of the disease [2]. There are virtually no effective pharmacological treatments for most of neurological conditions, with the notable exceptions of mood disorders, epilepsy, and chronic pain. The only effective treatment for stroke is thrombolysis, which is a vascular treatment, not a neurological one. Effective treatments for Alzhiemer's disease, Parkinson's disease, stroke, traumatic brain injury, multiple sclerosis, amyotrophic lateral sclerosis (ALS) and brain tumors do not exist yet. The problem with current therapeutic approaches is not only delivery but also inadequate efficacy, so, the development of specific drug directed at a CNS target is necessary. Therefore, there is a clear imbalance between the health needs of the population and efficient therapeutic tools. Adequate treatments could allow a reduction in morbidity and mortality of these diseases and, probably, a decrease of the associated costs.

THE BLOOD-BRAIN BARRIER: ANATOMY AND FUNCTIONS

The Blood Brain Barrier is a physical and a biochemical frontier between the blood and the brain comprising a dense cells layer surrounding the brain blood vessels.

In 1885, Paul Ehrlich injected aniline dyes (IV) into rats and noted that all organs except the brain were blue-dyed. Subsequently, Edwin Goldman using trypan blue demonstrated the existence of a "physiological membrane" that protects the brain [3]. The function of this anatomic barrier is to maintain the homeostasis into the brain by restricting the passage of a great number of molecules [4]. Neurons communicate via chemical messages, consequently, the composition of the extracellular fluid must be kept constant to ensure that the interneuronal signals are sent and received successfully. Thus, the barrier allows the passage of nutrients and substances necessary for proper neuronal functioning and prevents access to potentially harmful substances to the brain. In addition to regulate the transport of substances, the blood brain barrier also acts as a metabolic and immune barrier.

Anatomically, the barrier is constituted by three so-called by Abbott et al 'interfaces' [4]. The first and largest interface is the Blood Brain Barrier (BBB) structure constituted by the surface area of the brain microvessels. Microvessels wall contain endothelial cells, astrocytes, pericytes and an extracellular matrix. Endothelial cells of blood vessels in CNS are special, without fenestrations and pinocytic vesicles and sealed with tight junctions [5]. Some proteins are associated with the formation and maintenance of the tight junctions: transmembrane proteins (occludins, claudins and intercellular adhesion

molecules) and cytoplasmic proteins as zonula occludens ZO-1, ZO-2 and ZO-3. It has been speculated that the tightness of the blood brain barrier depends not only on the characteristics of endothelial cells but the presence of other molecules that create the necessary environment for the manifestation of the peculiar characteristics of the barrier. Endothelial cells of capillaries supplying the brain are covered by a basal membrane (collagen type IV, laminin, fibronectin and heparan sulfate proteoglycan, together with collagen type IV, provides a structural support layer), extracellular matrix, pericytes, neuronal axons and an almost continuous layer of astrocytes. In this sense, it is believed that astrocytes and pericytes play a fundamental role in maintaining the structure and there are many research groups studying their influence on the development of *in vitro* models of blood-brain barrier. In fact, incorporation of pericytes and astrocytes to endothelial cell cultures provide higher transendothelial electrical resistance than other models [6]. However, the complete functions that have astrocytes and pericytes cells in the blood brain barrier are one of the outstanding issues to be determined in future. The role of the extracellular matrix is also not clear but there is evidence that contributes to vessels integrity and function. Figure 1 shows a schematic picture of Blood Brain Barrier structure.

The epithelial cells of the choroid plexus constitute the second interface, the blood-cerebrospinal fluid barrier (BCSFB). This barrier regulates diffusion, facilitated diffusion and active transport into CSF, as well as active transport of metabolites from cerebrospinal fluid (CSF) to blood [4].

The third interface is constituted by the avascular arachnoid epithelium which envelops completely the Central Nervous System (CNS). The cells of this membrane also are linked by tight junctions.
All these components determine the low barrier permeability. However, barrier function is not only determined by the interendothelial tight junctions, other factors are involved. The presence of enzymes such as alkaline phosphatase, glutamyl transpeptidases, esterases and monoamine oxidase, which are either absent or expressed at low levels in peripheral vessels, provide an enzymatic protection. The overexpression of active transporters for uptake and efflux of substances limit the access of a great number of xenobiotics. Efflux transporters, which have promiscuous selectivity return into blood many substances which attempt to cross the barrier. There are also a number of transporters selective for brain nutrients that are potential targets for structural analogue drugs. Moreover, the negative charge of the endothelial cells surface repels the negative charged compounds preventing their passage to the other side of the barrier.

This means that many drugs that could be useful for the treatment of disorders of the central nervous system are ineffective when administered by conventional way due to a not reach their therapeutic target. The BBB is the major obstacle, though not the only one in limiting the options for treatment of neurological and psychiatric diseases. Inadequate drug levels due to several reasons such as metabolic drug interactions play an important role in the clinical efficacy and safety of drugs [7].

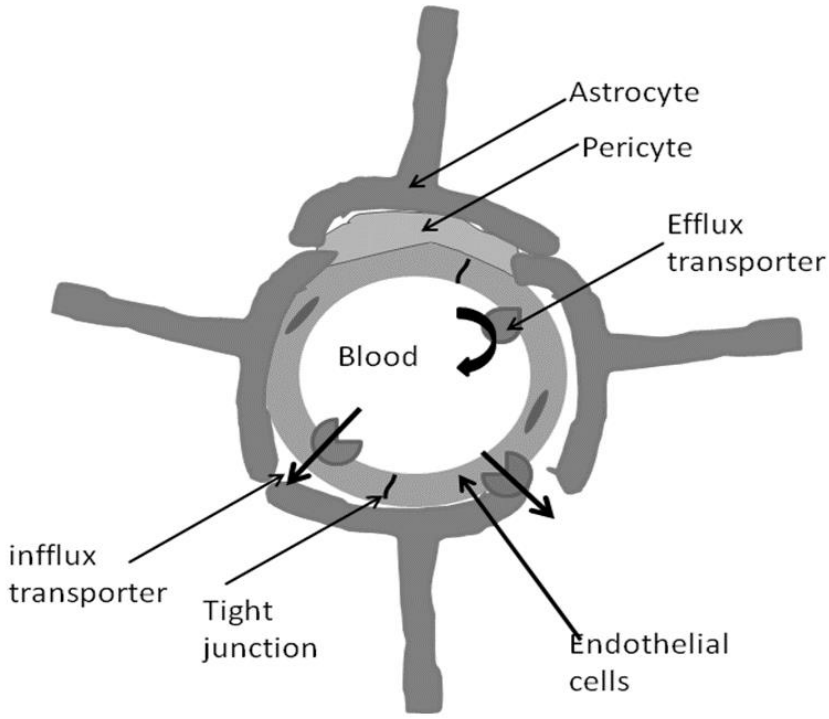

Figure1. Scheme of Structure of Blood Brain Barrier. Adapted from Nicolazzo et al, [5] and reproduced with permission from Mangas-Sanjuan et al. Future Science, 2010 [8].

TRANSPORT ACROSS THE BLOOD-BRAIN BARRIER

The most important function of the blood brain barrier is to maintain the optimal environment for neural function. It means regulating the access of both xenobiotics and normal factors (found within the peripheral circulation) that can alter neuronal function (ions, cytokines, hormones, lipids, amino acids, etc.). The diffusion across the barrier is determined by physicochemical parameters such as lipophilicity, polar surface, molecular weight, charge and others. For example, lipophilic molecules of small size (e.g. ethanol and caffeine)

can pass across the barrier following a transendothelial pathway but this option is not suitable for hydrophilic molecules. Moreover, the lack of fenestrations between endothelial cells of the blood-brain barrier restricts access of hydrophilic molecules via the paracellular pathway. However, the barrier is permeable to substances such as glucose (the main energetic substrate), oxygen, pyruvate, lactate, ketone bodies, aminoacid precursors of neurotransmitters and vitamins that cannot be synthesized in the central nervous system thanks to specific transporters. The BBB expressed an important number of transport proteins. The increased research in the role and function of the transporter systems can be used to facilitate the access to chemical molecules into the brain and to improve the clinical efficacy and safety of the neurological treatments. Transporter systems are illustrated in figure 2 and summarized in table 1. These are different types of mechanisms:

(a) Carrier-mediated transporters

Specific uptake transporters facilitate the access of endogenous or exogenous molecules to central nervous system. The most studied and one of the most effectively targeted transporters is LAT1 that allows not only the access of amino acids to the brain but also of drugs such as L-DOPA and metyl-DOPA. This transporter has clinical relevance in the treatment of Parkinson disease [9]. GLUT1 is one of the most expressed transporters in BBB and has special importance because facilitates the uptake of glucose which is the main energy source for the brain [10]. Interactions of GLUT1 with drugs used for the treatment of neurological diseases have been described, but the clinical relevance of these findings is not well-known yet. Moreover, a reduction

of GLUT1 expression in Alzheimer disease patients has been described that suggest a continuous energy restriction in the AD patients brains [11]. An important number of transporters including ENT1 (mediates the access of nucleoside drugs) [12], MCT1 (transporter of monocarboxylate drugs) or OATP family (mediate brain influx of amphiphilic compounds) have been identified and can be useful to mediate the access of drugs structural analogues of carrier substrates [7]. In order to regulate pH, the BBB has mechanisms that allow the ion access to central nervous system. These transporters are expressed in the abluminal, luminal or both sides of the membrane. The best characterized are the sodium pump, the sodium-potassium-two chloride cotransporter, the sodium-hydrogen exchanger and the chloride-bicarbonate exchanger.

(b) Receptor mediated transport.

This system requires the presence of membrane receptors, which recognize specific molecules and bind to them. This binding allows access of macromolecules by endocytosis. Endothelial cells express endogenous peptide receptor to mediate the transport of neuroactive peptides and proteins. Using these membrane receptors molecules such as insulin, transferrin, insulin-like growth factors, leptin and some lipoproteins can cross the BBB [13]. While this mechanism is very specific, their use for delivery to the brain of high molecular weight drugs with molecular Trojan horses has been investigated [14]. Several studies have shown the delivery of non-viral gene or recombinant proteins attached to molecular Trojan horses, following IV administration [13]. Especially relevant are the pharmacological effects obtained with gene therapy. Administration of molecular Trojan horse

liposomes that contain non-viral plasmid DNA has allowed 90-100% increase in survival time in mice with intra-cranial human brain cancer [15, 16] or complete normalization of striatal enzyme activity, which is 90% decreased in Parkinson Disease [17].

(c) Active efflux transporters.

The so-called multidrug pumps can be defined as a series of relatively nonspecific transporters, which are capable of handling a large number of structurally unrelated substrates. The best known and the most representative is P-glycoprotein (P-gp) that reduces the access into the brain of a wide range of cationic and lipophilic compounds. BCRP is a well-studied efflux transporter too but this transporter does not extensively limit brain penetration of its substrates by itself. However, a 'P-gp-BCRP synergy effect' has been observed, which has been the subject of several hypotheses and whose mechanism still remains unclear. The BBB also expresses other efflux transporters in the MRP protein family [18]. Recent studies indicate that human and rodent BBB only express MRP4 at quantifiable levels [7]. The role of the efflux transporters in the treatment of brain disorders is well-known and extensively accepted. An obvious and promising strategy to increase access of these drugs into the brain is to minimize the effects of the efflux transporters. This objective may be attempted through different strategies including inhibiting the efflux transporter with a substrate with higher affinity than the drug itself or encapsulating the drug to mask the xenobiotic from the efflux [19]. However, excessive efflux transporter inhibition can result in adverse effects due to the indiscriminate access of xenobiotics to the brain.

Table 1 Examples of relevant families of transporters for BBB drug delivery. Compiled from data presented in tables in Abbott et al. [4].

	Transport system	Substrate	BBB direction		Reference
			Influx	Efflux	
ATPases	ABC transporters	Lipid soluble non-polar molecules and conjugates		X	Begley 2004 [60, 61]
	ABCB1 (P-gp)			X	
	ABCC1-3 (MRP proteins)			X	
	ABCC4-5	Nucleosides		X	
	ABCG2 (BCRT)				Begley 2004 [60] Dauchy et al, [62]
Solute carriers (SLC)	LAT1	Aminoacids	X	X	Uchida, et al. [63]
	GLUT1	Glucose	X	X	Simpson [64]; Uchida, et al [63]
	ENT1	Nucleosides	X	X	Parkinson [65]
	MCT1	Monocarboxilates	X	X	Kalvass, et al [66]; Roiko et al [67]
	OCTs	Organic cations	X	X	Kalvass, et al [66]
	OATs	Organic anions	X	X	Gao et al [68]; Iusuf, D [69]
Receptor mediated transport (RMT)	RMT Insulin	Insulin	X		Banks [70]
	RMT Leptin	Leptin	X		Banks [71]
	RMT Transferrin (TfR)	Transferrin	X		Visser et al. [72]
	RMT Apolipoprotein E receptor 2 (ApoER2)	Lipoproteins	X		Herz and Marschang, [73]
	RMT LDL-receptor-related protein 1 (LRP1)	Lipoproteins, Amiloid-β, lactoferrin α	X		Herz and Marschang, [73] Pan and Kastin, [74]
	RMT Tumor necrosis factor (TNFα)	TNFα	X	X	Pan and Kastin, [75]
	RMT Epidermal growth factor	EGF	X		Stern et al [76]; Deane et al. [77]
	RMT Receptor for advanced glycosylation	Glycosylated proteins	X		
Adsorptive-mediated transport (AMT)	AMT Cationised proteins	Cationised albumin	X		Pardridge et al. [78]
	AMT Cell penetrating peptides	SynB5/pAnt (43-58)	X		Drin et al. [79]

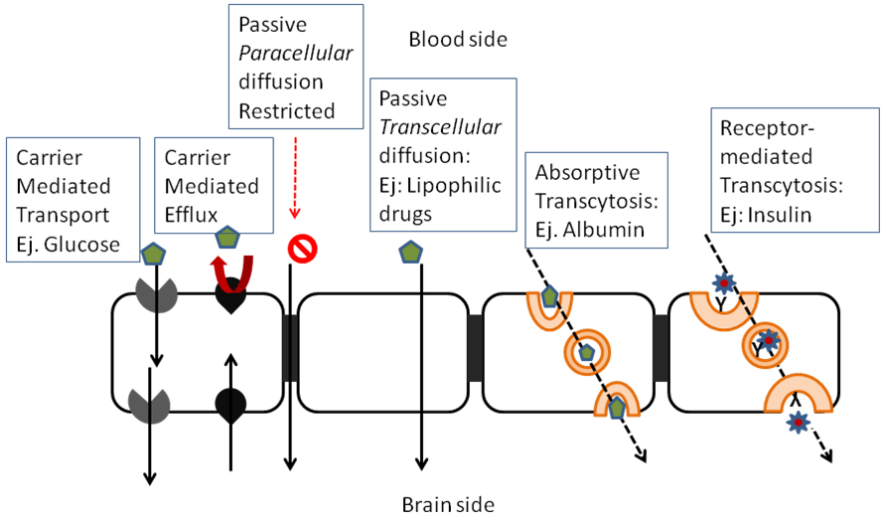

Figure 2: Permeation mechanisms through the endothelial cells. Reproduced with permission from Mangas-Sanjuan et al. Future Science, 2010 [8].

From a pharmacokinetic point of view, brain could be considered as a separate compartment. Level of drugs in the brain depends a priori on effective permeability through the barrier. The permeability depends on the ability of the drug to diffuse passively combined with access through transporters. At first, it would be thought that the permeability depends especially on lipophilicity but experimental evidence indicates that correlations between lipophilicity and permeability are not very good [36]. In fact, though lipophilic derivatives are more permeable across the BBB their effective uptake to CNS may be lower due to reduction of the plasma concentration. The increased clearance of lipidized forms reduces the area under the curve in plasma concentration-time profile [19]. The identification of the

parameters that influence the permeability through the blood brain barrier and the determination of the different mechanisms for brain access are being studied by several research groups [37]. This information can help to the design of molecules that could get their therapeutic target by crossing the barrier and to development of strategies to facilitate the passage of existing active molecules.

It has been postulated that the main factors, which influence the unbound drug concentration in the brain thus determining the pharmacological activity, are the drug plasma concentration, the extent of drug binding to plasma proteins, the enzymatic modification in the barrier and the drug affinity for the brain tissue [36].

IMPORTANCE OF THE DRUG DELIVERY INTO THE BRAIN

Currently, the prevalence of neurological and psychiatric disorders is very high [1]. The treatment of these diseases is not easy due to, as already mentioned, the BBBs role in protecting the central nervous system by preventing the access of virus and xenobiotics. This maintains a constant composition of cerebrospinal fluid and extracellular fluid, allowing optimal neuronal activity. The barrier is specialized in this role and is so effective that it limits access of therapeutics to the central nervous system.

From a pharmacokinetic point of view, it is well established that only the unbound or free drug in plasma (not bound to plasma proteins or blood cells) is distributed to body tissues. The unbound drug is able to diffuse out of the vascular space and cross the tissue membranes. For a drug targeting the CNS, the relevant concentration is the free drug within in the interstitial fluid. As it has been mentioned ISF

concentration when drug is in steady state (after multiple dosing once the input and output rate in the body are in equilibrium) will be influenced by the extent of binding to plasma proteins and the drug affinity for the brain tissue, however the ultimate regulator of ISF concentration is the drug's ability to cross the barrier. As in any oral drug the pharmacological effect is dependent on the drug bioavailability (rate and extend of access to the systemic circulation) in a CNS drug its effect is conditioned by its bioaccesibility to the brain tissue. This has been a challenge for so called small chemical entities and is still more challenging to the new biopharmaceuticals with higher molecular weights and a much lower ability to cross any biological barrier. However, BBB permeation is the necessary but not sufficient condition for a successful CNS drug because other factors control the concentration-time profile at the brain target sites. CNS drug distribution must be also optimized and this aspect is not always reflected in the BBB models [37].

On the other hand BBB disruptions and changes are common in some CNS conditions and neurodegenerative disorders and could be viewed also as a potential target for CNS therapies.

The potential strategies to deliver the drug to its targets in the CNS include invasive approaches (injections or implants) of limited utility due to damage risk, cost and inconveniences to the patient. The second option is either chemical modification of the candidate or formulation approaches. Drug modifications often affect therapeutic activity and modulation of BBB properties with excipients is not free of risk. The most promising strategy is the utilization of the physiological pathways to deliver endogenous substances and nutrients to the brain

i.e. targeted transporter mediated delivery and receptor mediated delivery [38, 39].

The development and research of these strategies requires adequate and validated models to obtain the proof of concept for efficacy of the delivery method. The BBB models for drug delivery need to encompass their complexity depending on their final purpose either screening among a big number of compounds or producing clinically relevant outputs (plasma and brain time profiles and concentration effects relationships). In this sense the development of physiology based pharmacokinetic pharmacodynamics models would allow the integration of the *in vitro* and the *in silico* information, the interspecies extrapolation and the incorporation of the pathological changes in the system responses. This bottom-up approach has proven its utility in other barrier modeling and in other ADME processes as intestinal absorption or hepatic metabolism. The bases of a mechanism-based or physiological based PK-PD model (PBPK-PD) are the characterization of the system parameters (blood flow, tissue weight or volume, enzyme levels or transporter expressions) that can be extrapolated among species or changed in pathological conditions and the input of the drug-specific parameters including physicochemical properties, target affinity and any other *in vitro* measured property. The combination of the system parameters with the drug information (inputs) generate as output the plasma or tissue concentration times profiles. These models can be constructed using programming packages such as MATLAB®, acslX®, or Berkeley Madonna® and there are examples of successful commercial PBPK simulation tools for absorption and metabolism as GastroPlusTM® (Simulations Plus Inc., www.simulations-plus.com),

SimCyp® (Simcyp, www.simcyp.com), and PK-Sim® (Bayer Technology Services, www.pksim.com) [40, 41].

The applicability of this methodology to predict brain concentration time profiles and CNS drug distribution requires the identification of critical system parameters such as cerebral blood flow, effective brain capillary surface area, CSF turnover, extracellular fluid (ECF) bulk flow, metabolic enzymes and transporter expression levels among others i.e. the models are expensive and time consuming to construct, but the feasibility of the approach has been already successful in other areas.

Considering the above challenges current research efforts for improving drug delivery to the brain should focus on:

- Understanding physiological changes in the BBB barrier in pathological conditions and generating models able to mimic these changes.
- Developing both cost-effective and fast *in vitro* screening methods to reduce later attrition rate as well as physiological meaningful *in vitro* tests to study drug transport mechanisms and testing delivery strategies
- Identifying system physiological parameters in humans and animal and their equivalent on *in vitro* models and their mutual relationships to construct predictive PBPK-PD models.

CONCLUSION

Even nowadays, one of the most challenging aspect of developing CNS drugs is ensuring their ability to cross the blood-brain barrier (BBB). Our knowledge about BBB structure and function has improved dramatically in the last decades as well as the availability of

screening methods from *in silico*, *in vitro* to *in situ* and *in vivo* models. A growing number of innovative technologies have been developed to overcome the barrier properties. However, there are still many unclear aspects about the factors that modulate drug access and disposition in the brain: passive BBB permeability, carrier mediated transport (absorptive or secretive) and the relative degree of tissue binding between brain and plasma as those factors will govern the interstitial drug concentration-time profiles. In addition, the development of physiology-based pharmacokinetic-pharmacodynamic models would allow the integration of the *in vitro* and *in silico* information to obtain clinically relevant outputs (i.e. plasma and brain time profiles and concentration effect relationships). This bottom-up approach has proven its utility in other barrier modeling as the intestinal one and can incorporate all the recent knowledge in the area of BBB transporters and tight junction formation and changes under pathological conditions

EXECUTIVE SUMMARY

- The Blood Brain Barrier is a physical and a biochemical frontier between the blood and the brain. This selective barrier is derived from the tight junctions of the endothelial cells at the brain blood vessels and their increased expression of transporters and metabolic enzymes as well as the surrounding astrocytes, pericytes and extracellular matrix.
- There are two ways for molecules to cross the BBB: passive diffusion (paracelular and transendothelial transport) for small and lipophilic compounds and via endogenous transport system for hydrophilic and large molecules.
- The three essential parameters to describe rate and extent of access to the CNS are: the effective permeability (as a composite of

diffusive and other transport mechanisms), the ratio of unbound drug in brain over unbound drug in plasma at steady state (extent) and the intra brain distribution volume.

- Not a single *in vitro* model mimicking all the BBB features is currently available. The appearance of hybrid (*in vitro*/*in silico*) models capable of predicting both passive and transport-mediated function and software tools for screening drugs is needed but this also needs the validation with *in vivo* data. Generation of larger databases of *in vivo* data (rate and extent) in humans and animal experiments would be desirable.
- PBPK-PD modeling strategies would allow to obtain clinically relevant outputs but the construction of the models still needs the characterization of many physiological parameters and their relationships between animal models and humans.
- The utilization of non-invasive strategies by using physiological pathways is the most promising strategy to deliver drugs into the CNS.

ACKNOWEDGEMENT

The authors acknowledge financial support to projects: DCI ALA/19.09.01/10/21526/245-297/ALFA 111(2010)29: Red-Biofarma. Red para el desarrollo de metodologias biofarmaceuticas racionales que incrementen la competencia y el impacto social de las Industrias Farmaceuticas Locales.

Victor Mangas-Sanjuan acknowledges to the Ministry of Education and Science of Spain and Miguel Hernandez University the FPU grant. (FPU AP2010-2372).

REFERENCES

1. Kessler RC, Demler O, Frank RG et al.: Prevalence and treatment of mental disorders, 1990 to 2003. N Engl J Med 352(24), 2515-2523 (2005).

2. Pangalos MN, Schechter LE, Hurko O: Drug development for CNS disorders: strategies for balancing risk and reducing attrition. Nat Rev Drug Discov 6(7), 521-532 (2007).

3. Ehrlich P: Das Sauerstoffbedürfnis des Organismus. In: Eine Farbenanalytische Studie, (Ed.^(Eds). Hirschwald, Berlin (1885).

4. Abbott NJ, Patabendige AA, Dolman DE, Yusof SR, Begley DJ: Structure and function of the blood-brain barrier. Neurobiol Dis 37(1), 13-25 (2010).

5. Nicolazzo JA, Charman SA, Charman WN: Methods to assess drug permeability across the blood-brain barrier. J Pharm Pharmacol 58(3), 281-293 (2006).

6. Nakagawa S, Deli MA, Nakao S et al.: Pericytes from brain microvessels strengthen the barrier integrity in primary cultures of rat brain endothelial cells. Cell Mol Neurobiol 27(6), 687-694 (2007).

7. Kalvass JC, Polli JW, Bourdet DL et al.: Why clinical modulation of efflux transport at the human blood-brain barrier is unlikely: the ITC evidence-based position. Clin Pharmacol Ther 94(1), 80-94 (2013).

8. Mangas-Sanjuan V, Gonzalez-Alvarez M, Gonzalez-Alvarez I, Bermejo M: Drug penetration across the blood-brain barrier: an overview. Ther Deliv 1(4), 535-562 (2010).

9. Uchida Y, Ohtsuki S, Katsukura Y et al.: Quantitative targeted absolute proteomics of human blood-brain barrier transporters and receptors. J Neurochem 117(2), 333-345 (2011).

10. Simpson IA, Carruthers A, Vannucci SJ: Supply and demand in cerebral energy metabolism: the role of nutrient transporters. J Cereb Blood Flow Metab 27(11), 1766-1791 (2007).

11. Zlokovic BV: The blood-brain barrier in health and chronic neurodegenerative disorders. Neuron 57(2), 178-201 (2008).

12. Parkinson FE, Damaraju VL, Graham K et al.: Molecular biology of nucleoside transporters and their distributions and functions in the brain. Curr Top Med Chem 11(8), 948-972 (2011).

13. Pardridge WM: Blood-brain barrier delivery. Drug Discov Today 12(1-2), 54-61 (2007).

14. De Boer AG, Van Der Sandt IC, Gaillard PJ: The role of drug transporters at the blood-brain barrier. Annu Rev Pharmacol Toxicol 43, 629-656 (2003).

15. Zhang Y, Zhu C, Pardridge WM: Antisense gene therapy of brain cancer with an artificial virus gene delivery system. Mol Ther 6(1), 67-72 (2002).

16. Zhang Y, Zhang YF, Bryant J, Charles A, Boado RJ, Pardridge WM: Intravenous RNA interference gene therapy targeting the human epidermal growth factor receptor prolongs survival in intracranial brain cancer. Clin Cancer Res 10(11), 3667-3677 (2004).

17. Zhang Y, Schlachetzki F, Zhang YF, Boado RJ, Pardridge WM: Normalization of striatal tyrosine hydroxylase and reversal of motor impairment in experimental parkinsonism with intravenous nonviral gene therapy and a brain-specific promoter. Hum Gene Ther 15(4), 339-350 (2004).

18. Nagengast WB, Oude Munnink TH, Dijkers EC et al.: Multidrug resistance in oncology and beyond: from imaging of drug efflux pumps to cellular drug targets. Methods Mol Biol 596, 15-31 (2010).

19. Pardridge WM: The blood-brain barrier: bottleneck in brain drug development. NeuroRx 2(1), 3-14 (2005).

20. Begley DJ: ABC transporters and the blood-brain barrier. Curr Pharm Des 10(12), 1295-1312 (2004).

21. Begley DJ: Delivery of therapeutic agents to the central nervous system: the problems and the possibilities. Pharmacol Ther 104(1), 29-45 (2004).

22. Dauchy S, Dutheil F, Weaver RJ et al.: ABC transporters, cytochromes P450 and their main transcription factors: expression at the human blood-brain barrier. J Neurochem 107(6), 1518-1528 (2008).

23. Roiko SA, Felmlee MA, Morris ME: Brain uptake of the drug of abuse gamma-hydroxybutyric acid in rats. Drug Metab Dispos 40(1), 212-218 (2012).

24. Gao B, Hagenbuch B, Kullak-Ublick GA, Benke D, Aguzzi A, Meier PJ: Organic anion-transporting polypeptides mediate transport of opioid peptides across blood-brain barrier. J Pharmacol Exp Ther 294(1), 73-79 (2000).

25. Iusuf D, Van De Steeg E, Schinkel AH: Functions of OATP1A and 1B transporters *in vivo*: insights from mouse models. Trends Pharmacol Sci 33(2), 100-108 (2012).

26. Banks WA: The source of cerebral insulin. Eur J Pharmacol 490(1-3), 5-12 (2004).

27. Banks WA, Niehoff ML, Martin D, Farrell CL: Leptin transport across the blood-brain barrier of the Koletsky rat is not mediated by a product of the leptin receptor gene. Brain Res 950(1-2), 130-136 (2002).

28. Visser CC, Voorwinden LH, Crommelin DJ, Danhof M, De Boer AG: Characterization and modulation of the transferrin receptor on brain capillary endothelial cells. Pharm Res 21(5), 761-769 (2004).

29. Herz J, Marschang P: Coaxing the LDL receptor family into the fold. Cell 112(3), 289-292 (2003).

30. Pan W, Kastin AJ: TNFalpha transport across the blood-brain barrier is abolished in receptor knockout mice. Exp Neurol 174(2), 193-200 (2002).

31. Pan W, Kastin AJ: Entry of EGF into brain is rapid and saturable. Peptides 20(9), 1091-1098 (1999).

32. Stern D, Yan SD, Yan SF, Schmidt AM: Receptor for advanced glycation endproducts: a multiligand receptor magnifying cell stress in diverse pathologic settings. Adv Drug Deliv Rev 54(12), 1615-1625 (2002).

33. Deane R, Wu Z, Zlokovic BV: RAGE (yin) versus LRP (yang) balance regulates alzheimer amyloid beta-peptide clearance through transport across the blood-brain barrier. Stroke 35(11 Suppl 1), 2628-2631 (2004).

34. Pardridge WM, Triguero D, Buciak J, Yang J: Evaluation of cationized rat albumin as a potential blood-brain barrier drug transport vector. J Pharmacol Exp Ther 255(2), 893-899 (1990).

35. Drin G, Cottin S, Blanc E, Rees AR, Temsamani J: Studies on the internalization mechanism of cationic cell-penetrating peptides. J Biol Chem 278(33), 31192-31201 (2003).

36. Alavijeh MS, Chishty M, Qaiser MZ, Palmer AM: Drug metabolism and pharmacokinetics, the blood-brain barrier, and central nervous system drug discovery. NeuroRx 2(4), 554-571 (2005).

37. De Lange EC: The mastermind approach to CNS drug therapy: translational prediction of human brain distribution, target site kinetics, and therapeutic effects. Fluids Barriers CNS 10(1), 12 (2013).

38. Gabathuler R: Approaches to transport therapeutic drugs across the blood-brain barrier to treat brain diseases. Neurobiol Dis 37(1), 48-57 (2010).

39. Gabathuler R: Development of new peptide vectors for the transport of therapeutic across the blood-brain barrier. Ther Deliv 1(4), 571-586 (2010).

40. Stevens J, Ploeger BA, Hammarlund-Udenaes M et al.: Mechanism-based PK-PD model for the prolactin biological system response following an acute dopamine inhibition challenge: quantitative extrapolation to humans. J Pharmacokinet Pharmacodyn 39(5), 463-477 (2012).

41. Westerhout J, Ploeger B, Smeets J, Danhof M, De Lange EC: Physiologically based pharmacokinetic modeling to investigate regional brain distribution kinetics in rats. Aaps J 14(3), 543-553 (2012).

Chapter 3

In Vitro Methods for Assesing the Drug Acces to the Brain

Mangas-Sanjuan, V.[1,2]; Gonzalez-Alvarez, M.[2]; Gonzalez-Alvarez, I.[2]; Bermejo, M.[2]

[1]Pharmaceutics and Pharmaceutical Technology Department. University of Valencia.
[2]Department of Engineering, Pharmaceutics and Pharmaceutical Technology Area. University Miguel Hernández, Elche.

Advances in Non-Invasive Drug Delivery to the Brain
Future Science
Accepted

INTRODUCTION

The success of new CNS drug development can be evaluated in terms of number of new medicines and time needed for their marketing approval. Drugs that affect the CNS have low percentages of success and much time is spent on developing new formulations (10.5 years) [1]. However, CNS therapy is the second largest therapeutic area in the pharmaceutical industry. This discrepancy is mainly attributed to the complexity of the brain, potential side effects of centrally acting agents, and the low predictability of CNS animal models for humans [1]. Therefore, in addition to a better understanding of physiological and pathophysiological conditions of the brain and its diseases, methods are needed that are able to select drug candidates more efficiently in the early preclinical stages.

In silico, *in vitro* and *in vivo* methodologies have been the subject of much research and development in recent years [1-3]. Several *in silico* and *in vivo* methods are accredited and well-established in the development of new drugs. *In vitro* methods are, however, the focus of much debate. There are currently no fully accepted criteria about what is required for an *in vitro* cell line method. There are many factors to take into account in selection of an *in vitro* method: transepithelial resistance of cell monolayers, transporter expression, ease and reproducibility and high ability to screen molecules. *In vitro* methods are however a very useful, even necessary, component of initial preclinical drug discovery. There are significant differences between the different *in vitro* methods in terms of complexity and, consequently, cost and information that each method can provide (Table 1). The development of these methodologies is essential for high throughput screening of molecules that allows the selection of optimal candidates for further evaluation *in*

vivo. *In vitro* methods are not, nor will be, a substitute for the *in vivo* tests, but allow further analysis of molecules, impossible to make *in vivo* due to ethical and economic reasons. It is therefore necessary that *in vitro* systems are capable of simulating the BBB more accurately.

PHYSICOCHEMICAL METHODS FOR BBB

Traditionally, some simple methods have been used to select candidates for central nervous system diseases based on their physiochemical properties. Immobilized artificial membrane chromatography, parallel artificial permeability assays and lipophilicity measurements are the most commonly used.

Immobilized artificial membrane chromatography

Taking into account that transcellular permeation is the main mechanism to cross the BBB, the ability of drugs to cross the membrane can be well-correlated with the membrane partition and, in many cases, with its lipophilicity. The immobilized artificial membrane (IAM) stationary phase is constituted by a monolayer of phosphatidylcoline covalently bound to an inert silica support which is able to simulate the biological cell membrane [4]. A recent study carried out by Grumetto [5], in which interactions between acidic drugs and membrane phospholipids were examined, revealed that IAM technique is suitable to investigate drug membrane interactions and the permeation through the BBB, allowing the opportunity to optimize the pharmacokinetic properties of the candidates at the early stages in some cases.

Table 1 Relevant *in vitro* models and type of information and parameters that can be obtained. Cps: compound. Pers: person

	Physicochemical models		Cellular models			Ex vivo models	
	IAM	**PAMPA models**	**Traditional cell models**	**Stem cells models**	**Tridimensional models**	**Isolated microvessels**	**Brain slices**
Throughput	500 cps/pers/day	100 cps/pers/day	10 cps/pers/day	10 cps/pers/day	Not determined	10-20 cps/pers/month	10 cps/pers/day
Parameters obtained	Partition coefficients aqueous phase/phospholipid	Permeability (cm/s) (passive component)	Permeability (cm/s)	Permeability (cm/s)	Permeability (cm/s)	Permeability (cm/s)	Fu, brain Vu, Brain
Information provided	Partial information of passive diffusion Drug membrane interactions	Passive diffusion	Passive diffusion and transporters contribution BBB functionality	Passive diffusion and transporters contribution BBB functionality	Passive diffusion and transporters contribution BBB functionality	Passive diffusion and transporters contribution Morphological, pathological and biomedical details	Passive diffusion and transporters contribution
Utility for study of effect of disease on BBB	No	No	Possible	Yes	Yes	Yes	No

Parallel artificial permeability assay

Parallel artificial permeability assay (PAMPA) is a high throughput methodology, based on a lipid artificial membrane, useful to predict passive oral absorption. Different modifications have been made over the last years to improve it as a BBB permeabilityscreen [3] but, due to the artificial origin, no transport processes are evaluated and only passive diffusion correlations might be applied. Despite its limitations, PAMPA is able to identify compounds that pass the BBB (CNS+) and those that poorly penetrate the BBB (CNS-). Also, better predictions in brain penetration are observed compared to log D [1, 3] and good correlation with MDCK cell line were obtained in the prediction of the rate of brain penetration [1, 6, 7]. An exhaustive study carried out by Dagenais and colleagues [8] validated PAMPA assays versus *in situ* permeability values, demonstrating that PAMPA assay was able to predict 82% of the variance in the intrinsic BBB permeability. PAMPA assay, and the IAM previously described, can be considered practical, low-cost and high-throughput methods to evaluate BBB passive transport and facilitate chemical optimization of molecules at early stages in order to optimize the CNS drug discovery process.

Lipophilicity measurements

It is well-known that lipophilic compounds cross biological membranes more easily than hydrophilic. For these reason some models have been developed in order to try to predict CNS drug uptake using lipophilicity measurements. n-Octanol partition coefficient can be used for initial screening of passive permeability. From the currently available experimental data, it is possible to establish the lipophilicity

cut off to ensure a passive permeability above 150 nm/s [9]. Taking into account that a poor passive permeability could be compensated by other properties of the compound and that it does not imply necessarily poor brain penetration due to the fact there is no limit in the transit time as it occurs in the gastrointestinal system [10, 11]. In fact, despite more lipophilic derivatives increase the passage across the BBB they also increases the penetration across other biological membranes. More lipophilic derivatives could provide an increase of brain uptake but it coexists with a reduction of the plasma concentration under the curve (AUC) due to the coexistence of an increased clearance of lipophilic forms. It is well known that drug uptake in CNS is function of plasma AUC, so, this factor minimizes the potential increase of drug uptake produced by lipidization of the molecule. This pharmacokinetic rule described by Pardridge [12] indicates that drug passage across the BBB does not correlate well with lipophilic measurements

Another useful tool to predict the brain permeation, thanks to the lipophilicity value, is the brain-plasma (B-P) assay, which is able to predict the *in vivo* brain/plasma (B/P) ratio [13]. This dialysis assay can predict the extent of the drug in the brain, based on the unbound fraction relationship between brain homogenate and buffer and plasma and buffer. The B/P ratio, as the other physicochemical measures described, can be used as an indicative parameter of brain penetration to guide structure modification to obtain derivatives with optimal brain access [1]. The predictability of the B-P assay was enhanced by introducing into the calculation the P-gp efflux ratio from the MDR1-MDCKII assay [14]. Therefore, B/P dialysis is a helpful tool in drug discovery.

EX-VIVO AND CELL-BASED *IN VITRO* METHODS

In order to obtain more reliable predictions, cell-based *in vitro* methods were developed. The quality of the predictions of these methods has been increasing but there is still a way to go in this field.

Isolated brain microvessels.

The *in vitro* isolation of intact brain microvessels (capillaries, venules or arterioles) was a crucial step to study of the morphology, physiology and pathophysiology of the BBB. Isolated microvessels have been used for morphological, pathological, biochemical and drug delivery studies of the BBB and for identification of transporters and membrane receptors. The advantages of isolated capillary systems include the three-dimensional structure, cell differentiation and availability. However, the viability of the endothelium is limited, the isolation procedure is complicated and the isolation protocol can induce metabolic deficiencies. In order to overcome this disadvantages cell culture-based systems were developed and acquired great relevance as *in vitro* models for drug screening.

Isolated brain microvessels have been successfully used to study the expression and activity of transporters. Miller et al [15-17] have used isolated capillaries of rodent or fish to exhaustively study the role of efflux transporters in limiting brain entry, the factors that regulate their expression and the potential targets for inhibition. Results indicate that the expression and activity of efflux transporters are affected by the presence of xenobiotics, diet, stress or disease. Their findings have contributed to understand the mechanisms of the barrier function and have offered opportunities to developed therapies or preventive measures for neurodegenerative diseases and brain cancer.

Primary or low passage brain capillary endothelial cell cultures

The use of brain capillary endothelial cells (BCECs) is one of the most obvious options to predict the brain penetration. Due to the use of human cells is restricted by ethical reasons, bovine or porcine endothelial cells have been selected because of their phenotypic similarity to the human BCECs and their relative viability compared to isolated microvessels [18]. The process involves the isolation of capillaries and culture of endothelial cells alone or in combination with astrocytes or astrocyte-conditioned medium. Assays and analysis show a considerable loss of BBB features on primary cultured cells. For example, there is a down regulation of BBB transporters and enzymes when the endothelial cells are removed from the brain and grown in culture [19].

Tight intercellular junctions are the most important element to consider in an *in vitro* model. Tightness of the monolayer can be evaluated by measuring transendothelial electrical resistance (TEER). Primary culture of brain endothelium alone is not able to achieve high TEER values. So, it is necessary to co-culture with astrocytes [20] which increase the tight junctions and induce the expression of specific BBB biomarkers including GGTP, the glucose transporter isotype (GLUT-1), transferrin receptor and P-glycoprotein (P-gp) [18]. Astrocytes isolated from newborn rats together with bovine or porcine endothelial cells are used as xenogenic co-culture systems, which are very useful in studying drug transport and BBB functionality.

Different co-culture systems have been investigated, as pericytes and fibroblast, neurons, microglia and monocytes or pericytes-astrocytes with endothelial cells in order to improve some properties of the cell model. Pericytes are of special relevance because they are

normally present at the BBB surrounded by the basement membrane and are responsible for inducing specific enzymes. So, it has been argued that pericytes are necessary to establish a cell culture model [21].

The complete procedure to obtain BCECs and the various other cells for co-culture is time consuming. Another disadvantage is that BCECs rapidly de-differentiate *in vitro* and lose the characteristics of BBB endothelial cells after a few passages in culture [22], which produces variability depending on the passage BCECs regarding phenotypic, permeability properties and cell contaminants (pericytes, leptomeningeal cells, smooth muscle cells) [22] [23]. The monitoring criteria to guarantee the quality of monolayers in transport studies include TEER and permeability to hydrophilic markers such as 14C-sucrose, which reflect the degree of tight junction formation. However, BCECs are still not able to reach the *in vivo* conditions (TEER in the range >2 k·Ω·cm^2 ≤ 8 k·Ω·cm^2 [24] and sucrose permeability of approximately $0.3 \cdot 10^{-7}$cm·s^{-1}) [25].

One of the most relevant application of this model has been the use of cultures of primary cells isolated from mice to examine mechanistic aspects of neurological diseases. For example, Miller and coworkers [26] developed a system consists of a coculture with primary cells isolated from mice to study inflammatory events in cerebral endothelium.

Immortalized brain endothelial cells

Due to the disadvantages of primary BCECs described above, different immortalized BCECs have been used to assess endothelial cell uptake of compounds and to perform mechanistic and biochemical studies [23, 27, 28]. Table 2 summarizes the most important

immortalized BCECs and their TEER (transendothelial electrical resistance) values. The development of immortalized BCECs has resulted in more reproducible results with less variation between studies compared to primary BCECs, due to the ease of culture, less contamination and no isolation process and a slower dedifferentiation. However, though immortalized cells lines are useful to overcome the limitations of the primary cultures, they are still limited by the loss of brain barrier phenotype, compared to *in vivo*. The generation of incomplete tight junctions restricts its use for BBB permeability screening. Most of the cell lines have been obtained by transfection of primary rat brain endothelial cells (RBE), including RBE4 cell line, RBEC1 cell line [29] and TR-BBB13 cell line [30]. In order to increase their barrier properties and improve their predictive capacity several different strategies have been used, including addition of phosphodiesterase inhibitors, glucocorticoids or interferons to the media [31, 32]. Due to the increasing number of immortalized RBE cell lines appearing, Roux et al. [22, 33] published a criteria in order to better characterize immortalized BCECs. They consider that the most important characteristics that have to be present in cell lines to better mimic BBB conditions are non-transformed phenotype, the expression of endothelial cell markers and the presence of BBB specific transport proteins.

In contrast to RBEC, a human brain immortalized endothelial (hCMEC/D3) cell line was generated by transfection of the human telomerase or SV40 T antigen. The result is a stable, well characterized and cell differentiated human brain endothelial cell line [34], exhibiting unlimited and robust cell proliferation, tight junctions and efflux transporters expression. Recent proteomic studies demonstrated that

hCMEC/D3 cells retain the expression of most transporters, thus this cell line is useful for examining drug transport across the BBB. However, some differences have been observed compared with isolated human brain microvessels [35].

Table 2 Most important immortalized BCECs lines and TEER values. Adapted from Tetsuya et al, 2003 [36].

Source	Cell line name	TEER value ($k\Omega cm^2$)	Reference
Rat	RBE4	<30	Roux F. et al. [80]
Rat	RBEC1		Kido et al. [81]
Rat	TRBBB	99-109	Hosoya et al. [82]
Rat	GPNT	<30	Weksler B. et al [83]
Mouse	TM-BBBs	105-118	Hosoya et al [84]
Mouse	MBEC4	40-50	Garberg P et al. [14]
Pig	PBMEC	300-550	Zhang et al. [85]
Human	ECV	30	Garberg P et al. [14]
Human	ECV-C6	100	Garberg P et al. [14]
Human	hCMEC/D3	30-40	Weksler B. et al [83]
Human	-	300-400	Stins M.F. et al [86]
Human	TY08	35-43	Sano Y. et al [87]
Dog	MDCK	130-150	Garberg P et al. [14]
Dog	MDCK-MDR1	120-140	Garberg P et al. [14]

Cells of non-cerebral origin

One of the most characterized and used cell line is the Madin-Darby Canine Kidney (MDCK) cell line, which is easy to grow, achieves a reproducible TEER value and can be transfected with the MDR1 gene, resulting in the polarized expression of P-gp [4]. MDR1-transfected MDCK cells have also shown high absorptive transport for CNS(+) drugs and low absorptive transport for CNS(-) drugs [7] and, consequently, may be a suitable model for BBB permeation due to the overexpression of P-gp. This cell line is characterized by a high restrictive paracellular transport [44]. Nevertheless its epithelial origin results in significant differences in morphology metabolic and transport

parameters. Despite these shortcomings a recent study based on a modified set up for MDCK cell experiments has demonstrated its ability to predict $f_{u, plasma}$, $V_{u, brain}$ and $Kp_{,uu, brain}$ (the most relevant parameters for rate and extend of CNS access) which make this model an useful tool at the screening stage [45].

Binding studies in brain slices

Becker and Liu [46] and Friden [47] have proposed a method to estimate free fraction in brain ($f_{u, brain}$) in which they used brain slices instead of brain homogenate. This modification of the technique retains the cellular structure of the brain and, in con¬sequence, any differences between ISF and ICF can be captured in the obtained $f_{u, brain}$ values. This methodology may be applied as a high throughput, evaluating different compounds in the same buffer, which allows to a high screening in the early phases of drug development [47]. However, because the brain slices should be kept in the best possible physiological conditions, it requires controlled experimental conditions and only small brain areas are used in the experimental setup. On the other hand, only when equilibrium between buffer and slices has been achieved, it is possible to measure $f_{u, brain}$ and $V_{u, brain}$.

Endothelial cells derived from pluripotent stem cells

Due to the limitations of the *in vitro* models described above there is still not a fully validated and human-origin *in vitro* model for high-throughput screening of potential CNS candidates. Lippmann and coworkers have developed recently a promising model based on human pluripotent stem cells (hPSCs). They describe how some neural

progenitor cells differentiated to mature neurons and astrocytes that can be used in co-culture to modeling a robust BBB model with excellent barrier properties, expression of transport systems and cells of adequate size. Permeability values obtained from co-cultures of endothelial cells obtained from hPSCs and astrocytes correlate well with *in vivo* brain uptake. Moreover, the versatility of the system to generate barrier models from modified material opens the possibility of investigating the development, regulation and drug access in disease conditions [48].

Tridimensional hollow-fiber BBB model

Traditional techniques for mimicking the BBB described above are based on static two chamber systems separated by a cell monolayer grown on a polycarbonate membrane that represents the barrier. These static models have limitations mainly because they do not reproduce the anatomical and physiological features of the blood-brain-barrier and, most of them, provide poor correlations with *in vivo* data. In order to address these limitations, dynamic *in vitro* models with tridimensional architecture were developed to reproduce more accurately the physiological features of the brain vascular segments and to take into account the blood flow in the prediction of brain permeation. In these systems, cell lines are cultured in the lumen of the tridimensional hollow fibers and exposed to flow and in the second compartment astrocytes are seeded providing a strong BBB model. This approach, used successfully by different research groups with different cell lines, has allowed an increase of the knowledge and predictability in CNS drug development [49, 50]. Studies carried out by Cucullo et al. have confirmed by genomic and proteomic analysis that physiological

environment (included mechanical stimuli) is crucial for the differentiation of endothelial cells [51]. Their research has provided evidence of the importance of the shear stress in the formation and maintenance of BBB features, suggesting that changes in the flow could play a role in neurological diseases. Subsequently, this system has been refined in order to establish a dynamic capillary-venule system capable of reproducing more accurately different vascular segments of the brain vascular network [52]. The main goal of this model is to explore the cerebrovascular response to pathophysiological stimuli and develop therapeutic strategies for neurological pathologies including epilepsy [53]. Moreover, this technical approach could be combined with the hPSC-derived BMECs to better mimic physiological conditions and improve the relevance and predictive power of the preclinical screens [54].

Microfluidic blood brain barrier model

Despite their many advantages conventional dynamic *in vitro* BBB models lack a thin dual cell layer interface. To overcome this limitation microfluidic *in vitro* models have been recently designed and developed. They are constituted by a microfluidic chip with microcirculation sized two-compartment chamber. Endothelial cells are seeded in the apical compartment and media or support neuronal cells are placed in the basolateral one. The devices have sufficient key characteristics to be considered a good model useful for studies of BBB function or drug delivery. It has many advantages such as low cost, controlled growth conditions and dynamic microenvironment with shear stress stimulation. Effectively, this method mimics the

cerebrovascular environment and thinner culture membrane even better than tridimensional models. Booth and Kim [55] developed a microfluidic BBB in where cultured b.End3 endothelial cells with and without co-cultured C6-D1A astrocytes in order to reproduce the BBB microenvironment. Prabhakarpandian et al [56] designed a similar system called "Synthetic Microvasculature Model of the blood-Brain-Barrier" which used the rat brain endothelial cell line (RBE4) and a perfusate of astrocyte conditioned media. Griep et al [57] have reported a promising microfluidic chip with immortalized human brain endothelial cell line hCMEC/D3. These realistic models are versatile and, for this reason, suitable to study barrier function and dysfunction and evaluate drug delivery in pathological and non-pathological conditions

CONCLUSIONS

In the CNS drug development, the main objective is to achieve free drug concentrations sufficient to obtain the desired therapeutic effect. According to the free (or unbound) drug hypothesis, unbound drug plasma concentration is directly related to unbound drug brain concentration and in consequence high plasma protein binding can reduce unbound concentration in the brain [1]. On the other hand, if there is any active process involved in the drug permeation across the BBB this relationship is no longer direct. Therefore, the three major factors governing free concentrations in brain are: BBB permeability, P-gp efflux transport, and plasma protein and brain tissue binding [1]. These characteristics must be represented in the model selected *in vitro*, in order to predict more accurately the drug access to the CNS.

High BBB permeability is important in achieving rapid onset. But there is also a practical upper limit of convenient or adequate BBB permeability (e.g., > 15 cm/s in MDCK). Extremely high permeability can be counterproductive owing to increased non-specific binding and, consequently, lower unbound drug concentration in the brain. BBB permeability for screening purposes can be measured by *in vitro* methods such as PAMPA-BBB or MDCK assays.

P-gp efflux is a major obstacle for brain penetration. Compounds with a high P-gp efflux ratio have low chance to become successful CNS agents. Conversely, P-gp efflux characteristics are beneficial for non-CNS therapies to limit CNS side effects. Saturation of P-gp at the BBB is unlikely. P-gp efflux is mostly species independent with some exceptions. MDR1-MDCKII and MDR1a/1b double knockout mouse models are effective tools to detect P-gp efflux mechanisms.

Tissue binding studies (to estimate the distribution volume in brain Vu) need *in vivo* methods or *in vitro* models as brain slices but there are preliminary promising results with some cell culture studies [45].

On the other hand some new approaches as cultures based on pluripotent stem cells or three-dimension models could add the advantage of rendering kinetic parameters (as permeability values) while also informing about the effect of pathological and physiological changes as transporters expression levels, alteration of the barrier properties or blood flow changes. Ultimately there will not be a single *in vitro* model but their selections have to be based on the final purpose, either screening of candidates or a mechanistic study for new drug design.

FUTURE PERSPECTIVES

In the early phases of CNS drug development, still many questions have to be answered using different methodologies thus making complicate the high throughput screening of candidates. *In vitro* methods have been recognized in their capability to predict the drug access rate into the brain, the role of different transporters in drug permeation and the relevance of some biomarkers in the signal transduction but the measurement of the extent and the drug brain distribution require separate experimental systems. A whole *in vitro* single system able to provide a complete characterization of the relevant drug parameters would be a relevant improvement for accelerating candidate screening. On the other hand, more research is necessary to obtain more reliable and stable *in vitro* cell lines reflecting either the healthy and ill brain conditions. These new *in vitro* systems have to be able to test the efficacy of the new technologies to cross the BBB thus, it would be desirable a flexible system with a tunable enzymatic and transporter expression levels. Finally, to fully exploit the *in vitro* results their integration in physiology-based pharmacokinetic-pharmacodynamic models would lead to obtain clinically relevant outputs (i.e. plasma and brain time profiles and concentration effect relationships) and to reduce the attrition rate.

EXECUTIVE SUMMARY

- There are no fully accepted criteria about what *in vitro* methods are the most convenient for predicting rate and extend of drug access to the brain.
- Simple methods based on the physicochemical properties as Immobilized artificial membrane chromatography, parallel artificial

permeability assays and lipophilicity measurements are the most commonly used in early screening but are mainly useful for compounds transported by passive diffusion.

- Isolated microvessels have three dimensional structure, differentiation and availability. They are useful to study morphological aspects, the expression and activity of transporters and carry out drug delivery assays.
- Primary or low passage brain capillary endothelial cell cultures are not able to retain blood brain barrier properties. Co cultures with astrocytes and pericytes are time consuming and still do not fully reproduce *in vivo* conditions.
- Immortalized brain endothelial cells of animal and human origin have been developed, resulting in easy culture cell lines, no isolation needed and less contamination observed. However, low tight junctions were obtained which limits its application in permeability studies.
- Among the cultures with cells of non-cerebral origin, MDCK and MDCK-MDR1 are the most promising cell lines thanks to their high TEER values and the possibility of obtaining stably transfected clones with the transporter of interest.
- Controlled and standardized Brain slices experiments allow the measurement of $f_{u,\ brain}$ and $V_{u\ ,brain}$. This model may be used in a high throughput mode and has the advantage of capturing the differences between ISF and ICF.
- Endothelial cells derived from pluripotent stem cells constitute a promising approach of human origin. Co-cultures of mature neurons and astrocytes provide a robust BBB model useful to study physiological and pathological aspects of the BBB and drug access in disease conditions.

- Tridimensional hollow-fiber models reproduce more accurately the physiological features of the brain vascular segments and allow exploring the response to pathophysiological stimuli.
- Microfluidic blood brain barrier models are realistic and versatile devices suitable to mimic the cerebrovascular environment. They are promising models to study barrier function and dysfunction and evaluate drug delivery in pathological and non-pathological conditions.

ACKNOWEDGEMENT

The authors acknowledge to projects: DCI ALA/19.09.01/10/21526/245-297/ALFA 111(2010)29: Red-Biofarma. Red para el desarrollo de metodologias biofarmaceuticas racionales que incrementen la competencia y el impacto social de las Industrias Farmaceuticas Locales. AGL2011-29857-C03-03 (Spanish Ministry of Science and Innovation).

Victor Mangas-Sanjuan acknowledges to the Ministry of Education and Science of Spain and Miguel Hernandez University for a FPU grant (FPU AP2010-2372).

REFERENCES

1. Di L, Kerns EH, Carter GT: Strategies to assess blood-brain barrier penetration. Expert Opin Drug Discov 3(6), 677-687 (2008).
2. Abbott NJ, Dolman DE, Patabendige AK: Assays to predict drug permeation across the blood-brain barrier, and distribution to brain. Curr Drug Metab 9(9), 901-910 (2008).
3. Avdeef A, Bendels S, Di L et al.: PAMPA--critical factors for better predictions of absorption. J Pharm Sci 96(11), 2893-2909 (2007).

4. Nicolazzo JA, Charman SA, Charman WN: Methods to assess drug permeability across the blood-brain barrier. J Pharm Pharmacol 58(3), 281-293 (2006).

5. Grumetto L, Carpentiero C, Di Vaio P, Frecentese F, Barbato F: Lipophilic and polar interaction forces between acidic drugs and membrane phospholipids encoded in IAM-HPLC indexes: their role in membrane partition and relationships with BBB permeation data. J Pharm Biomed Anal 75, 165-172 (2013).

6. Carrara S, Reali V, Misiano P, Dondio G, Bigogno C: Evaluation of *in vitro* brain penetration: optimized PAMPA and MDCKII-MDR1 assay comparison. Int J Pharm 345(1-2), 125-133 (2007).

7. Wang Q, Rager JD, Weinstein K et al.: Evaluation of the MDR-MDCK cell line as a permeability screen for the blood-brain barrier. Int J Pharm 288(2), 349-359 (2005).

8. Dagenais C, Avdeef A, Tsinman O, Dudley A, Beliveau R: P-glycoprotein deficient mouse *in situ* blood-brain barrier permeability and its prediction using an in combo PAMPA model. Eur J Pharm Sci 38(2), 121-137 (2009).

9. Mahar Doan KM, Wring SA, Shampine LJ et al.: Steady-state brain concentrations of antihistamines in rats: interplay of membrane permeability, P-glycoprotein efflux and plasma protein binding. Pharmacology 72(2), 92-98 (2004).

10. Friden M, Winiwarter S, Jerndal G et al.: Structure-brain exposure relationships in rat and human using a novel data set of unbound drug concentrations in brain interstitial and cerebrospinal fluids. J Med Chem 52(20), 6233-6243 (2009).

11. Reichel A: Addressing central nervous system (CNS) penetration in drug discovery: basics and implications of the evolving new concept. Chem Biodivers 6(11), 2030-2049 (2009).

12. Pardridge WM: The blood-brain barrier: bottleneck in brain drug development. NeuroRx 2(1), 3-14 (2005).

13. Kalvass JC, Maurer TS: Influence of nonspecific brain and plasma binding on CNS exposure: implications for rational drug discovery. Biopharm Drug Dispos 23(8), 327-338 (2002).

14. Summerfield SG, Stevens AJ, Cutler L et al.: Improving the *in vitro* prediction of *in vivo* central nervous system penetration: integrating permeability, P-glycoprotein efflux, and free fractions in blood and brain. J Pharmacol Exp Ther 316(3), 1282-1290 (2006).

15. Durk MR, Chan GN, Campos CR et al.: 1alpha,25-Dihydroxyvitamin D3-liganded vitamin D receptor increases expression and transport activity of P-glycoprotein in isolated rat brain capillaries and human and rat brain microvessel endothelial cells. J Neurochem 123(6), 944-953 (2012).

16. Miller DS: Confocal imaging of xenobiotic transport across the blood-brain barrier. J Exp Zool A Comp Exp Biol 300(1), 84-90 (2003).

17. Miller DS: Regulation of P-glycoprotein and other ABC drug transporters at the blood-brain barrier. Trends Pharmacol Sci 31(6), 246-254 (2010).

18. Grant GA, Abbott NJ, Janigro D: Understanding the Physiology of the Blood-Brain Barrier: *In Vitro* Models. News Physiol Sci 13, 287-293 (1998).

19. Calabria AR, Shusta EV: A genomic comparison of *in vivo* and *in vitro* brain microvascular endothelial cells. J Cereb Blood Flow Metab 28(1), 135-148 (2008).

20. Gaillard PJ, De Boer AB, Breimer DD: Pharmacological investigations on lipopolysaccharide-induced permeability changes in the blood-brain barrier *in vitro*. Microvasc Res 65(1), 24-31 (2003).

21. Kim JA, Tran ND, Li Z, Yang F, Zhou W, Fisher MJ: Brain endothelial hemostasis regulation by pericytes. J Cereb Blood Flow Metab 26(2), 209-217 (2006).

22. Roux F, Couraud PO: Rat brain endothelial cell lines for the study of blood-brain barrier permeability and transport functions. Cell Mol Neurobiol 25(1), 41-58 (2005).

23. Mensch J, Oyarzabal J, Mackie C, Augustijns P: *In vivo*, *in vitro* and *in silico* methods for small molecule transfer across the BBB. J Pharm Sci 98(12), 4429-4468 (2009).

24. Butt AM, Jones HC, Abbott NJ: Electrical resistance across the blood-brain barrier in anaesthetized rats: a developmental study. J Physiol 429, 47-62 (1990).

25. Bickel U: How to measure drug transport across the blood-brain barrier. NeuroRx 2(1), 15-26 (2005).

26. Coisne C, Dehouck L, Faveeuw C et al.: Mouse syngenic *in vitro* blood-brain barrier model: a new tool to examine inflammatory events in cerebral endothelium. Lab Invest 85(6), 734-746 (2005).

27. Toimela T, Maenpaa H, Mannerstrom M, Tahti H: Development of an *in vitro* blood-brain barrier model-cytotoxicity of mercury and aluminum. Toxicol Appl Pharmacol 195(1), 73-82 (2004).

28. Lauer R, Bauer R, Linz B et al.: Development of an *in vitro* blood-brain barrier model based on immortalized porcine brain microvascular endothelial cells. Farmaco 59(2), 133-137 (2004).

29. Nagasawa K, Ito S, Kakuda T et al.: Transport mechanism for aluminum citrate at the blood-brain barrier: kinetic evidence implies involvement of system Xc- in immortalized rat brain endothelial cells. Toxicol Lett 155(2), 289-296 (2005).

30. Tetsuka K, Takanaga H, Ohtsuki S, Hosoya K, Terasaki T: The l-isomer-selective transport of aspartic acid is mediated by ASCT2 at the blood-brain barrier. J Neurochem 87(4), 891-901 (2003).

31. Gaillard PJ, Voorwinden LH, Nielsen JL et al.: Establishment and functional characterization of an *in vitro* model of the blood-brain barrier,

comprising a co-culture of brain capillary endothelial cells and astrocytes. Eur J Pharm Sci 12(3), 215-222 (2001).

32. Tan KH, Dobbie MS, Felix RA, Barrand MA, Hurst RD: A comparison of the induction of immortalized endothelial cell impermeability by astrocytes. Neuroreport 12(7), 1329-1334 (2001).

33. Couraud PO, Greenwood J, Roux F, Adamson P: Development and characterization of immortalized cerebral endothelial cell lines. Methods Mol Med 89, 349-364 (2003).

34. Weksler BB, Subileau EA, Perriere N et al.: Blood-brain barrier-specific properties of a human adult brain endothelial cell line. Faseb J 19(13), 1872-1874 (2005).

35. Ohtsuki S, Ikeda C, Uchida Y et al.: Quantitative targeted absolute proteomic analysis of transporters, receptors and junction proteins for validation of human cerebral microvascular endothelial cell line hCMEC/D3 as a human blood-brain barrier model. Mol Pharm 10(1), 289-296 (2013).

36. Terasaki T, Ohtsuki S, Hori S, Takanaga H, Nakashima E, Hosoya K: New approaches to *in vitro* models of blood-brain barrier drug transport. Drug Discov Today 8(20), 944-954 (2003).

37. Kido Y, Tamai I, Okamoto M, Suzuki F, Tsuji A: Functional clarification of MCT1-mediated transport of monocarboxylic acids at the blood-brain barrier using *in vitro* cultured cells and *in vivo* BUI studies. Pharm Res 17(1), 55-62 (2000).

38. Hosoya KI, Takashima T, Tetsuka K et al.: mRna expression and transport characterization of conditionally immortalized rat brain capillary endothelial cell lines; a new *in vitro* BBB model for drug targeting. J Drug Target 8(6), 357-370 (2000).

39. Hosoya K, Tetsuka K, Nagase K et al.: Conditionally immortalized brain capillary endothelial cell lines established from a transgenic mouse harboring temperature-sensitive simian virus 40 large T-antigen gene. AAPS PharmSci 2(3), E27 (2000).

40. Garberg P, Ball M, Borg N et al.: *In vitro* models for the blood-brain barrier. Toxicol *In Vitro* 19(3), 299-334 (2005).

41. Zhang Y, Li CS, Ye Y et al.: Porcine brain microvessel endothelial cells as an *in vitro* model to predict *in vivo* blood-brain barrier permeability. Drug Metab Dispos 34(11), 1935-1943 (2006).

42. Stins MF, Badger J, Sik Kim K: Bacterial invasion and transcytosis in transfected human brain microvascular endothelial cells. Microb Pathog 30(1), 19-28 (2001).

43. Sano Y, Shimizu F, Abe M et al.: Establishment of a new conditionally immortalized human brain microvascular endothelial cell line retaining an *in vivo* blood-brain barrier function. J Cell Physiol 225(2), 519-528 (2010).

44. Di L, Kerns EH: Methods for Assissing Blood-Brain Barrier Penetration in Drug Discovery. In: ADME-Enabling Technologies in Drug Design and Development, Zhang D,Surapaneni S (Ed.^(Eds). Wiley and Sons, 169-174 (2012).

45. Mangas-Sanjuan V, Gonzalez-Alvarez I, Gonzalez-Alvarez M, Casabo VG, Bermejo M: Innovative *in Vitro* Method To Predict Rate and Extent of Drug Delivery to the Brain across the Blood-Brain Barrier. Mol Pharm 10(10), 3822-3831 (2013).

46. Becker S, Liu X: Evaluation of the utility of brain slice methods to study brain penetration. Drug Metab Dispos 34(5), 855-861 (2006).

47. Friden M, Ducrozet F, Middleton B, Antonsson M, Bredberg U, Hammarlund-Udenaes M: Development of a high-throughput brain slice method for studying drug distribution in the central nervous system. Drug Metab Dispos 37(6), 1226-1233 (2009).

48. Lippmann ES, Azarin SM, Kay JE et al.: Derivation of blood-brain barrier endothelial cells from human pluripotent stem cells. Nat Biotechnol 30(8), 783-791 (2012).

49. Neuhaus W, Lauer R, Oelzant S, Fringeli UP, Ecker GF, Noe CR: A novel flow based hollow-fiber blood-brain barrier *in vitro* model with immortalised cell line PBMEC/C1-2. J Biotechnol 125(1), 127-141 (2006).

50. Santaguida S, Janigro D, Hossain M, Oby E, Rapp E, Cucullo L: Side by side comparison between dynamic versus static models of blood-brain barrier *in vitro*: a permeability study. Brain Res 1109(1), 1-13 (2006).

51. Cucullo L, Hossain M, Puvenna V, Marchi N, Janigro D: The role of shear stress in Blood-Brain Barrier endothelial physiology. BMC Neurosci 12, 40 (2011).

52. Cucullo L, Hossain M, Tierney W, Janigro D: A new dynamic *in vitro* modular capillaries-venules modular system: cerebrovascular physiology in a box. BMC Neurosci 14, 18 (2013).

53. Cucullo L, Hossain M, Rapp E, Manders T, Marchi N, Janigro D: Development of a humanized *in vitro* blood-brain barrier model to screen for brain penetration of antiepileptic drugs. Epilepsia 48(3), 505-516 (2007).

54. Lippmann ES, Al-Ahmad A, Palecek SP, Shusta EV: Modeling the blood-brain barrier using stem cell sources. Fluids Barriers CNS 10(1), 2 (2013).

55. Booth R, Kim H: Characterization of a microfluidic *in vitro* model of the blood-brain barrier (muBBB). Lab Chip 12(10), 1784-1792 (2012).

56. Prabhakarpandian B, Shen MC, Nichols JB et al.: SyM-BBB: a microfluidic Blood Brain Barrier model. Lab Chip 13(6), 1093-1101 (2013).

57. Griep LM, Wolbers F, De Wagenaar B et al.: BBB on chip: microfluidic platform to mechanically and biochemically modulate blood-brain barrier function. Biomed Microdevices 15(1), 145-150 (2013).

Chapter 4

Modified Non-Sink Equation for Permeability Estimation in Cell Monolayers: Comparison with Standard Methods

Mangas-Sanjuan, V.[1,2]; Gonzalez-Alvarez, M.[2]; Gonzalez-Alvarez, I.[2]; Casabo, VG.[1,ω]; Bermejo, M.[2]

[1]Pharmaceutics and Pharmaceutical Technology Department. University of Valencia.
[2]Department of Engineering, Pharmaceutics and Pharmaceutical Technology Area. University Miguel Hernández, Elche.
[ω]Deceased, July 7, 2013.

Molecular Pharmaceutics, 2014, March 25
DOI: 10.1021/mp400555e
Accepted

INTRODUCTION

The relevance of cell culture permeation assays in drug development

Drug development can be evaluated in terms of success rate and time to market of new drug products. Obtaining molecules with high activity does not warrant their effectiveness *in vivo* because the drug must achieve therapeutic concentrations at the sites of action. The access to the therapeutic targets implies crossing biological barriers. This question is of great relevance especially in two groups of drug products: 1) Oral drug products in which the drug must be absorbed through the intestinal barrier to reach the systemic circulation and 2) those drugs whose sites of action are located in the so-called "drug sanctuaries" as the Central Nervous System (CNS) that must cross a blood-brain tight barrier.

Oral route is the preferred one in terms of patient compliance [1]. However, not all the drugs are suitable for oral administration. Drug dissolution and permeation through the intestinal membrane are the essential steps to reach the systemic circulation, consequently solubility and permeability are two of the key biopharmaceutical properties that determines drug product "developability". In 1995, Amidon et al. developed the Biopharmaceutics Classification System (BCS) [2] as a framework to classify drugs and to forecast *in vivo* drug product performance from *in vitro* data (i.e. permeability solubility and dissolution rate). The FDA in 2000 presented the guideline for waiver of *in vivo* bioavailability and bioequivalence studies for immediate-release solid oral dosage forms based on the Biopharmaceutics Classification System (BCS) [3] in which an exemption of *in vivo* bioequivalence studies ("biowaiver") can be requested for comparison

of drug products containing class 1 drugs. Class 1 drugs are those exhibiting high permeability (defined as an oral fraction absorbed >90%) and high solubility. EMA [4] and WHO [5] established the cut off for drug high permeability when the oral fraction absorbed is ≥85%. FDA accepts *in vitro* estimation of permeability using assays in cell monolayers as a method for permeability classification under certain conditions, i.e., passively absorbed drugs, epithelial cell monolayers, and the demonstrated suitability of the assay [3]. However EMA and WHO consider *in vitro* permeability estimations only as supportive data [4, 5].

On the other hand CNS drugs have in general lower success rates and longer development times (10.5 years) [6-9] than in other therapeutic areas because of the complexity of the brain, the blood brain barrier and the low predictability of CNS animal models.6 For these reasons many groups are working on the development of predictive preclinical models [10-26].

Recently an innovative *in vitro* method to predict rate and extent of drug delivery to the brain across the Blood-Brain Barrier has been published by our group [27]. The system permits the estimation of $f_{u, plasma}$, $V_{u, brain}$ and $Kp_{,uu, brain}$ in a single experimental system, using *in vitro* cell monolayers in different conditions.

In summary, cell culture permeability experiments are very valuable tools in drug development and candidate selection in the preclinical stage and also in clinical phases and generic development. A cell monolayer permeability assay consists of two chambers separated by a porous support material in which a single cell thickness layer of cells grows until confluence is attained and sufficient cell differentiation is reached. The drug solution is placed in one of the chambers and samples are taken in the opposite chamber at different times in order to

estimate permeability. The monolayer preparation protocols (seeding density, growth time, media composition and change frequency), the experimental conditions (apical and basolateral media composition, filter porosity, agitation conditions, temperature etc.) and the calculations procedures can affect the permeability estimation. Hence, standardization and method suitability demonstration are necessary steps for using permeability data for regulatory purposes.

Permeability estimation methods

The permeability is calculated from the drug concentrations and accumulated amounts in acceptor chamber using either linear or nonlinear regression models, depending of the assumption about sink conditions on the receptor side [28, 29]. Tavelin et al. [29] described the different profiles that are usually observed between accumulated amounts of drug in the acceptor side versus time. Three examples of these profiles are represented in Figure 1.

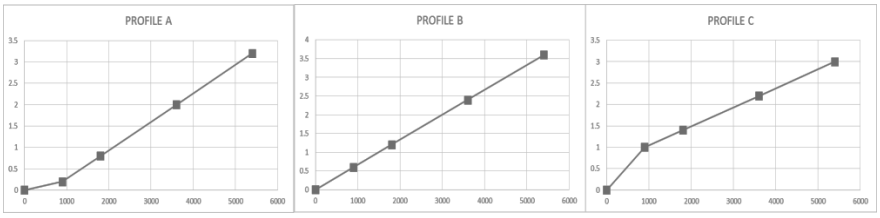

Figure 1. Profiles of accumulated amounts of drug in acceptor chamber versus time in permeability experiments in cell monolayers. Profile A: Drug is transported during the first sampling interval at a lower rate than expected; Profile B: Drug is transported linearly with a constant rate; Profile C: Drug is transported at a higher rate during the first sampling interval.

Tavelin et al. [28] highlighted the existence of atypical profiles (Profiles A and C on Figure 1) and explained the possible reasons to these profiles. Profile A may be caused by poor temperature control at

the beginning of the experiment, or by the fact that partitioning of the drug into the cell monolayer is the rate-limiting step. Profile C is sometimes observed when the transport of radiolabeled drugs is studied. The reason may be that radiolabeled low molecular weight impurities (such as 3H-water) are present in the drug solution and are transported at a higher rate than the drug. Another reason may be that the cell monolayer is affected by a too harsh application of the drug solution. In such cases, the estimation of the permeability by the standard linear regression methods or even non-linear regression methods may not be correct. Therefore, a good estimation of permeability is needed to correctly classify drugs under BCS criteria.

Simulation is an important tool for the evaluation of pharmacokinetic models that allows analyzing different scenarios and a more efficient decision making during drug development [30-38]. Regulatory agencies, FDA and EMA, encourage model simulation as a tool to increase predictability and efficiency in preclinical and clinical phases [39-41].

The aim of this study was to use a simulation strategy to explore the performance of a Modified Non-Sink equation, MNS; (in terms of precision and accuracy) for permeability estimation in different types of profiles and scenarios of variability, to compare the new proposed model with the classical sink and non-sink approaches and to explore its usefulness for BCS classification. Data from cell culture experiments representing the different experimental profiles have been analyzed with all the equations to validate the new approach. The limitations ad advantages of the MNS equation are discussed.

MATERIAL AND METHODS

Permeability calculations

Sink (S) equation

Permeability values in sink conditions are estimated from the first Fick's law equation under the assumption of sink condition (i.e. negligible drug concentration in acceptor versus donor or in mathematical terms acceptor concentration<10% of donor concentration), no change of drug donor concentration during the assay and under a linear approximation of the appearance rates.

$$P_{eff} = ({}^{dQ}/_{dt})/S \cdot C_0 \quad (1)$$

where dQ/dt is the apparent appearance rate of drug in the receiver side, calculated using linear regression of amounts in the receiver chamber versus time, S is the surface area of the monolayer C0 is the drug concentration in the donor chamber and P_{eff} is the permeability value. When the transport rate is low, neither the donor nor the receiver concentrations will change significantly with time, and sink conditions are assumed as a reasonable approximation.

Sink Corrected (SC) equation

Artursson et al. proposed a modified equation, in order to avoid the limitations of classical equation of sink conditions because even under sink conditions the change in donor concentration affects to the driving force and may not be negligible. In this new equation the concentration in the donor chamber changes in each sample interval [28].

$$P_{eff} = ({}^{dQ}/_{dt})/S \cdot C_D \quad (2)$$

where C_D is the concentration in the donor chamber at each sample interval.

Non-sink (NS) equation

Under non sink conditions, the apparent permeability coefficient was calculated according the following equation:

$$C_{receiver,t} = \frac{Q_{total}}{V_{receiver}+V_{donor}} + \left(\left(C_{receiver,t-1} \cdot f \right) - \frac{Q_{total}}{V_{receiver}+V_{donor}} \right) \cdot e^{-P_{eff} \cdot S \cdot \left(\frac{1}{V_{receiver}} + \frac{1}{V_{donor}} \right) \cdot \Delta t} \quad (3)$$

where $C_{receiver,t}$ is the drug concentration in the receiver chamber at time t, Q_{total} is the total amount of drug in both chambers, $V_{receiver}$ and V_{donor} are the volumes of each chamber, $C_{receiver,t-1}$ is the drug concentration in receiver chamber at previous time, f is the sample replacement dilution factor, S is the surface area of the monolayer, Δt is the time interval and P_{eff} is the permeability coefficient. This equation considers a continuous change of the donor and receiver concentrations, and it is valid in either sink or non-sink conditions. The curve-fitting is performed by nonlinear regression, by minimization of the Sum of Squared Residuals (SSR), where:

$$SSR = \sum \left[C_{r,i,obs} - C_{r,i}(t_{end,i}) \right]^2 \quad (4)$$

$C_{r,i,obs}$ is the observed receiver concentration at the end of interval i, and $C_{r,i(tend,i)}$ is the corresponding concentration at the same time calculated according to Eq. 3 [42].

New proposed equation: Modified Non-Sink (MNS)

$$C_{receiver,t} = \frac{Q_{total}}{V_{receiver}+V_{donor}} + \left(\left(C_{receiver,t-1} \cdot f \right) - \frac{Q_{total}}{V_{receiver}+V_{donor}} \right) \cdot e^{-\mathbf{P_{eff\,0,1}} \cdot S \cdot \left(\frac{1}{V_{receiver}} + \frac{1}{V_{donor}} \right) \cdot \Delta t} \quad (5)$$

where all the terms are defined in the previous equation and P_{eff} is the permeability coefficient, which might be $P_{eff\ 0}$ or $P_{eff\ 1}$. This equation, as equation 3 considers a continuous change of the donor and receiver concentrations, and it is valid in either sink or non-sink conditions. The new feature is the option to estimate two permeability coefficients ($P_{eff\ 0}$ and $P_{eff\ 1}$) to account for the atypical profiles A and C in which the initial rate is different.

The non-linear regressions to fit equation 3 (NS) and 5 (MNS) to data can be performed in Excel using Solver tool for minimization of the Sum of Squared Residuals. Equation 1 (S) and equation 2 (SC) are linear regression models that can be also executed in Excel.

Model Validation

Simulation step

In order to validate the modification in the Non-sink equation, different scenarios were simulated. 1000 experiments, 3 wells per experiment were generated combining different initial setups. Simulated data were obtained using Modified Non-sink (MNS) equation 5. Simulations have been performed with MSN equation that is the more general case but when $P_{eff\ 0} = P_{eff\ 1}$ it matches the Non-sink equation. Moreover when $P_{eff\ 0}$ (= $P_{eff\ 1}$) is small, sink conditions prevails, then sink experiments have been also simulated. In other words, changing the parameters in the MSN model, that is a generalized model is equivalent to performing simulations with non-sink model (when $P_{eff\ 0} = P_{eff\ 1}$), sink model (when permeability is small) and MSN. Simulated data analysis in this case, permits evaluate which of the equations is able

to grasp the atypical profiles and to render a permeability estimation closer to the "real or true" one.

Preset conditions during the simulation step are the user-defined parameters values. All values are summarized in Table 1-2. Data were simulated either in sink (Table 1) or non-sink (Table 2) conditions. Samples times were established to be 900, 1800, 3600 and 5400 sec. Inter-individual (inter-well) variability was added to the set permeability value and residual variability was added to the simulated concentrations. Variability in both cases followed an exponential error model (equation 6-7). For each well, an individual permeability was assigned, depending on the coefficient of variation (CV) defined in each scenario of variability. A combination of high (H=20% CV) or low (L=5% CV) interindividual and residual variability were selected in order to evaluate four different variability combinations.

$$\theta_i = \theta_p \cdot e^{\eta} \quad \eta \in N(0, \omega^2) \tag{6}$$

$$y_i = y_p \cdot e^{\varepsilon} \quad \varepsilon \in N(0, \sigma^2) \tag{7}$$

$\mathbf{P_{eff\,0}\,(cm/s)}$	$\mathbf{10^{-8}}$	$\mathbf{10^{-6}}$	$\mathbf{5{\cdot}10^{-6}}$
$P_{eff\,1}$ (cm/s)	10^{-6}	10^{-6}	10^{-6}
C_0 (μM)		100	
V_D (mL)		2	
V_R (mL)		3	
V_S (mL)		0.2	

Table 1. Parameter values of the preset conditions in Sink conditions.

$P_{eff\,0}$ (cm/s)	10^{-8}	$5{\cdot}10^{-5}$	10^{-4}
$P_{eff\,1}$ (cm/s)	$5{\cdot}10^{-5}$	$5{\cdot}10^{-5}$	$5{\cdot}10^{-5}$
C_0 (μM)		100	
V_D (mL)		2	
V_R (mL)		3	
V_S (mL)		0.2	

Table 2. Parameter values of the preset conditions in Non-sink conditions.

Permeability estimation

Permeability values were estimated from simulated concentrations in the receiver chamber, obtained in the previous step, using four different equations: Modified Non-sink (MNS) (equation 5), Non-sink (NS) (equation 3), Sink (S) (equation 1) and Corrected Sink (SC) (equation 2). The permeability coefficient estimations in sink and non-sink conditions were carried out in an Excel® worksheet.

Validation of model with experimental data.

MDCKII cells were grown in Dubelcco's Modified Eagle's Media containing L-glutamine, fetal bovine serum and penicillin-streptomycin. Each two days the media was replaced. Cells monolayers were prepared by seeding 400000 cells/cm^2 on a polycarbonate membrane which surface area was 4.2 cm^2. They were maintained at 37°C temperature, 90% humidity and 5% CO_2 and medium was replaced each two days until confluence (7-9 days). Afterwards, the integrity of the each cell monolayer was evaluated by measuring the trans-epithelial electrical resistance (TEER). In experiment Hank's balanced salt solution (HBSS) supplemented with HEPES was used to

fill the receiver chamber and to prepare the drug solution that was placed in the donor chamber after adjusting pH to 7.

Transport studies were conducted in an orbital environmental shaker at constant temperature (37°C) and agitation rate (50 rpm). *In vitro* studies were performed in both directions, from apical-to-basal (AB) and from basal-to-apical (BA) sides. The volume was 2 mL and 3 mL in apical and basolateral chamber respectively. Four samples of 200 μL each one were taken, and replaced each time with HBSS supplemented with HEPES from the receiver side at 15, 30, 45 and 90 minutes. Samples of the donor side were taken at the beginning and the end of the experiment. Moreover, the amount of compound in cell membranes and inside the cells was determined at the end of experiments in order to check the mass balance and the percentage of compound retained in the cell compartment (always less than 5%.)

Drugs used were Metoprolol, Caffeine, Verapamil, Zidovudine Atenolol and Norfloxacin. They were selected for having high or moderate permeability values (Metoprolol, Caffeine and Verapamil) or low ones (Zidovudine Atenolol and Norfloxacin) to obtain sink and non-sink conditions on the experimental system. Samples were analyzed by a validated HPLC procedure previously described [43].

Individual profiles of amounts or concentrations in acceptor chamber were carefully examined to identify atypical ones. Approximately 10% of the wells presented some degree of deviation from linearity (amount/concentration versus time profiles). Some examples and the result of their analysis are shown in Figure 2.

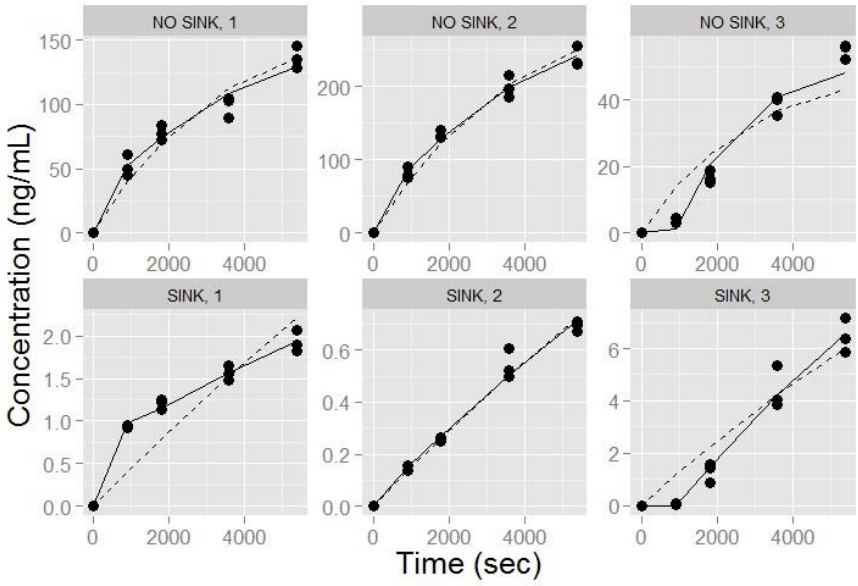

Figure 2. Concentrations in acceptor chamber versus time on individual wells for the following compounds Metoprolol, Caffeine, Verapamil, (no sink 1; no sink 2 and no sink 3 respectively) Zidovudine, Atenolol and Norfloxacin (sink 1; sink 2 and sink 3). Red line corresponds to the fit of the non-sink equation and the blue one is the fit of the MNS model to the data.

Graphical analysis

Receiver simulated concentrations are plotted versus population predicted concentrations obtained by NS and MNS equations. Plots were obtained using S-Plus 6.0 and RStudio using R version 2.14.

Estimation error

Once permeability coefficients were estimated for each well with the different methods, the average permeability of the experiment was calculated as the arithmetic mean of the three individual well permeability values. Then, mean estimation error, intra-assay estimation error and individual estimation error were determined as follow:

$$Mean\ Estimation\ Error = \frac{P_{eff\ ESTIMATED} - P_{eff}}{P_{eff}} \qquad (6)$$

where $P_{eff\ ESTIMATED}$ is the mean estimated permeability of each experiment and P_{eff} is the simulated permeability in the preset conditions (without variability). Mean estimation error, evaluates the capacity of each model to replicate the three observed scenarios.

$$Intraassay\ Estimation\ Error = \frac{P_{eff\ ESTIMATED} - P_{eff\ WELL}}{P_{eff\ WELL}} \quad (7)$$

where $P_{eff\ WELL}$ is the mean value of the three individual permeability values assigned in the simulation step to the wells. Intra-assay estimation error, evaluates the performance of each method to predict the mean permeability of the well in different variability scenarios

$$Individual\ Estimation\ Error = \frac{P_{eff\ ESTIMATED\ A} - P_{eff\ A}}{P_{eff\ A}} \quad (8)$$

where $P_{eff\ ESTIMATED}$ A is the estimated permeability in well A and P_{eff} A is the individual permeability of well A assigned in the simulation step. Error estimations were carried out in an Excel® worksheet.

Statistical analysis

Analysis of variance (ANOVA) was performed in order to detect statistical differences in the mean estimation error in each scenario of variability. Scheffe test was selected as a post-hoc analysis to detect differences between equations with α=0.05. All statistical procedures were performed using SPSS 20.0.

Model Comparison

Simulation step

At this point, in order to evaluate the performance of permeability estimation by each method to classify drugs in the BCS

framework, simulations were performed in a set of borderline scenarios regarding BCS. The question to be answered in this exercise was the following: in a borderline situation for BCS classification as high permeability compound i.e. test permeability closer to the high permeability cutoff, could the estimation method of test or reference permeability bias the classification result? Or in another words, which method would give a more accurate classification?

The high permeability cutoff was set at $2.0 \cdot 10^{-5}$ cm·sec^{-1} [44, 45]. To perform the simulations, test and reference permeability values were set at three levels of $2.0 \cdot 10^{-5}$ cm·sec^{-1}, (average value), $1.8 \cdot 10^{-5}$ cm·sec^{-1} (80% or lower limit) and $2.5 \cdot 10^{-5}$ cm·sec^{-1} (125% or upper limit). These levels were set to use a bioequivalence-like approach in the permeability classification [46]. 108 scenarios were generated combining 3 levels of permeability (upper limit, average or lower limit) for test * 3 levels of permeability for reference * 4 variability scenarios (as in the model validation step) * 3 profiles types (A, B or C).

Simulated data were obtained using Modified Non-sink (MNS) equation (3). Preset simulation conditions were fixed to a donor volume of 0.5 mL, receptor volume of 1.2 mL and sample volume of 0.2 mL; initial concentration in the donor chamber of 100 μM; and surface area of the monolayer of 0.9 cm^2. Samples times considered were 900, 1800, 3600 and 5400 sec. Initial permeability ($P_{eff\,0}$) and final permeability ($P_{eff\,1}$) were used to simulate different profiles, both in the reference as in the test compound. In order to be able to detect the effect in the permeability estimation, profiles simulated for reference and test compounds were Profile A, where less drug is transported during the first sampling interval ($P_{eff\,0} = 10^{-8}$ cm·sec-1); Profile B, where there is a constant permeation during the first sampling interval ($P_{eff\,0} = P_{eff\,1}$); and

Profile C, where more drug is transported during the first sampling interval ($P_{eff\,0} = 5 \cdot 10^{-5}$ cm·sec^{-1}). In each profile, different scenarios of variability were simulated considering an exponential model with high (20% CV) or low (5% CV) interindividual variability (IIV) high or low residual variability (RSV) i.e. each profile was simulated in four different scenarios of variability (2 interindividual*2 residual). Each scenario contained 1000 simulated experiments (500 simulated test experiments and 500 simulated reference experiments). Considering 3 wells per experiment it gives a total of 3000 wells per scenario.

Permeability estimation

Permeability values were estimated from simulated concentrations in the receiver chamber obtained in the previous step using four different equations: Modified Non-sink (MNS) (equation 5), Non-sink (NS) (equation 3), Sink (S) (equation 1) and Corrected Sink (SC) (equation 2). From the permeability coefficients obtained for each well the average permeability of the experiment was calculated as the arithmetic mean of the three wells. The permeability coefficient estimations in sink and non-sink conditions were carried out in an Excel® worksheet.

In order to evaluate the performance for classification of each estimation method the results were evaluated and labeled as following: Label OK; label ERROR and label VARIABILITY.

The OK result was established when the relationship between the preset simulation conditions (without variability) with simulation conditions specifically assigned to the well (IIV and RSV variability) and the result of the estimated permeability coefficient by each method were the same.

ERROR result was established when preset simulation conditions (without variability) matched with simulation conditions specifically assigned to the well (IIV and RSV variability), but not with the result of the permeability coefficient estimated by each method. This label means that the estimation method was not able to estimate correctly the rank order of the test regarding the reference (higher, similar or lower). ERROR label was also assigned when preset simulation conditions (without variability) did not match with simulation conditions specifically assigned to the well (IIV and RSV variability) and the estimated permeability value did not match the permeability assigned to that well.

VARIABILITY result was established when preset simulation conditions (without variability) did not match with simulation conditions specifically assigned to the well (IIV and RSV variability), but the result of the estimated permeability coefficient matched to the simulation conditions specifically assigned to the well. In another words the label VARIABILITY represents the situation in which the theoretical permeability value used for data simulation and the rank order of test and reference did not correspond to the particular permeability (and rank order) assigned to a particular well of the experiments, even if the estimation method was able to correctly estimate the well permeability.

An example of labeling results for one scenario is represented in Table 3 in order to clarify the label meaning.

PRESET SIMULATION CONDITIONS	SIMULATIONS CONDITIONS WITH VARIABILITY	ESTIMATION RESULT AND LABEL	
1500 SIMULATED TEST COMPOUND			
$T > R$	$P_{SIM-T} \geq R$	$P_{EST} \geq R$	OK
$T > R$	$P_{SIM-T} \geq R$	$\mathbf{P_{EST} < R}$	ERROR
$T > R$	$\mathbf{P_{SIM-T} < R}$	$\mathbf{P_{EST} \geq R}$	ERROR
$T > R$	$\mathbf{P_{SIM-T} < R}$	$P_{EST} < R$	VARIABILITY
1500 SIMULATED REFERENCE COMPOUND			
$R < T$	$P_{SIM-R} < T$	$P_{EST} < T$	OK
$R < T$	$P_{SIM-R} < T$	$\mathbf{P_{EST} \geq T}$	ERROR
$R < T$	$\mathbf{P_{SIM-R} \geq T}$	$\mathbf{P_{EST} < T}$	ERROR
$R < T$	$\mathbf{P_{SIM-R} \geq T}$	$P_{EST} \geq T$	VARIABILITY

Table 3. Example of a scenario with the possible results obtained regarding the simulation and estimation process. T is referred to Test compound, R is reference compound. In the preset simulation conditions a particular rank order is selected, for instance theoretical permeability value of test T is higher than the reference one (T>R). PSIM is the permeability value assigned to the well (due to the interindividual variability) and PEST is the estimated permeability value by any of the used methods.

Statistical analysis

Results from each model were analyzed using a crosstab and chi-square test to detect statistical differences between methods used (MNS, NS, S, SC) and results obtained. A statistical p-value of 0.05 was established. All statistical procedures were executed using SPSS 20.0.

RESULTS

Model Validation

Graphical analysis

Simulated concentration in the receiver chamber was plotted versus time by each profile and scenario of variability generated (high (H) and low (L) interindividual variability (IIV) and residual variability (RSV)) are represented in Figure 3.

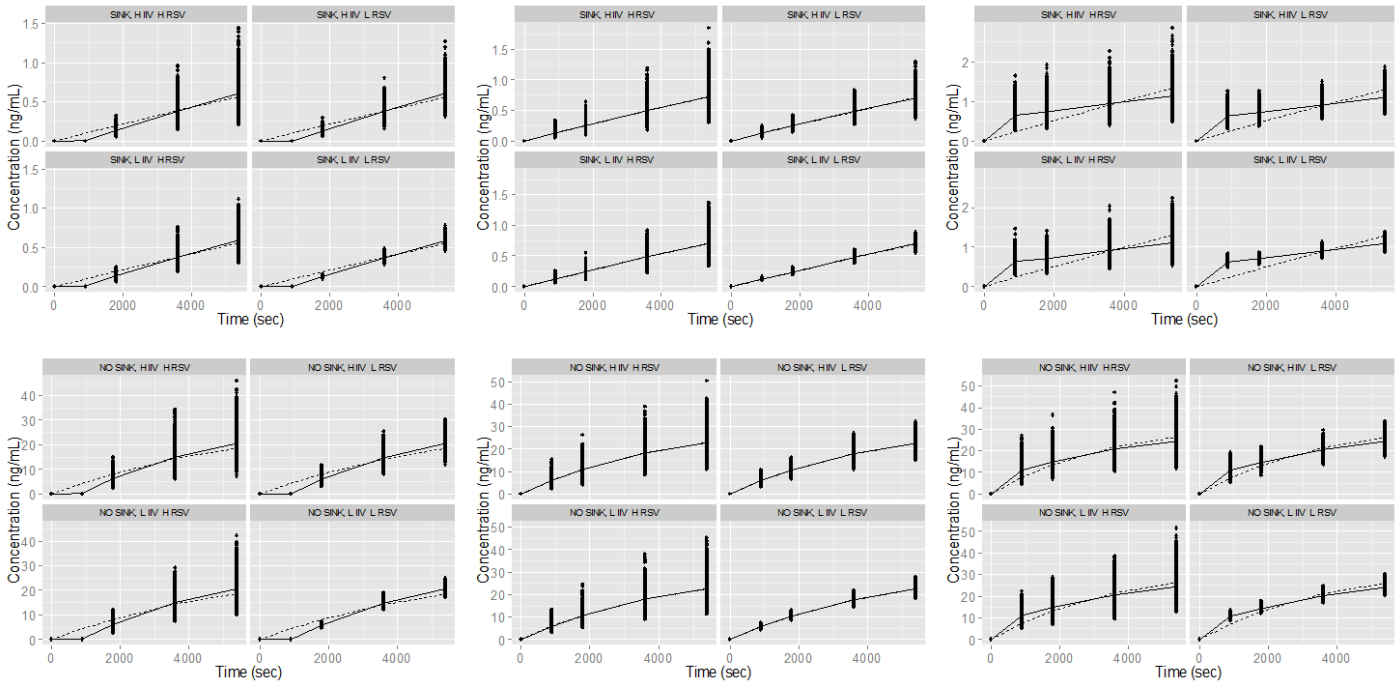

Figure 3. Profile A, B and C (left, middle and right groups) by scenarios of variability in sink conditions are represented in the upper line and non-sink conditions are plotted in the lower line. Blue dots are simulated concentrations (ng/mL) in 3000 wells, solid line is the population predicted values obtained by MNS equation and dotted line is the population predicted value by NS.

Validation of model with experimental data.

Results of permeability experiments in MDCKII cells were selected for model validation. Figure 2 represents the concentrations in acceptor chamber versus time on individual wells for the following compounds Metoprolol, Caffeine, Verapamil, (non-sink 1 ; non-sink 2 and non-sink 3) Zidovudine Atenolol and Norfloxacin (sink 1; sink 2 and sink 3). Red line corresponds to the fit of the non-sink equation and the blue one is the fit of the MNS model to the data. Fits of the non-sink and MNS models were compared with Snedecor's F test. F calculated and tabulated values are summarized in Table 4.

PROFILE A

	SINK				**NON SINK**			
	H IIV H RSV	H IIV L RSV	L IIV H RSV	L IIV L RSV	H IIV H RSV	H IIV L RSV	L IIV H RSV	L IIV L RSV
	MNS	**MNS**	**MNS**	**MNS**	**MNS**	**MNS**	**MNS**	**MNS**
NS	**Sig**	**Sig**	**Sig**	**Sig**	**Sig**	**Sig**	**Sig**	**Sig**
S	NS	NS	NS	NS	**Sig**	**Sig**	**Sig**	**Sig**
SC	NS	NS	**Sig**	**Sig**	**Sig**	**Sig**	**Sig**	**Sig**

Table 4. ANOVA results of Profile A data sets in each scenario of variability between methods of estimation (MSN, NS, S and SC). Sig means statistical differences and NS no statistical differences were observed.

Estimation error

Results from mean, intra-assay and individual estimation error are shown on Figures 4, 5 and 6. Red dots are the mean values of estimation error of each method (MNS, NS, S, SC), grey box is one standard deviation (SD) of the mean and lines are two SD of the mean value.

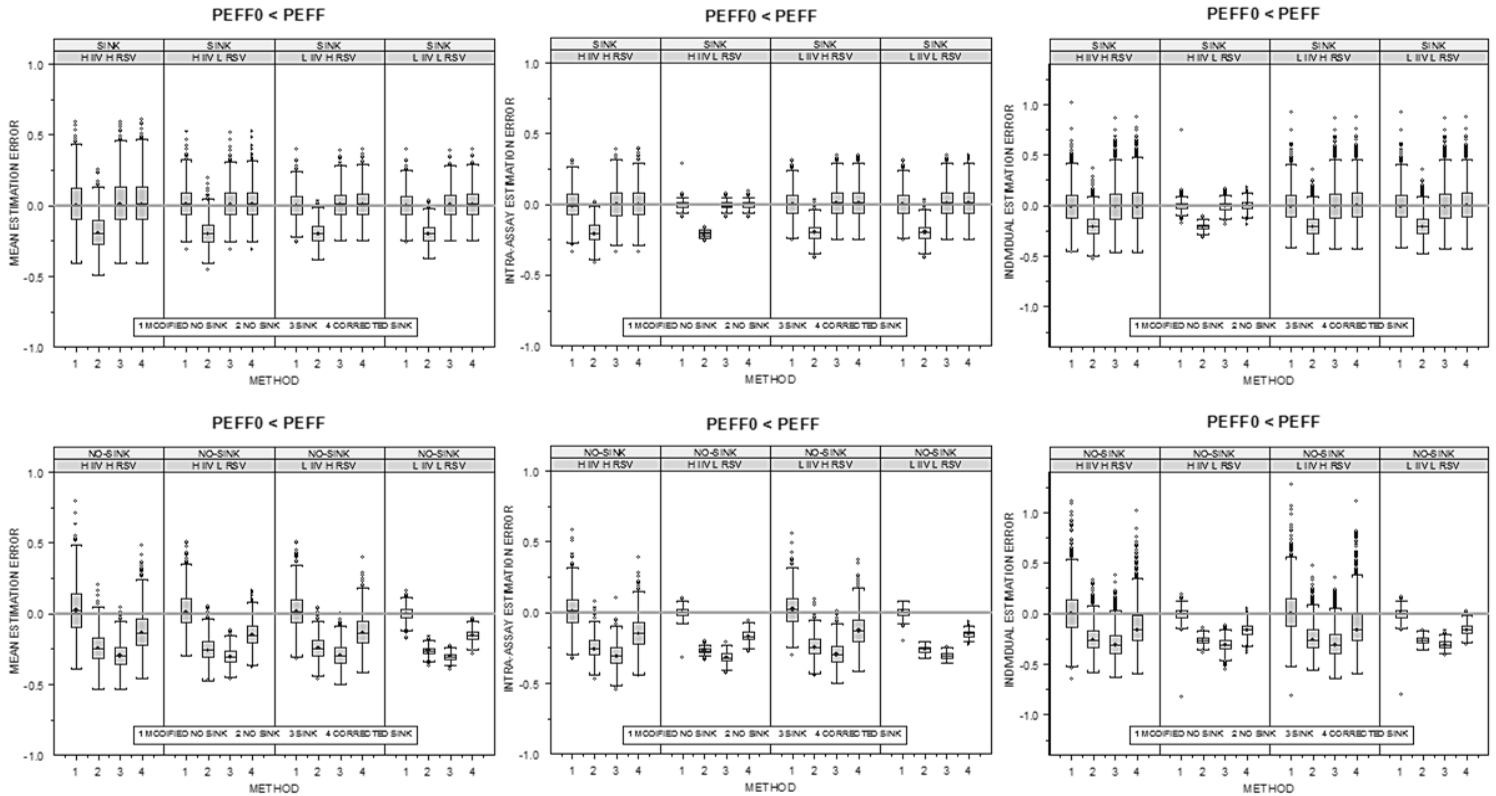

Figure 4. Estimation errors of Profile A in sink and non-sink conditions, by each scenario of variability and by each method of estimation.

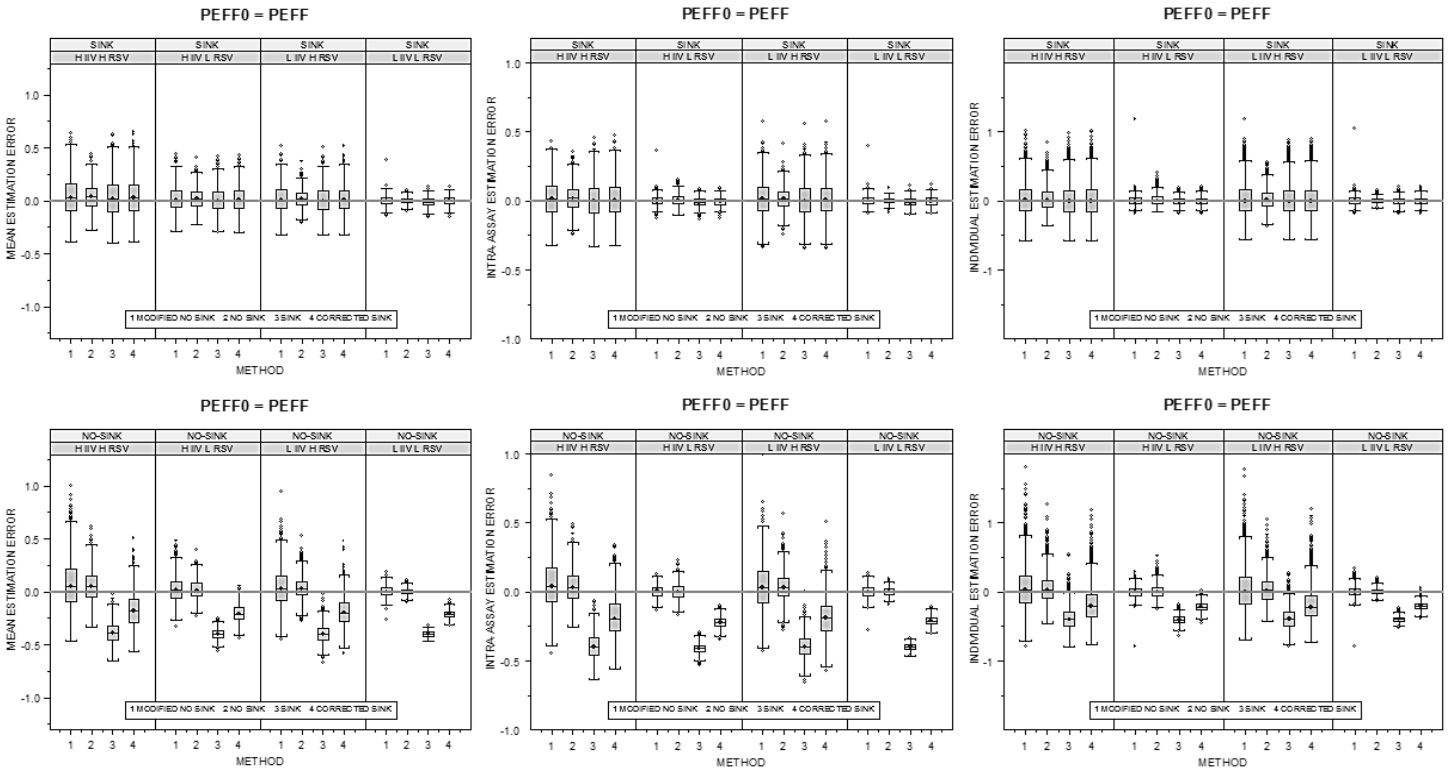

Figure 5. Estimation errors of Profile B in sink and non-sink conditions, by each scenario of variability and by each method of estimation.

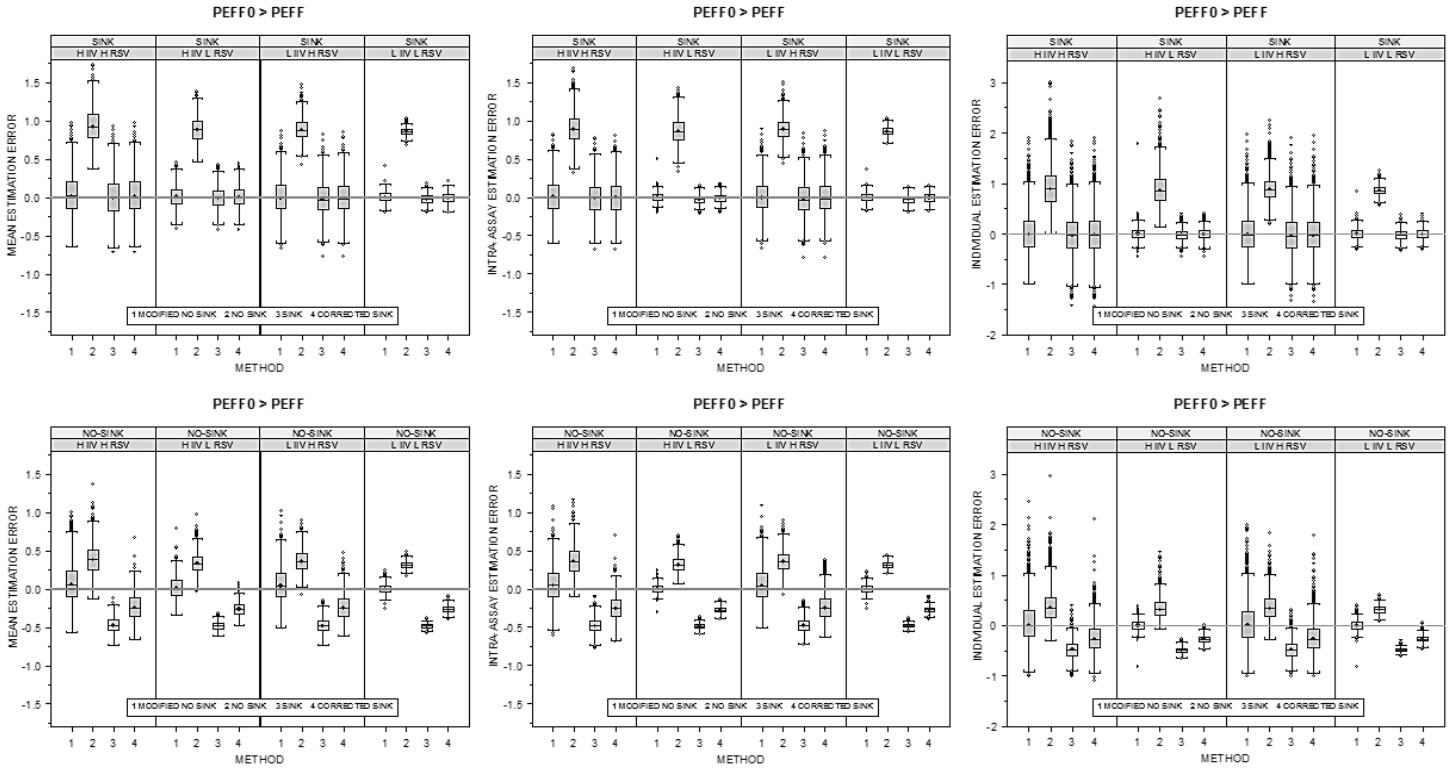

Figure 6. Estimation errors of Profile C in sink and non-sink conditions, by each scenario of variability and by each method of estimation.

Statistical analysis

ANOVA of the mean estimation errors was performed with Scheffe as post-hoc test. Results are summarized in Table 5-7.

PROFILE A

	SINK				NON SINK			
	H IIV H RSV	H IIV L RSV	L IIV H RSV	L IIV L RSV	H IIV H RSV	H IIV L RSV	L IIV H RSV	L IIV L RSV
	MNS	**MNS**	**MNS**	**MNS**	**MNS**	**MNS**	**MNS**	**MNS**
NS	**Sig**	**Sig**	**Sig**	**Sig**	**Sig**	**Sig**	**Sig**	**Sig**
S	NS	NS	NS	NS	**Sig**	**Sig**	**Sig**	**Sig**
SC	NS	NS	**Sig**	**Sig**	**Sig**	**Sig**	**Sig**	**Sig**

Table 5. ANOVA results of Profile A data sets in each scenario of variability between methods of estimation (MSN, NS, S and SC). Sig means statistical differences and NS no statistical differences were observed.

PROFILE B

	SINK				NON SINK			
	H IIV H RSV	H IIV L RSV	L IIV H RSV	L IIV L RSV	H IIV H RSV	H IIV L RSV	L IIV H RSV	L IIV L RSV
	MNS	**MNS**	**MNS**	**MNS**	**MNS**	**MNS**	**MNS**	**MNS**
NS	NS	NS	NS	NS	NS	NS	NS	NS
S	NS	NS	NS	**Sig**	**Sig**	**Sig**	**Sig**	**Sig**
SC	NS	NS	NS	NS	**Sig**	**Sig**	**Sig**	**Sig**

Table 6. ANOVA results of Profile B data sets in each scenario of variability between methods of estimation (MSN, NS, S and SC). Sig means statistical differences and NS no statistical differences were observed.

PROFILE C

	SINK				NON SINK			
	H IIV H RSV	H IIV L RSV	L IIV H RSV	L IIV L RSV	H IIV H RSV	H IIV L RSV	L IIV H RSV	L IIV L RSV
	MNS	**MNS**	**MNS**	**MNS**	**MNS**	**MNS**	**MNS**	**MNS**
NS	**Sig**	**Sig**	**Sig**	**Sig**	**Sig**	**Sig**	**Sig**	**Sig**
S	NS	S	NS	**Sig**	**Sig**	**Sig**	**Sig**	**Sig**
SC	NS	NS	NS	**Sig**	**Sig**	**Sig**	**Sig**	**Sig**

Table 7. ANOVA results of Profile C data sets in each scenario of variability between methods of estimation (MSN, NS, S and SC). Sig means statistical differences and NS no statistical differences were observed.

Model comparison

Permeability estimation

Results of the classification from 108 scenarios with each method of estimation are summarized in Table 8. (Chi-square results are in Tables 1 to 3 in supporting information file).

Results were classified in OK, ERROR or VARIABILITY. Considering the meaning of these labels (as the examples presented in Table 3) the objective would be finding which method is able to obtain the higher number of OK results, the lower number of ERROR labels and it is not biased by the variability of the experiment. After performing the chi-square test, the number of occasions that the MNS method produced better results than the others was computed and these results are displayed in Table 8. For instance, MNS estimation method obtained a statistically higher number of OK results in 59 scenarios compared with NS method, the same number in 12 and less OK results than NS in 37 scenarios (108 total scenarios). Regarding the

ERROR results, MNS method produced less times ERROR results in 75 scenarios compared with NS method, the same number in 12 scenarios and more ERROR results in 21 scenarios. In VARIABILITY results, MNS method led to a higher number of VARIABILITY results compared with NS in 40 scenarios, a similar number in 49 scenarios and less number of VARIABILITY results in 19 scenarios.

	OK			ERROR			VARIABILITY		
	NS	**S**	**SC**	**NS**	**S**	**SC**	**NS**	**S**	**SC**
BETTER	**59**	**83**	24	**75**	**90**	44	**40**	**42**	4
SIMILAR	12	25	**82**	12	15	**62**	**49**	**66**	**104**
WORSE	37	0	2	21	3	2	19	0	0

Table 8. Comparison of statistically significant differences between MNS and NS, MNS and S and MNS versus SC. In the Columns OK and VARIABILITY, BETTER is considered when the number of results, either OK or VARIABILITY was significantly higher in MNS than the other methods; SIMILAR is when the differences were not significant; WORSE when the number of results (OK or VARIABILITY) was significantly lower in MNS than the other methods. In the Column ERROR, BETTER corresponds to a significant lower number of ERROR results, SIMILAR means a non-significant difference and WORSE implies a significantly higher number of ERROR results.

DISCUSSION

Drugs for oral administration and CNS drugs are two therapeutic groups which need to cross biological barriers; in consequence, to increase the success rate during development a good preclinical screening system of the membrane permeability of the candidates is essential.

The *in vitro* permeability studies are a fundamental tool in the preclinical development of new drugs [28, 47-51]. Permeability is the ability of a molecule to cross biological barriers and several cell monolayers are used in the *in vitro* permeation studies [49, 52-54]. On top of that, an accurate estimation of permeability is relevant for correct

classification and selection of optimal candidates for further preclinical and clinical evaluation. For this reason, in this work we have evaluated the standard procedures for permeability estimation from experimental data and we have compared them with a modified equation in order to accommodate all the experimental profiles that are usually obtained in these *in vitro* permeability experiments.

Model Performance with Simulated data

As published by Tavelin et al. [28] the profiles of accumulated amount of drug versus time are not always perfectly linear but might have initial atypical behaviors (called Profile A and C). Figures 1 shows the prediction of MNS and NS methods for a simulated database in different initial conditions of permeation and different scenarios of variability, both in low permeability (sink) and high permeability (non-sink) conditions. When there is no alteration in the initial permeation of the drug across the cell monolayer, NS and MNS predicted equally well the simulated concentrations in the receiver chamber. But if there is any initial alteration (Profile A and C), only MNS is able to estimate accurately the "true" permeability due its ability to discriminate the initial permeability until the first sampling interval ($P_{eff\,0}$) and the final (or "true") permeability ($P_{eff\,1}$), i.e. this method takes into account the behavior in the initial phase and it avoids that this initial alteration affects the estimation of the permeability. Therefore, NS method underestimates in Profile A and overestimates in Profile C the permeability value in all scenarios of variability and sink and non-sink conditions.

When comparing the results of the estimation errors (Figure 3-5), no significant differences are observed between the behavior of the

mean, intra-assay and individual estimation errors. In all the profiles (A, B and C), under sink conditions linear regression models (S and SC) achieved similar estimation errors compared with MNS method. These results are expected because the linear sink and sink corrected models allow the intercept of the regression to be different from 0. However, when conditions are non-sink and linearity is affected, S and SC underestimate in Profile A and overestimate in Profile C across all variability scenarios.

On the other hand, NS method produces estimation errors different from 0 when the initial permeation across the monolayer is affected (in all scenarios of variability) and under sink and non-sink conditions (Figures 3-5). The single permeability parameter in the equation is not able to satisfy, by nonlinear regression, all experimental concentrations in the receiver chamber. However, when there is no alteration in the initial phase (Figure 2) NS method is able to predict an accurate permeability value under sink and non-sink conditions in all scenarios of variability.

NS presents statistically significant differences in average estimation error compared to MNS, under sink and non-sink, in the Profile A and C in all variability scenarios proposed. Therefore NS method underestimates or overestimates statistically the permeability. There were no significant differences in Profile B between NS and MNS method.

Linear regression models (S and SC) showed statistically significant differences when non-sink conditions existed in each of the profiles and scenarios of variability proposed. In some cases, under sink conditions, significant differences were observed between S and SC and MNS, usually when IIV and RSV variability was low. This could be

explained because as the variance of the mean estimation errors is small, small differences in the mean error between methods could be significant in Scheffe test.

Therefore, these differences observed in Figures 3 to 6 and the statistical differences in estimation errors evidenced in the ANOVA (Tables 5-7) demonstrated that linear regression models are not valid at any level of variability under non-sink, and even in scenarios with low variability under sink conditions. Likewise, NS method is not useful for calculating the permeability when there is an alteration of the permeation through the cell monolayer in the initial stages in all scenarios of variability and under sink and non-sink conditions.

Model validation with experimental data

As it can be observed in Figure 2 and Table 4 MNS method provided a better fit with atypical values (Metoprolol and Verapamil) under non sink conditions and as well under sink conditions (Zidovudine and Norfloxacin). In other words the more complex model offers a statistically significant better fit when in those cases with an apparent lag time for permeation or a higher transport in the earlier times either in sink and non-sink conditions. In profiles without these problems non sink equation performs well and it is not necessary to include a new parameter to describe the data.

Model Comparison

The importance of a correct estimation of the permeability of new drugs in development lies in an efficient selection of the candidates to ensure a greater chance of reaching the market. This fact is, in

particular, relevant when the classification of the candidate by comparison with a reference could be biased if the estimation is not accurate.

The designed scenarios to perform the simulations are focused on a borderline situation for classification as high permeability compound (in BCS framework) that is test and reference permeability values very similar. This particular case was selected because, obviously, when the classification is clear, or in other words, with a test permeability value much higher or lower than the reference one, the bias due to the estimation method could be neglected, as it could affect test or reference in a different magnitude but it would never mask the existing differences. Thus, actually a biased permeability estimates would not affect the comparison. The problem of the estimation method could arise when the candidate compound is near the cutoff value. In this situation, a bioequivalence-like approach could be useful to ensure the statistical significance of the test-reference difference but it should not be forgotten that if the average value for 90% confidence interval construction is biased the comparison would be also erroneous.

The main objective in this section is to compare the number of satisfactory estimation results i.e. correct classification (OK and VARIABILITY) (given a particular scenario) produced by each estimation method. Results summarized in Table 7 demonstrated that the MNS method would conclude a correct classification in more potential scenarios even when the designed scenarios were borderline situations. Given a theoretical difference of 20% in test and reference compound, when the experimental variability is added to the system, the MNS equation led to a correct rank order, matching the "true" parameters in a higher number of occasions, including those with

"atypical" profiles of cumulative amounts versus time. It is important to point out that the so called atypical profiles are actually not unusual but often neglected and then, the standard calculation methods are used without considering their influence in the estimation error. In the present simulation it is demonstrated that when these profiles arise the new Modified Non Sink equation gives the most accurate estimate. Therefore, the main conclusion of this section is that the MNS method is able to correctly estimate the permeability in a larger number of cases compared to the proposed models and it has fewer errors in the classification of the compound. This is essential for a more efficient candidate selection.

Regarding of the limitation of the present approach it is necessary to point out the three tested models (Sink, Non-sink and MNS) include the assumption that permeability is equal in both directions and, thus, they would predict equal concentration in apical and basolateral compartments at equilibrium. However, oftentimes this assumption does not hold. For instance, active transport and pH gradient for ionizable compounds, lead to direction dependent permeability. Even in these cases the new MNS model would capture the loss of sink condition or would describe the altered initial rate.

In order to accommodate for non-equal concentration in both chambers at equilibrium and then estimate in a single step the different apical to basal and basal to apical permeability a differential equation model have to be used as it has been already proposed [55, 56]. On the other hand the simplest approach to detect direction dependent phenomena is to estimate the unidirectional permeability and evaluate the basal to apical and apical to basal ratios. The new proposed method

is intended for this purpose and has demonstrated its better performance.

CONCLUSION

Modified Non Sink equation (Mangas-Casabó method) is a precise and accurate equation for calculating the apparent unidirectional permeability in any type of profile and under different scenarios of variability, as well as sink and non-sink conditions, while the NS method fails in obtaining good permeability estimates in those situations in which the initial permeation rate is altered.

Linear regression models (S and SC), are not valid under strong non-sink conditions as expected as the underlying assumptions (sink conditions) do not hold but also in situations in which sink conditions are fulfilled but the system variability is high.

MSN method would be the recommended one as it accommodates not only sink and non-sink conditions but also all type of profiles with altered initial rates. Sink corrected could be a good approximation (in slightly non sink conditions) even better than Non Sink method because NS does not fit well the atypical profiles.

ACKNOWLEDGEMENTS

The authors acknowledge partial financial support to projects: DCI ALA/19.09.01/10/21526/245-297/ALFA 111(2010)29: Red-Biofarma. Red para el desarrollo de metodologias biofarmaceuticas racionales que incrementen la competencia y el impacto social de las Industrias Farmaceuticas Locales. AGL2011-29857-C03-03, Foodomics evaluation of dietary polyphenols against colon cancer using *in vitro* and *in vivo* models from Spanish Ministry of Science and

Innovation. Victor Mangas-Sanjuán received a grant from Ministry of Education and Science of Spain and Miguel Hernandez University (FPU AP2010-2372).

REFERENCES

1. Buckley, S. T.; Fischer, S. M.; Fricker, G.; Brandl, M. *In vitro* models to evaluate the permeability of poorly soluble drug entities: challenges and perspectives. Eur J Pharm Sci 2012, 45, (3), 235-50.

2. Amidon, G. L.; Lennernas, H.; Shah, V. P.; Crison, J. R. A theoretical basis for a biopharmaceutic drug classification: the correlation of *in vitro* drug product dissolution and *in vivo* bioavailability. Pharm Res 1995, 12, (3), 413-20.

3. FDA Waiver of *In Vivo* Bioavailability and Bioequivalence Studies for Immediate-Release Solid Oral Dosage Forms Based on a Biopharmaceutics Classification System; Center for Drug Evaluation and Research: August 2000, 2000.

4. EMA GUIDELINE ON THE INVESTIGATION OF BIOEQUIVALENCE; European Medicines Agency: 1 August 2010, 2010.

5. WHO. WHO EXPERT COMMITTEE ON SPECIFICATIONS FOR PHARMACEUTICAL PREPARATIONS. 2006.

6. Di, L.; Kerns, E. H.; Carter, G. T. Strategies to assess blood-brain barrier penetration. Expert Opin Drug Discov 2008, 3, (6), 677-87.

7. Kessler, R. C.; Demler, O.; Frank, R. G.; Olfson, M.; Pincus, H. A.; Walters, E. E.; Wang, P.; Wells, K. B.; Zaslavsky, A. M. Prevalence and treatment of mental disorders, 1990 to 2003. N Engl J Med 2005, 352, (24), 2515-23.

8. Kola, I.; Landis, J. Can the pharmaceutical industry reduce attrition rates? Nat Rev Drug Discov 2004, 3, (8), 711-5.

9. Pangalos, M. N.; Schechter, L. E.; Hurko, O. Drug development for CNS disorders: strategies for balancing risk and reducing attrition. Nat Rev Drug Discov 2007, 6, (7), 521-32.

10. Bickel, U. How to measure drug transport across the blood-brain barrier. NeuroRx 2005, 2, (1), 15-26.

11. Broccatelli, F.; Larregieu, C. A.; Cruciani, G.; Oprea, T. I.; Benet, L. Z. Improving the prediction of the brain disposition for orally administered drugs using BDDCS. Adv Drug Deliv Rev 2012, 64, (1), 95-109.

12. Cabrera, M. A.; Bermejo, M.; Perez, M.; Ramos, R. TOPS-MODE approach for the prediction of blood-brain barrier permeation. J Pharm Sci 2004, 93, (7), 1701-17.

13. Carrara, S.; Reali, V.; Misiano, P.; Dondio, G.; Bigogno, C. Evaluation of *in vitro* brain penetration: optimized PAMPA and MDCKII-MDR1 assay comparison. Int J Pharm 2007, 345, (1-2), 125-33.

14. Culot, M.; Lundquist, S.; Vanuxeem, D.; Nion, S.; Landry, C.; Delplace, Y.; Dehouck, M. P.; Berezowski, V.; Fenart, L.; Cecchelli, R. An *in vitro* blood-brain barrier model for high throughput (HTS) toxicological screening. Toxicol *In Vitro* 2008, 22, (3), 799-811.

15. Friden, M.; Ducrozet, F.; Middleton, B.; Antonsson, M.; Bredberg, U.; Hammarlund-Udenaes, M. Development of a high-throughput brain slice method for studying drug distribution in the central nervous system. Drug Metab Dispos 2009, 37, (6), 1226-33.

16. Friden, M.; Gupta, A.; Antonsson, M.; Bredberg, U.; Hammarlund-Udenaes, M. *In vitro* methods for estimating unbound drug concentrations in the brain interstitial and intracellular fluids. Drug Metab Dispos 2007, 35, (9), 1711-9.

17. Friden, M.; Winiwarter, S.; Jerndal, G.; Bengtsson, O.; Wan, H.; Bredberg, U.; Hammarlund-Udenaes, M.; Antonsson, M. Structure-brain exposure relationships in rat and human using a novel data set of unbound drug concentrations in brain interstitial and cerebrospinal fluids. J Med Chem 2009, 52, (20), 6233-43.

18. Geldenhuys, W. J.; Manda, V. K.; Mittapalli, R. K.; Van der Schyf, C. J.; Crooks, P. A.; Dwoskin, L. P.; Allen, D. D.; Lockman, P. R. Predictive

screening model for potential vector-mediated transport of cationic substrates at the blood-brain barrier choline transporter. Bioorg Med Chem Lett 2010, 20, (3), 870-7.

19. Hammarlund-Udenaes, M.; Bredberg, U.; Friden, M. Methodologies to assess brain drug delivery in lead optimization. Curr Top Med Chem 2009, 9, (2), 148-62.

20. Hansen, D. K.; Scott, D. O.; Otis, K. W.; Lunte, S. M. Comparison of *in vitro* BBMEC permeability and *in vivo* CNS uptake by microdialysis sampling. J Pharm Biomed Anal 2002, 27, (6), 945-58.

21. Hanson, L. R.; Frey, W. H., 2nd. Intranasal delivery bypasses the blood-brain barrier to target therapeutic agents to the central nervous system and treat neurodegenerative disease. BMC Neurosci 2008, 9 Suppl 3, S5.

22. Kataoka, M.; Masaoka, Y.; Yamazaki, Y.; Sakane, T.; Sezaki, H.; Yamashita, S. *In vitro* system to evaluate oral absorption of poorly water-soluble drugs: simultaneous analysis on dissolution and permeation of drugs. Pharm Res 2003, 20, (10), 1674-80.

23. Lacombe, O.; Videau, O.; Chevillon, D.; Guyot, A. C.; Contreras, C.; Blondel, S.; Nicolas, L.; Ghettas, A.; Benech, H.; Thevenot, E.; Pruvost, A.; Bolze, S.; Krzaczkowski, L.; Prevost, C.; Mabondzo, A. *In vitro* primary human and animal cell-based blood-brain barrier models as a screening tool in drug discovery. Mol Pharm 2011, 8, (3), 651-63.

24. Mabondzo, A.; Bottlaender, M.; Guyot, A. C.; Tsaouin, K.; Deverre, J. R.; Balimane, P. V. Validation of *in vitro* cell-based human blood-brain barrier model using clinical positron emission tomography radioligands to predict *in vivo* human brain penetration. Mol Pharm 2010, 7, (5), 1805-15.

25. Wan, H.; Rehngren, M.; Giordanetto, F.; Bergstrom, F.; Tunek, A. High-throughput screening of drug-brain tissue binding and *in silico* prediction for assessment of central nervous system drug delivery. J Med Chem 2007, 50, (19), 4606-15.

26. Wang, Q.; Rager, J. D.; Weinstein, K.; Kardos, P. S.; Dobson, G. L.; Li, J.; Hidalgo, I. J. Evaluation of the MDR-MDCK cell line as a permeability screen for the blood-brain barrier. Int J Pharm 2005, 288, (2), 349-59.

27. Mangas-Sanjuan, V.; Gonzalez-Alvarez, I.; Gonzalez-Alvarez, M.; Casabo, V. G.; Bermejo, M. Innovative *in vitro* method to predict rate and extent of drug delivery to the brain across the Blood-Brain Barrier. Mol Pharm 2013.

28. Tavelin, S.; Grasjo, J.; Taipalensuu, J.; Ocklind, G.; Artursson, P. Applications of epithelial cell culture in studies of drug transport. Methods Mol Biol 2002, 188, 233-72.

29. Palm, K.; Luthman, K.; Ros, J.; Grasjo, J.; Artursson, P. Effect of molecular charge on intestinal epithelial drug transport: pH-dependent transport of cationic drugs. The Journal of pharmacology and experimental therapeutics 1999, 291, (2), 435-43.

30. Jonsson, S.; Henningsson, A.; Edholm, M.; Salmonson, T. Role of modelling and simulation: a European regulatory perspective. Clin Pharmacokinet 2012, 51, (2), 69-76.

31. Sheiner, L. B. Learning versus confirming in clinical drug development. Clin Pharmacol Ther 1997, 61, (3), 275-91.

32. Breimer, D. D.; Danhof, M. Relevance of the application of pharmacokinetic-pharmacodynamic modelling concepts in drug development. The "wooden shoe' paradigm. Clin Pharmacokinet 1997, 32, (4), 259-67.

33. Derendorf, H.; Meibohm, B. Modeling of pharmacokinetic/pharmacodynamic (PK/PD) relationships: concepts and perspectives. Pharm Res 1999, 16, (2), 176-85.

34. Holford, N. H.; Kimko, H. C.; Monteleone, J. P.; Peck, C. C. Simulation of clinical trials. Annu Rev Pharmacol Toxicol 2000, 40, 209-34.

35. Aarons, L.; Karlsson, M. O.; Mentre, F.; Rombout, F.; Steimer, J. L.; van Peer, A. Role of modelling and simulation in Phase I drug development. Eur J Pharm Sci 2001, 13, (2), 115-22.

36. Chaikin, P.; Rhodes, G. R.; Bruno, R.; Rohatagi, S.; Natarajan, C. Pharmacokinetics/pharmacodynamics in drug development: an industrial perspective. J Clin Pharmacol 2000, 40, (12 Pt 2), 1428-38.

37. Reigner, B. G.; Williams, P. E.; Patel, I. H.; Steimer, J. L.; Peck, C.; van Brummelen, P. An evaluation of the integration of pharmacokinetic and pharmacodynamic principles in clinical drug development. Experience within Hoffmann La Roche. Clin Pharmacokinet 1997, 33, (2), 142-52.

38. Lockwood, P.; Ewy, W.; Hermann, D.; Holford, N. Application of clinical trial simulation to compare proof-of-concept study designs for drugs with a slow onset of effect; an example in Alzheimer's disease. Pharm Res 2006, 23, (9), 2050-9.

39. FDA Innovation or stagnation: challenge and opportunity on the critical path to new medical products. http://www.fda.gov/ScienceResearch/SpecialTopics/CriticalPathInitiative/CriticalPathOpportunitiesReports/ucm077262.htm (Accessed 2 May 2010),

40. Edholm, M.; Gil Berglund, E.; Salmonson, T. Regulatory aspects of pharmacokinetic profiling in special populations: a European perspective. Clin Pharmacokinet 2008, 47, (11), 693-701.

41. Manolis, E.; Pons, G. Proposals for model-based paediatric medicinal development within the current European Union regulatory framework. Br J Clin Pharmacol 2009, 68, (4), 493-501.

42. Bevington, P. a. R., D., Data reduction and error analysis for the physical sciences. 2nd ed. ed.; McGraw-Hill: New York, 1992.

43. Mangas-Sanjuan, V.; Gonzalez-Alvarez, I.; Gonzalez-Alvarez, M.; Casabo, V. G.; Bermejo, M. Innovative *in vitro* method to predict rate and extent of drug delivery to the brain across the blood-brain barrier. Mol Pharm 2013, 10, (10), 3822-31.

44. Pham-The, H.; Garrigues, T.; Bermejo, M.; Gonzalez-Alvarez, I.; Monteagudo, M. C.; Cabrera-Perez, M. A. Provisional classification and *in*

silico study of biopharmaceutical system based on caco-2 cell permeability and dose number. Mol Pharm 2013, 10, (6), 2445-61.

45. Pham-The, H. G.-Á., I.; Bermejo, M.; Mangas-Sanjuan, V.; Centelles, I.; Garrigues, T.; Cabrera-Pérez, MA. *In Silico* Prediction of Caco-2 Cell Permeability by a Classification QSAR Approach. Molecular Informatics 2011, 30, (4), 376-385.

46. Kim, J. S.; Mitchell, S.; Kijek, P.; Tsume, Y.; Hilfinger, J.; Amidon, G. L. The suitability of an *in situ* perfusion model for permeability determinations: utility for BCS class I biowaiver requests. Mol Pharm 2006, 3, (6), 686-94.

47. Sarmento, B.; Andrade, F.; da Silva, S. B.; Rodrigues, F.; das Neves, J.; Ferreira, D. Cell-based *in vitro* models for predicting drug permeability. Expert Opin Drug Metab Toxicol 2012, 8, (5), 607-21.

48. Skolnik, S.; Lin, X.; Wang, J.; Chen, X. H.; He, T.; Zhang, B. Towards prediction of *in vivo* intestinal absorption using a 96-well Caco-2 assay. J Pharm Sci 2010, 99, (7), 3246-65.

49. Turco, L.; Catone, T.; Caloni, F.; Di Consiglio, E.; Testai, E.; Stammati, A. Caco-2/TC7 cell line characterization for intestinal absorption: how reliable is this *in vitro* model for the prediction of the oral dose fraction absorbed in human? Toxicol *In Vitro* 2011, 25, (1), 13-20.

50. Volpe, D. A. Drug-permeability and transporter assays in Caco-2 and MDCK cell lines. Future Med Chem 2011, 3, (16), 2063-77.

51. Youdim, K. A.; Avdeef, A.; Abbott, N. J. *In vitro* trans-monolayer permeability calculations: often forgotten assumptions. Drug Discov Today 2003, 8, (21), 997-1003.

52. Bermejo, M.; Avdeef, A.; Ruiz, A.; Nalda, R.; Ruell, J. A.; Tsinman, O.; Gonzalez, I.; Fernandez, C.; Sanchez, G.; Garrigues, T. M.; Merino, V. PAMPA--a drug absorption *in vitro* model 7. Comparing rat *in situ*, Caco-2, and PAMPA permeability of fluoroquinolones. Eur J Pharm Sci 2004, 21, (4), 429-41.

53. Hilgendorf, C.; Spahn-Langguth, H.; Regardh, C. G.; Lipka, E.; Amidon, G. L.; Langguth, P. Caco-2 versus Caco-2/HT29-MTX co-cultured cell lines: permeabilities via diffusion, inside- and outside-directed carrier-mediated transport. J Pharm Sci 2000, 89, (1), 63-75.

54. Volpe, D. A. Variability in Caco-2 and MDCK cell-based intestinal permeability assays. J Pharm Sci 2008, 97, (2), 712-25.

55. Gonzalez-Alvarez, I.; Fernandez-Teruel, C.; Garrigues, T. M.; Casabo, V. G.; Ruiz-Garcia, A.; Bermejo, M. Kinetic modelling of passive transport and active efflux of a fluoroquinolone across Caco-2 cells using a compartmental approach in NONMEM. Xenobiotica 2005, 35, (12), 1067-88.

56. Troutman, M. D.; Thakker, D. R. Novel experimental parameters to quantify the modulation of absorptive and secretory transport of compounds by P-glycoprotein in cell culture models of intestinal epithelium. Pharmaceutical research 2003, 20, (8), 1210-24.

Chapter 5

Variability of Permeability Estimation from Different Protocols of Subculture and Transport Experiments in Cell Monolayers

Oltra-Noguera, D.[1,a], Mangas-Sanjuan, V.[1,2,a], Centelles-Sangüesa, A.[1,a], Gonzalez-Garcia, I.[1,2], Sanchez-Castaño, G.[1], Gonzalez-Alvarez, M.[2], Casabo, VG.[1,ω], Merino, V.[1], Gonzalez-Alvarez, I.[2], Bermejo, M.[2]

[1]Pharmaceutics and Pharmaceutical Technology Department. University of Valencia.

[2]Department of Engineering, Pharmaceutics and Pharmaceutical Technology Area. University Miguel Hernández, Elche.

[ω]Deceased, July 7, 2013.

[a]These authors made equal contributions and are considered first co-authors.

Submitted

INTRODUCTION

In vitro models with high predictive ability have been revealed as strong tools for pharmaceutical industry. The use of validated *in vitro* models also means lower development cost and less time-consuming processes. Moreover, the use of a good predictive model in the early phases of drug discovery could prevent sub-optimal drug candidates from reaching clinical development with the associated waste of time, resources and money. Current *in vitro* models for the predictions of drug transport across biological membranes include cell cultures that reproduce physiological characteristics of different barriers, such as the intestine, the blood-brain barrier or the kidney and liver. However, it has been reported that *in vitro* models have some limitations. For instance, the variability in permeability estimations complicates the comparison and combination of data from different laboratories and it makes necessary the careful validation of the model and the continuous suitability demonstration. Permeability values and their associated variability from cell culture transport experiments is influenced by several factors that can be classified in three groups, pre-experimental, experimental and post-experimental factors. The adequate standardization of these factors can help to reduce the inter- and intra-laboratory variability in permeability values.

Among the pre-experimental factors the most relevant are the cell type and source and passage number which could affect the monolayer differentiation, membrane composition, transporter expression and tight junction resistance (1-2). In fact, some research works describe differences in cell shape and size, multilayer formation and actin staining between the same cell sources (3). Several cellular

lines have been traditionally used in order to determine the *in vitro* permeability values. Caco-2, MDCK or MDCK-MDR1 cell lines are the most commonly used for this purpose. Caco-2 cells are the most widely used model for estimation of drug intestinal permeability despite its colonic origin (4-5). On the other hand MDCK epithelial cells despite of its non-human and non-intestinal origin have demonstrated a good correlation with Caco-2 cells results and good predictive performance of human oral fraction absorbed (6-7). MDCK-Mdr1 cells correspond to the P-gp transfected clone from MDCK and are used for the study of P-gp substrates (8-9). MDCK and MDCK-Mdr1 lines with low values of trans-epithelial resistance (TEER) are used also as blood brain barrier model (10-12). These three cell lines have been included in this study as the most representative barrier models to compare its intrinsic variability when used with the same protocol. The culture conditions, such as the components of the culture medium or the cell density, the pH or the temperature also affect the final characteristics of the monolayer (13-14). Subculture details such as the frequency of culture media renewal affect the expression of several enzymes and the kinetic parameters of the transport substrates (15-16).

Regarding the passage number, many researchers have demonstrated that changes in TEER, cell growth, mannitol flux and active transport are observed with passage number (17-19). However, there is no consensus regarding the optimal interval of passages for conducting assays in order to obtain adequate and reproducible permeability values.

The experimental factors can also affect the monolayer absorption and metabolic properties. The literature describe parameters involved in monolayer permeability such as media composition and pH

of both chambers, seeding density, system shaking, plastic support material type, solute concentration, temperature, etc. which also affect the barrier properties (integrity, permeability and transporter expression) and the thickness of the unstirred water layer (2-20). Differentiation period after confluence is a crucial parameter in order to obtain reproducible results as the cells suffer important changes in morphology, barrier properties and expression of transporters with time (17-19-21-22). With increasing age, changes in cell height and shape, cell junction formation, TEER values, metabolic activity, P-gp, MRP2, OATB OCTN2 and PePT1 transporters expression and brush border microvilli were observed (23). The challenge is to determine the optimum culture period for performing transport assays. Moreover, features such as the sampling schedule (only acceptor chamber or both, number of samples, media replacement), the maintenance or not of sink conditions are determinant of the calculation method and thus influence the permeability estimate obtained.

Among the post experimental factors, the variability associated with the analytical method is an important aspect to take into account as well as the estimation method (and its underlying mathematical assumptions) that it is an aspect often neglected (24).

The objective of this paper is the evaluation of the effect of passage number, experimental protocol, maturation time after seeding and calculation method on the permeability values and their associated variability in cell culture transport experiments conducted in our laboratory using three cell lines, Caco-2, MDCK and MDCK-Mdr1. The final goal is to select the best experimental conditions for further method validation and to determine the sample size for detecting a given difference in permeability values. Three compound markers of

transcellular permeability (Metoprolol), paracellular permeability (Lucifer Yellow) and P-gp functionality (Rhodamine-123) were used to check the performance of the cell lines and their ability to reach pre-established specifications.

MATERIALS AND METHODS

Compounds assayed and cell lines

Metoprolol, Rhodamine and Lucifer Yellow were purchased from Sigma (Barcelona, Spain. Compounds transport was studied at 100 μM for Metoprolol, at 5.5 μM for Rhodamine and at 2 mM for Lucifer Yellow.

Samples were analyzed by HPLC using a 5 μm, 3.9 x 150 mm Novapack C18 column.

Metoprolol samples were analyzed with fluorescence detection (λexcitation=231 nm and λemission=307 nm). The mobile phase was 60:20:20, water: methanol: acetonitrile, with a flow rate of 1 mL/min and the injected volume was 20 μL. In these conditions, the retention time of Metoprolol was around 2.5 min. Rhodamine samples were analyzed with fluorescence detection (λexcitation=485 nm and λemission=546 nm). The mobile phase was 60:40, water: acetonitrile, with a flow rate of 1 mL/min and the injected volume was 20 μL. In these conditions, the retention time of Rhodamine was around 4.5 min. Lucifer Yellow samples were analyzed with fluorescence detection (λexcitation=430 nm and λemission=530 nm). The mobile phase was 80:20, water: acetonitrile, with a flow rate of 1 mL/min and the injected volume was 20 μL. In these conditions, the retention time of Lucifer Yellow was around 3 min.

Caco-2 cell lines were provided by Dr. Hu (Washington State University, Pullman). MDCK and MDCK-MDR1 cell lines were provided by Dr. Gottesman, MM. (National Institutes of Health, Bethesda).

Cell culture and transport studies

Pre-experimental factors:

Passage number

The passage numbers used were between 10 to 80 post defrosting cell lines. Cell monolayers were grown in Dulbecco's modified Eagle's media as described previously (Hu M et al. 1994; Hu M et al. 1994). Cell cultures were maintained at 37ºC under 90% humidity and 5% CO2.

SOPs

Two different experimental protocols have been used to grow the cells and perform the experiments. Protocols for transport experiment differ mainly in the filter support coating and the medium and plastic ware brands and in the batch homogenization of some medium components (as the serum growth factor). Both protocols used tissue culture flasks 25 cm2 (T-25) or 75 cm2 (T-75) (Falcon, Beckton Dickinson). DMEM (Dulbecco's Modified Eagle's Medium With 4500 mg/L glucose, L-glutamine sodium bicarbonate, without sodium pyruvate from Sigma D5796) (89%) was adding by Gentamicin G1272 from Sigma (0.25%), MEM Non-Essential Aminoacid from Gibco 11140-035 (1%), Foetal Bovine Serum F7524 from Sigma (10%) and HEPES 1M 15630-056 by Gibco.

Solutions for cell trypsinization were done with PBS-CMF (Phosphate-buffered saline PBS, Calcium and Magnesium Free from Gibco 10010-015, 12 ml during 10 minutes and 0.25% Trypsin, 1mM EDTA.4Na in HBSS-CMF (2.5 g/L trypsin; 0.38 g/L EDTA.4Na) from Gibco 25200-056.

In the first protocol cells grew in a collagen coated polycarbonate membrane (Costar inserts, surface area 0.9 cm2, 0.4 μm pore size) (SOP 1) and, in the second one cells grew in a polycarbonate membrane without collagen coated. (MILLICEL-PCF, surface area 0.9 cm2, 0.4 μm pore size) (SOP 2).

Experimental factors:

Days between seeding

Experiments in Caco-2 cell monolayers were developed at 4, 15 or 21 days and in MDCK /MDCK-MDR1 at 4 or 9 days.

Experiment

All experimental conditions below explained were the same for all experiments. The integrity of each cell monolayer was checked by measuring its transepithelial electrical resistance (TEER) value before an experiment. Normal TEER values were typically 250 $\Omega \cdot cm^2$ for Caco-2 cells (21) and 190 $\Omega \cdot cm^2$ for MDCK or MDCK-MDR1 (25). Cell monolayers with TEER values less than 180 $\Omega \cdot cm^2$ or 150 $\Omega \cdot cm^2$ respectively were not used. Hank's balanced salt solution (HBSS) (9.8 g/L) supplemented with NaHCO3 (0.37 g/L), HEPES (5.96 g/L) and glucose (3.5 g/L) 14025-050 form Gibco was used for all the experiments after adjusting pH to the desired value in both protocols (26-27).

Transport studies were conducted in an orbital environmental shaker at constant temperature (37ºC) and agitation rate (100 rpm). Four samples of 200 μL each one were taken, and replaced with fresh buffer, from the receiver side at 30, 60, 90 and 120 minutes. Samples of the donor side were taken at the beginning and the end of the experiment. Moreover, the amount of compound in cell membranes and inside the cells was determined at the end of experiments in order to check the mass balance. The percentage of compound retained in the cell compartment was always less than 5%.

Transport studies were performed in both directions, from apical-to-basal (A-to-B) and from basal-to-apical (B-to-A) sides. The volume of donor compartment was 0.5 mL in A-to-B direction and 1.2 mL in B-to-A direction.

Post-experimental factor

Data analysis

The permeability was calculated from the drug concentrations and accumulated amounts in acceptor chamber using either linear or nonlinear regression models, depending of the assumption about sink conditions on the receptor side (28). The permeability calculation can be done according Sink (S) equation, Sink Corrected (SC) equation, Non-sink (NS) equation, Modified Non-Sink (MNS) equation (a recently developed modification of the non-sink analysis to accommodate lag times and higher permeability in the initial times).

Sink (S) equation

Permeability values in sink conditions are estimated from the first Fick's law equation under the assumption of sink condition (i.e.

negligible drug concentration in acceptor versus donor or in mathematical terms acceptor concentration<10% of donor concentration), no change of drug donor concentration during the assay and under a linear approximation of the appearance rates.

$$P_{eff} = ({}^{dQ}/_{dt})/S \cdot C_0 \quad (1)$$

where dQ/dt is the apparent appearance rate of drug in the receiver side, calculated using linear regression of amounts in the receiver chamber versus time, S is the surface area of the monolayer C0 is the drug concentration in the donor chamber and Peff is the permeability value. When the transport rate is low, neither the donor nor the receiver concentrations will change significantly with time, and sink conditions are assumed as a reasonable approximation.

Sink Corrected (SC) equation

Artursson et al. proposed a modified equation, in order to avoid the limitations of classical equation of sink conditions because even under sink conditions the change in donor concentration affects to the driving force and may not be negligible. In this new equation the concentration in the donor chamber changes in each sample interval (28).

$$P_{eff} = ({}^{dQ}/_{dt})/S \cdot C_D \quad (2)$$

where CD is the concentration in the donor chamber at each sample interval.

Non-sink (NS) equation

Under non sink conditions, the apparent permeability coefficient is calculated according the following equation:

$$C_{receiver,t} = \frac{Q_{total}}{V_{receiver}+V_{donor}} + \left(\left(C_{receiver,t-1} \cdot f \right) - \frac{Q_{total}}{V_{receiver}+V_{donor}} \right) \cdot e^{-P_{eff} \cdot S \cdot \left(\frac{1}{V_{receiver}} + \frac{1}{V_{donor}} \right) \cdot \Delta t} \quad (3)$$

where $C_{receiver,t}$ is the drug concentration in the receiver chamber at time t, Q_{total} is the total amount of drug in both chambers, $V_{receiver}$ and V_{donor} are the volumes of each chamber, $C_{receiver,t-1}$ is the drug concentration in receiver chamber at previous time, f is the sample replacement dilution factor, S is the surface area of the monolayer, Δt is the time interval and P_{eff} is the permeability coefficient. This equation considers a continuous change of the donor and receiver concentrations, and it is valid in either sink or non-sink conditions.

Modified Non-Sink (MNS) equation

$$C_{receiver,t} = \frac{Q_{total}}{V_{receiver}+V_{donor}} + \left(\left(C_{receiver,t-1} \cdot f \right) - \frac{Q_{total}}{V_{receiver}+V_{donor}} \right) \cdot e^{-\boldsymbol{P_{eff\ 0,1}} \cdot S \cdot \left(\frac{1}{V_{receiver}} + \frac{1}{V_{donor}} \right) \cdot \Delta t} \quad (4)$$

All the terms are defined in the previous equation and Peff is the permeability coefficient, which might be Peff 0 or Peff 1. This equation, as equation 3 considers a continuous change of the donor and receiver concentrations, and it is valid in either sink or non-sink conditions. The new feature is the option to estimate two permeability coefficients (Peff 0 and Peff 1) to account for atypical profiles in which the initial rate is different (24).

The non-linear regressions to fit equation 3 (NS) and 4 (MNS) to data can be performed in Excel using Solver tool for minimization of the Sum of Squared Residuals. Equation 1 (S) and equation 2 (SC) are linear regression models that can be also executed in Excel.

Studies were performed by triplicate and the data were presented as mean ± standard deviation (SD). ANOVA and Scheffe post hoc tests and Student's t-test were performed with PASW Statistics 17 (SPSS Inc.) in order to determine statistically significant differences between A-to-B and B-to-A permeability values, as well as the influence of factors than can affect permeability values.

Akaike criterion (AIC), weighted sum of squared residuals (SSR), were used to evaluate the goodness of fit and to select the best data analysis. The improvement of the sum of squared residuals value by a more complex model was statistically assessed with a Snedecor's F test. The more complex model was accepted at a significance value $p<0.05$.

RESULTS

Post-experimental factors

Data analysis

The selection of the best permeability estimation model is required in order to obtain less biased values ant to compare experimental conditions and protocols. Table 1 summarizes the analysis of the modelling strategies for permeability estimation. In the first place it was determined if sink conditions prevailed or not in each well before selecting the equation to estimate the permeability. In "sink conditions" wells the linear approximations were used and the best fit models were

selected. In non-sink conditions, non-sink equation and the modified non sink equation were used. Table 1 reflects the percentage of wells accomplishing sink or not sink conditions and the best fit model for each situation.

Table 5. Comparison of models for permeability estimation under sink and non-sink conditions. *Model comparison by AIC value. **Models compared by Snedecor's F test over the sum of squared residuals corrected by the degrees of freedom.

Conditions prevailing in the experiment	Best fit model
Sink (47% of wells) *	Sink Model 0 % Sink corrected model 100%
Non-Sink (53 % of wells)**	Non sink 12% Modified Non sink 88%

Consequently the permeability estimation was performed with Sink corrected approach when sink conditions prevailed and Modified non-sink model in all the non-sink conditions.

Pre-experimental factors

Passage number

Figures 1 and 3 represent permeability values of Metoprolol obtained at different passage number after thawing the three cell lines Caco-2, MDCK and MDCK-MDR1 using both protocols (SOP). Figure 2 and 4 represent the variability (expressed as coefficient of variation) in each passage number and cell line. In this set of experiments SOP 1 experiments were performed 21 days after seeding while SOP 2 maturation time after seeding was 15 days.

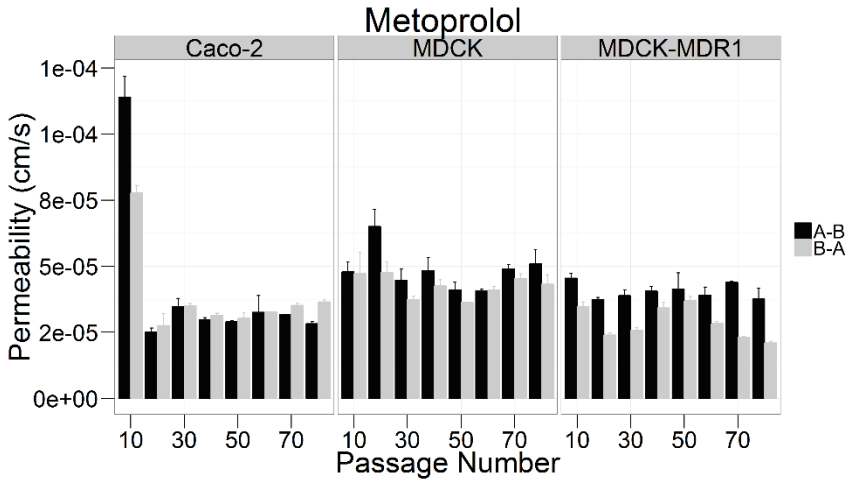

Figure 1. Permeability values of Metoprolol (100 μM) obtained at different passage number after thawing process in 3 cell lines. (SOP1)

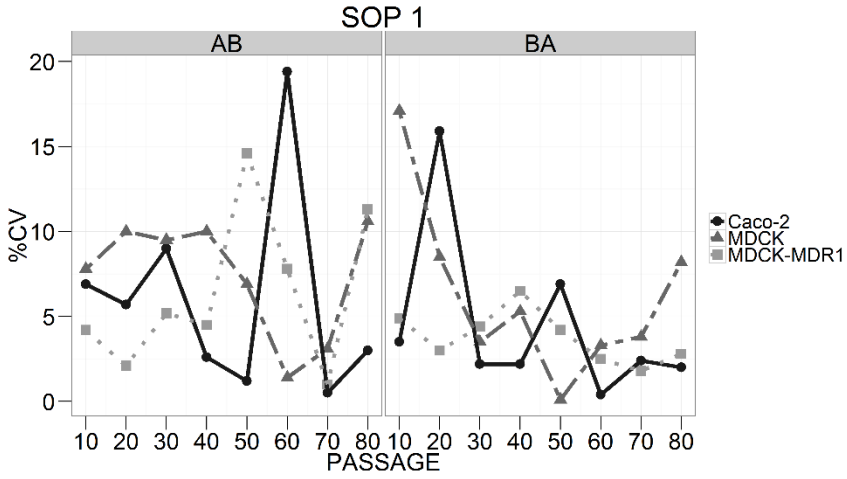

Figure 2. Variability in the estimation of permeability values obtained with SOP 1, expressed as coefficient of variation in both directions and in the three cell lines

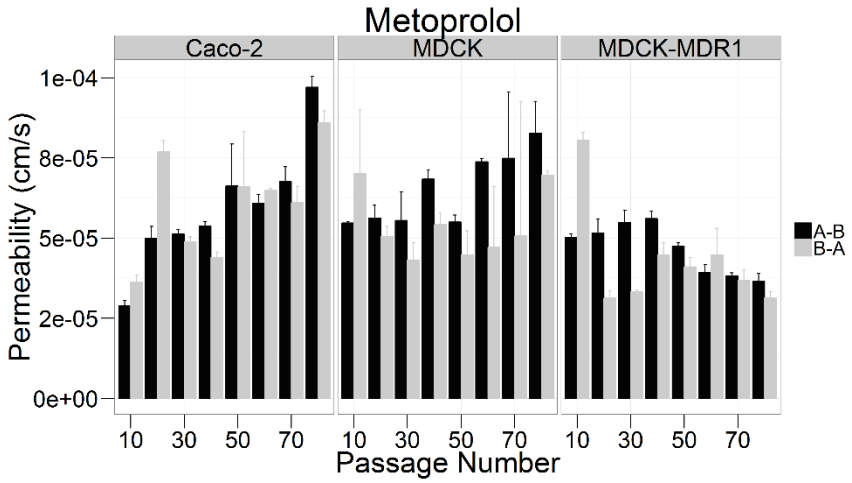

Figure 3. Permeability values of Metoprolol (100 μM) obtained at different passage number after defrost process in 3 cell lines. (SOP2)

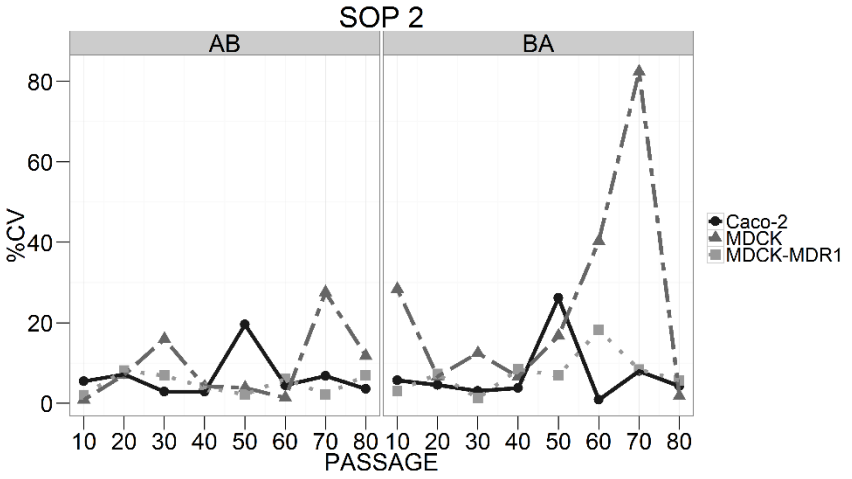

Figure 4. Variability in the estimation of permeability values obtained with SOP 2, expressed as coefficient of variation in both directions and in the three cell lines

In SOP 1 the one-way analysis of variance detected differences in permeability values with passage number only in Caco-2 cells. Post hoc Scheffe test concluded statistical significant differences among all passages versus passage 10 in Caco-2 cells (in AB and BA directions).

No differences in permeability values with passage number were detected in MDCK and MDR cell lines

In SOP 2 the one-way analysis of variance detected differences in permeability values in each direction with passage number in the three cell lines. Post hoc Scheffe test concluded statistical significant differences among all passages versus passage 10 in MDR cells (in AB and BA directions). Differences are detected (with passage 10) after passage 60 in MDCK and after passage 20 in Caco-2 cells (in both directions).

Protocol (SOP)

Both SOPs were compared in 3 cell lines and using early (10 passages after defrost), intermediate (40 passages after defrost) or late (80 passages after defrosting) passages. Permeability values of typical marker compounds as LY (paracellular marker), Metoprolol (transcellular marker) and Rhodamine 123 (secretion marker due to P-pg) were investigated. Results are summarized in Figures 5 to 7. The coefficients of variation of permeability values of each compound in each cell line and protocol are represented in Tables 2 to 4.

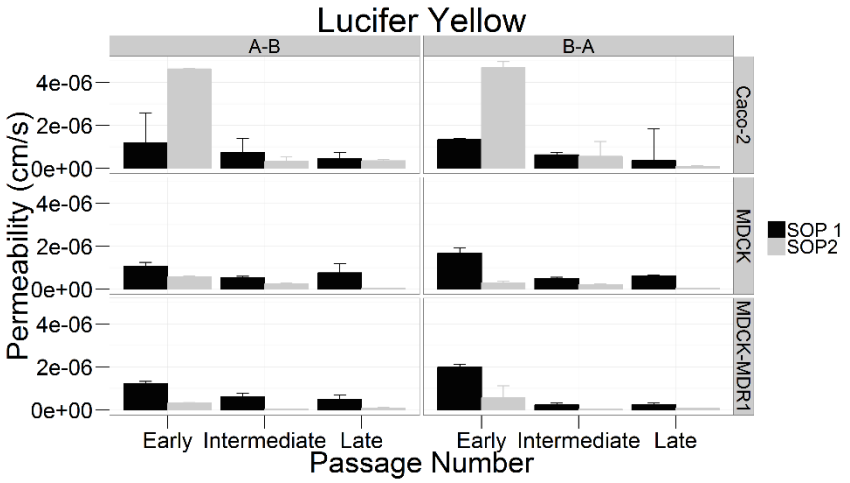

Figure 5. Permeability values of LY (2mM) obtained with both harvesting protocols (SOPs) at different passage number after defrosting process in 3 cell lines.

Table 2. Variability in Lucifer Yellow permeability values in both protocols, in different passage numbers and cell lines.

Lucifer Yellow	Passage	CV% SOP1	CV% SOP2
Caco2	Early	7.3	3.0
Caco2	Intermediate	11.8	90.8
Caco2	Late	5.1	23.2
MDCK	Early	15.6	15.2
MDCK	Intermediate	10.3	9.7
MDCK	Late	4.8	18.7
MDR	Early	7.1	9.6
MDR	Intermediate	2.8	38.3
MDR	Late	16.1	28.0
Average		9.0	26.3

Anova analysis and Scheffe post-hoc comparison showed differences in both SOP's in LY permeability values among all passages (in both directions).

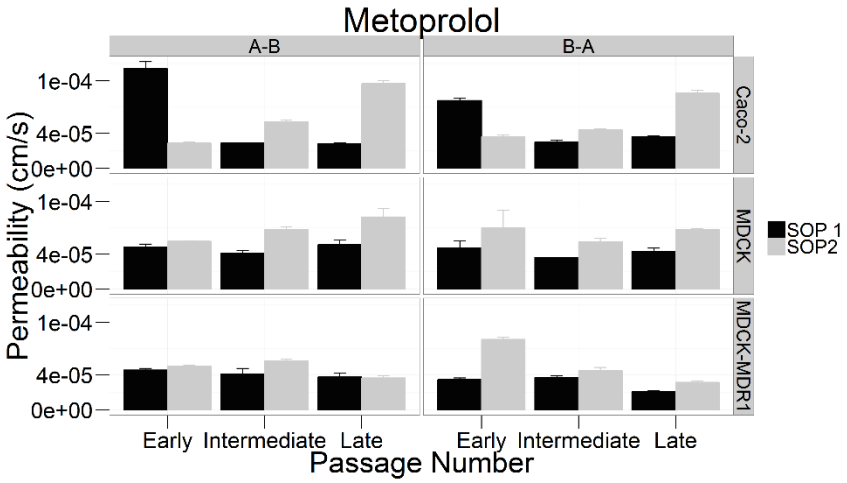

Figure 6. Permeability values of Metoprolol (100 μM) obtained with both harvesting protocols (SOPs) at different passage number after defrosting process in 3 cell lines.

Table 3. Variability in Metoprolol permeability values in both protocols, in different passage numbers and cell lines.

Metoprolol	Passage	CV% SOP1	CV% SOP2
Caco2	Early	4.1	5.4
Caco2	Intermediate	8.8	9.4
Caco2	Late	7.4	4.5
MDCK	Early	8.6	6.6
MDCK	Intermediate	3.5	4.2
MDCK	Late	2.2	8.0
MDR	Early	3.1	6.3
MDR	Intermediate	4.0	17.5
MDR	Late	2.5	7.1
Average		4.9	7.7

Anova analysis and Scheffe post-hoc comparison showed differences in both SOP's in Metoprolol permeability values in early passage compared with late (in both directions and all cell lines)

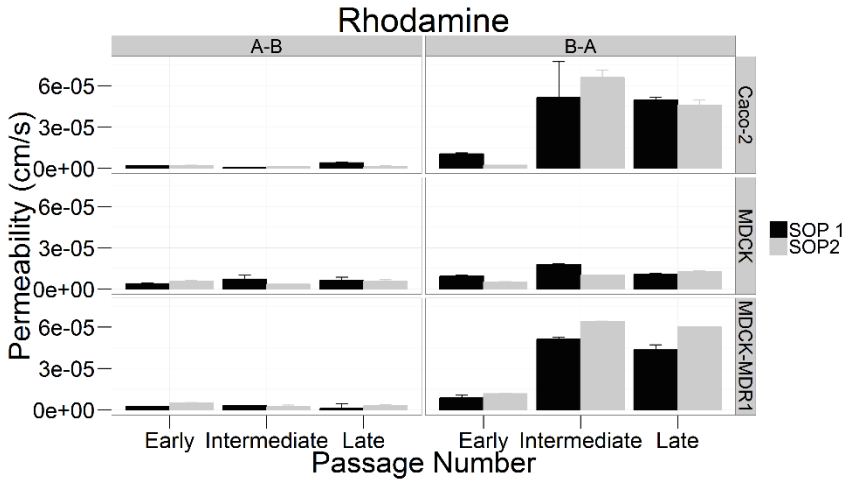

Figure 7. Permeability values of Rhodamine (5.5 μM) obtained with both harvesting protocols (SOPs) at different passage number after defrosting process in 3 cell lines.

Table 4. Variability in Rhodamine permeability values in both protocols, in different passage numbers and cell lines

Rhodamine	Passage	CV% SOP1	CV% SOP2
Caco2	Early	4.6	6.2
Caco2	Intermediate	36.5	5.7
Caco2	Late	145.7	27.2
MDCK	Early	4.0	16.5
MDCK	Intermediate	5.5	4.9
MDCK	Late	47.1	7.6
MDR	Early	29.0	7.5
MDR	Intermediate	8.4	4.0
MDR	Late	2.3	0.5
Average		31.5	8.9

Anova analysis and Scheffe post-hoc comparison showed differences in both SOP's in Rhodamine permeability values in early

passage compared with late in BA direction in MDCK and MDR but not in Caco-2 cells.

Experimental factors

Days between seeding and experiment

One of the factors affecting permeability values is the time between seeding cells and performing the experiment as it could affect to the transporter expression and cell maturation. The usual maturation time depends on the kind of cells and it used to be from 4 to 21 days in Caco2 cell line and from 4 to 9 in MDCK and MDR1. Our aim was to confirm the influence of the maturation time in SOP1 in order to select the best option for further experiments. For this reason, transport experiments were performed at different time post seeding according to the cell line assayed. For Metoprolol and Lucifer Yellow an intermediate passage number was used while for Rhodamine it has also been checked the relevance of the passage number as from the previous experiments it was shown that for a carrier mediated compound the influence of the passage number was a relevant factor on the transporter expression.

Figures 8, 9 and 10 show the permeability values of Lucifer Yellow, Metoprolol and Rhodamine respectively obtained at different times post seeding and passages in the three cell lines.

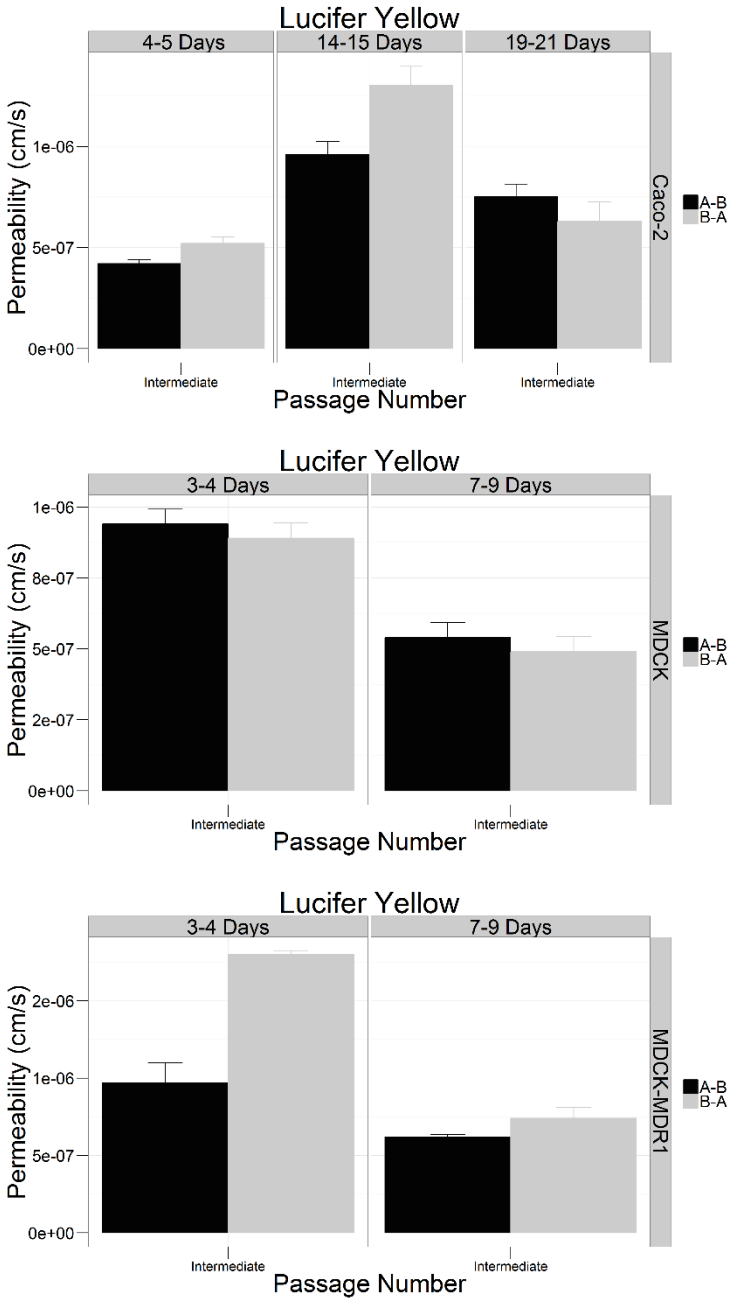

Figure 8. Permeability values of LY (2mM) obtained at different times post seeding and passages in the three cell lines.

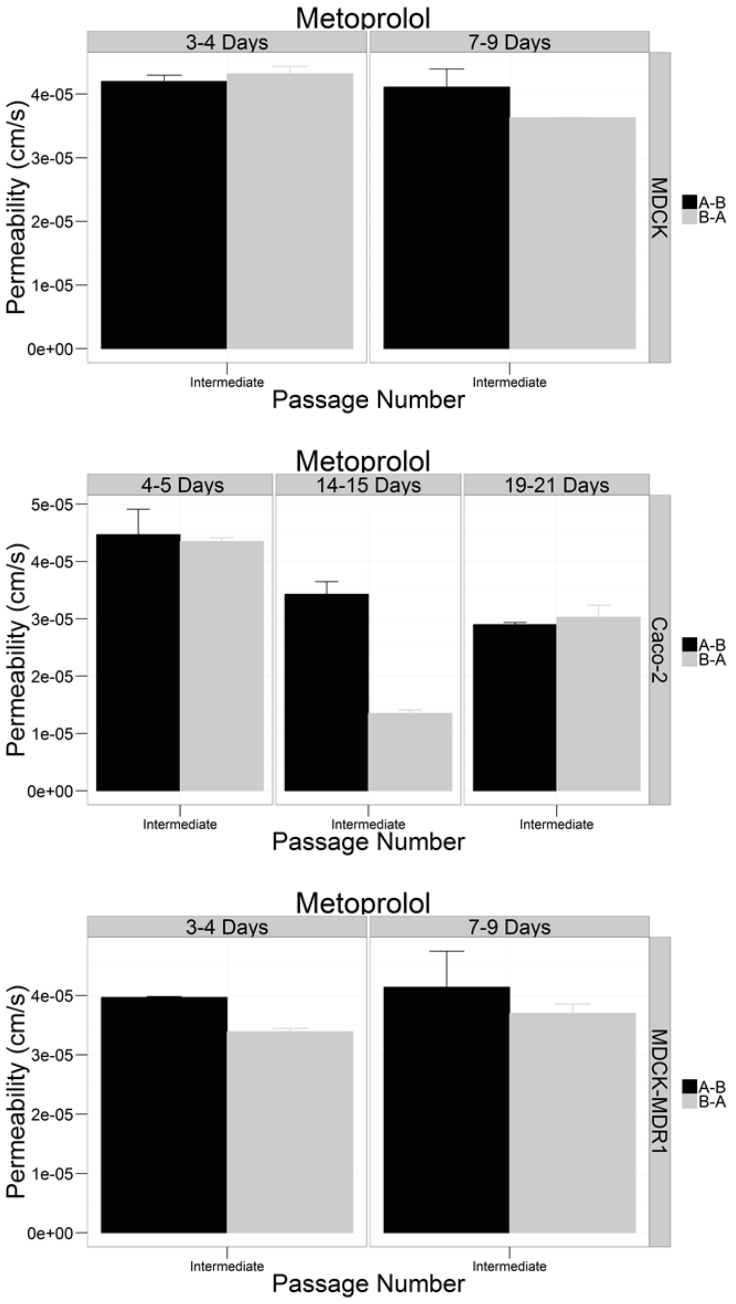

Figure 9. Permeability values of Metoprolol (100 μM) obtained at different times post seeding and passages in the three cell lines.

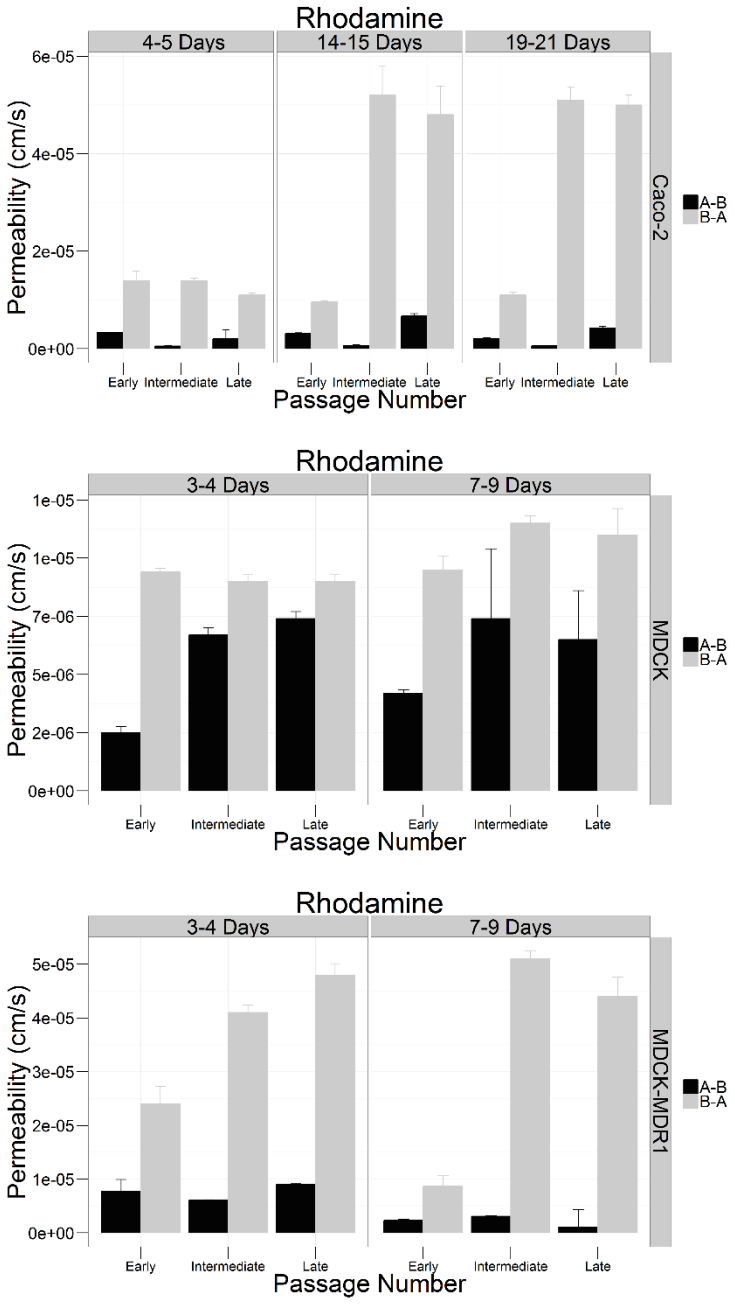

Figure 10. Permeability values of Rhodamine (5.5 μM) obtained at different times post seeding and passages in the three cell lines.

The two-way analysis of variance and scheffe post hoc analysis demonstrated statistical significant differences in permeability values with the time after seeding in the three cell lines and for all the compounds.

Tables 5 to 7 summarized the average coefficient of variation in AB and BA permeability values in the different conditions (passage and time after seeding) for all cell lines and compounds.

Table 5. Variability in permeability values of Rhodamine obtained in different cell lines and passages with different maturation days after seeding.

Rhodamine			
Line	**Passage**	**Days**	**Mean CV%**
Caco2	Early	4	7.1
		15	3.5
		21	5.0
	Intermediate	4	10.4
		15	11.6
		21	4.9
	Late	4	**46.6**
		15	9.7
		21	6.4
MDCK	Early	4	5.9
		9	4.9
	Intermediate	4	4.0
		9	21.6
	Late	4	3.7
		9	21.2
MDR	Early	4	21.2
		9	15.5
	Intermediate	4	2.4
		9	2.6
	Late	4	3.6
		9	149.5

Table 6. Variability in permeability values of Lucifer Yellow obtained in different cell lines and passages with different maturation days after seeding

Lucifer Yellow		
Line	**Days**	**Mean CV%**
Caco 2	4	5.1
	15	7.0
	21	11.8
MDCK	4	5.8
	9	10.3
MDR	4	7.3
	9	6.2

Table 7. Variability in permeability values of Metoprolol obtained in different cell lines and passages with different maturation days after seeding

Metoprolol		
Line	**Days**	**Mean CV%**
Caco 2	4	3.8
	15	8.4
	21	8.5
MDCK	4	3.6
	9	3.0
MDR	4	1.4
	9	3.0

DISCUSSION

Pre-experimental factors

Passage number

The effect of passage number was studies in both protocols with Metoprolol. The effect of passage number was different in SOP 1 versus SOP 2. In SOP 1 with Caco-2 cells after passage 10 the permeability values decreased and remained fairly constant in the subsequent passages. In MDCK and MDR1 passage number does not

seem to affect to the permeability values at least in the range of passages assayed (Figure 1).

In SOP 2 on the contrary the passage number had a marked effect on Metoprolol permeability in particular in Caco-2 cells where there is a trend with higher permeability values of Metoprolol with higher passages (Figure 2). This result is in contradiction with other studies in which lower permeability values are found with higher passages due to tighter paracellular space [88]. In order to explain these differences further experiments with Lucifer Yellow and Rhodamine were performed to compare both protocols. (See next section)

On the other hand the variability in permeability estimation showed a trend to decrease in MDCK and Caco-2 cells with SOP1 but a tendency to increase in SOP 2. MDCK-Mdr1 showed the lower variability in both protocols (ranged between 5 and 7% as average values), without any relevant change with passage number.

Considering these results, SOP 1 at intermediate passage number seems to be the best experimental conditions to compare drugs absorbed by passive diffusion by transcellular route.

Protocol

Coating with collagen is the main difference between both protocols and it has been show that rat collagen type I coating leads to a quicker confluence and higher cell density in caco-2 cells compared with filters without coating. Collagen coating also affect to transport expression and enzyme activity (2).

A more detailed comparison between protocols was done using three model compounds to check changes in paracellular, transcellular and P-gp expression. With SOP 1 as well as SOP 2 Lucifer Yellow

permeability decreased with higher passages in all cell lines, but Metoprolol permeability values decreased with higher passages in SOP 1 but increased in SOP 2 in Caco- 2 cells. These differences were lower in MDCK and MDR lines. For both compounds variability in average CV was lower for SOP 1 (see Tables 2 and 3). It seems that with both protocols in all cell lines the paracellular route becomes more restricted with higher passage numbers. The increase in Metoprolol permeability in SOP 2 with higher passage numbers is difficult to explain but it reflects a loss of the trans-cellular barrier properties with higher passages.

These results confirm the conclusion of the previous experiments, indicating that coating in SOP 1 helps to cell differentiation in a more stable manner compared to SOP 2 which showed permeability changes with passage and also more variable values

Regarding Rhodamine permeability, it was not affected by passage number in Caco-2 cells with any of the protocols, but variability increased with higher passage numbers. This result is in contradiction with the observed by Siisalo et al. (29) who observe a clear effect of passage number in P-gp and other transporters expression in Caco-2 cell. In accordance with Siisalo et al in MDCK and MDR P-gp functionality is increased at higher passage numbers in both protocols. In this compound variability is lower with SOP 2.

The differences in SOP 1 and 2 regarding the effect of passage number on the different permeation routes show the complexity of the involved mechanisms. For P-gp interaction studies in this case would be more convenient SOP 2 at intermediate or late passage numbers.

Experimental factors

Days between seeding and experiment

The time post seeding had the expected effect in particular in Rhodamine permeability for which higher maturation times lead to a higher expression of the transporter (see Figure 7). The influence on Metoprolol and Lucifer Yellow is less clear and even if statistical differences are detected there is not a clear trend neither in permeability values nor in variability. These results support the idea of developing "fast maturation" models that can be useful for screening compounds absorbed by passive mechanism (30).

Post-experimental factors

Data analysis

The analysis of permeability data was performed with the four possible approximations but the final model was selected based on goodness of fit criteria (AIC and Snedecor's F test). The selection of the analysis method is a relevant aspect to reduce inter- and intra-laboratory variability as the estimated permeability value can change up to a 100% in value with different methods. On the other hand in order to obtain the most accurate estimate it is necessary to use a calculation method with accurate implicit assumptions. Even when sink conditions prevail, the donor concentration changes with time thus sink corrected equation gave better fit in 100% of the linear cases. For non-sink conditions the percent of wells with some deviation in the first data point (lag time or higher permeation rate) is about 30% thus making necessary to include a second parameter in the model to account for the deviation and avoid

the bias in slope estimation. Our new approach gave a better fit to experimental data in most non-sink wells.

CONCLUSIONS

The results obtained in this study confirm the complexity of the interaction between cell culturing protocols and cell lines and the need for standardization and characterization of the culture properties to optimize the conditions depending on the study objectives. In our study, the average variability observed in permeability values in all cell lines is around 10%-15% that means that for detecting a 15% difference in permeability values the required number of individual estimations would be between 8 and 12, i.e. one plate of 12 wells. The variability is lower in intermediate passages in Caco-2 cells supporting the recommendation of use a short range of passages to a particular study. MDCK was more influenced by the passage number, with less CV in lower passages. MDCK-MDR1 showed constant CV among passages, protocols and experimental conditions but permeability values were affected by all the studied conditions, indicating that for this cell line standardization of experimental conditions is in particular relevant to obtain comparable results between different laboratories.

As conclusion, we have confirmed the influence of maturation conditions, passage number in permeability values and in their variability. Based in our results protocol with coating would be more adequate for studies of compounds absorbed by passive diffusion but the protocol without coating gave us better results for studies about P-gp interactions. A similar study should be done in each laboratory to

understand the influence of their protocols in the monolayer properties in order to standardizing conditions and setting the acceptance criteria.

ACKNOWLEDGEMENTS

The authors acknowledge partial financial support to projects: DCI ALA/19.09.01/10/21526/245-297/ALFA 111(2010)29: Red-Biofarma. Red para el desarrollo de metodologias biofarmaceuticas racionales que incrementen la competencia y el impacto social de las Industrias Farmaceuticas Locales. AGL2011-29857-C03-03, Foodomics evaluation of dietary polyphenols against colon cancer using *in vitro* and *in vivo* models from Spanish Ministry of Science and Innovation, STREP project: MEMTRANS: Membrane transporters: *In vitro* models for the study of their role in drug fate (FP6 LSHB-CT-2006- 518246). Victor Mangas-Sanjuán received a grant from Ministry of Education and Science of Spain and Miguel Hernandez University (FPU AP2010-2372)..

REFERENCES

1. W.J. Roth, D.J. Lindley, S.M. Carl, and G.T. Knipp. The effects of intralaboratory modifications to media composition and cell source on the expression of pharmaceutically relevant transporters and metabolizing genes in the Caco-2 cell line. Journal of pharmaceutical sciences. 2012; 101:3962-3978.

2. Y. Sambuy, I. De Angelis, G. Ranaldi, M.L. Scarino, A. Stammati, and F. Zucco. The Caco-2 cell line as a model of the intestinal barrier: influence of cell and culture-related factors on Caco-2 cell functional characteristics. Cell Biol Toxicol. 2005; 21:1-26.

3. I. Behrens, W. Kamm, A.H. Dantzig, and T. Kissel. Variation of peptide transporter (PepT1 and HPT1) expression in Caco-2 cells as a function of cell origin. Journal of pharmaceutical sciences. 2004; 93:1743-1754.

4. P. Artursson. Epithelial transport of drugs in cell culture. I: A model for studying the passive diffusion of drugs over intestinal absorptive (Caco-2) cells. Journal of pharmaceutical sciences. 1990; 79:476-482.

5. P. Arturssonand R.T. Borchardt. Intestinal drug absorption and metabolism in cell cultures: Caco-2 and beyond. Pharmaceutical research. 1997; 14:1655-1658.

6. S. Tavelin, J. Taipalensuu, L. Soderberg, R. Morrison, S. Chong, and P. Artursson. Prediction of the oral absorption of low-permeability drugs using small intestine-like 2/4/A1 cell monolayers. Pharmaceutical research. 2003; 20:397-405.

7. A. Dahan, J.M. Miller, J.M. Hilfinger, S. Yamashita, L.X. Yu, H. Lennernas, and G.L. Amidon. High-permeability criterion for BCS classification: segmental/pH dependent permeability considerations. Mol Pharm. 2010; 7:1827-1834.

8. Y. Adachi, H. Suzuki, and Y. Sugiyama. Comparative studies on *in vitro* methods for evaluating *in vivo* function of MDR1 P-glycoprotein. Pharmaceutical research. 2001; 18:1660-1668.

9. T. Watanabe, R. Onuki, S. Yamashita, K. Taira, and Y. Sugiyama. Construction of a functional transporter analysis system using MDR1 knockdown Caco-2 cells. Pharmaceutical research. 2005; 22:1287-1293.

10. S. Lundquist, M. Renftel, J. Brillault, L. Fenart, R. Cecchelli, and M.P. Dehouck. Prediction of drug transport through the blood-brain barrier *in vivo*: a comparison between two *in vitro* cell models. Pharmaceutical research. 2002; 19:976-981.

11. P. Garberg, M. Ball, N. Borg, R. Cecchelli, L. Fenart, R.D. Hurst, T. Lindmark, A. Mabondzo, J.E. Nilsson, T.J. Raub, D. Stanimirovic, T. Terasaki,

J.O. Oberg, and T. Osterberg. *In vitro* models for the blood-brain barrier. Toxicol *In Vitro*. 2005; 19:299-334.

12. Q. Wang, J.D. Rager, K. Weinstein, P.S. Kardos, G.L. Dobson, J. Li, and I.J. Hidalgo. Evaluation of the MDR-MDCK cell line as a permeability screen for the blood-brain barrier. Int J Pharm. 2005; 288:349-359.

13. S. Ferruzza, C. Rossi, Y. Sambuy, and M.L. Scarino. Serum-reduced and serum-free media for differentiation of Caco-2 cells. Altex. 2013; 30:159-168.

14. S.M. Moyes, J.F. Morris, and K.E. Carr. Culture conditions and treatments affect Caco-2 characteristics and particle uptake. International journal of pharmaceutics. 2010; 387:7-18.

15. C.S. Bestwickand L. Milne. Alteration of culture regime modifies antioxidant defenses independent of intracellular reactive oxygen levels and resistance to severe oxidative stress within confluent Caco-2 "intestinal cells". Dig Dis Sci. 2001; 46:417-423.

16. X.W. Wu, R.F. Wang, M. Yuan, W. Xu, and X.W. Yang. Dulbecco's modified eagle's medium and minimum essential medium--which one is more preferred for establishment of Caco-2 cell monolayer model used in evaluation of drug absorption? Pharmazie. 2013; 68:805-810.

17. S.A. Bravo, C.U. Nielsen, J. Amstrup, S. Frokjaer, and B. Brodin. In-depth evaluation of Gly-Sar transport parameters as a function of culture time in the Caco-2 cell model. European journal of pharmaceutical sciences : official journal of the European Federation for Pharmaceutical Sciences. 2004; 21:77-86.

18. S. Lu, A.W. Gough, W.F. Bobrowski, and B.H. Stewart. Transport properties are not altered across Caco-2 cells with heightened TEER despite underlying physiological and ultrastructural changes. Journal of pharmaceutical sciences. 1996; 85:270-273.

19. H. Yu, T.J. Cook, and P.J. Sinko. Evidence for diminished functional expression of intestinal transporters in Caco-2 cell monolayers at high passages. Pharmaceutical research. 1997; 14:757-762.

20. D.A. Volpe. Variability in Caco-2 and MDCK cell-based intestinal permeability assays. Journal of pharmaceutical sciences. 2008; 97:712-725.

21. I.J. Hidalgo, T.J. Raub, and R.T. Borchardt. Characterization of the human colon carcinoma cell line (Caco-2) as a model system for intestinal epithelial permeability. Gastroenterology. 1989; 96:736-749.

22. M. Markowska, R. Oberle, S. Juzwin, C.P. Hsu, M. Gryszkiewicz, and A.J. Streeter. Optimizing Caco-2 cell monolayers to increase throughput in drug intestinal absorption analysis. J Pharmacol Toxicol Methods. 2001; 46:51-55.

23. G. Englund, F. Rorsman, A. Ronnblom, U. Karlbom, L. Lazorova, J. Grasjo, A. Kindmark, and P. Artursson. Regional levels of drug transporters along the human intestinal tract: co-expression of ABC and SLC transporters and comparison with Caco-2 cells. European journal of pharmaceutical sciences : official journal of the European Federation for Pharmaceutical Sciences. 2006; 29:269-277.

24. V. Mangas-Sanjuan, I. Gonzalez-Alvarez, M. Gonzalez-Alvarez, V.G. Casabo, and M. Bermejo. Modified Nonsink Equation for Permeability Estimation in Cell Monolayers: Comparison with Standard Methods. Mol Pharm. 2014.

25. C. Navarro, I. Gonzalez-Alvarez, M. Gonzalez-Alvarez, M. Manku, V. Merino, V.G. Casabo, and M. Bermejo. Influence of polyunsaturated fatty acids on Cortisol transport through MDCK and MDCK-MDR1 cells as blood-brain barrier *in vitro* model. European journal of pharmaceutical sciences : official journal of the European Federation for Pharmaceutical Sciences. 2011; 42:290-299.

26. M. Hu, J. Chen, D. Tran, Y. Zhu, and G. Leonardo. The Caco-2 cell monolayers as an intestinal metabolism model: metabolism of dipeptide Phe-Pro. J Drug Target. 1994; 2:79-89.

27. M. Hu, J. Chen, Y. Zhu, A.H. Dantzig, R.E.J. Stratford, and M.T. Kuhfeld. Mechanism and kinetics of transcellular transport of a new beta-lactam antibiotic loracarbef across an intestinal epithelial membrane model system (Caco-2). Pharm Res. 1994; 11:1405-1413.

28. S. Tavelin, J. Grasjo, J. Taipalensuu, G. Ocklind, and P. Artursson. Applications of epithelial cell culture in studies of drug transport. Methods Mol Biol. 2002; 188:233-272.

29. S. Siissalo, L. Laitinen, M. Koljonen, K.S. Vellonen, H. Kortejarvi, A. Urtti, J. Hirvonen, and A.M. Kaukonen. Effect of cell differentiation and passage number on the expression of efflux proteins in wild type and vinblastine-induced Caco-2 cell lines. European journal of pharmaceutics and biopharmaceutics : official journal of Arbeitsgemeinschaft fur Pharmazeutische Verfahrenstechnik eV. 2007; 67:548-554.

30. K.A. Lentz, J. Hayashi, L.J. Lucisano, and J.E. Polli. Development of a more rapid, reduced serum culture system for Caco-2 monolayers and application to the biopharmaceutics classification system. International journal of pharmaceutics. 2000; 200:41-51.

Chapter 6

Innovative *In Vitro* Method to Predict Rate and Extent of Drug Delivery to the Brain across the Blood-Brain Barrier

Mangas-Sanjuan, V.[1,2]; Gonzalez-Alvarez, I.[2]; Gonzalez-Alvarez, M.[2]; Casabo, VG.[1,2]; Bermejo, M.[2]

[1]Pharmaceutics and Pharmaceutical Technology Department. University of Valencia.
[2]Department of Engineering, Pharmaceutics and Pharmaceutical Technology Area. University Miguel Hernández, Elche.
[ω]Deceased, July 7, 2013.

Molecular Pharmaceutics, 2013
Volume 10, Pages 3822-3821

INTRODUCTION

The prevalence of central nervous system (CNS) disorders worldwide is around 30% and it is estimated that 65% of CNS patients do not receive any or correct treatment [1]. For instance, the health costs related to stroke, depression, schizophrenia and Alzheimer's disease patients in United States are estimated to be over US$250 billion. This tendency is expected to raise [2] because most of the CNS drugs are used to treat symptoms rather than the etiology [3] and due to other factors like ageing society and unhealthy life styles [4].

The drug development process has shown its sub-optimal efficiency on the light of the increasing cost and time to reach the market and the decreasing number of drugs approved in the last years [5]. In the CNS related drugs, the probability of success in obtaining a marketing authorization is less than 7% [6] and the time needed, considering clinical and regulatory phases, is around 10.5 years, the longest compared to other therapeutic areas [7]. Thereby, reliable methods for selecting the best candidates in the early preclinical phases are urgently needed in order to reduce the risk of costly later failures in clinical phases [3, 8].

Blood-brain barrier (BBB) controls the access of endogenous substances and xenobiotics to the extracellular fluid (ECF) and intracellular cerebral fluid (ICF). BBB is an active barrier with important functions for brain homeostasis and protection, formed by endothelial cells with high expression of tight junctions and transporters. Only the unbound fraction of drug in plasma can permeate through the BBB and interact with the target in the brain [4, 9-11]. The most important parameters that govern the pharmacokinetics of drug in the CNS are $f_{u,\ plasma}$, $Kp_{,uu,\ brain}$ and $V_{u,\ brain}$. $f_{u,\ plasma}$ is the unbound fraction of drug in

plasma, $Kp_{uu,\ brain}$ represents the ratio between unbound drug concentrations in brain and in blood and $V_{u,\ brain}$ is the apparent distribution volume in brain. ECF concentrations could only be obtained using microdialysis. For ethical reasons, human cerebrospinal fluid concentrations (CSF) have been used as a surrogate measure of the ECF concentrations. De Lange et al. has recently published the utility of human $Kp_{uu,\ CSF}$ as reference of the ECF concentrations in brain [4].

In silico, *in vitro*, *in situ* or *in vivo* methodologies have been employed to evaluate the pharmacokinetic of new drug candidates in the CNS [12]. *In vitro* cell culture experiments are used as a high throughput method to select best candidates for further stages of the drug development process, however permeability coefficients (P_{app}) are relevant only for the rate of access and the onset of action but do not determine the extent as in a steady state drug administration there is not a limited time for the permeation process. Consequently the range of adequate permeability values for BBB barrier is wider than that used for intestinal permeability screening [10, 13]. Different *in vitro* cell models have been used to mimic the blood-brain barrier (BBB) [14-18]. Madin-Darby canine kidney II (MDCKII) cells and MDCKII transfected with the human multidrug resistance gene 1 (encoding P- glycoprotein, P-gp) (MDCKII-MDR1) are commonly used to evaluate the blood–brain barrier permeability of drugs [16, 19, 20] MDCK I cells show much higher transepithelial electric resistance (TEER) than MDCK II cells, although they bear similar numbers of tight junction (TJ) strands [21]. These cells display morphological, enzymatic, and antigenic cell markers, also found in cerebral endothelial cells and have been reported as a suitable model for this barrier. The MDCKII-MDR1 cell line was

identified as the most promising cell line among several cell lines, for qualitative predictions of brain distribution, and to distinguish between compounds that pass the blood–brain barrier by passive diffusion and those that are substrates for active efflux by P-glycoprotein, P-gp [22-24]. The P-gp transporter and other membrane transporters belonging to the ATP-binding cassette family of transporters have been extensively described to regulate intracellular concentrations of different compounds [25-27].

The *in vivo* microdialysis is the gold standard technique, allowing continuous monitoring with high-resolution concentration profiles of drugs and metabolites from (freely moving) individual subjects. Measurements are obtained from brain extracellular fluid, inserting one probe into the brain tissue and from peripheral blood stream. Then, unbound brain and plasma concentrations are estimated as the best reference to explore drug permeation and distribution across the BBB [9, 10, 28-30]. However, the main disadvantage of this technique is the high time-consuming, which reduces its application as a high screening method for new drug candidates.

The aim of the present work was to develop a new whole *in vitro* high throughput method to predict drug rate and extent of access across the BBB. The system permits using apparent permeability values (Papp) from *in vitro* cell monolayers experiments in different conditions to estimate $f_{u,\,plasma}$, $V_{u,\,brain}$, and $Kp_{uu,\,brain}$.

In order to explore the feasibility of the *in vitro* system as a screening method for CNS compounds the predicted *in vitro* values have been correlated to *in vivo* $f_{u,\,plasma}$, $Kp_{uu,\,brain}$, human $Kp_{uu,\,CSF}$ and $V_{u,\,brain}$ values obtained by microdialysis by Friden et al. [31] (Table 1). Cell cultures of MDCKII and MDCKII-MDR1 have been used to compare

its prediction performance and to determine the transport mechanism for each compound tested.

						RAT				HUMAN
COMPOUND	**MW (g/mol)**	**log P**	**HBA**	**P-gp**	**CNS**	**Cu (µM)**	**Vu,brain (ml/g brain)**	**fup**	**Kpuu,brain**	**Kpuu,csf**
Amitriptyline	277.39	4.41	1	+	+	0.022	310	0.09	0.73	0.18
Atenolol	266	0.335	5	-	-	1.5	2.5	1	0.026	0.54
Diphenhydramine	291.82	2.997	2	-	+	0.051	32	0.48	1.05	
Ethyl-phenyl malonamide	206.24	0.348	4	-	+	4.3	0.9	0.55	1.25	
Levofloxacin	361.37	1.855	7	+	+	0.59	1.7	0.82	0.12	0.18
Metoprolol	267.38	1.632	4	-	-	0.75	5.5	0.9	0.64	0.93
Norfloxacin	319.13	1.744	6	+	-	0.7	2.9	0.87	0.028	0.11
Propranolol	259.4	2.9	3	+	+	0.051	118	0.09	0.61	0.42
Verapamil	454.6	3.899	6	+	-	0.075	54	0.12	0.053	1.13
Zidovudine	267.24	0.052	9	-	+	1.2	1.1	0.64	0.09	1.04

Table 1. *In vivo* data for each compound tested.[89] MW means molecular weight, HBA is hydrogen bond acceptor. Cu is the unbound plasma concentration in rat, Vu,brain refers to apparent volume of distribution in brain, fu,p is the unbound fraction in plasma, Kp,uu,brain is the unbound relationship between brain and plasma in rat and Kp,uu,CSF is the unbound relationship between cerebrospinal fluid in human

EXPERIMENTAL SECTION

Chemicals. Amitriptyline, Atenolol, Diphenhydramine, Ethyl-Phenyl Malonamide, Levofloxacin, Metoprolol, Norfloxacin, Propranolol, Verapamil and Zidovudine were purchased by Sigma Aldrich. Sodium azide (Az) as inhibitor was purchased from Sigma (Barcelona, Spain). All other reactives were HPLC grade. Experiments were conducted in four different concentrations and in the presence of sodium azide (1 mM) to detect and eliminate carrier mediated processes in order to estimate the passive diffusion component of the transport (Table 2). All concentrations were assayed in all types of experiments and both cell cultures

.

COMPOUND	CONCENTRATION (µM)	ACID WATER	METHANOL	ACETONITRILE	λ	RETENTION TIME (min)	DETECTOR
Amitriptyline	1500 1000 500 100 100 + 1 mM Azide	40		60	240	1.36	UV
Atenolol	1000 500 100 50 100 + 1 mM Azide	90	5	5	231-307	3.51	FLUO
Diphenhydramine	1500 1000 500 100 100 + 1 mM Azide	70		30	245	2.88	UV
Ethyl-phenyl malonamide	1500 1000 750	40	60		205	1.59	UV

	500 500 + 1 mM Azide						
Levofloxacin	1000 500 100 50 100 + 1 mM Azide	60	40		282-450	1.75	UV
Metoprolol	1000 500 100 50 100 + 1 mM Azide	60	20	20	231-307	1.38	FLUO
Norfloxacin	1000 500 100 50 100 + 1 mM Azide	60	20	20	300-500	1.16	FLUO
Propranolol	1000 500 100 50 100 + 1 mM Azide	50	30	20	254-350	1.6	FLUO

Verapamil	1000 500 100 50 100 + 1 mM Azide	62		38	275-350	3.17	FLUO
Zidovudine	1000 500 100 50 100 + 1 mM Azide	70	30		276	2	UV

Table 2. Drug concentrations and analytical methods used in HPLC. Acid water was prepared with 0.5 mL Trifuoroacetic acid in 1 L water. Water, Methanol and Acetonitrile were purchased by Sigma, HPLC grade. Novapack C18 3.9x150mmm was used.

Cell culture and transport studies.

MDCKII and MDCKII-MDR1 cells were grown in Dubelcco's Modified Eagle's Media containing L-glutamine, fetal bovine serum and penicillin-streptomycin. Each two days the media was replaced. Cells monolayers were prepared by seeding 400000 cells/cm^2 for MDCKII and 20000 cells/cm^2 for MDCKII-MDR1 on a polycarbonate membrane which surface area was 4.2 cm^2. They were maintained at 37°C temperature, 90% humidity and 5% CO_2 and medium was replaced each two days until confluence (7-9 days). Afterwards, the integrity of the each cell monolayer was evaluated by measuring the trans-epithelial electrical resistance (TEER). In experiment Hank's balanced salt solution (HBSS) supplemented with HEPES was used to fill the receiver chamber and to prepare the drug solution that was placed in the donor chamber after adjusting pH to 7.

Transport studies were conducted in an orbital environmental shaker at constant temperature (37°C) and agitation rate (50 rpm). Four samples of 200 μL each one were taken, and replaced each time with HBSS supplemented with HEPES from the receiver side at 15, 30, 45 and 90 minutes. Samples of the donor side were taken at the beginning and the end of the experiment. Moreover, the amount of compound in cell membranes and inside the cells was determined at the end of experiments in order to check the mass balance and the percentage of compound retained in the cell compartment (always less than 5%.) standard one with the same buffer for apical and basolateral compartment were conducted in apical to basolateral (AB) and basolateral to apical (BA) direction, the albumin experiments with presence of albumin in apical compartment were performed in AB direction (mimicking blood compartment) and the homogenate

experiments with brain homogenate in basolateral compartment were conducted in BA direction (mimicking brain compartment). Solutions were prepared 24h before the experiment and stored at 4°C. Drug concentrations assayed are summarized in Table 2. Samples were stored at -20ºC until analyzed. A scheme of the three different experimental settings is represented in Figure 1.

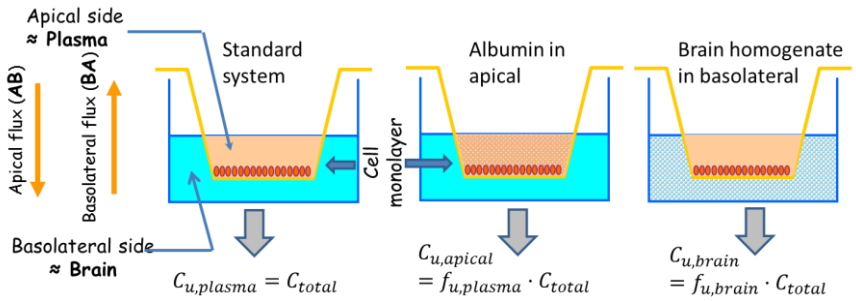

Figure 1. Scheme of the system based in three experimental settings to obtain permeability values used to estimate extent and rate of brain access. Two cell lines, MDCK and MDCK-MDR1 were checked to establish their predictive performance in this new experimental system by comparison with *in vivo* data.

Standard Experiments

In vitro studies were performed in both directions, from apical-to-basal (AB) and from basal-to-apical (BA) sides. The volume was 2 mL and 3 mL in apical and basolateral chamber respectively.

Albumin Experiments

The concentration of albumin used was 4%, in similar percentage to human blood. Drug solution with albumin was placed in the apical chamber (blood compartment). Albumin transport experiments were performed in MDCKII and MDCKII-MDR1 cells in AB direction.

Homogenate Experiments

Animals: Male Landrace-Large White pigs weighing 15-20 kg were purchased from Animal house at University of Valencia. All animals were pair-housed at 18–22°C under a 12-h light/dark cycle with free access to food and water. The pre-anesthesia was composed by ketamine, medetomidine and azaperone by intramuscular injection. Animals were intubated and moved to the operation room with intravenous anesthesia and spontaneous ventilation. All procedures were performed by responsible veterinarian. The animal study was approved by the Scientific Committee of the Faculty of Pharmacy and followed the guidelines described in the EC Directive 86/609, the Council of the Europe Convention ETS 123 and Spanish national laws governing the use of animals in research (Real Decreto 223/1988, BOE 67, 18-3-98: 8509-8511).

Homogenate brain dilution: Drug-naive pigs were sacrificed under overdose of anesthesia, the brain was removed and homogenized as described by Friden et al. [31]. Brain homogenate was mixed with phosphate buffer (180 mM pH 7.4) in 1:3 ratio to obtain the brain homogenate dilution. The same amount of each drug than in the standard experiments were dissolved in 3mL of brain homogenate dilution to be placed in the basolateral chamber in MDCKII and MDCKII-MDR1 cell monolayers.

Drug analysis

Analytical methods for each drug are described in Table 2. All samples were analyzed using Waters 2695 separations module, Waters 2487 ultraviolet and Waters 2475 Fluorescence detector. The standard

calibration curves were prepared by dilution from the drug solution assayed. Acid water was prepared with 0.5 mL Trifluoroacetic acid in 1 L water. Water, Methanol and Acetonitrile were purchased by Sigma, HPLC grade. A Novapack C18 3.9x150mmm cartridge was used.

The concentration of all the samples was within the linear range of quantitation for all the assays. Analytical methods were validated with regard to specificity, selectivity, linearity, precision and accuracy.

Albumin samples (200 μL) were diluted in 400 μL acetonitrile to precipitate albumin. Afterwards, all samples from standard transport experiment, albumin and homogenate samples were centrifuged at 6150 G for 10 minutes and aliquots of supernatant were transferred to vials and analyzed using HPLC.

Data analysis

The apparent permeability coefficient was calculated according to the following equation:

$$C_{receiver,t} = \frac{Q_{total}}{V_{receiver}+V_{donor}} + \left(\left(C_{receiver,t} \cdot f \right) - \frac{Q_{total}}{V_{receiver}+V_{donor}} \right) \cdot e^{-P \cdot S \cdot \left(\frac{1}{V_{receiver}} + \frac{1}{V_{donor}} \right) \cdot \Delta t} \quad (1)$$

where $C_{receiver,\ t}$ is concentration of drug in the receiver chamber at time t, Q_{total} is the total amount of drug in both chambers, $V_{receiver}$ and V_{donor} are the volumes of each chamber, $C_{receiver,\ t-1}$ is drug concentration in receiver chamber at previous time, f is the sample replacement dilution factor, S is the surface area of the monolayer, Δt is the time interval and P is the permeability coefficient. This equation considers a continuous change of the donor and receiver concentrations, and it is

valid in either sink or non-sink conditions [32, 33]. The permeability coefficient estimations in sink and non-sink conditions were carried out in an Excel® worksheet. When the experiments are performed at the same pH in donor and acceptor chambers the ratio of the basal to apical (P_{BA}) and apical to basal (P_{AB}) permeability values can be used to detect the presence of secretion ($P_{BA}/P_{AB}>2$) or absorption carrier mediated transport mechanisms ($P_{BA}/P_{AB}<0.8$).

In vitro BBB parameters were derived as explained below. *In vitro* $f_{u,\,plasma}$ is obtained from the ratio of the permeability obtained in the AB direction in the albumin experiments, $P_{app\ ALB}$, and the permeability in the AB direction in the standard experiment, $P_{app\ A\rightarrow B}$, the rational is the following. In the absence of albumin (as in the standard experiments) the flux of drug from apical to basolateral chamber is expressed by this equation based on Fick's first law, assuming sink conditions (i.e. negligible drug concentration at the receiver chamber):

$$\frac{dQ}{dt} = P_{app\ A\rightarrow B} \cdot C_A \qquad (2)$$

where Q is the amount of drug, S the surface of the membrane, C_A the drug concentration in the apical chamber and $P_{app\ A\rightarrow B}$ the intrinsic permeability of the drug in the membrane.

In the presence of albumin in the apical chamber (plasma), only the unbound drug is available for permeation, then the unbound drug concentration, $C_{u,\,plasma}$ is the responsible of the concentration gradient driving the diffusion step. Unbound drug concentration can be estimated from the total drug concentration in apical chamber C_A as:

$$C_{u,plasma} = f_{u,plasma} \cdot C_A \qquad (3)$$

The drug flux in AB direction in presence of albumin is then:

$$\frac{dQ}{S \cdot dt} = P_{app\ A \to B} \cdot C_{u,plasma} \quad (4)$$

$$\frac{dQ}{S \cdot dt} = P_{app\ A \to B} \cdot f_{u,plasma} \cdot C_A \quad (5)$$

As in the permeability calculations the total drug concentration in apical chamber C_A is used (because fu is unknown) actually the permeability value obtained in presence of albumin is an "apparent value", $P_{app\ ALB}$,

$$\frac{dQ}{S \cdot dt} = P_{app\ ALB} \cdot C_A \quad (6)$$

Dividing equation 5 and 6 it is easy to obtain the relationship between the permeability in presence and in absence of albumin that corresponds to *in vitro* $f_{u,\ plasma}$

$$P_{app\ ALB} = P_{app\ A \to B} \cdot f_{u,plasma} \quad (7)$$

If the *in vitro* unbound fraction in plasma is close to 1 (no drug is bound to albumin), both permeability values should be equal at the same concentration. If *in vitro* unbound fraction in plasma is lower than 1 (drug is bounded to albumin), $P_{app\ ALB}$ should be lower than $P_{app\ A \to B}$, as less free drug is available for diffusion.

In vivo $f_{u,\ brain}$ is related to the unbound concentration in brain and the total concentration in brain.

$$C_{u,brain} = C_{total,brain} \cdot f_{u,brain} \quad (8)$$

Following the same rational that that used for albumin experiments , *in vitro* $f_{u,\ brain}$ may be obtained from the ratio between the BA apparent permeability values obtained in presence of homogenate, $P_{app\ HOM}$ and $P_{app\ B \to A}$ the permeability in the basal-to-apical direction of the standard experiments.

$$P_{app\ HOM} = P_{app\ B\to A} \cdot f_{u,brain} \quad (9)$$

$$f_{u,brain} = P_{app\ HOM}/P_{app\ B\to A} \quad (10)$$

In vivo $Kp_{uu,\ brain}$ is defined as the relation between unbound concentration in brain and unbound concentration in plasma at steady state. These concentrations are the driving forces to achieve a pharmacological effect. This ratio describes quantitatively how the BBB controls the drug permeation by passive diffusion or active influx/efflux transport. $Kp_{uu,\ brain}$ is determined by the relationship between the influx and efflux clearances.10

$$K_{p,uu,brain} = Cl_{in}/Cl_{out} \quad (11)$$

If passive diffusion is the only mechanism involved in the transport of the drug across BBB, $Kp_{uu,\ brain}$ is equal to 1. If $Kp_{uu,\ brain}$ is lower than 1, it means there is efflux transport (out from the brain) whereas if $Kp_{uu,\ brain}$ is higher than 1, an influx transport mechanism is present.

Taking into account that clearance is defined as:

$$CL = P_{app} \cdot S \quad (12)$$

in vitro $Kp_{uu,\ brain}$ may be defined as the ratio between apical-to-basolateral and basolateral-to-apical apparent permeability values obtained in the standard experiments.

$$K_{p,uu,brain} = P_{app\ A\to B}/P_{app\ B\to A} \quad (13)$$

In vivo $V_{u,\ brain}$ is defined as [10]

$$V_{u,brain} = A_{total,brain}/C_{u,brain} \quad (14)$$

Where $A_{total,\ brain}$ represents total amount of drug in brain and $C_{u,\ brain}$ is the unbound concentration in brain. *In vivo* apparent volume in brain can be also estimated with the following equation10

$$V_{u,brain} = V_{ECF} + \left(1/f_{u,brain}\right) \cdot V_{ICF} \quad (15)$$

where V_{ECF} is the volume of the extracellular fluid (brain interstitial fluid) and V_{ICF} is the brain intracellular volume. If there is no binding in brain parenchyma (i.e. drug does bind to any cell component), fu, brain is almost one, and $V_{u,\ brain}$ is equal to V_{ECF} +V_{ICF}, which is typically around 0.8 ml·g brain^{-1})(0.2 ml·g brain^{-1} +0.6 ml·g brain^{-1})[10]. Likewise, $V_{u,\ brain}$ is larger than 0.8 ml·g brain^{-1} when $f_{u,\ brain}$ is small.

Methods of *in vitro in vivo* correlation

In order to estimate the *in vivo* relevance of this *in vitro* method, *in vivo* rat $f_{u,\ plasma}$, $Kp_{uu,\ brain}$, $V_{u,\ brain}$ and human $Kp_{uu,\ CSF}$ data were obtained from Friden et al. [31]. The next step is to calculate from the above equations all the *in vitro* parameters and for these purpose there are three possible alternatives considering that P_{app} values have been obtained at different initial concentrations.

First option is to estimate *in vitro* parameters using the P_{app} obtained at the lowest assayed concentrations (at which supposedly the saturable transport processes are not saturated. The second option is to estimate the *in vitro* parameters from each P_{app} and averaging the *in vitro* parameters obtained and, finally, using and extrapolation strategy to take into account the transport mechanism and the differences between the *in vivo* human concentrations (i.e. steady state concentrations) and the *in vitro* concentrations used.

Extrapolation: For some of the assayed compounds, apparent permeability values were concentration dependent due to the existence of carrier mediated influx or efflux processes. As the *in vitro* values are obtained from the apparent permeability values it is necessary to use those apparent permeability values obtained at the same unbound plasma concentrations reported by Friden et al. [34]. For this reason an extrapolation procedure was used in order to compare *in vitro* and *in vivo* BBB parameters at the same concentration.

Permeability as a function of concentration models were fitted using linear or nonlinear regression in Excel® with Solver tool. The best model was selected by comparing the residual variances with an F-Snedecor's test at α=0.05 significance level.

Extrapolation models: Passive diffusion model assumed that permeability is not concentration dependent thus the effective permeability is the average of the experimental values at all the concentrations assayed:

$$P_{app,extrapolated} = \overline{P_{app}} \quad (16)$$

where P_{app} is the mean apparent permeability value obtained by Solver minimization of the sum of squares residuals (SSR). Consequently the extrapolated value corresponds to the mean value.

Linear model was also fitted to the P_{app} values for each cell line versus the assayed concentrations:

$$P_{app} = Slope \cdot C + b \quad (17)$$

where C is the concentration and b represents the intercept of the model obtained by Solver minimization of the SSR. With the parameter values b and slope the P_{app}, extrapolated was estimated at the *in vivo* concentration.

Influx model parameters were estimated by fitting this equation to the P_{app} versus concentration data

$$P_{app} = P_{dif} + V_{max}/(K_M + C) \quad (18)$$

where V_{MAX} represents de maximal rate of transport, K_M is the concentration at the half V_{MAX} and P_{dif} represents the diffusion permeability obtained by Solver minimization of the SSR. Pdif, V_{MAX} and K_M were then used to estimate P_{app}, extrapolated.

Finally, the efflux model is represented by the following equation:

$$P_{app} = P_{dif} - V_{max}/(K_M + C) \quad (19)$$

where V_{MAX} represents de maximal rate of transport, K_M is the concentration at the half V_{MAX} and P_{dif} represents the diffusion permeability obtained by Solver minimization of the SSR.

For each drug the best model was selected and used for obtaining by extrapolation the apparent permeability value, P_{app}, extrapolated, at the *in vivo* concentration in each experimental setting. P_{app}, extrapolated values were used for the calculation of the *in vitro* $f_{u, plasma}$, $Kp_{uu, brain}$, $V_{u, brain}$ as described previously and correlated with the *in vivo* values. The linear regression plots and the 95% confidence prediction intervals were estimated using S-Plus 6.1

RESULTS

Permeability values

In Table 3 the extrapolated permeability values at the *in vivo* concentrations for all the compounds, cell line and type of experiment are shown.

COMPOUND	CONCENTRATION (μM)	MDCKII P_{app} (x10^{-6} cm/sec)					MDCKII-MDR1 P_{app} (x10^{-6} cm/sec)				
		A→B	B→A	ALB	HOM	$P_{B→A}/P_{A→B}$	A→B	B→A	ALB	HOM	$P_{B→A}/P_{A→B}$
Amitriptyline	0.022	74.77 P	178.48 P	6.02 P	6.54 P	2.39	17.95 P	16.91 P	3.45 P	1.76 P	0.94
Atenolol	1.5	1.32 P	1.49 P	1.12 P	1.59 P	1.13	0.49 P	0.88 P	0.42 P	0.74 P	1.80
Diphenhydramine	0.051	91.72 P	79.62 P	13.12 P	25.31 P	0.87	99.97 P	58.40 P	15.42 P	11.75 P	0.58
Ethyl-phenyl malonamide	4.3	18.11 P	19.73 P	9.40 P	17.43 P	1.09	5.80 P	11.28 P	6.38 P	9.42 P	1.94
Levofloxacin	0.59	3.90 L	6.67 P	3.47 P	5.84 P	1.71	1.83 P	25.00 P	0.92 P	21.61 P	13.67
Metoprolol	0.75	94.66 P	112.07 P	78.33 P	35.91 P	1.18	57.30 P	52.09 P	27.51 P	21.22 P	0.91
Norfloxacin	0.7	2.51 P	8.16 P	1.84 P	5.79 P	3.25	0.94 P	2.15 P	0.63 P	1.93 P	2.28
Propranolol	0.051	68.37 P	89.08 P	7.24 P	8.18 P	1.30	110.65 P	52.75 P	13.29 P	7.38 P	0.48
Verapamil	0.075	58.29 P	49.22 P	15.54 P	15.83 P	0.84	82.73 P	51.66 P	8.66 P	17.89 P	0.62
Zidovudine	1.2	11.39 P	14.03 P	7.74 P	14.50 P	1.23	2.73 P	28.41 P	1.98 P	28.84 P	10.41

Table 3. Extrapolated permeability values, $P_{app,extrapolated}$ at the *in vivo* relevant concentration in MDCKII and MDCKII-MDR1 cell lines and in the different experimental settings (standard, albumin and brain homogenate presence). P(passive), L (lineal), I (influx) and E (efflux) are the model used for extrapolation.

In vitro BBB parameters

The *in vitro* estimated $f_{u, plasma}$, $Kp_{uu, CSF}$, $V_{u, brain}$ in MDCKII are summarized in table 4. *In vivo* data were obtained from Friden et al. [34] and *in vitro* data were calculated according to equations described above.

In Table 5 *in vitro* estimated of $f_{u, plasma}$, $Kp_{uu, brain}$, $V_{u, brain}$ in MDCKII-MDR1 are reported. *In vivo* data were obtained from Friden et al. [34] and *in vitro* data were calculated according to equations described above.

Correlations

MDCKII

Figure 2 shows the correlation obtained between *in vivo* $f_{u, plasma}$ and *in vitro* $f_{u, plasma}$ values obtained with MDCK cells. The *in vitro* values of $Kp_{uu, brain}$ predicted with MDCK cells and the correlation with *in vivo* values is represented in Figure 3. Figure 4 shows the correlation obtained between *in vivo* $V_{u, brain}$ and *in vitro* $V_{u, brain}$ from MDCK cells. Parameters of the linear correlations, Pearson coefficient and squared Pearson correlation coefficients are displayed in the figures.

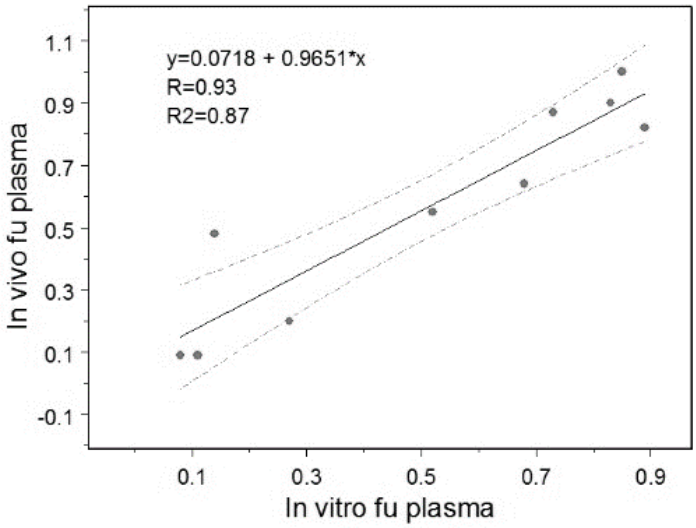

Figure 2. Correlation obtained between in vivo fu,p and in vitro fu,p in MDCKII cell line for ten compounds. The solid line represents the linear regression, and the dotted line represents the 95% confidence interval of the predictions. R is Pearson correlation coefficient and R2 is the square of Pearson correlation coefficient that reflects the percent of total variance of the dependent variable that is explained by the independent one.

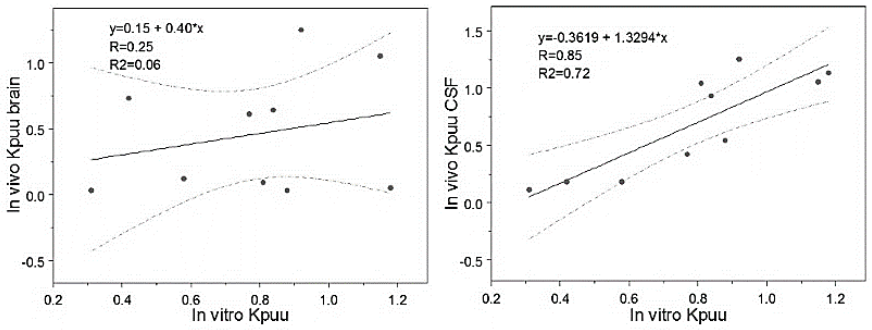

Figure 3. Correlation obtained between rat in vivo Kp,uu,brain and in vitro Kp,uu,brain (left) and between human in vivo Kp,uu,CSF and in vitro Kp,uu,brain (right) in MDCKII cell line. The solid line represents the linear regression, and the dotted line represents the 95% confidence interval of the predictions. R is Pearson correlation coefficient and R2 is the square of Pearson correlation coefficient reflecting the percent of total variance of dependent variable explained by the independent one.

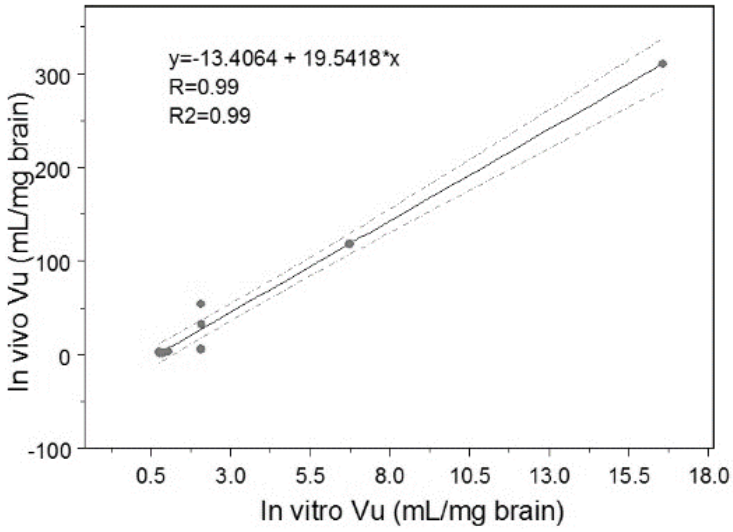

Figure 4. Correlation obtained between *in vivo* $V_{u,brain}$ and *in vitro* $V_{u,brain}$ in MDCKII cell line for the ten assayed drugs. The solid line represents the linear regression, and the dotted line represents the 95% confidence interval of the predictions. R is Pearson correlation coefficient and R2 is the square of Pearson correlation coefficient.

MDCKII-MDR1

The correlation obtained between *in vivo* $f_{u,\ plasma}$ and *in vitro* $f_{u,\ plasma}$ values obtained with MDCK-MDR1 cells is represented in Figure 5. The *in vitro* values of $Kp_{uu,\ brain}$ predicted with MDCK-MDR1 cells versus the *in vivo* values is represented in Figure 6. Figure 7 shows the correlation obtained between *in vivo* $V_{u,\ brain}$ and *in vitro* $V_{u,\ brain}$ from MDCK-MDR1 cells. Parameters of the linear correlations, Pearson coefficient and squared Pearson correlation coefficients are displayed in the figures.

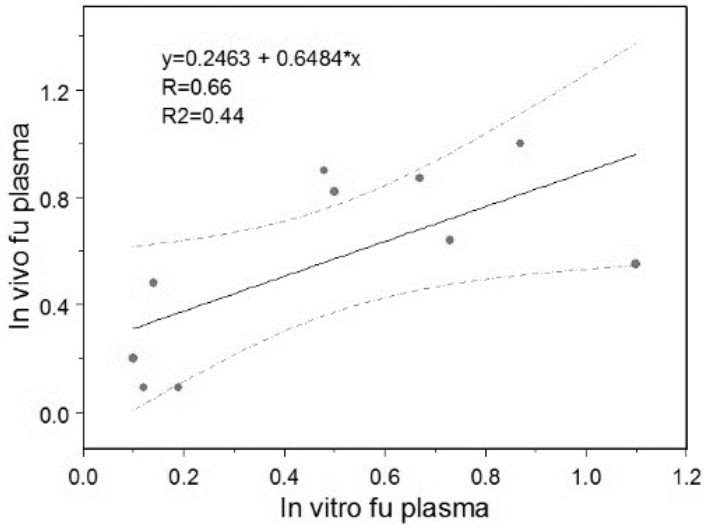

Figure 5. Correlation obtained between *in vivo* $f_{u,p}$ and *in vitro* $f_{u,p}$ in MDCKII-MDR1 cell line for ten compounds. The solid line represents the linear regression, and the dotted line represents the 95% confidence interval of the predictions. R is Pearson correlation coefficient and R2 is the square of Pearson correlation coefficient.

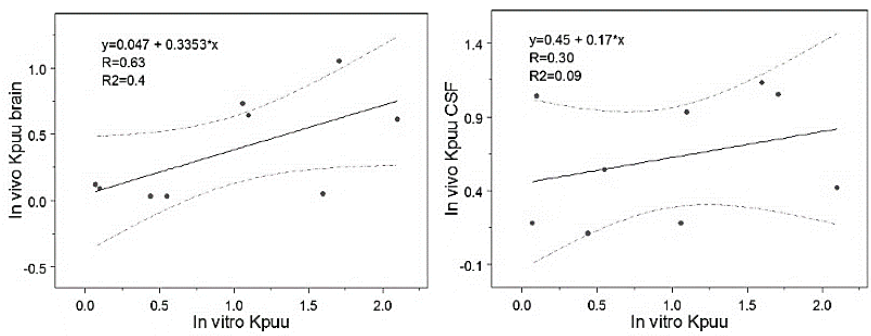

Figure 6. Correlation obtained between rat *in vivo* $Kp_{,uu,brain}$ and *in vitro* $Kp_{,uu,brain}$ (left) and between human *in vivo* $Kp_{,uu,CSF}$ and *in vitro* $Kp_{,uu,brain}$ (right) in MDCKII-MDR1 cell line for nine compounds (Ethyl-phenyl malonamide was not considered). The solid line represents the linear regression, and the dotted line represents the 95% confidence interval of the predictions. R is Pearson correlation coefficient and R2 is the square of Pearson correlation coefficient.

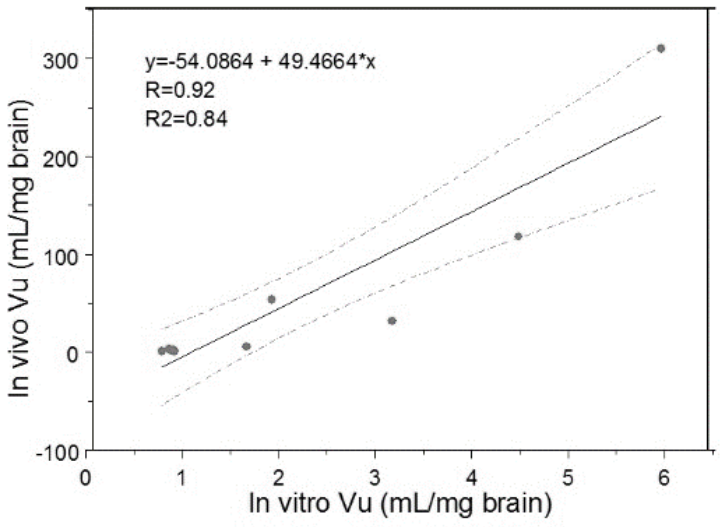

Figure 7. Correlation obtained between *in vivo* $V_{u,brain}$ and *in vitro* $V_{u,brain}$ in MDCKII-MDR1 cell line for ten compounds. The solid line represents the linear regression, and the dotted line represents the 95% confidence interval of the predictions. R is Pearson correlation coefficient and R2 is the square of Pearson correlation coefficient.

DISCUSSION

The Blood-Brain barrier is a restrictive membrane which limits the access and distribution into the brain to many different molecules. It preserves the brain environment due to tight junctions between endothelial cells and transport mechanisms. The rate of success of CNS drugs in drug development is limited by a lack of reliable screening methods which may select the most valuables candidates for further analysis. Therefore, in this article a new *in vitro* methodology to predict the access and distribution of drugs into the brain is proposed and its predictive performance is evaluated. The method is developed in MDCKII and MDCKII-MDR1 cell lines because they closely reflect the tightness and transporters expression of the blood brain barrier in a

more reliable and constant manner than non-immortalized cell lines [19, 20].

The relevant BBB parameters for predicting rate and extent of access are: $f_{u,\ plasma}$, $V_{u,\ brain}$, and $Kp_{uu,\ brain}$. $f_{u,\ plasma}$ explains the drug's affinity to blood proteins and this parameter quantify the free concentration that is able to cross the BBB and reach the target. However, the amount of drug that is able to reach the target depends also on the free drug concentration in brain. Therefore, $Kp_{uu,\ brain}$ is a measurement in equilibrium of the relationship between free brain concentrations and free plasma concentrations. The value of $Kp_{uu,\ brain}$ indicates the extent of the drug that crossed the blood-brain barrier and is highly related to the effect. When $Kp_{uu,\ brain}$ is greater than 1, an influx transporter is involved in the permeation of the drug (i.e. drug transport into the brain is favored); passive diffusion occurs when $Kp_{,uu,\ brain}$ is equal to 1 and when $Kp_{,uu,brain}$ is less than 1, the drug is transported by an efflux mechanism (i.e. is permeation into the brain is interfered by the transporter). The parameter that describes the distribution of the drug in brain is $V_{u,\ brain}$. The brain may be divided in two different compartments, extracellular fluid (ECF) and intracellular fluid (ICF). The ECF+ICF real volume is the minimum volume in which the drug may be distributed if it does not bind to the cells components. If the drug is accumulated in cells, then $V_{u,\ brain}$ is greater than (ECF+ICF) volume.

The experimental determination of these three parameters required different and independent experimental setups. $f_{u,\ plasma}$ is determined *in vitro*, $Kp_{uu,\ brain}$ requires *in vivo* microdialysis studies to estimate the ECF and plasma concentrations and $V_{u,\ brain}$ may also be obtained using *in vitro* methods [9]. A reliable and easy experimental

system, which allows the screening of CNS compounds, is needed to select the best candidates for future *in vivo* analysis [3, 8]. It could redirect the expensive and time consuming drug development to a more efficient process. The ideal situation would be having a single system able to predict the three relevant parameters and amenable to be miniaturized and robotized for high throughput screening. With this aim a new *in vitro* model is proposed, based on cell monolayer permeability experiments, in order to allow the simultaneous determination of $f_{u, plasma}$, $V_{u, brain}$, and $Kp_{uu, brain}$ thanks to the modification of the experimental standard setting and to the adequate mathematical modeling.

Model compounds

Model compounds were selected to include CNS and non-CNS drugs, as well as considering their affinity to P-gp transporter [35-41]. Drugs with high and low degree of plasma protein binding were included as well as having a wide span of lipophilicity -values from clearly hydrophilic (Atenolol, Ethyl-phenyl Malonamide and Zidovudine) to highly lipophilic (Amitriptyline, Diphenhydramine and Verapamil). The molecular weight range was not as wide as it goes from 250 to 450. The final set of ten compounds fulfilling these characteristics was selected based on the *in vivo* data availability as the final purpose was checking the predictability of the *in vitro* model (Table 1).

Experimental setting

The use of *in vitro* cells monolayers with albumin in the acceptor (basolateral) chamber has been proposed in models of the intestinal membrane in order to mimic the blood side after drug intestinal permeation [42]. On the other hand, the estimation of the unbound drug fraction in plasma based in the ratio of the permeability values in the absence and in the presence of albumin in the basolateral chamber has been also explored [42]. Based on this idea, an experimental setting with albumin in donor chamber to mimic the blood side is proposed in the BBB model. The derivation of the $f_{u,\ plasma}$ calculation follows the same rational that the previously reported. The albumin concentration was fixed to the average albumin concentration in human plasma [42]. The inclusion of brain homogenate in the basolateral chamber, following the same rational, should allow the estimation of $f_{u,\ brain}$ by comparison of the permeability values obtained with and without brain homogenate in the system. Different buffer/brain homogenate ratios were examined to select the most adequate ratio in terms of adherence, sampling feasibility and physiological resemblance. A 3:1 ratio of buffer/brain homogenate was selected as it was reported by Friden et al. [31].

Correlations

All the correlations *in vitro* versus *in vivo* parameters were done using the three proposed correlation methods, i.e. from the P_{app} at the lowest concentrations, by averaging the *in vitro* estimates at all the concentrations and from the extrapolation strategy. The last method produced the best correlations (higher correlation coefficients) in both cell lines.

MDCKII

In this cell line *In vitro* fu,p calculated from permeability values and *in vivo* fu,p presented a good correlation (Figure 1) in ten compounds tested (R=0.93). *In vitro* $Kp_{uu,\ brain}$ and *in vivo* human $Kp_{uu,\ CSF}$ correlation (Figure 2) was obtained with an R=0.85. Human $Kp_{uu,\ CSF}$ data were better correlated than rat $Kp_{uu,\ brain}$ values (R=0.25), probably due to the less transporter expression in MDCKII and human Blood-cerebrospinal fluid barrier (BCSFB). Good $V_{u,\ brain}$ correlation (Figure 3) was observed between *in vitro* $V_{u,\ brain}$ and *in vivo* $V_{u,\ brain}$ (R=0.99). Amitriptyline, Diphenhydramine, Propranolol and Verapamil showed 15-fold rank order, whereas Atenolol 3-fold, Levofloxacin, Metoprolol and Norfloxacin 2-fold and Ethyl-phenyl malonamide and Zidovudine close to 1-fold rank order (Table 4).

MDCKII						
COMPOUND	**$V_{u,brain}$ (ml/g brain)**		**$K_{puu,CSF}$**		**$f_{u,plasma}$**	
	In vitro	***In vivo***	***In vitro***	***In vivo***	***In vitro***	***In vivo***
Amitriptyline	16.58	310.00	0.42	0.18	0.08	0.09
Atenolol	0.76	2.50	0.88	0.54	0.85	1.00
Diphenhydramine	2.09	32.00	1.15	1.05	0.14	0.48
Ethyl-phenyl malonamide	0.88	0.90	0.92	1.25	0.52	0.55
Levofloxacin	0.89	1.70	0.58	0.18	0.89	0.82
Metoprolol	2.07	5.50	0.84	0.93	0.83	0.90
Norfloxacin	1.05	2.90	0.31	0.11	0.73	0.87
Propranolol	6.74	118.00	0.77	0.42	0.11	0.09
Verapamil	2.07	54.00	1.18	1.13	0.27	0.20
Zidovudine	0.78	1.10	0.81	1.04	0.68	0.64

Table 4. *In vitro* parameters in MDCKII cell line calculated from equations 4, 7, 9 and 11 and *in vivo* parameters published by Friden et al. [[89]].

MDCKII-MDR1

In the MDR1 transfected cell line, *in vitro* and *in vivo* $f_{u,\ p}$ correlation (Figure 4) was less accurate and precise. A Pearson

correlation coefficient of 0.66 is lower than observed than in MDCKII cell line (R=0.93). *In vitro* $Kp_{uu,\ brain}$ and *in vivo* $Kp_{uu,\ brain}$ correlation (Figure 5) was obtained with an R=0.66, removing Ethyl-phenyl malonamide data. Rat $Kp_{uu,\ brain}$ data were better correlated than human $Kp_{uu,\ CSF}$ values (R=0.30), but a good correlation was not achieved with any of the *in vivo* Kp_{uu} values. The higher expression level of P-gp in this cell line might not reflect the *in vivo* expression levels in BBB. Good $V_{u,\ brain}$ correlation (Figure 6) was observed between *in vitro* $V_{u,\ brain}$ and *in vivo* $V_{u,\ brain}$ (R=0.92). Similar behavior in rank order was observed as explained in MDCKII. Amitriptyline showed a 51-fold rank order, Propranolol and Verapamil showed 25-fold rank order, diphenhydramine 10-fold rank order, whereas Atenolol, Metoprolol, Norfloxacin 3-fold, Levofloxacin 2-fold and Ethyl-phenyl malonamide and Zidovudine close to 1-fold rank order (Table 5).

MDCKII-MDR1						
COMPOUND	**$V_{u,brain}$ (ml/g brain)**		**$K_{puu,brain}$**		**$f_{u,plasma}$**	
	In vitro	***In vivo***	***In vitro***	***In vivo***	***In vitro***	***In vivo***
Amitriptyline	5.97	310.00	1.06	0.73	0.19	0.09
Atenolol	0.91	2.50	0.55	0.03	0.87	1.00
Diphenhydramine	3.18	32.00	1.71	1.05	0.14	0.48
Ethyl-phenyl malonamide	0.92	0.90	0.00	1.25	1.10	0.55
Levofloxacin	0.89	1.70	0.07	0.12	0.50	0.82
Metoprolol	1.67	5.50	1.10	0.64	0.48	0.90
Norfloxacin	0.87	2.90	0.44	0.03	0.67	0.87
Propranolol	4.49	118.00	2.10	0.61	0.12	0.09
Verapamil	1.93	54.00	1.60	0.05	0.10	0.20
Zidovudine	0.79	1.10	0.10	0.09	0.73	0.64

Table 5. *In vitro* parameters in MDCKII-MDR1 cell line calculated from equations 4, 7, 9 and 11 and *in vivo* parameters published by Friden et al. [89]

Comparing both cell lines, in general the prediction performance of MDCKII cell lines is better than the MDCK-MDR1.

Nevertheless the worst predicted compounds are the same in both cell lines at least for Kp_{uu} and for f_u. For instance Zidovudine and Ethylphenylmalonamide *in vivo* Kp_{uu} are underestimated in both cell lines while Propranolol and atenolol are over estimated. Diphenhydramine f_u is underestimated in both cell lines. The reason for the deviation is not clear but it does not seem to be related with the different expression level of P-gp that is the most relevant difference between both cell lines.

CONCLUSION

The BBB parameters obtained with our new method were predictive of the *in vivo* behavior of candidates. *in vitro* $f_{u,\ plasma}$, $Kp_{uu\ ,brain}$ and $V_{u,\ brain}$ calculated with P_{app} from MDCKII cell line presented a good correlation with *in vivo* $f_{u,\ plasma}$, $Kp_{uu,\ brain}$ and $V_{u,\ brain}$ published values ($r=0.93$; $r=0.85$ and $r=0.99$ respectively). Despite its simplicity the predictive performance is fairly good considering the reduced number of tested compounds with different physicochemical and transport properties. Further experimental modifications could be checked to optimize the method but the present data support its feasibility. As other *in vitro* cell culture models the system is suitable for miniaturization and robotization to allow high throughput performance.

ACKNOWLEDGEMENTS

The authors acknowledge financial support to projects: DCI ALA/19.09.01/10/21526/245-297/ALFA 111(2010)29: Red-Biofarma. Red para el desarrollo de metodologias biofarmaceuticas racionales que incrementen la competencia y el impacto social de las Industrias Farmaceuticas Locales.

A grant from Ministry of Education and Science of Spain and Miguel Hernandez University (Beca Victor Mangas FPU AP2010-2372).

REFERENCES

1. Kessler, R. C.; Demler, O.; Frank, R. G.; Olfson, M.; Pincus, H. A.; Walters, E. E.; Wang, P.; Wells, K. B.; Zaslavsky, A. M. Prevalence and treatment of mental disorders, 1990 to 2003. N Engl J Med 2005, 352, (24), 2515-23.

2. Pangalos, M. N.; Schechter, L. E.; Hurko, O. Drug development for CNS disorders: strategies for balancing risk and reducing attrition. Nat Rev Drug Discov 2007, 6, (7), 521-32.

3. de Lange, E. C. The mastermind approach to CNS drug therapy: translational prediction of human brain distribution, target site kinetics, and therapeutic effects. Fluids Barriers CNS 2013, 10, (1), 12.

4. de Lange, E. C. Utility of CSF in translational neuroscience. J Pharmacokinet Pharmacodyn 2013.

5. Owens, J. 2006 drug approvals: finding the niche. Nat Rev Drug Discov 2007, 6, (2), 99-101.

6. Kola, I. The state of innovation in drug development. Clin Pharmacol Ther 2008, 83, (2), 227-30.

7. Kaitin, K. I.; DiMasi, J. A. Pharmaceutical innovation in the 21st century: new drug approvals in the first decade, 2000-2009. Clin Pharmacol Ther 2011, 89, (2), 183-8.

8. Reichel, A. The role of blood-brain barrier studies in the pharmaceutical industry. Curr Drug Metab 2006, 7, (2), 183-203.

9. Hammarlund-Udenaes, M.; Bredberg, U.; Friden, M. Methodologies to assess brain drug delivery in lead optimization. Curr Top Med Chem 2009, 9, (2), 148-62.

10. Hammarlund-Udenaes, M.; Friden, M.; Syvanen, S.; Gupta, A. On the rate and extent of drug delivery to the brain. Pharm Res 2008, 25, (8), 1737-50.

11. Hammarlund-Udenaes, M.; Paalzow, L. K.; de Lange, E. C. Drug equilibration across the blood-brain barrier--pharmacokinetic considerations based on the microdialysis method. Pharm Res 1997, 14, (2), 128-34.

12. Feng, M. R. Assessment of blood-brain barrier penetration: *in silico*, *in vitro* and *in vivo*. Curr Drug Metab 2002, 3, (6), 647-57.

13. Abbott, N. J.; Dolman, D. E.; Patabendige, A. K. Assays to predict drug permeation across the blood-brain barrier, and distribution to brain. Curr Drug Metab 2008, 9, (9), 901-10.

14. Mabondzo, A.; Bottlaender, M.; Guyot, A. C.; Tsaouin, K.; Deverre, J. R.; Balimane, P. V. Validation of *in vitro* cell-based human blood-brain barrier model using clinical positron emission tomography radioligands to predict *in vivo* human brain penetration. Mol Pharm 2010, 7, (5), 1805-15.

15. Hakkarainen, J. J.; Jalkanen, A. J.; Kaariainen, T. M.; Keski-Rahkonen, P.; Venalainen, T.; Hokkanen, J.; Monkkonen, J.; Suhonen, M.; Forsberg, M. M. Comparison of *in vitro* cell models in predicting *in vivo* brain entry of drugs. Int J Pharm 2010, 402, (1-2), 27-36.

16. Lundquist, S.; Renftel, M.; Brillault, J.; Fenart, L.; Cecchelli, R.; Dehouck, M. P. Prediction of drug transport through the blood-brain barrier *in vivo*: a comparison between two *in vitro* cell models. Pharm Res 2002, 19, (7), 976-81.

17. Omidi, Y.; Campbell, L.; Barar, J.; Connell, D.; Akhtar, S.; Gumbleton, M. Evaluation of the immortalised mouse brain capillary

endothelial cell line, b.End3, as an *in vitro* blood-brain barrier model for drug uptake and transport studies. Brain Res 2003, 990, (1-2), 95-112.

18. Perriere, N.; Yousif, S.; Cazaubon, S.; Chaverot, N.; Bourasset, F.; Cisternino, S.; Decleves, X.; Hori, S.; Terasaki, T.; Deli, M.; Scherrmann, J. M.; Temsamani, J.; Roux, F.; Couraud, P. O. A functional *in vitro* model of rat blood-brain barrier for molecular analysis of efflux transporters. Brain Res 2007, 1150, 1-13.

19. Garberg, P.; Ball, M.; Borg, N.; Cecchelli, R.; Fenart, L.; Hurst, R. D.; Lindmark, T.; Mabondzo, A.; Nilsson, J. E.; Raub, T. J.; Stanimirovic, D.; Terasaki, T.; Oberg, J. O.; Osterberg, T. *In vitro* models for the blood-brain barrier. Toxicol *In Vitro* 2005, 19, (3), 299-334.

20. Wang, Q.; Rager, J. D.; Weinstein, K.; Kardos, P. S.; Dobson, G. L.; Li, J.; Hidalgo, I. J. Evaluation of the MDR-MDCK cell line as a permeability screen for the blood-brain barrier. Int J Pharm 2005, 288, (2), 349-59.

21. Furuse, M.; Furuse, K.; Sasaki, H.; Tsukita, S. Conversion of zonulae occludentes from tight to leaky strand type by introducing claudin-2 into Madin-Darby canine kidney I cells. J Cell Biol 2001, 153, (2), 263-72.

22. Garberg, P.; Ball, M.; Borg, N.; Cecchelli, R.; Fenart, L.; Hurst, R. D.; Lindmark, T.; Mabondzo, A.; Nilsson, J. E.; Raub, T. J.; Stanimirovic, D.; Terasaki, T.; Oberg, J. O.; Osterberg, T. *In vitro* models for the blood-brain barrier. Toxicol *In Vitro* 2005, 19, (3), 299-334.

23. Veronesi, B. Characterization of the MDCK cell line for screening neurotoxicants. Neurotoxicology 1996, 17, (2), 433-43.

24. Wang, Q.; Rager, J. D.; Weinstein, K.; Kardos, P. S.; Dobson, G. L.; Li, J.; Hidalgo, I. J. Evaluation of the MDR-MDCK cell line as a permeability screen for the blood-brain barrier. International journal of pharmaceutics 2005, 288, (2), 349-59.

25. Xie, R.; Hammarlund-Udenaes, M.; de Boer, A. G.; de Lange, E. C. The role of P-glycoprotein in blood-brain barrier transport of morphine: transcortical microdialysis studies in mdr1a (-/-) and mdr1a (+/+) mice. Br J Pharmacol 1999, 128, (3), 563-8.

26. de Lange, E. C.; Marchand, S.; van den Berg, D.; van der Sandt, I. C.; de Boer, A. G.; Delon, A.; Bouquet, S.; Couet, W. *In vitro* and *in vivo* investigations on fluoroquinolones; effects of the P-glycoprotein efflux transporter on brain distribution of sparfloxacin. Eur J Pharm Sci 2000, 12, (2), 85-93.

27. Doran, A.; Obach, R. S.; Smith, B. J.; Hosea, N. A.; Becker, S.; Callegari, E.; Chen, C.; Chen, X.; Choo, E.; Cianfrogna, J.; Cox, L. M.; Gibbs, J. P.; Gibbs, M. A.; Hatch, H.; Hop, C. E.; Kasman, I. N.; Laperle, J.; Liu, J.; Liu, X.; Logman, M.; Maclin, D.; Nedza, F. M.; Nelson, F.; Olson, E.; Rahematpura, S.; Raunig, D.; Rogers, S.; Schmidt, K.; Spracklin, D. K.; Szewc, M.; Troutman, M.; Tseng, E.; Tu, M.; Van Deusen, J. W.; Venkatakrishnan, K.; Walens, G.; Wang, E. Q.; Wong, D.; Yasgar, A. S.; Zhang, C. The impact of P-glycoprotein on the disposition of drugs targeted for indications of the central nervous system: evaluation using the MDR1A/1B knockout mouse model. Drug Metab Dispos 2005, 33, (1), 165-74.

28. de Lange, E. C.; de Boer, A. G.; Breimer, D. D. Methodological issues in microdialysis sampling for pharmacokinetic studies. Adv Drug Deliv Rev 2000, 45, (2-3), 125-48.

29. de Lange, E. C.; Danhof, M.; de Boer, A. G.; Breimer, D. D. Critical factors of intracerebral microdialysis as a technique to determine the pharmacokinetics of drugs in rat brain. Brain Res 1994, 666, (1), 1-8.

30. de Lange, E. C.; Danhof, M.; de Boer, A. G.; Breimer, D. D. Methodological considerations of intracerebral microdialysis in pharmacokinetic studies on drug transport across the blood-brain barrier. Brain Res Brain Res Rev 1997, 25, (1), 27-49.

31. Friden, M.; Gupta, A.; Antonsson, M.; Bredberg, U.; Hammarlund-Udenaes, M. *In vitro* methods for estimating unbound drug concentrations in the brain interstitial and intracellular fluids. Drug Metab Dispos 2007, 35, (9), 1711-9.

32. Palm, K.; Luthman, K.; Ros, J.; Grasjo, J.; Artursson, P. Effect of molecular charge on intestinal epithelial drug transport: pH-dependent transport of cationic drugs. J Pharmacol Exp Ther 1999, 291, (2), 435-43.

33. Tavelin, S.; Grasjo, J.; Taipalensuu, J.; Ocklind, G.; Artursson, P. Applications of epithelial cell culture in studies of drug transport. Methods Mol Biol 2002, 188, 233-72.

34. Friden, M.; Ducrozet, F.; Middleton, B.; Antonsson, M.; Bredberg, U.; Hammarlund-Udenaes, M. Development of a high-throughput brain slice method for studying drug distribution in the central nervous system. Drug Metab Dispos 2009, 37, (6), 1226-33.

35. Uhr, M.; Grauer, M. T.; Yassouridis, A.; Ebinger, M. Blood-brain barrier penetration and pharmacokinetics of amitriptyline and its metabolites in p-glycoprotein (abcb1ab) knock-out mice and controls. J Psychiatr Res 2007, 41, (1-2), 179-88.

36. Kallem, R.; Kulkarni, C. P.; Patel, D.; Thakur, M.; Sinz, M.; Singh, S. P.; Mahammad, S. S.; Mandlekar, S. A simplified protocol employing elacridar in rodents: a screening model in drug discovery to assess P-gp mediated efflux at the blood brain barrier. Drug Metab Lett 2012, 6, (2), 134-44.

37. Neuhaus, W.; Mandikova, J.; Pawlowitsch, R.; Linz, B.; Bennani-Baiti, B.; Lauer, R.; Lachmann, B.; Noe, C. R. Blood-brain barrier *in vitro* models as tools in drug discovery: assessment of the transport ranking of antihistaminic drugs. Pharmazie 2012, 67, (5), 432-9.

38. Sikri, V.; Pal, D.; Jain, R.; Kalyani, D.; Mitra, A. K. Cotransport of macrolide and fluoroquinolones, a beneficial interaction reversing P-glycoprotein efflux. Am J Ther 2004, 11, (6), 433-42.

39. Cao, X.; Yu, L. X.; Barbaciru, C.; Landowski, C. P.; Shin, H. C.; Gibbs, S.; Miller, H. A.; Amidon, G. L.; Sun, D. Permeability dominates *in vivo* intestinal absorption of P-gp substrate with high solubility and high permeability. Mol Pharm 2005, 2, (4), 329-40.

40. Kuo, Y. C.; Lu, C. H. Modulation of efflux proteins by electromagnetic field for delivering azidothymidine and saquinavir into the brain. Colloids Surf B Biointerfaces 2012, 91, 291-5.

41. Yamaguchi, H.; Yano, I.; Hashimoto, Y.; Inui, K. I. Secretory mechanisms of grepafloxacin and levofloxacin in the human intestinal cell line caco-2. J Pharmacol Exp Ther 2000, 295, (1), 360-6.

42. Neuhoff, S.; Artursson, P.; Zamora, I.; Ungell, A. L. Impact of extracellular protein binding on passive and active drug transport across Caco-2 cells. Pharm Res 2006, 23, (2), 350-9.

General Results

PERMEABILITY ESTIMATION

Model Validation

Cell culture permeability experiments are valuable tools in drug development and candidate selection but the monolayer preparation protocols and the calculations procedures can affect the permeability estimation.

Calculations

There are different profiles that are usually observed between accumulated amounts of drug in the acceptor side versus time. Three examples of these profiles are represented in Figure 3.

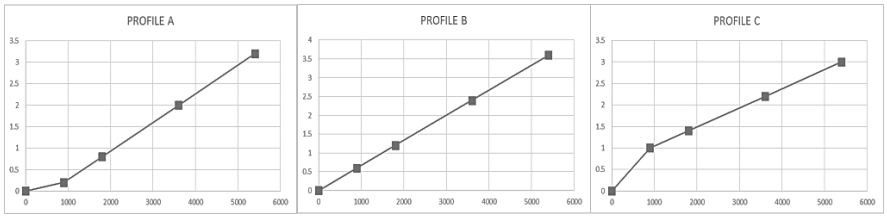

Figure 3. Profiles of accumulated amounts of drug in acceptor chamber versus time in permeability experiments in cell monolayers. Profile A: Drug is transported during the first sampling interval at a lower rate than expected; Profile B: Drug is transported linearly with a constant rate; Profile C: Drug is transported at a higher rate during the first sampling interval.

Tavelin et al. [24] highlighted the existence of these atypical profiles (Profiles A and C on Figure 3) that could be caused by poor control of temperature, partitioning of the drug into the cell monolayer, low molecular weight impurities (such as 3H-water) that are transported at a higher rate than the drug or harsh application of the drug solution leading to the disturbance of the monolayer.

An objective of this work was to use a simulation strategy to explore the performance of a new proposed Modified Non-Sink equation (MNS) for permeability estimation in different types of profiles, considering several levels of experimental variability and to compare MNS method with the classical sink and non-sink approaches and finally to explore its usefulness for BCS classification.

Simulated concentrations in the receiver chamber were plotted versus time by each profile and scenario of variability (high (H) and low (L) interindividual variability (IIV) and residual variability (RSV)) in Figure 4.

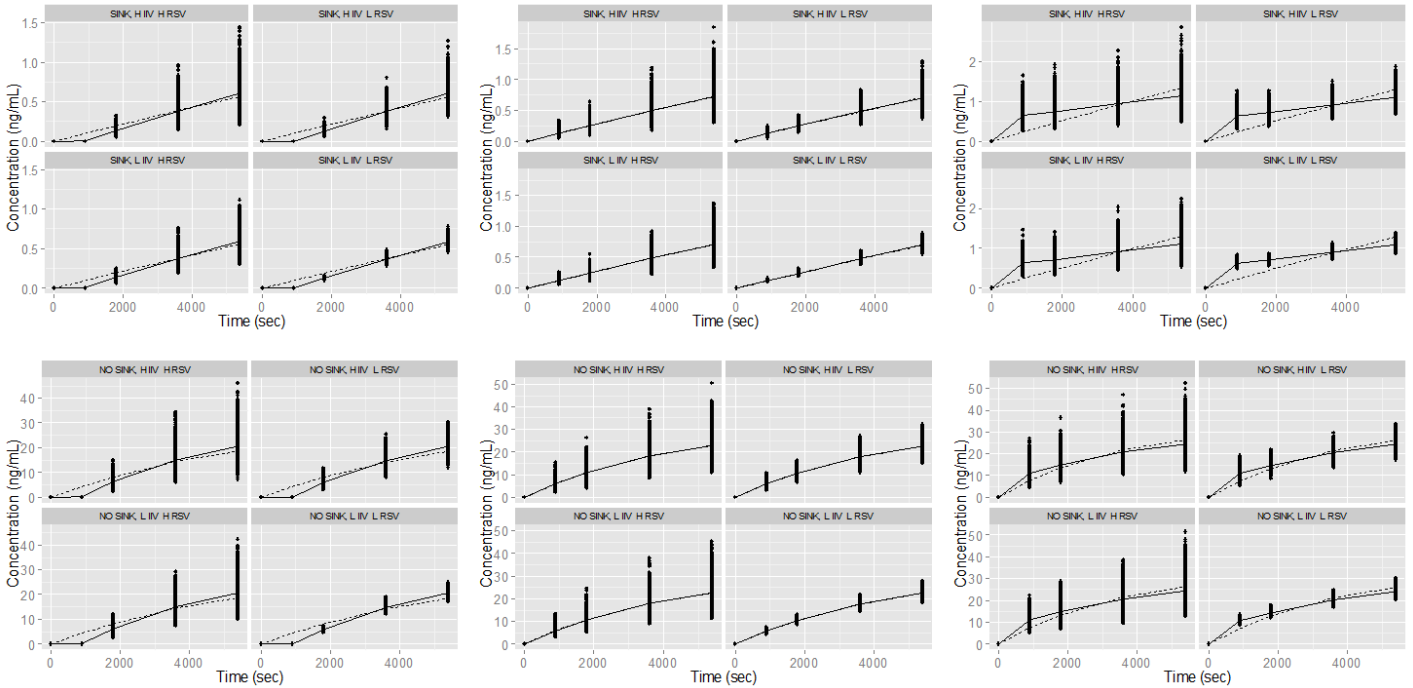

Figure 4. Profile A, B and C (left, middle and right groups) by scenarios of variability in sink conditions are represented in the upper line and non-sink conditions are plotted in the lower line. Blue dots are simulated concentrations (ng/mL) in 3000 wells, solid line is the population predicted values obtained by MNS equation and dotted line is the population predicted value by NS.

Estimation error

Results from mean, intra-assay and individual estimation error of Permeability values are calculated and depicted on Figures 5-7. Dots are the mean values of estimation error of each method (MNS, NS, S, SC), grey box is one standard deviation (SD) of the mean and lines are two SD of the mean value.

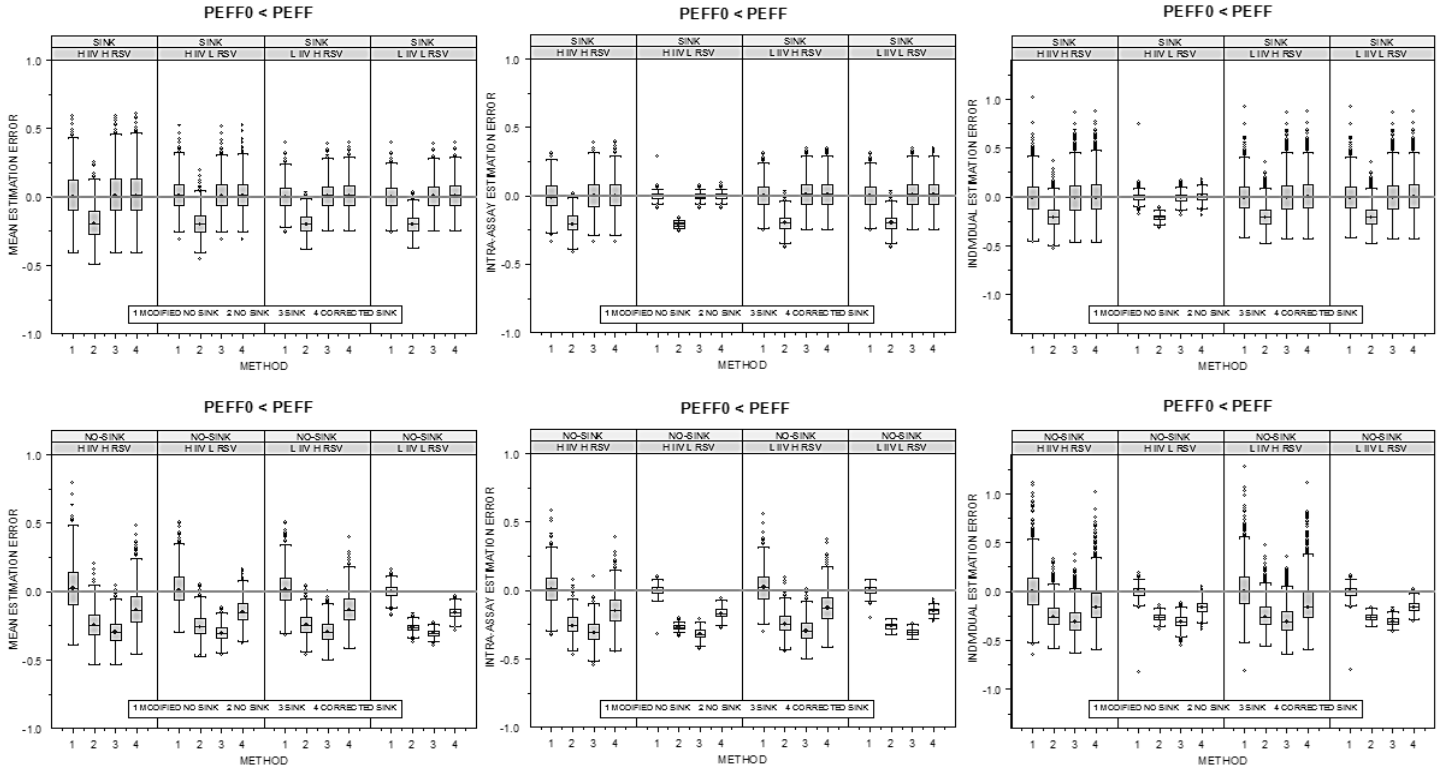

Figure 5. Estimation errors of Profile A in sink and non-sink conditions, by each scenario of variability and by each method of estimation.

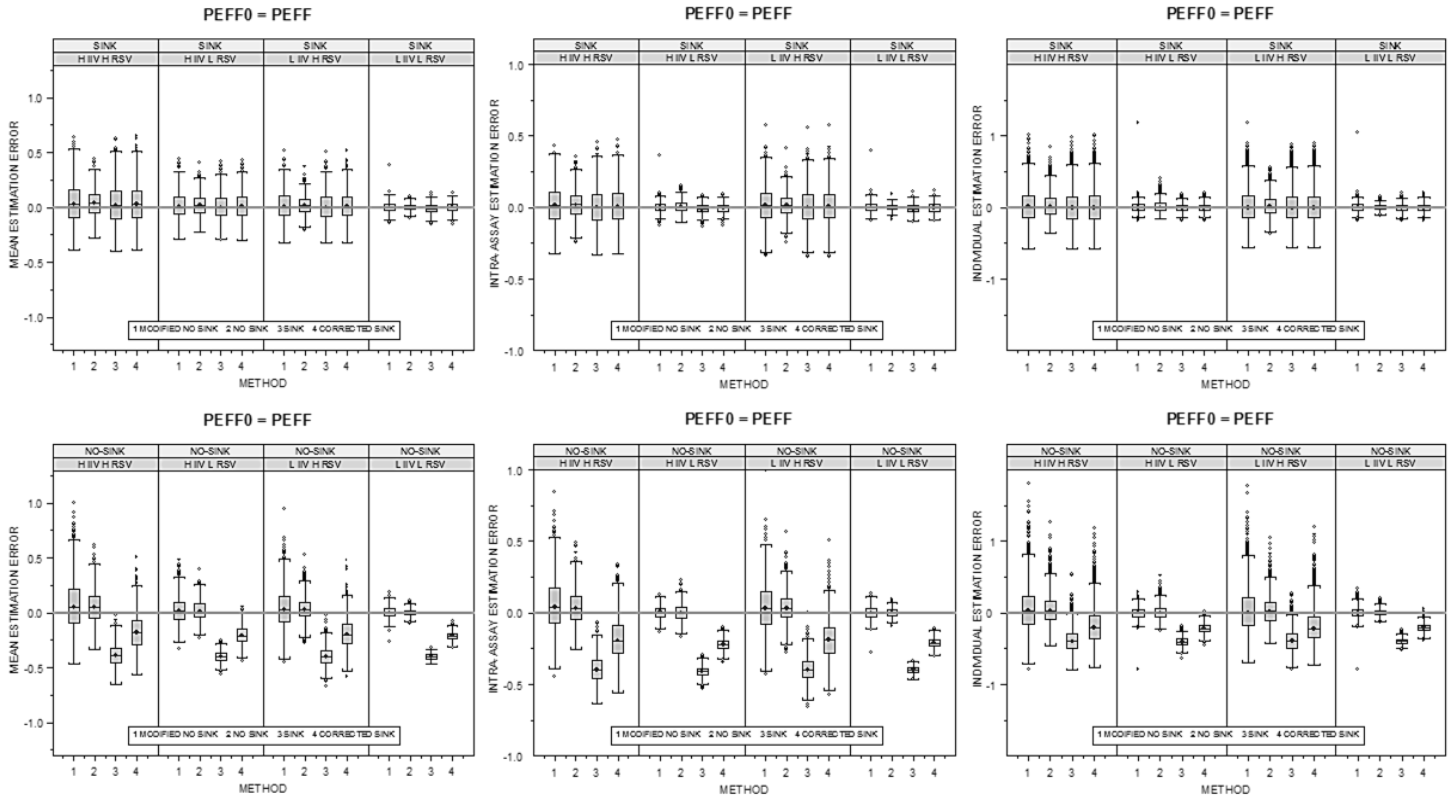

Figure 6. Estimation errors of Profile B in sink and non-sink conditions, by each scenario of variability and by each method of estimation.

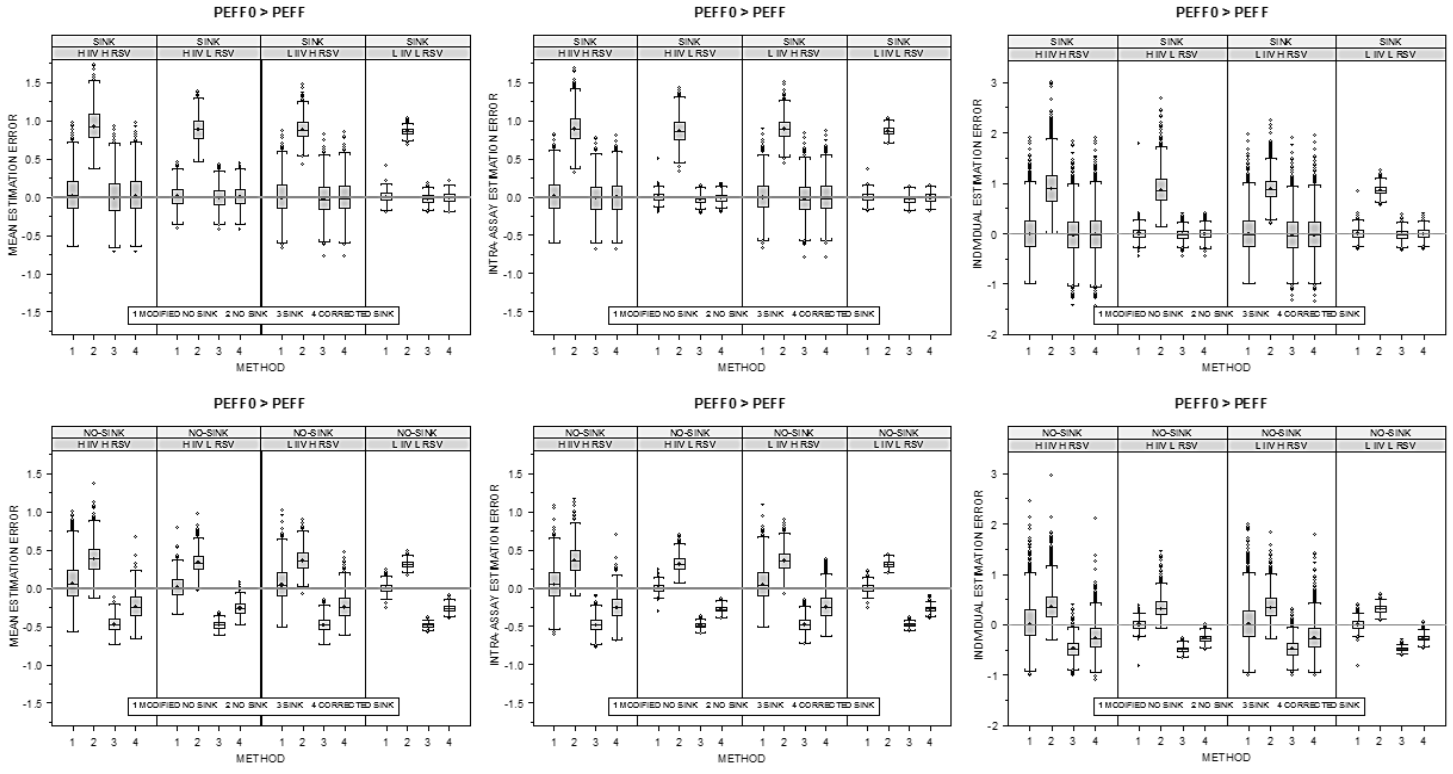

Figure 7. Estimation errors of Profile C in sink and non-sink conditions, by each scenario of variability and by each method of estimation.

Statistical analysis

ANOVA of the mean estimation errors was performed with Scheffe as post-hoc test. Results are summarized in Table 1-3.

PROFILE A

	SINK				NON SINK			
	H IIV H RSV	H IIV L RSV	L IIV H RSV	L IIV L RSV	H IIV H RSV	H IIV L RSV	L IIV H RSV	L IIV L RSV
	MNS	**MNS**	**MNS**	**MNS**	**MNS**	**MNS**	**MNS**	**MNS**
NS	**Sig**	**Sig**	**Sig**	**Sig**	**Sig**	**Sig**	**Sig**	**Sig**
S	NS	NS	NS	NS	**Sig**	**Sig**	**Sig**	**Sig**
SC	NS	NS	**Sig**	**Sig**	**Sig**	**Sig**	**Sig**	**Sig**

Table 1. ANOVA results of Profile A data sets in each scenario of variability between methods of estimation (MSN, NS, S and SC). Sig means statistical differences and NS no statistical differences were observed.

PROFILE B

	SINK				NON SINK			
	H IIV H RSV	H IIV L RSV	L IIV H RSV	L IIV L RSV	H IIV H RSV	H IIV L RSV	L IIV H RSV	L IIV L RSV
	MNS	**MNS**	**MNS**	**MNS**	**MNS**	**MNS**	**MNS**	**MNS**
NS	NS	NS	NS	NS	NS	NS	NS	NS
S	NS	NS	NS	**Sig**	**Sig**	**Sig**	**Sig**	**Sig**
SC	NS	NS	NS	NS	**Sig**	**Sig**	**Sig**	**Sig**

Table 2. ANOVA results of Profile B data sets in each scenario of variability between methods of estimation (MSN, NS, S and SC). Sig means statistical differences and NS no statistical differences were observed.

PROFILE C

	SINK				NON SINK			
	H IIV H RSV	H IIV L RSV	L IIV H RSV	L IIV L RSV	H IIV H RSV	H IIV L RSV	L IIV H RSV	L IIV L RSV
	MNS	**MNS**	**MNS**	**MNS**	**MNS**	**MNS**	**MNS**	**MNS**
NS	**Sig**	**Sig**	**Sig**	**Sig**	**Sig**	**Sig**	**Sig**	**Sig**
S	NS	S	NS	**Sig**	**Sig**	**Sig**	**Sig**	**Sig**
SC	NS	NS	NS	**Sig**	**Sig**	**Sig**	**Sig**	**Sig**

Table 3. ANOVA results of Profile C data sets in each scenario of variability between methods of estimation (MSN, NS, S and SC). Sig means statistical differences and NS no statistical differences were observed.

Model comparison

Permeability estimation

Results of the classification from 108 scenarios with each method of estimation are summarized in Table 4. Results were classified in OK, ERROR or VARIABILITY. Considering the meaning of these labels (as the examples presented in Table 3) the objective would be finding which method is able to obtain the higher number of OK results, the lower number of ERROR labels and it is not biased by the variability of the experiment. After performing the chi-square test, the number of occasions that the MNS method produced better results than the others was computed and these results are displayed in Table 4. For instance, MNS estimation method obtained a statistically higher number of OK results in 59 scenarios compared with NS method, the same number in 12 and less OK results than NS in 37 scenarios (108 total scenarios). Regarding the ERROR results, MNS method produced

less times ERROR results in 75 scenarios compared with NS method, the same number in 12 scenarios and more ERROR results in 21 scenarios. In VARIABILITY results, MNS method led to a higher number of VARIABILITY results compared with NS in 40 scenarios, a similar number in 49 scenarios and less number of VARIABILITY results in 19 scenarios.

	OK			**ERROR**			**VARIABILITY**		
	NS	**S**	**SC**	**NS**	**S**	**SC**	**NS**	**S**	**SC**
BETTER	**59**	**83**	24	**75**	**90**	44	**40**	**42**	4
SIMILAR	12	25	**82**	12	15	**62**	**49**	**66**	**104**
WORSE	37	0	2	21	3	2	19	0	0

Table 4. Comparison of statistically significant differences between MNS and NS, MNS and S and MNS versus SC. In the Columns OK and VARIABILITY, BETTER is considered when the number of results, either OK or VARIABILITY was significantly higher in MNS than the other methods; SIMILAR is when the differences were not significant; WORSE when the number of results (OK or VARIABILITY) was significantly lower in MNS than the other methods. In the Column ERROR, BETTER corresponds to a significant lower number of ERROR results, SIMILAR means a non-significant difference and WORSE implies a significantly higher number of ERROR results.

VARIABILITY OF PERMEABILITY ESTIMATION FROM DIFFERENT PROTOCOLS OF SUBCULTURE AND TRANSPORT EXPERIMENTS IN CELL MONOLAYERS

Protocol characterization and optimization

Other factor that can affect permeability values is the protocol for sub-culturing cell monolayers and performing transport experiments. In this work, insert type (polycarbonate membrane with or without collagen coating), passage number (10 40 and 80 after defrost) and time after seeding (4, 15, 21 days after seeding) were considered to evaluate the permeability values and their variability.

Metoprolol (Passive transport marker), Lucifer Yellow (paracelular transport markers) and Rhodamine-123 (P-gp substrate) were used to check the performance of the cell lines. Results are summarized in Figures 8 to 10. The coefficients of variation of permeability values of each compound in each cell line and protocol are represented in Tables 5 to 7.

Two different experimental protocols have been used to grow the cells and perform the experiments. Protocols for transport experiment differ mainly in the filter support coating and the medium and plastic ware brands and in the batch homogenization of some medium components (as the serum growth factor). In the first protocol cells grew in a collagen coated polycarbonate membrane (Costar inserts, surface area 0.9 cm2, 0.4 μm pore size) (SOP 1) and, in the second one cells grew in a polycarbonate membrane without collagen coated. (MILLICEL-PCF, surface area 0.9 cm2, 0.4 μm pore size) (SOP 2)

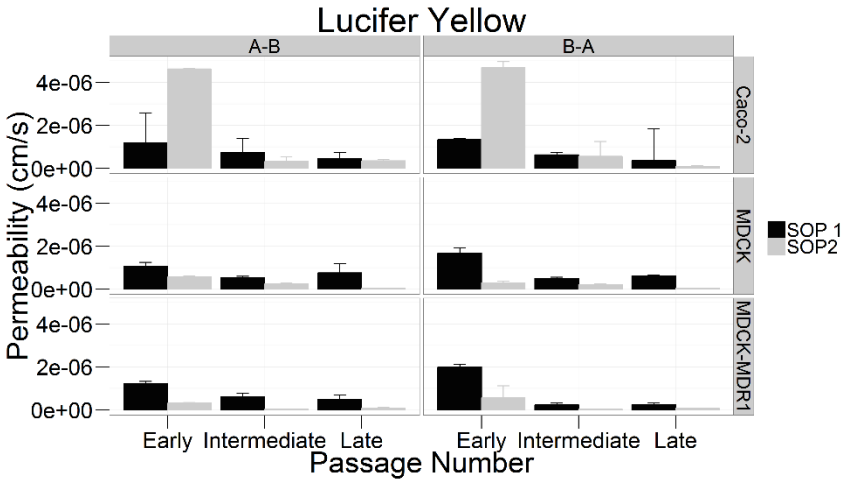

Figure 8. Permeability values of LY (2mM) obtained with both harvesting protocols (SOPs) at different passage number after defrosting process in 3 cell lines.

Lucifer Yellow	Passage	CV% SOP1	CV% SOP2
Caco2	Early	7.3	3.0
Caco2	Intermediate	11.8	90.8
Caco2	Late	5.1	23.2
MDCK	Early	15.6	15.2
MDCK	Intermediate	10.3	9.7
MDCK	Late	4.8	18.7
MDR	Early	7.1	9.6
MDR	Intermediate	2.8	38.3
MDR	Late	16.1	28.0
Average		9.0	26.3

Table 5. Variability in Lucifer Yellow permeability values in both protocols, in different passage numbers and cell lines.

Anova analysis and Scheffe post-hoc comparison showed differences in both SOP's in LY permeability values among all passages (in both directions).

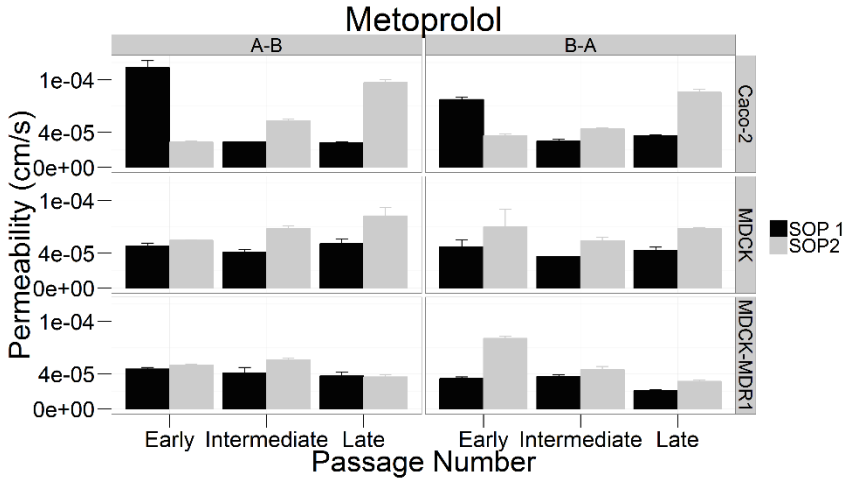

Figure 9. Permeability values of Metoprolol (100 μM) obtained with both harvesting protocols (SOPs) at different passage number after defrosting process in 3 cell lines.

Metoprolol	Passage	CV% SOP1	CV% SOP2
Caco2	Early	4.1	5.4
Caco2	Intermediate	8.8	9.4
Caco2	Late	7.4	4.5
MDCK	Early	8.6	6.6
MDCK	Intermediate	3.5	4.2
MDCK	Late	2.2	8.0
MDR	Early	3.1	6.3
MDR	Intermediate	4.0	17.5
MDR	Late	2.5	7.1
Average		4.9	7.7

Table 6. Variability in Metoprolol permeability values in both protocols, in different passage numbers and cell lines.

Anova analysis and Scheffe post-hoc comparison showed differences in both SOP's in Metoprolol permeability values in early passage compared with late (in both directions and all cell lines).

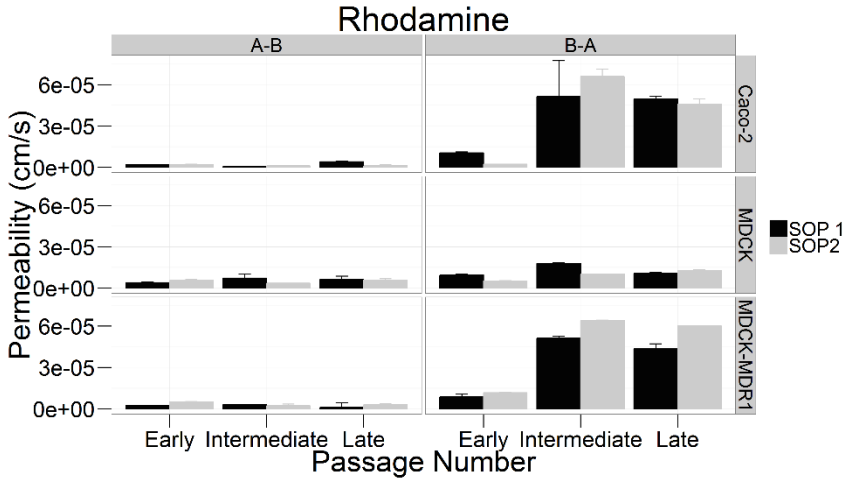

Figure 10. Permeability values of Rhodamine (5.5 μM) obtained with both harvesting protocols (SOPs) at different passage number after defrosting process in 3 cell lines.

Rhodamine	Passage	CV% SOP1	CV% SOP2
Caco2	Early	4.6	6.2
Caco2	Intermediate	36.5	5.7
Caco2	Late	145.7	27.2
MDCK	Early	4.0	16.5
MDCK	Intermediate	5.5	4.9
MDCK	Late	47.1	7.6
MDR	Early	29.0	7.5
MDR	Intermediate	8.4	4.0
MDR	Late	2.3	0.5
Average		31.5	8.9

Table 7. Variability in Rhodamine permeability values in both protocols, in different passage numbers and cell lines

Anova analysis and Scheffe post-hoc comparison showed differences in both SOP's in Rhodamine permeability values in early passage compared with late in BA direction in MDCK and MDCK-MDR1 but not in Caco-2 cells.

One of the factors affecting permeability values is the time between seeding cells and performing the experiment as it could affect to the transporter expression and cell maturation. The usual maturation time depends on the kind of cells and it used to be from 4 to 21 days in Caco2 cell line and from 4 to 9 in MDCK and MDCK-MDR1.

Figures 11, 12 and 13 show the permeability values of Lucifer Yellow, Metoprolol and Rhodamine respectively obtained at different times post seeding and passages in the three cell lines.

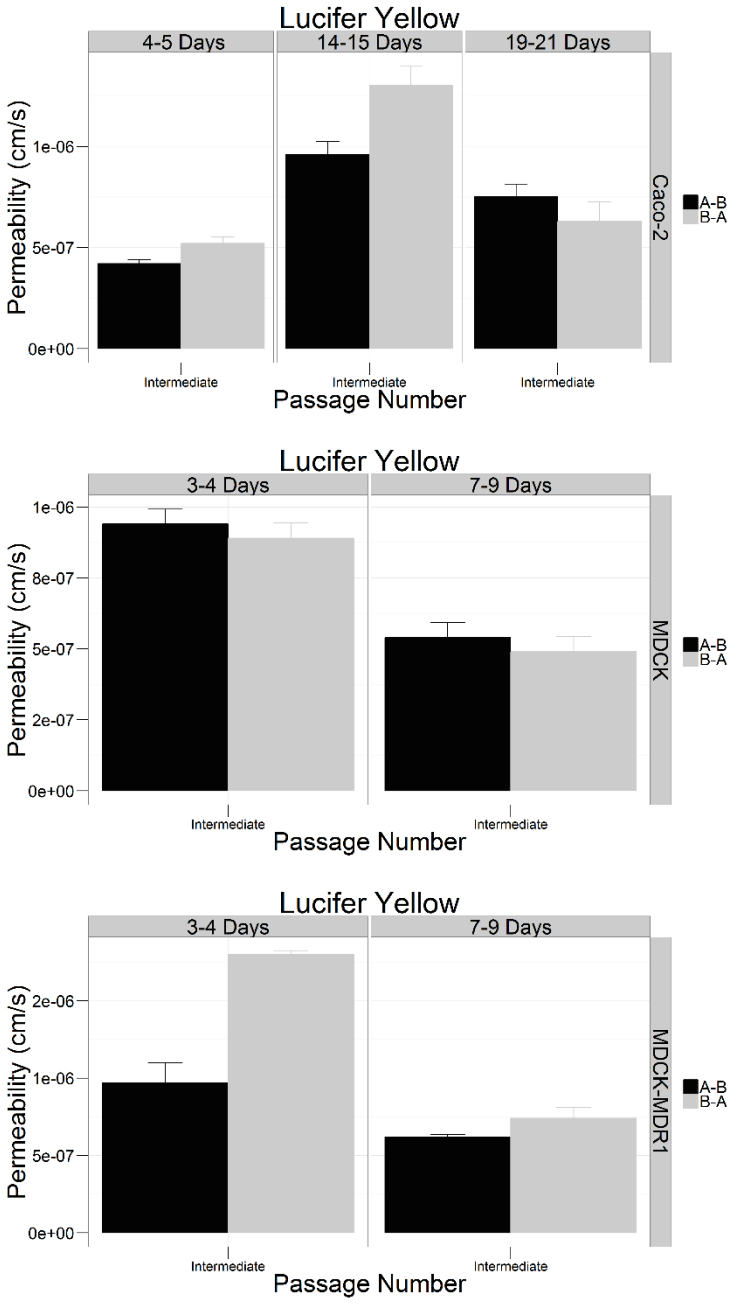

Figure 11. Permeability values of LY (2mM) obtained at different times post seeding and passages in the three cell lines.

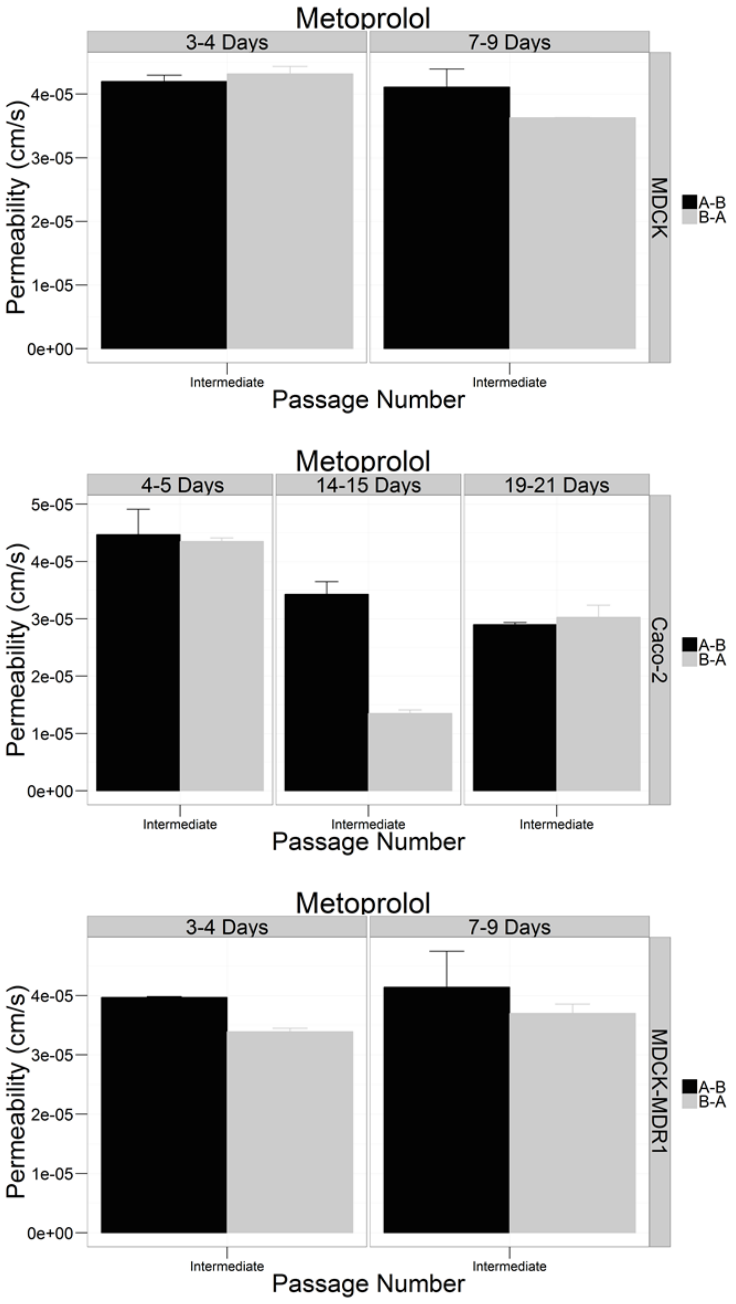

Figure 12. Permeability values of Metoprolol (100 μM) obtained at different times post seeding and passages in the three cell lines.

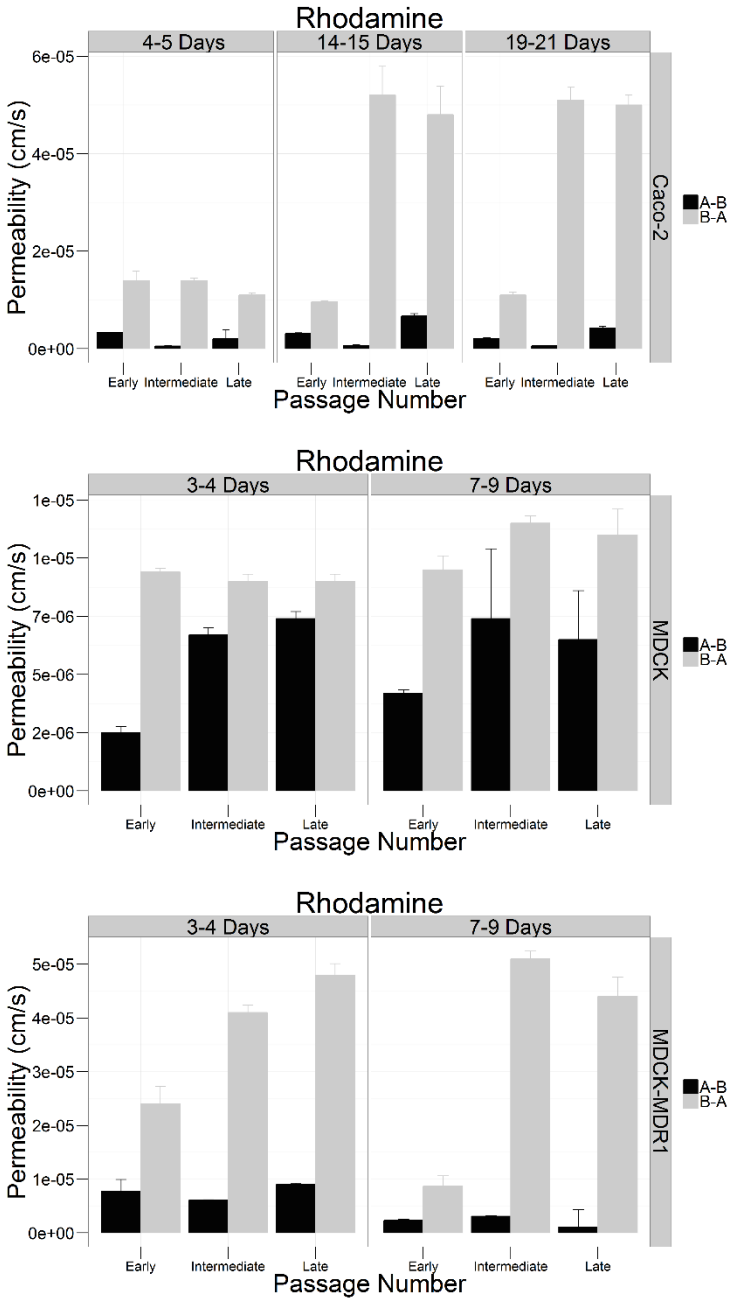

Figure 13. Permeability values of Rhodamine (5.5 μM) obtained at different times post seeding and passages in the three cell lines.

The analysis of variance test and scheffe post hoc analysis demonstrated statistical significant differences in permeabilities with the time after seeding in the three cell lines and for all the compounds. Tables 8 to 10 summarized the average coefficient of variation in AB and BA permeability values in the different conditions (passage and time after seeding) for all cell lines and compounds.

Rhodamine			
Line	**Passage**	**Days**	**Mean CV%**
Caco2	Early	4	7.1
		15	3.5
		21	5.0
	Intermediate	4	10.4
		15	11.6
		21	4.9
	Late	4	46.6
		15	9.7
		21	6.4
MDCK	Early	4	5.9
		9	4.9
	Intermediate	4	4.0
		9	21.6
	Late	4	3.7
		9	21.2
MDCK MDR1	Early	4	21.2
		9	15.5
	Intermediate	4	2.4
		9	2.6
	Late	4	3.6
		9	149.5

Table 8. Variability in permeability values of Rhodamine obtained in different cell lines and passages with different maturation days after seeding.

Lucifer Yellow		
Line	**Days**	**Mean CV%**
Caco 2	4	5.1
	15	7.0
	21	11.8
MDCK	4	5.8
	9	10.3
MDCK-MDR1	4	7.3
	9	6.2

Table 9. Variability in permeability values of Lucifer Yellow obtained in different cell lines and passages with different maturation days after seeding

Metoprolol		
Line	**Days**	**Mean CV%**
Caco 2	4	3.8
	15	8.4
	21	8.5
MDCK	4	3.6
	9	3.0
MDCK-MDR1	4	1.4
	9	3.0

Table 10. Variability in permeability values of Metoprolol obtained in different cell lines and passages with different maturation days after seeding.

The results obtained in this study confirmed the complexity of the interaction between cell culturing protocols and the need for standardization and characterization of the culture properties to optimize the conditions. These results allowed developing a new whole *in vitro* high throughput method to predict drug rate and extent of access across the BBB. The system permitted to estimate $f_{u,\ brain}$, $V_{u,\ brain}$ and $Kp_{uu,\ brain}$ in a single experimental system, using *in vitro* cell monolayers in different conditions.

In this work it was necessary to validate the prediction ability of the new *in vitro* models by comparison of the *in vitro* parameters with *in vivo* data.

INNOVATIVE *IN VITRO* METHOD TO PREDICT DRUG PERMEATION ACROSS THE BBB

Permeability Values of *In Vitro* BBB Experiments

In Table 11-12 the extrapolated permeability values at the *in vivo* concentrations for all the compounds, cell line and type of experiment are shown.

COMPOUND	CONCENTRATION (µM)	MDCKII P_{app} ($x10^{-6}$ cm/sec)				
		A→B	B→A	ALB	HOM	$P_{B\rightarrow A}/P_{A\rightarrow B}$
Amitriptyline	0.022	74.77 P	178.48 P	6.02 P	6.54 P	2.39
Atenolol	1.5	1.32 P	1.49 P	1.12 P	1.59 P	1.13
Diphenhydramine	0.051	91.72 P	79.62 P	13.12 P	25.31 P	0.87
Ethyl-phenyl malonamide	4.3	18.11 P	19.73 P	9.40 P	17.43 P	1.09
Levofloxacin	0.59	3.90 L	6.67 P	3.47 P	5.84 P	1.71
Metoprolol	0.75	94.66 P	112.07 P	78.33 P	35.91 P	1.18
Norfloxacin	0.7	2.51 P	8.16 P	1.84 P	5.79 P	3.25
Propranolol	0.051	68.37 P	89.08 P	7.24 P	8.18 P	1.30
Verapamil	0.075	58.29 P	49.22 P	15.54 P	15.83 P	0.84
Zidovudine	1.2	11.39 P	14.03 P	7.74 P	14.50 P	1.23

Table 61. Extrapolated permeability values, Papp,extrapolated at the *in vivo* relevant concentration in MDCKII and MDCKII-MDR1 cell lines and in the different experimental settings (standard, albumin and brain homogenate presence). P(passive), L (lineal), I (influx) and E (efflux) are the model used for extrapolation.

COMPOUND	CONCENTRATION (µM)	MDCKII-MDR1 P_{app} ($x10^{-6}$ cm/sec)				
		A→B	B→A	ALB	HOM	$P_{B\rightarrow A}/P_{A\rightarrow B}$
Amitriptyline	0.022	17.95 P	16.91 P	3.45 P	1.76 P	0.94
Atenolol	1.5	0.49 P	0.88 P	0.42 P	0.74 P	1.80
Diphenhydramine	0.051	99.97 P	58.40 P	15.42 P	11.75 P	0.58
Ethyl-phenyl malonamide	4.3	5.80 P	11.28 P	6.38 P	9.42 P	1.94
Levofloxacin	0.59	1.83 P	25.00 P	0.92 P	21.61 P	13.67
Metoprolol	0.75	57.30 P	52.09 P	27.51 P	21.22 P	0.91
Norfloxacin	0.7	0.94 P	2.15 P	0.63 P	1.93 P	2.28
Propranolol	0.051	110.65 P	52.75 P	13.29 P	7.38 P	0.48
Verapamil	0.075	82.73 P	51.66 P	8.66 P	17.89 P	0.62
Zidovudine	1.2	2.73 P	28.41 P	1.98 P	28.84 P	10.41

Table 72. Extrapolated permeability values, Papp,extrapolated at the *in vivo* relevant concentration in MDCKII and MDCKII-MDR1 cell lines and in the different experimental settings (standard, albumin and brain homogenate presence). P(passive), L (lineal), I (influx) and E (efflux) are the model used for extrapolation.

In Vitro BBB parameters

The *in vitro* estimated $f_{u,\ plasma}$, $Kp_{uu,\ CSF}$, $V_{u,\ brain}$ in MDCKII are summarized in Table 13. *In vivo* data were obtained from Friden et al. [89] and *in vitro* data were calculated according to equations described in Chapter 6.

	MDCKII					
COMPOUND	**$V_{u,brain}$ (ml/g brain)**		**$K_{puu,CSF}$**		**$f_{u,plasma}$**	
	In vitro	***In vivo***	***In vitro***	***In vivo***	***In vitro***	***In vivo***
Amitriptyline	16.58	310.00	0.42	0.18	0.08	0.09
Atenolol	0.76	2.50	0.88	0.54	0.85	1.00
Diphenhydramine	2.09	32.00	1.15	1.05	0.14	0.48
Ethyl-phenyl malonamide	0.88	0.90	0.92	1.25	0.52	0.55
Levofloxacin	0.89	1.70	0.58	0.18	0.89	0.82
Metoprolol	2.07	5.50	0.84	0.93	0.83	0.90
Norfloxacin	1.05	2.90	0.31	0.11	0.73	0.87
Propranolol	6.74	118.00	0.77	0.42	0.11	0.09
Verapamil	2.07	54.00	1.18	1.13	0.27	0.20
Zidovudine	0.78	1.10	0.81	1.04	0.68	0.64

Table 83. *In vitro* parameters in MDCKII cell line calculated from equations 4, 7, 9 and 11 and *in vivo* parameters published by Friden et al. [89].

In Table 14 *in vitro* estimated of $f_{u,plasma}$, $K_{p,uu,brain}$, $V_{u,brain}$ in MDCKII-MDR1 are reported. *In vivo* data were obtained from Friden et al. [89] and *in vitro* data were calculated according to equations described above.

MDCKII-MDR1						
COMPOUND	**$V_{u,brain}$ (ml/g brain)**		**$K_{puu,brain}$**		**$f_{u,plasma}$**	
	In vitro	***In vivo***	***In vitro***	***In vivo***	***In vitro***	***In vivo***
Amitriptyline	5.97	310.00	1.06	0.73	0.19	0.09
Atenolol	0.91	2.50	0.55	0.03	0.87	1.00
Diphenhydramine	3.18	32.00	1.71	1.05	0.14	0.48
Ethyl-phenyl malonamide	0.92	0.90	0.00	1.25	1.10	0.55
Levofloxacin	0.89	1.70	0.07	0.12	0.50	0.82
Metoprolol	1.67	5.50	1.10	0.64	0.48	0.90
Norfloxacin	0.87	2.90	0.44	0.03	0.67	0.87
Propranolol	4.49	118.00	2.10	0.61	0.12	0.09
Verapamil	1.93	54.00	1.60	0.05	0.10	0.20
Zidovudine	0.79	1.10	0.10	0.09	0.73	0.64

Table 94. *In vitro* parameters in MDCKII-MDR1 cell line calculated from equations 4, 7, 9 and 11 and *in vivo* parameters published by Friden et al. [89].

Correlations

To validate the reliability of the new method it was necessary to correlate *in vitro* vs *in vivo* BBB parameters.

MDCKII

Figure 14 shows the correlation obtained between *in vivo* $f_{u,plasma}$ and *in vitro* $f_{u,plasma}$. values obtained with MDCK cells. The *in vitro* values of $K_{p,uu,brain}$ predicted with MDCK cells and the correlation with *in vivo* values is represented in Figure 15. Figure 16 shows the correlation obtained between *in vivo* $V_{u,brain}$ and *in vitro* $V_{u,brain}$ from MDCK cells. Parameters of the linear correlations, Pearson coefficient and squared Pearson correlation coefficients are displayed in the figures.

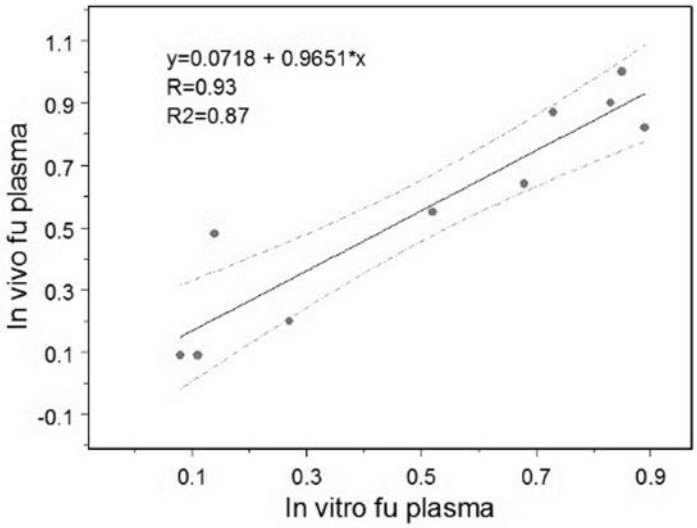

Figure 14. Correlation obtained between *in vivo* fu,p and *in vitro* fu,p in MDCKII cell line for ten compounds. The solid line represents the linear regression, and the dotted line represents the 95% confidence interval of the predictions. R is Pearson correlation coefficient and R^2 is the square of Pearson correlation coefficient that reflects the percent of total variance of the dependent variable that is explained by the independent one.

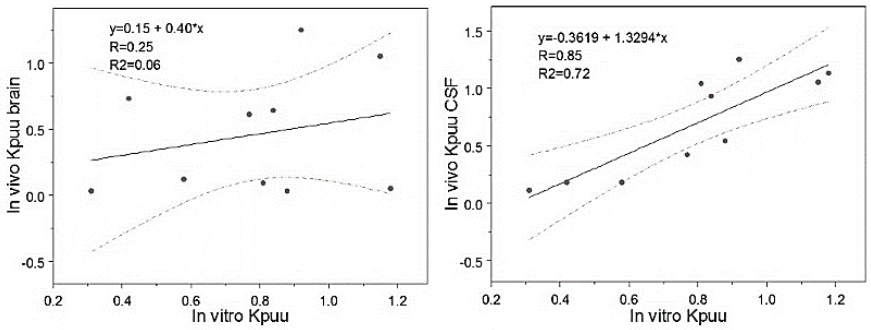

Figure 15. Correlation obtained between rat *in vivo* $K_{p,uu,brain}$ and *in vitro* $K_{p,uu,brain}$ (left) and between human *in vivo* $K_{p,uu,CSF}$ and *in vitro* $K_{p,uu,brain}$ (right) in MDCKII cell line. The solid line represents the linear regression, and the dotted line represents the 95% confidence interval of the predictions. R is Pearson correlation coefficient and R^2 is the square of Pearson correlation coefficient reflecting the percent of total variance of dependent variable explained by the independent one.

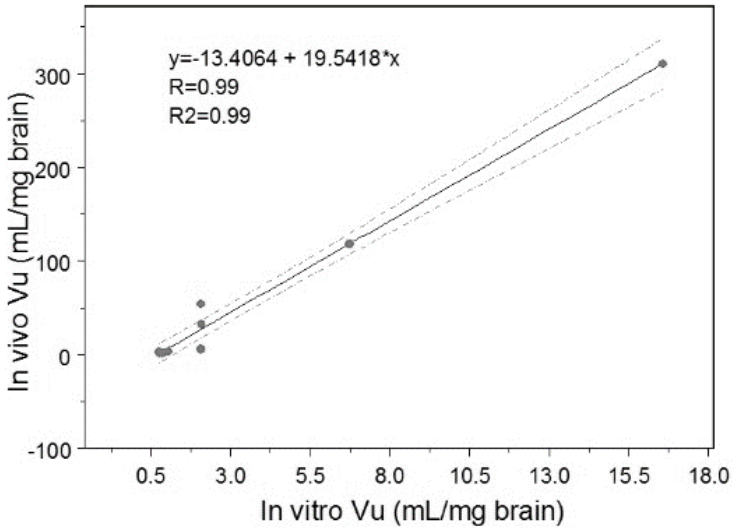

Figure 16. Correlation obtained between *in vivo* $V_{u,brain}$ and *in vitro* $V_{u,brain}$ in MDCKII cell line for the ten assayed drugs. The solid line represents the linear regression, and the dotted line represents the 95% confidence interval of the predictions. R is Pearson correlation coefficient and R^2 is the square of Pearson correlation coefficient.

MDCKII-MDR1

The correlation obtained between *in vivo* $f_{u,\ plasma}$ and *in vitro* $f_{u,\ plasma}$ values obtained with MDCK-MDR1 cells is represented in Figure 17. The *in vitro* values of $Kp_{uu,\ brain}$ predicted with MDCK-MDR1 cells versus the *in vivo* values are represented in Figure 18. Figure 19 shows the correlation obtained between *in vivo* $V_{u,\ brain}$ and *in vitro* $V_{u,\ brain}$ from MDCK-MDR1 cells. Parameters of the linear correlations, Pearson coefficient and squared Pearson correlation coefficients are displayed in the figures.

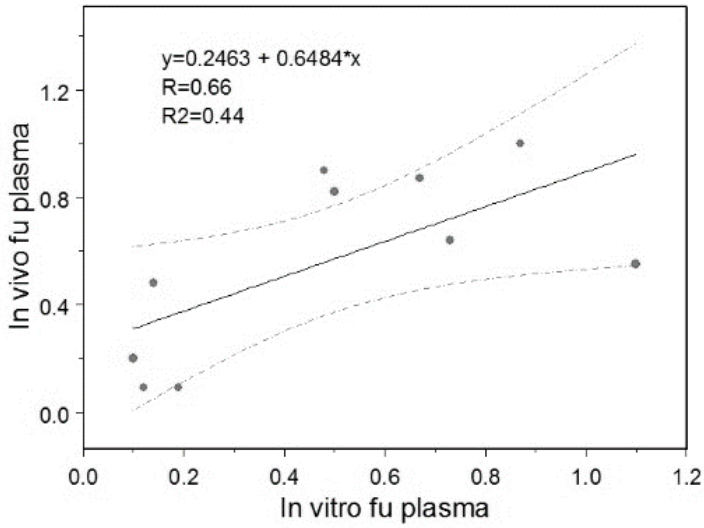

Figure 17. Correlation obtained between *in vivo* $f_{u,p}$ and *in vitro* $f_{u,p}$ in MDCKII-MDR1 cell line for ten compounds. The solid line represents the linear regression, and the dotted line represents the 95% confidence interval of the predictions. R is Pearson correlation coefficient and R^2 is the square of Pearson correlation coefficient.

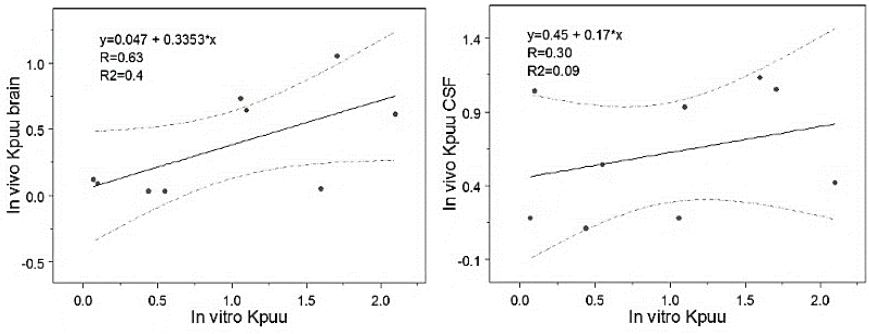

Figure 18. Correlation obtained between rat *in vivo* $K_{p,uu,brain}$ and *in vitro* $K_{p,uu,brain}$ (left) and between human *in vivo* $K_{p,uu,CSF}$ and *in vitro* $K_{p,uu,brain}$ (right) in MDCKII-MDR1 cell line for nine compounds (Ethyl-phenyl malonamide was not considered). The solid line represents the linear regression, and the dotted line represents the 95% confidence interval of the predictions. R is Pearson correlation coefficient and R2 is the square of Pearson correlation coefficient.

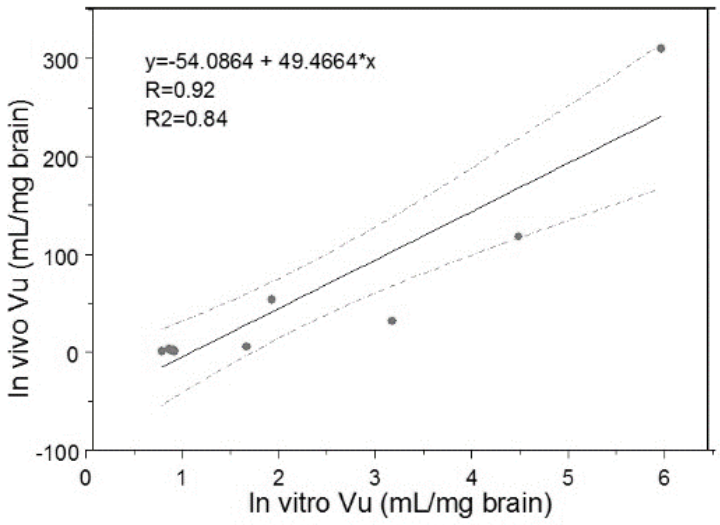

Figure 19. Correlation obtained between *in vivo* $V_{u,brain}$ and *in vitro* $V_{u,brain}$ in MDCKII-MDR1 cell line for ten compounds. The solid line represents the linear regression, and the dotted line represents the 95% confidence interval of the predictions. R is Pearson correlation coefficient and R2 is the square of Pearson correlation coefficient.

General Discussion

PERMEABILITY ESTIMATION

The *in vitro* permeability studies are a fundamental tool in the preclinical development of new drugs [24, 90-94].Permeability is the ability of a molecule to cross biological barriers and several cell monolayers are used in the *in vitro* permeation studies [54, 92, 95, 96]. The importance of a correct estimation of the permeability of new drugs in development lies in an efficient selection of the candidates to ensure a greater chance of reaching the market. This fact is, in particular, relevant when the classification of the candidate by comparison with a reference could be biased if the estimation is not accurate.

Model Validation

NS and MNS predicted equally well the simulated concentrations in the receiver chamber when there is no alteration in the initial phases of drug permeation. But if there is any initial alteration (Profile A and C Figure 2, only MNS is able to estimate accurately the "true" permeability due its ability to discriminate the initial permeability until the first sampling interval (P_{eff} 0) and the final (or "true") permeability (P_{eff} 1), i.e. this method takes into account the behavior in the initial phase and it avoids that this initial alteration affects the estimation of the permeability. Therefore, NS method underestimates in Profile A and overestimates in Profile C the permeability value in all scenarios of variability and sink and non-sink conditions.

When comparing the results of the estimation errors (Figure 8-10), no significant differences are observed between the behavior of the mean, intra-assay and individual estimation errors. In all the profiles (A, B and C), under sink conditions linear regression models (S and SC) achieved similar estimation errors compared with MNS method. These

results are expected because the linear sink and sink corrected models allow the intercept of the regression to be different from 0.

On the other hand, NS method produces estimation errors different from 0 when the initial permeation across the monolayer is affected (in all scenarios of variability) and under sink and non-sink conditions (Figures 8-10). The single permeability parameter in the equation is not able to satisfy, by nonlinear regression, all experimental concentrations in the receiver chamber. However, when there is no alteration in the initial phase (Figure 2) NS method is able to predict an accurate permeability value under sink and non-sink conditions in all scenarios of variability. NS presents statistically significant differences in average estimation error compared to MNS, under sink and non-sink, in the Profile A and C in all variability scenarios proposed.

Linear regression models (S and SC) showed statistically significant differences when non-sink conditions existed in each of the profiles and scenarios of variability proposed. In some cases, under sink conditions, significant differences were observed between S and SC and MNS, usually when IIV and RSV variability was low. This could be explained because as the variance of the mean estimation errors is small, small differences in the mean error between methods could be significant in Scheffe test.

Therefore, these differences observed in Figures 7 to 10 and the statistical differences in estimation errors evidenced in the ANOVA (Tables 1-3) demonstrated that linear regression models are not valid at any level of variability under non-sink, and even in scenarios with low variability under sink conditions. Likewise, NS method is not useful for calculating the permeability when there is an alteration of the

permeation through the cell monolayer in the initial stages in all scenarios of variability and under sink and non-sink conditions.

Model Comparison

The designed scenarios to perform the simulations are focused on a borderline situation for classification as high permeability compound (in BCS framework) that is test and reference permeability values very similar. This particular case was selected because, obviously, when the classification is clear, or in other words, with a test permeability value much higher or lower than the reference one, the bias due to the estimation method could be neglected, as it could affect test or reference in a different magnitude but it would never mask the existing differences. Thus, actually a biased permeability estimates would not affect the comparison. The problem of the estimation method could arise when the candidate compound is near the cutoff value.

Results from Chapter 4 demonstrated that the MNS method would conclude a correct classification in more potential scenarios even when the designed scenarios were borderline situations. Given a theoretical difference of 20% in test and reference compound, when the experimental variability is added to the system, the MNS equation led to a correct rank order, matching the "true" parameters in a higher number of occasions, including those with "atypical" profiles of cumulative amounts versus time. It is important to point out that the so called atypical profiles are actually not unusual but often neglected and then, the standard calculation methods are used without considering their influence in the estimation error. In the present simulation it is demonstrated that when these profiles arise the new Modified Non Sink

equation gives the most accurate estimate. Therefore, the main conclusion of this section is that the MNS method is able to correctly estimate the permeability in a larger number of cases compared to the proposed models and it has fewer errors in the classification of the compound. This is essential for a more efficient candidate selection.

VARIABILITY OF PERMEABILITY ESTIMATION FROM DIFFERENT PROTOCOLS OF SUBCULTURE AND TRANSPORT EXPERIMENTS IN CELL MONOLAYERS

In SOP 1 with Caco-2 cells after passage 10 the permeability values decreased and remained fairly constant in the subsequent passages. In MDCK and MDCK-Mdr1 passage number does not seem to affect to the permeability values at least in the range of passages assayed (Figure 1). In SOP 2 on the contrary the passage number had a marked effect on Metoprolol permeability in particular in Caco-2 cells where there is a trend with higher permeability values of Metoprolol with higher passages (Figure 2).

On the other hand the variability in permeability estimation showed a trend to decrease in MDCK and Caco-2 cells with SOP1 but a tendency to increase in SOP 2. MDCK-MDR1 showed the lower variability in both protocols (ranged between 5 and 7% as average values), without any relevant change with passage number.

Considering these results, SOP 1 at intermediate passage number seems to be the best experimental conditions to compare drugs absorbed by passive diffusion by transcellular route.

SOP 1 helps to cell differentiation in a more stable manner compared to SOP 2 which showed permeability changes with passage and also more variable values.

The differences in SOP 1 and 2 regarding the effect of passage number on the different permeation routes show the complexity of the involved mechanisms. For P-gp interaction studies in this case would be more convenient SOP 2 at intermediate or late passage numbers.

The results obtained in this study confirm the complexity of the interaction between cell culturing protocols and cell lines and the need for standardization and characterization of the culture properties to optimize the conditions depending on the study objectives. In our study, the average variability observed in permeability values in all cell lines is around 10%-15% that means that for detecting a 15% difference in permeability values the required number of individual estimations would be between 8 and 12, i.e. one plate of 12 wells. The variability is lower in intermediate passages in Caco-2 cells supporting the recommendation of use a short range of passages to a particular study. MDCK was more influenced by the passage number, with less CV in lower passages. MDCK-MDR1 showed constant CV among passages, protocols and experimental conditions but permeability values were affected by all the studied conditions, indicating that for this cell line standardization of experimental conditions is in particular relevant to obtain comparable results between different laboratories.

As conclusion, we have confirmed the influence of maturation conditions, passage number in permeability values and in their variability. Based in our results protocol with coating would be more adequate for studies of compounds absorbed by passive diffusion but the protocol without coating gave us better results for studies about P-gp interactions. A similar study should be done in each laboratory to understand the influence of their protocols in the monolayer properties in order to standardizing conditions and setting the acceptance criteria.

INNOVATIVE *IN VITRO* METHOD TO PREDICT DRUG PERMEATION ACROSS THE BBB

In vitro methods have been recognized in their capability to predict the drug access rate into the brain, the role of different transporters in drug permeation and the relevance of some biomarkers in the signal transduction, but the measurement of the extent and the drug brain distribution require separate experimental systems. A whole *in vitro* single system has been proposed using MDCKII and MDCKII-MDR1 cell lines because they closely reflect the tightness and transporters expression of the blood brain barrier in a more reliable and constant manner than non-immortalized cell lines [14, 15] and it provides a well characterization of the relevant drug parameters in order to improve candidate selection in the preclinical stages for further *in vivo* analysis [97, 98].

The relevant BBB parameters for predicting rate and extent of access are: $f_{u,\ plasma}$, $V_{u,\ brain}$, and $Kp_{,uu,\ brain}$. $f_{u,\ plasma}$ explains the drug's affinity to blood proteins and this parameter quantify the free concentration that is able to cross the BBB and reach the target. However, the amount of drug that is able to reach the target depends also on the free drug concentration in brain. Therefore, $Kp_{,uu,\ brain}$ is a measurement in equilibrium of the relationship between free brain concentrations and free plasma concentrations. The value of $Kp_{,uu,\ brain}$ indicates the extent of the drug that crossed the blood-brain barrier and is highly related to the effect. The parameter that describes the distribution of the drug in brain is $V_{u,\ brain}$. The brain may be divided in two different compartments, extracellular fluid (ECF) and intracellular fluid (ICF). The ECF+ICF real volume is the minimum volume in which the drug may be distributed if it does not bind to the cells

components. If the drug is accumulated in cells, then $V_{u, brain}$ is greater than (ECF+ICF) volume. The experimental determination of these three parameters required different and independent experimental setups. $f_{u, plasma}$ is determined *in vitro*, $Kp_{uu, brain}$ requires *in vivo* microdialysis studies to estimate the ECF and plasma concentrations and $V_{u, brain}$ may also be obtained using *in vitro* methods [4].

Correlations

All the correlations *in vitro* versus *in vivo* parameters were done using the three proposed correlation methods, i.e. from the Papp at the lowest concentrations, by averaging the *in vitro* estimates at all the concentrations and from the extrapolation strategy. The last method produced the best correlations (higher correlation coefficients) in both cell lines.

MDCKII

In this cell line *in vitro* fu,p calculated from permeability values and *in vivo* $f_{u, plasma}$ presented a good correlation (Figure 15) in ten compounds tested (R=0.93). *In vitro* $Kp_{uu, brain}$ and *in vivo* human $Kp_{uu, CSF}$ correlation (Figure 16) was obtained with an R=0.85. Human $Kp_{uu, CSF}$ data were better correlated than rat $Kp_{uu, brain}$ values (R=0.25), probably due to the less transporter expression in MDCKII and human Blood-cerebrospinal fluid barrier (BCSFB). Good $V_{u, brain}$ correlation (Figure 17) was observed between *in vitro* $V_{u, brain}$ and *in vivo* $V_{u, brain}$ (R=0.99).

MDCKII-MDR1

In the MDR1 transfected cell line, *in vitro* and *in vivo* $f_{u,plasma}$ correlation (Figure 18) was less accurate and precise. A Pearson correlation coefficient of 0.66 is lower than observed than in MDCKII

cell line (R=0.93). *In vitro* $Kp_{uu,\ brain}$ and *in vivo* $Kp_{uu,\ brain}$ correlation (Figure 19) was obtained with an R=0.66, removing Ethyl-phenyl malonamide data. Rat $Kp_{uu,\ brain}$ data were better correlated than human $Kp_{uu,\ CSF}$ values (R=0.30), but a good correlation was not achieved with any of the *in vivo* Kp_{uu} values. The higher expression level of P-gp in this cell line might not reflect the *in vivo* expression levels in BBB. Good $V_{u,\ brain}$ correlation (Figure 20) was observed between *in vitro* $V_{u,\ brain}$ and *in vivo* $V_{u,\ brain}$ (R=0.92). Similar behavior in rank order was observed as explained in MDCKII.

Comparing both cell lines, in general the prediction performance of MDCKII cell lines is better than the MDCK-MDR1. Nevertheless the worst predicted compounds are the same in both cell lines at least for Kp_{uu} and for $f_{u,\ plasma}$. For instance Zidovudine and Ethyl-phenylmalonamide *in vivo* Kp_{uu} are underestimated in both cell lines while Propranolol and Atenolol are over estimated. Diphenhydramine $f_{u,\ plasma}$ is underestimated in both cell lines. The reason for the deviation is not clear but it does not seem to be related with the different expression level of P-gp that is the most relevant difference between both cell lines.

Conclusions

1. Modified Non-Sink equation (Mangas-Casabó method) is a precise and accurate equation for calculating the apparent unidirectional permeability in any type of profile and under different scenarios of variability, as well as sink and non-sink conditions, while the Non-Sink equation fails in obtaining good permeability estimates in those situations in which the initial permeation rate is altered.

2. Linear regression models (S and SC), are not valid under strong non-sink conditions as expected as the underlying assumptions (sink conditions) do not hold but also in situations in which sink conditions are fulfilled but the system variability is high.

3. MSN method would be the recommended one as it accommodates not only sink and non-sink conditions but also all type of profiles with altered initial rates. Sink corrected could be a good approximation (in slightly non sink conditions) even better than Non Sink method because NS does not fit well the atypical profiles.

4. The sub-culturing protocols, passage number and days after seeding before the experiment have an important influence in permeability values and in their variability.

5. SOP 1 (with collagen coating) at intermediate passage number seems to be the best experimental conditions in our laboratory

and cell lines to compare drugs absorbed by passive diffusion by transcellular route.

6. The differences in SOP 1 and 2 regarding the effect of passage number on the different permeation routes show the complexity of the involved mechanisms. For P-gp interaction studies in this case would be more convenient SOP 2 at intermediate or late passage numbers.

7. The variability in permeability estimation showed a trend to decrease in MDCK and Caco-2 cells with SOP1 but a tendency to increase in SOP 2. MDCK-Mdr1 showed the lower variability in both protocols (ranged between 5 and 7% as average values), without any relevant change with passage number.

8. The time post seeding had the expected effect in particular in Rhodamine permeability for which higher maturation times lead to a higher expression of the transporter Nevertheless for passive diffusion transported drugs there is not a clear trend neither in permeability values nor in variability. These results support the idea of developing "fast maturation" models that can be useful for screening compounds absorbed by passive mechanism.

9. In our study, the average variability observed in permeability values in all cell lines is around 10%-15% that means that for detecting a 15% difference in permeability values the required

number of individual estimations would be between 8 and 12, i.e. one plate of 12 wells.

10. The in vitro cell monolayer system (in MDCK and MDCK-MDR1) with albumin in apical chamber in comparison with the standard system without albumin allows the estimation of the fraction unbound in plasma.

11. The inclusion of brain homogenate in the basolateral chamber allows the estimation of $f_{u,\ brain}$ by comparison of the permeability values obtained with and without brain homogenate in the system. The most adequate ratio in terms of adherence, sampling feasibility and physiological resemblance was a 3:1 ratio of buffer/brain homogenate.

12. *In vitro* $f_{u,\ plasma}$, $Kp_{uu,\ brain}$ and $V_{u,\ brain}$ calculated with the apparent permeabilities Papp in the proposed cell culure system presented a good correlation with *in vivo* $f_{u,\ plasma}$, $Kp_{,uu,\ brain}$ and $V_{u,\ brain}$ published values. Despite its simplicity the predictive performance is fairly good considering the reduced number of tested compounds with different physicochemical and transport properties.

13. In summary, a innovative "three step" whole in vitro cell monolayer system have been developed including a standard set up of apical and basolateral chamber of same composition a second model with albumin in apical chamber and a third step

with brain homogenate in basolateral chamber. The comparison of the effective permeabilities in the three steps allows the estimation of the relevant kinetic parameters for Blood Brain Barrier with the proposed mathematical analysis.

References

1. Pavan, B., et al., *Progress in drug delivery to the central nervous system by the prodrug approach.* Molecules, 2008. **13**(5): p. 1035-65.
2. Pangalos, M.N., L.E. Schechter, and O. Hurko, *Drug development for CNS disorders: strategies for balancing risk and reducing attrition.* Nature reviews. Drug discovery, 2007. **6**(7): p. 521-32.
3. de Lange, E.C., *Utility of CSF in translational neuroscience.* Journal of pharmacokinetics and pharmacodynamics, 2013.
4. Hammarlund-Udenaes, M., U. Bredberg, and M. Friden, *Methodologies to assess brain drug delivery in lead optimization.* Current topics in medicinal chemistry, 2009. **9**(2): p. 148-62.
5. Hammarlund-Udenaes, M., et al., *On the rate and extent of drug delivery to the brain.* Pharmaceutical research, 2008. **25**(8): p. 1737-50.
6. Hammarlund-Udenaes, M., L.K. Paalzow, and E.C. de Lange, *Drug equilibration across the blood-brain barrier--pharmacokinetic considerations based on the microdialysis method.* Pharmaceutical research, 1997. **14**(2): p. 128-34.
7. Feng, M.R., *Assessment of blood-brain barrier penetration: in silico, in vitro and in vivo.* Current drug metabolism, 2002. **3**(6): p. 647-57.
8. Abbott, N.J., D.E. Dolman, and A.K. Patabendige, *Assays to predict drug permeation across the blood-brain barrier, and distribution to brain.* Current drug metabolism, 2008. **9**(9): p. 901-10.
9. Hakkarainen, J.J., et al., *Comparison of in vitro cell models in predicting in vivo brain entry of drugs.* International journal of pharmaceutics, 2010. **402**(1-2): p. 27-36.
10. Lundquist, S., et al., *Prediction of drug transport through the blood-brain barrier in vivo: a comparison between two in vitro cell models.* Pharmaceutical research, 2002. **19**(7): p. 976-81.
11. Mabondzo, A., et al., *Validation of in vitro cell-based human blood-brain barrier model using clinical positron emission tomography radioligands to predict in vivo human brain penetration.* Molecular pharmaceutics, 2010. **7**(5): p. 1805-15.
12. Omidi, Y., et al., *Evaluation of the immortalised mouse brain capillary endothelial cell line, b.End3, as an in vitro blood-brain barrier model for drug uptake and transport studies.* Brain research, 2003. **990**(1-2): p. 95-112.
13. Perriere, N., et al., *A functional in vitro model of rat blood-brain barrier for molecular analysis of efflux transporters.* Brain research, 2007. **1150**: p. 1-13.

14. Garberg, P., et al., *In vitro models for the blood-brain barrier.* Toxicology in vitro : an international journal published in association with BIBRA, 2005. **19**(3): p. 299-334.
15. Wang, Q., et al., *Evaluation of the MDR-MDCK cell line as a permeability screen for the blood-brain barrier.* International journal of pharmaceutics, 2005. **288**(2): p. 349-59.
16. Furuse, M., et al., *Conversion of zonulae occludentes from tight to leaky strand type by introducing claudin-2 into Madin-Darby canine kidney I cells.* The Journal of cell biology, 2001. **153**(2): p. 263-72.
17. de Lange, E.C., et al., *In vitro and in vivo investigations on fluoroquinolones; effects of the P-glycoprotein efflux transporter on brain distribution of sparfloxacin.* European journal of pharmaceutical sciences : official journal of the European Federation for Pharmaceutical Sciences, 2000. **12**(2): p. 85-93.
18. Doran, A., et al., *The impact of P-glycoprotein on the disposition of drugs targeted for indications of the central nervous system: evaluation using the MDR1A/1B knockout mouse model.* Drug metabolism and disposition: the biological fate of chemicals, 2005. **33**(1): p. 165-74.
19. Xie, R. and M. Hammarlund-Udenaes, *Blood-brain barrier equilibration of codeine in rats studied with microdialysis.* Pharmaceutical research, 1998. **15**(4): p. 570-5.
20. de Lange, E.C., et al., *Critical factors of intracerebral microdialysis as a technique to determine the pharmacokinetics of drugs in rat brain.* Brain research, 1994. **666**(1): p. 1-8.
21. de Lange, E.C., et al., *Methodological considerations of intracerebral microdialysis in pharmacokinetic studies on drug transport across the blood-brain barrier.* Brain research. Brain research reviews, 1997. **25**(1): p. 27-49.
22. de Lange, E.C., A.G. de Boer, and D.D. Breimer, *Methodological issues in microdialysis sampling for pharmacokinetic studies.* Advanced drug delivery reviews, 2000. **45**(2-3): p. 125-48.
23. Jonsson, S., et al., *Role of modelling and simulation: a European regulatory perspective.* Clinical pharmacokinetics, 2012. **51**(2): p. 69-76.
24. Tavelin, S., et al., *Applications of epithelial cell culture in studies of drug transport.* Methods in molecular biology, 2002. **188**: p. 233-72.
25. Aarons, L., et al., *Role of modelling and simulation in Phase I drug development.* European journal of pharmaceutical sciences : official journal of the European Federation for Pharmaceutical Sciences, 2001. **13**(2): p. 115-22.

26. Breimer, D.D. and M. Danhof, *Relevance of the application of pharmacokinetic-pharmacodynamic modelling concepts in drug development. The "wooden shoe' paradigm.* Clinical pharmacokinetics, 1997. **32**(4): p. 259-67.
27. Chaikin, P., et al., *Pharmacokinetics/pharmacodynamics in drug development: an industrial perspective.* Journal of clinical pharmacology, 2000. **40**(12 Pt 2): p. 1428-38.
28. Derendorf, H. and B. Meibohm, *Modeling of pharmacokinetic/pharmacodynamic (PK/PD) relationships: concepts and perspectives.* Pharmaceutical research, 1999. **16**(2): p. 176-85.
29. FDA, *Innovation or stagnation: challenge and opportunity on the critical path to new medical products*, 2010.
30. Holford, N.H., et al., *Simulation of clinical trials.* Annual review of pharmacology and toxicology, 2000. **40**: p. 209-34.
31. Lockwood, P., et al., *Application of clinical trial simulation to compare proof-of-concept study designs for drugs with a slow onset of effect; an example in Alzheimer's disease.* Pharmaceutical research, 2006. **23**(9): p. 2050-9.
32. Reigner, B.G., et al., *An evaluation of the integration of pharmacokinetic and pharmacodynamic principles in clinical drug development. Experience within Hoffmann La Roche.* Clinical pharmacokinetics, 1997. **33**(2): p. 142-52.
33. Sheiner, L.B., *Learning versus confirming in clinical drug development.* Clinical pharmacology and therapeutics, 1997. **61**(3): p. 275-91.
34. Edholm, M., E. Gil Berglund, and T. Salmonson, *Regulatory aspects of pharmacokinetic profiling in special populations: a European perspective.* Clinical pharmacokinetics, 2008. **47**(11): p. 693-701.
35. Manolis, E. and G. Pons, *Proposals for model-based paediatric medicinal development within the current European Union regulatory framework.* British journal of clinical pharmacology, 2009. **68**(4): p. 493-501.
36. Roth, W.J., et al., *The effects of intralaboratory modifications to media composition and cell source on the expression of pharmaceutically relevant transporters and metabolizing genes in the Caco-2 cell line.* Journal of pharmaceutical sciences, 2012. **101**(10): p. 3962-78.
37. Sambuy, Y., et al., *The Caco-2 cell line as a model of the intestinal barrier: influence of cell and culture-related factors on Caco-2 cell functional characteristics.* Cell biology and toxicology, 2005. **21**(1): p. 1-26.
38. Behrens, I., et al., *Variation of peptide transporter (PepT1 and HPT1) expression in Caco-2 cells as a function of cell origin.* Journal of pharmaceutical sciences, 2004. **93**(7): p. 1743-54.

39. Artursson, P., *Epithelial transport of drugs in cell culture. I: A model for studying the passive diffusion of drugs over intestinal absorptive (Caco-2) cells.* Journal of pharmaceutical sciences, 1990. **79**(6): p. 476-82.
40. Artursson, P. and R.T. Borchardt, *Intestinal drug absorption and metabolism in cell cultures: Caco-2 and beyond.* Pharmaceutical research, 1997. **14**(12): p. 1655-8.
41. Tavelin, S., et al., *Prediction of the oral absorption of low-permeability drugs using small intestine-like 2/4/A1 cell monolayers.* Pharmaceutical research, 2003. **20**(3): p. 397-405.
42. Dahan, A., et al., *High-permeability criterion for BCS classification: segmental/pH dependent permeability considerations.* Molecular pharmaceutics, 2010. **7**(5): p. 1827-34.
43. Adachi, Y., H. Suzuki, and Y. Sugiyama, *Comparative studies on in vitro methods for evaluating in vivo function of MDR1 P-glycoprotein.* Pharmaceutical research, 2001. **18**(12): p. 1660-8.
44. Watanabe, T., et al., *Construction of a functional transporter analysis system using MDR1 knockdown Caco-2 cells.* Pharmaceutical research, 2005. **22**(8): p. 1287-93.
45. Ferruzza, S., et al., *Serum-reduced and serum-free media for differentiation of Caco-2 cells.* ALTEX, 2013. **30**(2): p. 159-68.
46. Moyes, S.M., J.F. Morris, and K.E. Carr, *Culture conditions and treatments affect Caco-2 characteristics and particle uptake.* International journal of pharmaceutics, 2010. **387**(1-2): p. 7-18.
47. Bestwick, C.S. and L. Milne, *Alteration of culture regime modifies antioxidant defenses independent of intracellular reactive oxygen levels and resistance to severe oxidative stress within confluent Caco-2 "intestinal cells".* Digestive diseases and sciences, 2001. **46**(2): p. 417-23.
48. Wu, X.W., et al., *Dulbecco's modified eagle's medium and minimum essential medium--which one is more preferred for establishment of Caco-2 cell monolayer model used in evaluation of drug absorption?* Die Pharmazie, 2013. **68**(10): p. 805-10.
49. Bravo, S.A., et al., *In-depth evaluation of Gly-Sar transport parameters as a function of culture time in the Caco-2 cell model.* European journal of pharmaceutical sciences : official journal of the European Federation for Pharmaceutical Sciences, 2004. **21**(1): p. 77-86.
50. Lu, S., et al., *Transport properties are not altered across Caco-2 cells with heightened TEER despite underlying physiological and ultrastructural changes.* Journal of pharmaceutical sciences, 1996. **85**(3): p. 270-3.

51. Yu, H., T.J. Cook, and P.J. Sinko, *Evidence for diminished functional expression of intestinal transporters in Caco-2 cell monolayers at high passages.* Pharmaceutical research, 1997. **14**(6): p. 757-62.
52. Artursson, P., K. Palm, and K. Luthman, *Caco-2 monolayers in experimental and theoretical predictions of drug transport.* Advanced drug delivery reviews, 2001. **46**(1-3): p. 27-43.
53. Dahan, A., et al., *High-Permeability Criterion for BCS Classification: Segmental/pH Dependent Permeability Considerations.* Molecular pharmaceutics, 2010.
54. Volpe, D.A., *Variability in Caco-2 and MDCK cell-based intestinal permeability assays.* Journal of pharmaceutical sciences, 2008. **97**(2): p. 712-25.
55. Hidalgo, I.J., T.J. Raub, and R.T. Borchardt, *Characterization of the human colon carcinoma cell line (Caco-2) as a model system for intestinal epithelial permeability.* Gastroenterology, 1989. **96**(3): p. 736-49.
56. Markowska, M., et al., *Optimizing Caco-2 cell monolayers to increase throughput in drug intestinal absorption analysis.* Journal of pharmacological and toxicological methods, 2001. **46**(1): p. 51-5.
57. Englund, G., et al., *Regional levels of drug transporters along the human intestinal tract: co-expression of ABC and SLC transporters and comparison with Caco-2 cells.* European journal of pharmaceutical sciences : official journal of the European Federation for Pharmaceutical Sciences, 2006. **29**(3-4): p. 269-77.
58. Mangas-Sanjuan, V., et al., *Modified Nonsink Equation for Permeability Estimation in Cell Monolayers: Comparison with Standard Methods.* Molecular pharmaceutics, 2014.
59. Friden, M., et al., *In vitro methods for estimating unbound drug concentrations in the brain interstitial and intracellular fluids.* Drug metabolism and disposition: the biological fate of chemicals, 2007. **35**(9): p. 1711-9.
60. Begley, D.J., *ABC transporters and the blood-brain barrier.* Current pharmaceutical design, 2004. **10**(12): p. 1295-312.
61. Begley, D.J., *Delivery of therapeutic agents to the central nervous system: the problems and the possibilities.* Pharmacology & therapeutics, 2004. **104**(1): p. 29-45.
62. Dauchy, S., et al., *ABC transporters, cytochromes P450 and their main transcription factors: expression at the human blood-brain barrier.* Journal of neurochemistry, 2008. **107**(6): p. 1518-28.

63. Uchida, Y., et al., *Quantitative targeted absolute proteomics of human blood-brain barrier transporters and receptors.* Journal of neurochemistry, 2011. **117**(2): p. 333-45.
64. Simpson, I.A., A. Carruthers, and S.J. Vannucci, *Supply and demand in cerebral energy metabolism: the role of nutrient transporters.* Journal of cerebral blood flow and metabolism : official journal of the International Society of Cerebral Blood Flow and Metabolism, 2007. **27**(11): p. 1766-91.
65. Parkinson, F.E., et al., *Molecular biology of nucleoside transporters and their distributions and functions in the brain.* Current topics in medicinal chemistry, 2011. **11**(8): p. 948-72.
66. Kalvass, J.C., et al., *Why clinical modulation of efflux transport at the human blood-brain barrier is unlikely: the ITC evidence-based position.* Clinical pharmacology and therapeutics, 2013. **94**(1): p. 80-94.
67. Roiko, S.A., M.A. Felmlee, and M.E. Morris, *Brain uptake of the drug of abuse gamma-hydroxybutyric acid in rats.* Drug metabolism and disposition: the biological fate of chemicals, 2012. **40**(1): p. 212-8.
68. Gao, B., et al., *Organic anion-transporting polypeptides mediate transport of opioid peptides across blood-brain barrier.* The Journal of pharmacology and experimental therapeutics, 2000. **294**(1): p. 73-9.
69. Iusuf, D., E. van de Steeg, and A.H. Schinkel, *Functions of OATP1A and 1B transporters in vivo: insights from mouse models.* Trends in pharmacological sciences, 2012. **33**(2): p. 100-8.
70. Banks, W.A., *The source of cerebral insulin.* European journal of pharmacology, 2004. **490**(1-3): p. 5-12.
71. Banks, W.A., et al., *Leptin transport across the blood-brain barrier of the Koletsky rat is not mediated by a product of the leptin receptor gene.* Brain research, 2002. **950**(1-2): p. 130-6.
72. Visser, C.C., et al., *Characterization and modulation of the transferrin receptor on brain capillary endothelial cells.* Pharmaceutical research, 2004. **21**(5): p. 761-9.
73. Herz, J. and P. Marschang, *Coaxing the LDL receptor family into the fold.* Cell, 2003. **112**(3): p. 289-92.
74. Pan, W. and A.J. Kastin, *TNFalpha transport across the blood-brain barrier is abolished in receptor knockout mice.* Experimental neurology, 2002. **174**(2): p. 193-200.
75. Pan, W. and A.J. Kastin, *Entry of EGF into brain is rapid and saturable.* Peptides, 1999. **20**(9): p. 1091-8.

76. Stern, D., et al., *Receptor for advanced glycation endproducts: a multiligand receptor magnifying cell stress in diverse pathologic settings.* Advanced drug delivery reviews, 2002. **54**(12): p. 1615-25.
77. Deane, R., Z. Wu, and B.V. Zlokovic, *RAGE (yin) versus LRP (yang) balance regulates alzheimer amyloid beta-peptide clearance through transport across the blood-brain barrier.* Stroke; a journal of cerebral circulation, 2004. **35**(11 Suppl 1): p. 2628-31.
78. Pardridge, W.M., et al., *Evaluation of cationized rat albumin as a potential blood-brain barrier drug transport vector.* The Journal of pharmacology and experimental therapeutics, 1990. **255**(2): p. 893-9.
79. Drin, G., et al., *Studies on the internalization mechanism of cationic cell-penetrating peptides.* The Journal of biological chemistry, 2003. **278**(33): p. 31192-201.
80. Roux, F. and P.O. Couraud, *Rat brain endothelial cell lines for the study of blood-brain barrier permeability and transport functions.* Cellular and molecular neurobiology, 2005. **25**(1): p. 41-58.
81. Kido, Y., et al., *Functional clarification of MCT1-mediated transport of monocarboxylic acids at the blood-brain barrier using in vitro cultured cells and in vivo BUI studies.* Pharmaceutical research, 2000. **17**(1): p. 55-62.
82. Hosoya, K.I., et al., *mRna expression and transport characterization of conditionally immortalized rat brain capillary endothelial cell lines; a new in vitro BBB model for drug targeting.* Journal of drug targeting, 2000. **8**(6): p. 357-70.
83. Weksler, B.B., et al., *Blood-brain barrier-specific properties of a human adult brain endothelial cell line.* FASEB journal : official publication of the Federation of American Societies for Experimental Biology, 2005. **19**(13): p. 1872-4.
84. Hosoya, K., et al., *Conditionally immortalized brain capillary endothelial cell lines established from a transgenic mouse harboring temperature-sensitive simian virus 40 large T-antigen gene.* AAPS pharmSci, 2000. **2**(3): p. E27.
85. Zhang, Y., et al., *Porcine brain microvessel endothelial cells as an in vitro model to predict in vivo blood-brain barrier permeability.* Drug metabolism and disposition: the biological fate of chemicals, 2006. **34**(11): p. 1935-43.
86. Stins, M.F., J. Badger, and K. Sik Kim, *Bacterial invasion and transcytosis in transfected human brain microvascular endothelial cells.* Microbial pathogenesis, 2001. **30**(1): p. 19-28.

87. Sano, Y., et al., *Establishment of a new conditionally immortalized human brain microvascular endothelial cell line retaining an in vivo blood-brain barrier function.* Journal of cellular physiology, 2010. **225**(2): p. 519-28.
88. Peng, Y., et al., *Applications of a 7-day Caco-2 cell model in drug discovery and development.* European journal of pharmaceutical sciences : official journal of the European Federation for Pharmaceutical Sciences, 2014. **56**: p. 120-30.
89. Friden, M., et al., *Development of a high-throughput brain slice method for studying drug distribution in the central nervous system.* Drug metabolism and disposition: the biological fate of chemicals, 2009. **37**(6): p. 1226-33.
90. Sarmento, B., et al., *Cell-based in vitro models for predicting drug permeability.* Expert opinion on drug metabolism & toxicology, 2012. **8**(5): p. 607-21.
91. Skolnik, S., et al., *Towards prediction of in vivo intestinal absorption using a 96-well Caco-2 assay.* Journal of pharmaceutical sciences, 2010. **99**(7): p. 3246-65.
92. Turco, L., et al., *Caco-2/TC7 cell line characterization for intestinal absorption: how reliable is this in vitro model for the prediction of the oral dose fraction absorbed in human?* Toxicology in vitro : an international journal published in association with BIBRA, 2011. **25**(1): p. 13-20.
93. Volpe, D.A., *Drug-permeability and transporter assays in Caco-2 and MDCK cell lines.* Future medicinal chemistry, 2011. **3**(16): p. 2063-77.
94. Youdim, K.A., A. Avdeef, and N.J. Abbott, *In vitro trans-monolayer permeability calculations: often forgotten assumptions.* Drug discovery today, 2003. **8**(21): p. 997-1003.
95. Bermejo, M., et al., *PAMPA--a drug absorption in vitro model 7. Comparing rat in situ, Caco-2, and PAMPA permeability of fluoroquinolones.* European journal of pharmaceutical sciences : official journal of the European Federation for Pharmaceutical Sciences, 2004. **21**(4): p. 429-41.
96. Hilgendorf, C., et al., *Caco-2 versus Caco-2/HT29-MTX co-cultured cell lines: permeabilities via diffusion, inside- and outside-directed carrier-mediated transport.* Journal of pharmaceutical sciences, 2000. **89**(1): p. 63-75.
97. de Lange, E.C., *The mastermind approach to CNS drug therapy: translational prediction of human brain distribution, target site kinetics,*

and therapeutic effects. Fluids and barriers of the CNS, 2013. **10**(1): p. 12.
98. Reichel, A., *The role of blood-brain barrier studies in the pharmaceutical industry*. Current drug metabolism, 2006. **7**(2): p. 183-203.